

**THE UNIVERSITY OF HULL**

**The Synthesis and Evaluation of Side Chain Liquid Crystal Polymers.**

being a Thesis submitted for the Degree of PhD

in the University of Hull

by

**Philip James Smith BSc(Hons)**

March, 1993



## **IMAGING SERVICES NORTH**

Boston Spa, Wetherby

West Yorkshire, LS23 7BQ

[www.bl.uk](http://www.bl.uk)

**BEST COPY AVAILABLE.**

**VARIABLE PRINT QUALITY**

*I dedicate this thesis to my wife  
and best friend Helen,  
and my parents Doris and Derrick.*

## ACKNOWLEDGEMENTS

I would like to express my thanks to all the people who made this work possible, The Ministry of Defence for providing the funding and The University of Hull for providing the facilities.

I would also like to thank Dr. David Lacey for his help, guidance and friendship.

I am grateful for the help, support and useful discussions provided by many of the Liquid Crystal Group at The University of Hull. Especially Julie Haley for her great help and Chris (Vic Reeves) Booth for keeping me almost sane. I would like to thank the staff of the Chemistry Department for the excellent analytical services.

I am indebted to my friends and family for their constant support and understanding throughout the duration of this work.

Finally I must say a special thank you to my wife Helen for keeping my life running smoothly around me while I wrote this thesis.

## TABLE OF CONTENTS.

1. INTRODUCTION TO LIQUID CRYSTALS. . . . .	1
1.1 Introduction. . . . .	1
1.2 Thermotropic Liquid Crystalline Phases. . . . .	3
1.3 Calamitic Liquid Crystalline Phases . . . . .	5
1.4 Discussion of Phases Formed by Non-Chiral Materials. . . . .	6
1.4.1 Smectic/Crystal Phases. . . . .	6
1.4.2 The Nematic Phase. . . . .	9
1.5 Discussion of Phases Formed by Chiral Liquid Crystalline Materials . . . . .	11
1.5.1 Chiral Smectic C ( $S_C^*$ ) Phase . . . . .	11
1.5.2 The Cholesteric (Chiral Nematic) Phase . . . . .	13
1.5.3 Blue Phases . . . . .	15
1.5.4 Smectic A* Phase . . . . .	17
2. INTRODUCTION TO POLYMERS . . . . .	20
2.1 Polymers . . . . .	20
2.2 Definitions . . . . .	20
2.3 Types of Polymerization . . . . .	22
2.3.1 Step-Growth Polymerization . . . . .	22
2.3.2 Addition Polymerization . . . . .	25
2.3.2.1 Free Radical Initiators. . . . .	26
2.3.2.2 Initiation . . . . .	26
2.3.3 Formation of an Active Centre . . . . .	29

2.3.4 Propagation . . . . .	29
2.3.5 Termination . . . . .	30
2.4 Ionic Polymerization . . . . .	32
2.4.1 Cationic polymerization . . . . .	33
2.4.2 Anionic Polymerization . . . . .	34
2.4.3 Group Transfer Polymerization . . . . .	36
2.4.4 Comparison of Free Radical Polymerization to Group Transfer Polymerization . . . . .	38
3. INTRODUCTION TO LIQUID CRYSTAL POLYMERS . . . . .	40
3.1 Introduction . . . . .	40
3.2 Main Chain Liquid Crystal (MCLC) Polymers . . . . .	42
3.2.1 Thermotropic MCLC Polymers . . . . .	42
3.2.2 Phase Behaviour in Main Chain Liquid Crystal (MCLC) Polymers . . . . .	45
3.3 Side Chain Liquid Crystal (SCLC) Polymers . . . . .	48
3.3.1 Constituents of a Side Chain Liquid Crystal Polymer . . . . .	50
3.3.2 The Polymer Backbone . . . . .	51
3.3.2.1 Degree of Polymerization . . . . .	51
3.3.2.2 Polydispersity . . . . .	53
3.3.2.3 Chemical Constitution . . . . .	54
3.3.2.4 Lateral Attachment . . . . .	55
3.3.2.5 Linear Polysiloxanes . . . . .	58
3.3.2.6 Copolymer Linear Polysiloxanes. . . . .	60
3.3.2.7 Cyclic Polysiloxanes. . . . .	63

3.3.2.7 Polymer Architecture . . . . .	70
3.3.2.8 Mixed Lateral-Terminal Polysiloxanes . . . . .	71
3.4 The Flexible Spacer Group. . . . .	76
3.5 The Mesogenic Core . . . . .	79
3.6 The Terminal Group . . . . .	82
3.7 Summary . . . . .	83
4. AIMS. . . . .	85
5. EXPERIMENTAL. . . . .	87
5.1 Physical Characterization . . . . .	87
5.2 Purification of Solvents. . . . .	91
5.2.1 Dry Dichloromethane. . . . .	91
5.2.2 Dry Tetrahydrofuran. . . . .	92
5.2.3 Dry Toluene. . . . .	92
5.3 SCHEME 1 . . . . .	93
5.3.1 The Preparations of Compounds <b>Ia</b> to <b>If</b> are Exemplified by the Following Preparation of $\omega$ - Bromopropyl acrylate ( <b>Ia</b> ). . . . .	93
5.3.2 Preparation of $\omega$ -Bromopropyl methacrylate ( <b>Ib</b> ). . . . .	95
5.3.3 Preparation of $\omega$ -Chlorohexyl acrylate ( <b>Ic</b> ). . . . .	95
5.3.4 Preparation of $\omega$ -Chlorohexyl methacrylate ( <b>Id</b> ). . . . .	96
5.3.5 Preparation of $\omega$ -Bromoundecyl acrylate ( <b>Ie</b> ). . . . .	97
5.3.6 Preparation of $\omega$ -Bromoundecyl methacrylate ( <b>If</b> ). . . . .	97
5.4 SCHEME 2 . . . . .	99

5.4.1	Preparation of 4-(Methoxycarbonyloxy)benzoic Acid	
	(II). . . . .	100
5.4.2	Preparation of the Acid Chloride of	
	4-(Methoxycarbonyloxy)benzoic Acid (III) . . . . .	100
5.4.3	Preparation of 4-Methoxyphenyl	
	4-(methoxycarbonyloxy)benzoate (IVa). . . . .	101
5.4.4	Preparation of 4-Cyanophenyl	
	4-(methoxycarbonyloxy)benzoate (IVb). . . . .	101
5.4.5	Preparation of 4-Methoxyphenyl 4-hydroxybenzoate	
	(Va). . . . .	102
5.4.6	Preparation of 4-Cyanophenyl 4-hydroxybenzoate (Vb). . . . .	103
5.4.7	Preparation of Compounds VIa to VIg. . . . .	104
5.4.8	Preparation of 4-Methoxyphenyl	
	4-[3-(acryloyloxy)propyloxy]benzoate (VIa). . . . .	104
5.4.9	Preparation of 4-Methoxyphenyl	
	4-[6-(acryloyloxy)hexyloxy]benzoate (VIb). . . . .	105
5.4.10	Preparation of 4-Methoxyphenyl	
	4-[11-(acryloyloxy)undecyloxy]benzoate (VIc) . . . . .	106
5.4.11	Preparation of 4-Cyanophenyl	
	4-[6-(acryloyloxy)hexyloxy]benzoate (VIId). . . . .	107
5.4.12	Preparation of 4-Cyanophenyl	
	4-[6-(methacryloyloxy)hexyloxy]benzoate (VIe). . . . .	107
5.4.13	Preparation of 4-Cyanophenyl	
	4-[11-(acryloyloxy)undecyloxy]benzoate (VIIf). . . . .	108

5.4.14	Preparation of 4-Cyanophenyl	
	4-[11-(methacryloyloxy)undecyloxy]benzoate ( <b>VIg</b> ). . . . .	109
5.5	SCHEME 3 . . . . .	110
5.5.1	Preparation of 4'-Cyano-	
	4-[6-(acryloyloxy)hexoxy]biphenyl ( <b>VIIa</b> ). . . . .	111
5.5.2	Preparation of 4'-Cyano-	
	4-[6-(methacryloyloxy)hexoxy]biphenyl ( <b>VIIb</b> ). . . . .	111
5.5.3	Preparation of 4'-Cyano-	
	4-[11-(acryloyloxy)undecoxy]biphenyl ( <b>VIIc</b> ). . . . .	112
5.5.4	Preparation of 4'-Cyano-	
	4-[11-(methacryloyloxy)undecoxy]biphenyl ( <b>VIIId</b> ). . . . .	113
5.6	SCHEME 4 . . . . .	114
5.6.1	Preparation of 4'-Methoxycarbonyloxybiphenyl-	
	4-carboxylic acid ( <b>VIII</b> ). . . . .	115
5.6.2	Preparation of ( <i>S</i> )-(+)-1-Methylheptyl	
	4'-methoxycarbonyloxybiphenyl-4-carboxylate ( <b>IX</b> ). . . . .	115
5.6.3	Preparation of ( <i>S</i> )-(+)-1-Methylheptyl	
	4'-hydroxybiphenyl-4-carboxylate ( <b>X</b> ). . . . .	116
5.6.4	Preparation of ( <i>S</i> )-(+)-1-Methylheptyl 4'-[11-	
	(acryloyloxy)undecoxy]biphenyl-4-carboxylate ( <b>XI</b> ). . . . .	117
5.7	SCHEME 5 . . . . .	119
5.7.1	Preparation of ( <i>S</i> )-(-)-3,7-Dimethyl-1-octanol ( <b>XII</b> ). . . . .	120
5.7.2	Preparation of ( <i>S</i> )-(-)-3'',7''-Dimethyloctyl	
	4'-methoxycarbonyloxybiphenyl-4-carboxylate ( <b>XIII</b> ). . . . .	120

5.7.3	Preparation of ( <i>S</i> )-(-)-3'',7''-Dimethyloctyl- 4'-hydroxybiphenyl-4-carboxylate ( <b>XIV</b> ). . . . .	121
5.7.4	Preparation of ( <i>S</i> )-(-)-3'',7''-Dimethyloctyl 4'-[11- (acryloyloxy)undecoxy]biphenyl-4-carboxylate ( <b>XV</b> ). . .	122
5.8	SCHEME 6 . . . . .	124
5.8.1	Preparation of ( <i>S</i> )-(-)-Ethyl 2-(4'- methoxycarbonyloxybiphenyl- 4-carbonyloxy)propanoate ( <b>XVI</b> ). . . . .	125
5.8.2	Preparation of ( <i>S</i> )-(-)-Ethyl 2-(4'-hydroxybiphenyl- 4-carbonyloxy)propanoate ( <b>XVII</b> ). . . . .	126
5.8.3	Preparation of ( <i>S</i> )-(-)-Ethyl 2- {4'-[11-(acryloyloxy)undecoxy]biphenyl-4- carbonyloxy}propanoate ( <b>XVIII</b> ). . . . .	127
5.9	SCHEME 7 . . . . .	128
5.10	Polymerization Procedures. . . . .	129
5.10.1	Polymerization of Methyl Methacrylate Using Group Transfer Polymerization. . . . .	129
5.10.1.1	Purification of Starting Materials. . . . .	129
5.10.1.2	Group Transfer Polymerization. . . . .	131
5.10.2	Free Radical Polymerization. . . . .	135
5.10.2.1	Literature Procedure. . . . .	135
5.10.2.2	Modified Procedure. . . . .	135
5.10.3	Preparation of SCLC Cyclic Polysiloxanes. . . . .	136

5.10.3.1	Preparation of Hexachloroplatinic Acid (Speier's catalyst). . . . .	136
5.10.3.2	Hydrosilylation of Cyclic Polysiloxanes. . . . .	137
5.11	Microscopic Identification of Liquid Crystalline Phases. . . . .	137
5.11.1	Microscope Slide Preparation. . . . .	139
5.11.2	Homogeneous Alignment. . . . .	140
5.11.3	Homeotropic Alignment. . . . .	141
5.11.4	Sample Preparation. . . . .	143
6.	RESULTS AND DISCUSSION. . . . .	145
6.1	Group Transfer Polymerization. . . . .	145
6.1.1	Polymerization of Methyl Methacrylate. . . . .	145
6.1.2	Polymerization of Mesogenic Moieties. . . . .	152
6.2	Free Radical Polymerization . . . . .	154
6.2.1	Literature Procedure . . . . .	154
6.2.2	Polymerization of Simple Acrylates and Methacrylates. . . . .	156
6.2.2.1	Effect of the Solvent. . . . .	156
6.2.2.2	Effect of Concentration of AIBN. . . . .	167
6.2.2.3	The Effect of Pressure (Sealed Reaction Vessel). . . . .	171
6.2.2.4	The Combined Effect of Pressure and Ultrasound. . . . .	175
6.2.2.5	The Effect of Monomer Concentration. . . . .	176
6.2.2.6	Summary. . . . .	182
6.2.3	Free Radical Polymerization of Mesogenic Monomers. . . . .	183

6.2.3.1	Polymerization of Monomers VI(a - g). . . . .	187
6.2.3.2	Polymerization of Monomers VII(a - d). . . . .	190
6.3	Random Copolymerization of Mesogenic and Non-Mesogenic Acrylates and Methacrylates. . . . .	191
6.3.1	Free Radical Copolymerization of Mesogenic and Non- Mesogenic Monomers. . . . .	193
6.3.1.1	Methyl Acrylate and Methacrylate as the Non- Mesogenic Monomer. . . . .	194
6.3.1.2	Butyl Acrylate and Methacrylate as Non- Mesogenic Monomer. . . . .	198
6.4	Random Mesogenic Copolymers. . . . .	202
6.5	Alignment and Phase Identification of SCLC Polymers. . . . .	215
6.5.1	Limitations of the Alignment Procedure. . . . .	217
6.5.1	Mixed Lateral and Terminal Attachment of Side Chains to Cyclic Polysiloxanes. . . . .	229
6.5.2	Miscibility of Cyclic Polysiloxanes. . . . .	230
6.6	X-ray Diffraction Studies on Cyclic Polysiloxanes. . . . .	230
7.	CONCLUSIONS . . . . .	234
8.	BIBLIOGRAPHY . . . . .	239

## LIST OF FIGURES.

Figure 1.1 A schematic representation of the relationship between the solid, liquid and liquid crystalline phases . . . . .	2
Figure 1.2 A schematic representation of a calamitic liquid crystalline molecule . . . . .	3
Figure 1.3 An example of a calamitic molecule that exhibits liquid crystalline properties . . . . .	4
Figure 1.4 A schematic representation of a discotic liquid crystalline molecule . . . . .	4
Figure 1.5 An example of a discotic material that exhibits liquid crystalline properties . . . . .	4
Figure 1.6 A schematic representation of a smectic A phase . . . . .	7
Figure 1.7 A schematic representation of a smectic C phase . . . . .	8
Figure 1.8 Examples of molecules that exhibit smectic and crystal phases . . . .	9
Figure 1.9 An example of a molecule that exhibits a nematic phase . . . . .	10
Figure 1.10 A schematic representation of a nematic phase . . . . .	10
Figure 1.11 An example of a material that exhibits a chiral smectic C ( $S_C^*$ ) phase. . . . .	12
Figure 1.12 The structure of the chiral smectic C ( $S_C^*$ ) phase . . . . .	13
Figure 1.13 The relationship between compounds that show nematic and cholesteric phases . . . . .	14
Figure 1.14 A schematic representation of a cholesteric phase . . . . .	15
Figure 1.15 A schematic representation of a cubic blue phase . . . . .	16
Figure 1.16 An example of an ester that exhibits a chiral smectic A phase . . .	17

Figure 1.17 A schematic representation of the structure of the chiral smectic A phase .....	18
Figure 1.18 An example of a polymer which exhibits a chiral smectic A phase .....	18
Figure 1.19 A schematic representation of the structure of a polymeric chiral smectic A phase .....	19
Figure 2.1 A graph of the distribution of molecular weights of a polymer ...	22
Figure 2.2 An example of a condensation reaction .....	23
Figure 2.3 An example of a polycondensation reaction .....	23
Figure 2.4 A general example of a reaction that produces polyurethanes .....	24
Figure 2.5 An example of a reaction that can result in a linear polymer or a cyclized monomer .....	25
Figure 2.6 The effect of heat on benzoyl peroxide .....	27
Figure 2.7 The effect of heat on $\alpha,\alpha'$ -azoisobutyronitrile .....	28
Figure 2.8 A redox reaction that can be used to produce free radicals at low temperatures .....	28
Figure 2.9 The formation of an active centre .....	29
Figure 2.10 The reaction of a free radical with a monomer unit .....	30
Figure 2.11 Termination reactions in growing polymer chains .....	31
Figure 2.12 Chain Transfer reaction .....	32
Figure 2.13 The production of an ion pair by reaction of perchloric acid and a monomer .....	33
Figure 2.14 An example of cationic polymerization. ....	34
Figure 2.15 The initiation steps of an anionic polymerization .....	35

Figure 2.16 The classical anionic polymerization of methyl methacrylate using butyllithium as initiator . . . . .	36
Figure 2.17 The proposed mechanism for group transfer polymerization. . . . .	39
Figure 3.1 A summary of the different architectures that are possible for liquid crystal polymers . . . . .	41
Figure 3.2 An example of a main chain liquid crystal polymer, produced by Eastman Kodak . . . . .	43
Figure 3.3 An example of a main chain liquid crystal polymer produced by DuPont . . . . .	43
Figure 3.4 The structure of Kevlar . . . . .	44
Figure 3.5 An example of a main chain liquid crystal polymer incorporating different spacer lengths . . . . .	45
Figure 3.6 Schematic representations of a) a nematic phase and b) a smectic phase formed by main chain liquid crystal polymers . . . . .	46
Figure 3.7 A schematic representation of the main features of a side chain liquid crystal polymer . . . . .	51
Figure 3.8 A schematic representation of the variation of phase transition temperatures with degree of polymerization . . . . .	52
Figure 3.9 A schematic representation of a laterally attached side chain liquid crystal polymer . . . . .	58
Figure 3.10 The hydrosilylation reaction. . . . .	59
Figure 3.11 The structures of some commercially available polysiloxane backbones and their analogous SCLC polysiloxanes . . . . .	61

Figure 3.12 The structures of a) tetramethylcyclotetrasiloxane and b) pentamethylcyclopentasiloxane. . . . .	63
Figure 3.13 The four isomers of tetramethylcyclotetrasiloxane. . . . .	64
Figure 3.14 The four isomers of pentamethylcyclopentasiloxane. . . . .	65
Figure 3.15 The a) discotic and b) bundle structures for cyclic polysiloxanes. . . . .	66
Figure 3.16 The phase transitions of linear and cyclic polysiloxanes. . . . .	67
Figure 3.17 The method of preparing a cyclic polysiloxane with a moderate molecular weight side chain . . . . .	68
Figure 3.18 The structure of a cyclic polysiloxane with a high molecular weight side chain . . . . .	69
Figure 3.19 A schematic representation of a polymer with both laterally and terminally appended side chains . . . . .	72
Figure 3.20 An example of a mixed lateral-terminal copolysiloxane . . . . .	72
Figure 3.21 A schematic representation of a polymer containing mesogens in the main and side chains . . . . .	73
Figure 3.22 The variety of mesogenic cores that were examined by Gray, Hill and Lacey . . . . .	81
Figure 3.23 The efficiency of the ring system X in promoting liquid crystal properties . . . . .	82
Figure 3.24 Typical mesogenic side groups for a) ferroelectric, b) nonlinear optic applications. . . . .	83
Figure 5.1 The structure of the copolymer XIX + XV. . . . .	88
Figure 5.2 The $^1\text{H}$ nmr of the copolymer XIX + XV. . . . .	90

Figure 5.3 A schematic representation of the large apparatus used to carry out group transfer polymerization. . . . .	134
Figure 5.4 A schematic representation of the modified apparatus for carrying out Group Transfer Polymerization. . . . .	135
Figure 5.5 The preparation of homogeneously aligned SCLC polymers. . . . .	142
Figure 5.6 The preparation of homeotropically aligned SCLC polymers. . . . .	144
Figure 6.1 Effect of the ratio of initiator:catalyst (I:C) for the polymerization of methyl methacrylate by GTP (large apparatus). . . . .	149
Figure 6.2 Effect of the ratio of initiator:catalyst (I:C) for the polymerization of methyl methacrylate by GTP (small apparatus). . . . .	150
Figure 6.3 The mesogenic moiety <b>VIIId</b> used for group transfer polymerization. . . . .	152
Figure 6.4 Variation of a) $\bar{M}_w$ , b) $\bar{M}_n$ and c) $\bar{M}_w/\bar{M}_n$ with different solvents for methyl methacrylate. . . . .	159
Figure 6.5 Variation of a) $\bar{M}_w$ , b) $\bar{M}_n$ and c) $\bar{M}_w/\bar{M}_n$ with different solvents for methyl acrylate. . . . .	160
Figure 6.6 Variation of a) $\bar{M}_w$ , b) $\bar{M}_n$ and c) $\bar{M}_w/\bar{M}_n$ with different solvents for ethyl methacrylate. . . . .	161
Figure 6.7 Variation of a) $\bar{M}_w$ , b) $\bar{M}_n$ and c) $\bar{M}_w/\bar{M}_n$ with different solvents for ethyl acrylate. . . . .	162
Figure 6.8 Comparison of the effect of solvent on a) $\bar{M}_n$ and b) $\bar{M}_w/\bar{M}_n$ on the four non-mesogenic polymers. . . . .	164

Figure 6.9	Variation of a) $\bar{M}_w$ , b) $\bar{M}_n$ and c) $\bar{M}_w/\bar{M}_n$ with concentration of AIBN and different solvents, in the free radical polymerization of ethyl acrylate. . . . .	170
Figure 6.10	Variation of a) $\bar{M}_w$ , b) $\bar{M}_n$ and c) $\bar{M}_w/\bar{M}_n$ with sealed tubes and different solvents for the free radical polymerization of methyl methacrylate. . . . .	174
Figure 6.11	Variation of a) $\bar{M}_w$ , b) $\bar{M}_n$ and c) $\bar{M}_w/\bar{M}_n$ with ultrasound and different solvents in sealed tubes in the polymerization of methyl methacrylate. . . . .	178
Figure 6.12	Variation of a) $\bar{M}_w$ , b) $\bar{M}_n$ and c) $\bar{M}_w/\bar{M}_n$ with ultrasound and different solvents in sealed tubes in the polymerization of methyl methacrylate (2 mol %). . . . .	181
Figure 6.13	Variation of a) $\bar{M}_w$ , b) $\bar{M}_n$ and c) $\bar{M}_w/\bar{M}_n$ with different solvents for Monomer VIIIc . . . . .	186
Figure 6.14	The monomers used for the mesogenic copolymer study. . . . .	204
Figure 6.15	The DSC heating curve of the 1:5 copolymer XVIII + XIX. . . . .	207
Figure 6.16	The DSC cooling curve of the 1:5 copolymer XVIII + XIX. . . . .	208
Figure 6.17	The Cooling cycle of the 1:5 copolymer XVIII + XIX. . . . .	209
Figure 6.18	The cooling cycle 1E7; sector along 001 of the 1:5 copolymer XVIII + XIX. . . . .	210
Figure 6.19	The cooling cycle 5ES . . . . .	212
Figure 6.20	A polyacrylate supplied for phase identification by Merck (UK) (XX). . . . .	216

Figure 6.21 A polychloroacrylate supplied for phase identification by Merck (UK) (XXI). . . . .	216
Figure 6.22 Structure of cyclic polysiloxanes . . . . .	219
Figure 6.23 The X-ray diffraction patterns of polymers XLIIIa and XLIVa .	233

## LIST OF TABLES.

Table 1.1 A summary of the classification of smectic/crystal phases . . . . .	7
Table 3.1 A good example of the influence of the length of the flexible spacer group on the phase transitions of polymeric materials demonstrated by poly[ $\omega$ -(4'-methoxybiphenyl-4-oxy)alkyl] methacrylates . . . . .	50
Table 3.2 The effect of the polymer backbone on transition temperatures . . . .	56
Table 3.3 Influence of the polymer backbone on the phase transitions of polymers . . . . .	57
Table 3.4 The variation of transition temperatures produced by substituting a mesogenic side chain onto different copolymer backbones . . . . .	62
Table 3.5 Variations in transition temperatures with the length of the spacer group in polymers containing mesogenic units in both the polymer backbone and the side chain . . . . .	74
Table 3.6 Variations in transition temperature with spacer length for a cross-shaped polymer . . . . .	75
Table 3.7 The effect of spacer length on the phase transitions of <i>en-bloc</i> polymers . . . . .	76
Table 3.8 The effect of changing the chemical composition of the anchorage point of the flexible spacer group to the mesogenic core . . . . .	78
Table 3.9 Influence of the length of the spacer group and the nature of the polymer backbone on the phase transitions of polymers containing 4-cyanobiphenyl based mesogenic groups . . . . .	80
Table 6.1 GPC data for large scale GTP of methyl methacrylate. . . . .	147

Table 6.2 GPC data for small scale GTP of methyl methacrylate. . . . .	149
Table 6.3 A comparison of GPC results for large and small scale GTP reactions. . . . .	151
Table 6.4 The effect of solvent upon the physical properties of free radical polymerization of non-mesogenic monomers. . . . .	158
Table 6.5 The effect of concentration of initiator on the free radical polymerization of ethyl acrylate. . . . .	169
Table 6.6 The effect of sealed tubes on the free radical polymerization of methyl methacrylate. . . . .	173
Table 6.7 The effect of ultrasound on the free radical polymerization of methyl methacrylate. . . . .	177
Table 6.8 The effect of ultrasound on the polymerization of the same concentration of methyl methacrylate as for mesogenic monomers. . . .	180
Table 6.9 The effect of solvents on the physical properties of the free radical polymerization of monomer XIX. . . . .	185
Table 6.10 The physical and thermal properties of polymers VI (a - g). . . . .	189
Table 6.11 The physical and thermal properties of polymers VII(a - d). . . . .	191
Table 6.12 The physical and thermal properties of polymer XV. . . . .	192
Table 6.13 The results of the copolymerizations carried out by Platé <i>et al.</i> . . . .	195
Table 6.14 The results of the copolymerization of mesogenic and non- mesogenic monomers. . . . .	197
Table 6.15 The physical and thermal properties of the copolymerization of mesogenic and non-mesogenic monomers. . . . .	200

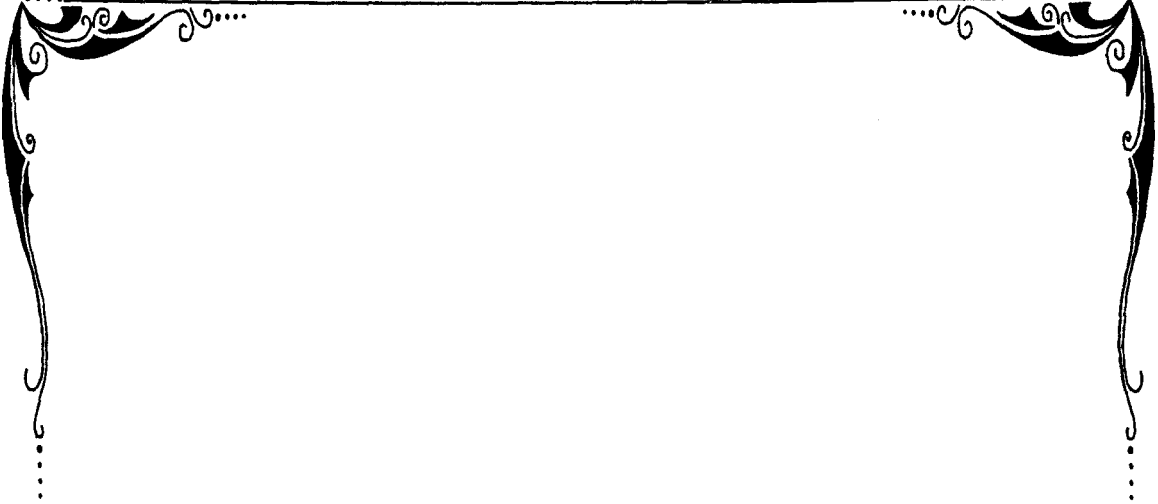
Table 6.16 The physical and thermal properties of copolymerization of mesogenic and non-mesogenic monomers. . . . .	201
Table 6.17 The physical and thermal properties of the mesogenic copolymers produced by free radical polymerization. . . . .	205
Table 6.18 The higher order reflections of the 1:5 copolymer XVIII + XIX. . .	211
Table 6.19 The variation of layer spacing with temperature for the copolymer . . . . .	213
Table 6.20 The length of the side chain units of the copolymer. . . . .	214
Table 6.21 The physical and thermal properties of Polymers XLIII(a + b). . .	221
Table 6.22 The physical and thermal properties of Polymers XLIV(a + b). . .	222
Table 6.23 The physical and thermal properties of Polymers XLV(a + b). . . .	223
Table 6.24 The physical and thermal properties of XLVI(a + b). . . . .	224
Table 6.25 The physical and thermal properties of Polymers XLVII(a + b). . .	224
Table 6.26 The physical and thermal properties of Polymers XLVIII(a + b). . .	225
Table 6.27 The thermal properties of laterally attached linear polysiloxanes. . .	226
Table 6.28 The physical and thermal properties of Polymers XLIX(a + b). . .	227
Table 6.29 The physical and thermal properties of Polymers L(a + b). . . . .	228
Table 6.30 The physical and thermal properties of Polymer LI. . . . .	228
Table 6.31 The physical and thermal properties of the fractionated mixed lateral / terminal cyclic polysiloxane. . . . .	231

**LIST OF SCHEMES.**

5.3 SCHEME 1 .....	93
5.4 SCHEME 2 .....	99
5.5 SCHEME 3 .....	110
5.6 SCHEME 4 .....	114
5.7 SCHEME 5 .....	119
5.8 SCHEME 6 .....	124
5.9 SCHEME 7 .....	128

## LIST OF PLATES.

Plate 1	The characteristic "sandy" texture of a side chain liquid crystal polymer. Polymer XIX, 150 °C (x100). . . . .	250
Plate 2	The Focal conic texture of the smectic A phase of Polymer XIX, no alignment, 150 °C (x100). . . . .	250
Plate 3	The schlieren texture of the smectic C phase of Polymer XXI, aligned homeotropically, 130 °C (x100). . . . .	251
Plate 4	The focal conic texture of the smectic A phase of Polymer XX, homogeneously aligned, 150 °C (x100). . . . .	251
Plate 5	The focal conic smectic A texture of Polymer XX, homogeneously aligned, 105 °C (x100). . . . .	252
Plate 6	The broken focal conic smectic C texture of Polymer XX, homogeneously aligned, cooled from the smectic A phase, 90 °C (x100). . . . .	252
Plate 7	The broken focal conic texture of the smectic I phase of Polymer XX, homogeneously aligned, cooled from the smectic C phase, 30 °C (x100). . . . .	253
Plate 8	The texture of Polymer XXVI, 145 °C (x100). . . . .	253
Plate 9	The texture of Polymer XXVII, 130 °C (x100). . . . .	254
Plate 10	The texture of Polymer XXXV, 100 °C (x100). . . . .	254
Plate 11	The focal conic texture of the chiral smectic C phase of Polymer XLIVa, 25 °C (x100). . . . .	255
Plate 12	The "discotic" texture of Polymer XLIVa, 25 °C after 24 h. (x100). . . . .	255



*Introduction*  
*to*  
*Liquid Crystals*



# 1. INTRODUCTION TO LIQUID CRYSTALS.

## 1.1 Introduction.

The phenomenon of liquid crystallinity was first reported by Reinitzer<sup>1</sup> for cholesteryl benzoate in 1888. It was observed that the melting behaviour of this compound was different from the classical melting behaviour of ordinary organic materials.<sup>2</sup> In a classical melting process the molecules in the solid are held in fixed positions at lattice sites with very little room for rotation or movement. As the sample is heated, the molecules gain energy and begin to vibrate. At a particular temperature known as the melting point, the forces which hold the molecules in position are overcome and the molecules become free to rotate and move. Above the melting point the molecules have no long range order and this state of matter is known as the *Isotropic Liquid*. There is a decrease in order on heating a sample from the solid phase, which has three dimensional order, to the isotropic liquid which has zero order. This melting process is found to exist in most organic molecules which have equal forces of attraction in all directions between molecules.

For the liquid crystalline system, because the molecules are lath-like in shape, the forces of attraction between the molecules are unequal in different directions and the system behaves as an anisotropic medium. The melting process now occurs in stages giving rise to stable intermediate states or *Mesophases*.<sup>3</sup> A simple picture of the melting process for such a liquid crystalline system can be described as follows. The

molecules in the solid are fixed in lattice positions and as the temperature is increased, the molecules gain energy and begin to vibrate. Once the molecules have gained sufficient energy, the weakest point of attraction between the molecules is broken, but due to the anisotropic nature of the system, some degree of order in the material is still maintained. This is known as a *Liquid Crystalline State*. On further heating the attractive forces which are maintaining order in the mesophase may be further weakened giving rise to either other mesophases or, once all the attractive forces between molecules have been broken completely, the isotropic liquid.

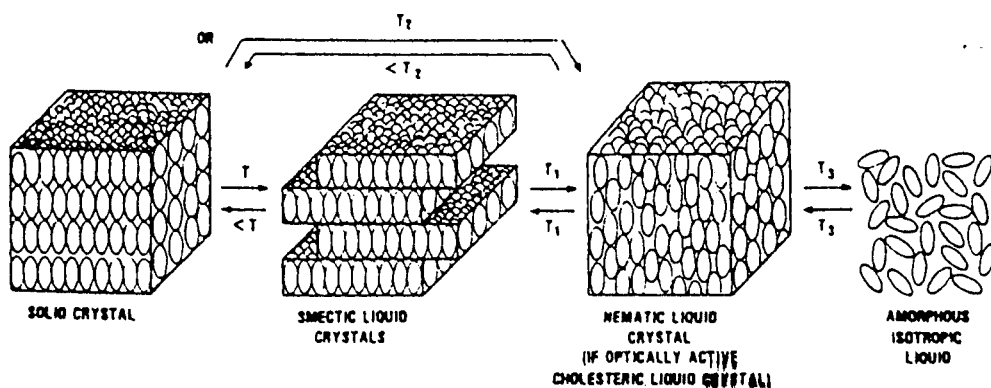


**Figure 1.1** A schematic representation of the relationship between the solid, liquid and liquid crystalline phases.

Many different types of mesophase are known and some of these will be described later. Liquid crystalline phases have the fluid properties of the isotropic liquid and some degree of order (but less than) of the solid crystal; hence their name *Liquid Crystals*.

The application of heat to a sample to form liquid crystalline phases (*Thermotropic* liquid crystal phases) is not the only method by which liquid crystalline phases can be produced. Another type of liquid crystalline phase known as *Lyotropic*, can be produced by the addition of a solvent (usually water) to certain amphiphilic compounds. At certain concentrations of the amphiphilic compound in a given solvent, ordered phases consisting of arrangements of micelles are formed. These exhibit anisotropic properties characteristic of liquid crystalline phases. Some examples of lyotropic systems are given below, but a detailed discussion of this type of mesophase is beyond the scope of this thesis; for reviews see references [4 - 7]. Examples of lyotropic systems include the surfactants  $C_{16}H_{25}NMe_3Cl$  and  $C_nH_{2n+1}NMe_3Br$  ( $n = 8 - 18$ ).

### 1.2 Thermotropic Liquid Crystalline Phases.

Thermotropic liquid crystalline phases may be produced by organic and organometallic compounds whose molecules are either rod shaped (*Calamitic*) or disc shaped (*Discotic*). Some examples of both types of system are given in Figures 1.2 to 1.5.

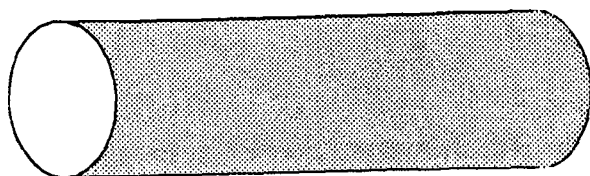


**Figure 1.2** A schematic representation of a calamitic liquid crystalline molecule.

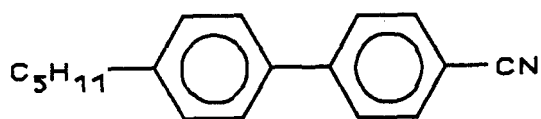


**Figure 1.3** An example of a calamitic molecule that exhibits liquid crystalline properties.<sup>8</sup>

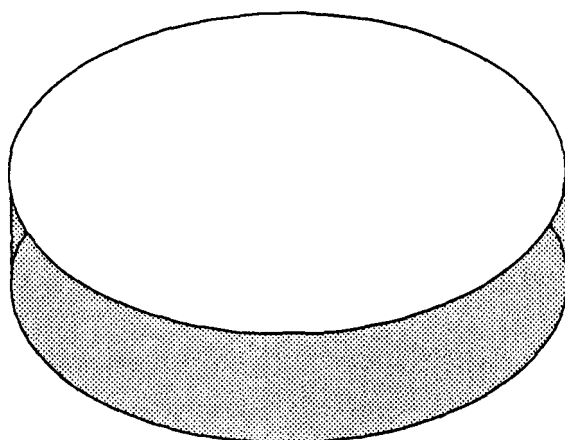


**Figure 1.4** A schematic representation of a discotic liquid crystalline molecule.

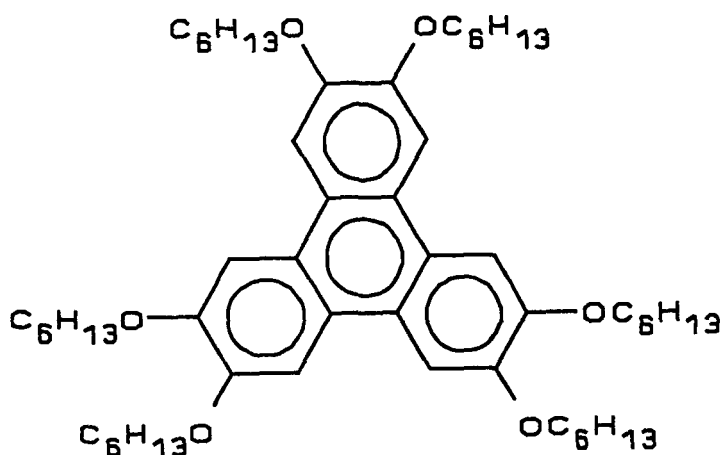


**Figure 1.5** An example of a discotic material that exhibits liquid crystalline properties.<sup>9</sup>

The content of this thesis is mainly concerned with calamitic thermotropic liquid crystals and so the description of the types of liquid crystalline phases will concentrate on these types of liquid crystals. For reviews of discotic phases, see the articles by Chandrasekhar<sup>10</sup> and Billard *et al.*<sup>11</sup>

### 1.3 Calamitic Liquid Crystalline Phases.

The type of phases produced by calamitic molecules is highly dependent upon the chemical structure of the compound. For non-chiral materials the types of phases that can be produced are classified as follows,

- Nematic (N), from *nematos*, Greek for thread-like.
- Smectic (S), from *smectos*, Greek for soap-like.

A more complex set of phases can be produced by materials which incorporate chiral centres.

- Blue phases (BP), named because they appeared blue under the microscope when they were discovered.<sup>12</sup>
- Cholesteric phase (Ch), named because the first compounds which showed this phase were derivatives of cholesterol.<sup>1</sup> This phase is now sometimes called a Chiral Nematic ( $N^*$ ).
- Chiral smectic phases ( $S^*$ ).

## 1.4 Discussion of Phases Formed by Non-Chiral Materials.

### 1.4.1 Smectic/Crystal Phases.

If the melting behaviour of a non-chiral liquid crystalline material is considered, the compound will not simply melt from the ordered structure of the solid to the disordered structure of the isotropic liquid. Instead the melting process may proceed *via* several stable intermediate phases.<sup>13</sup> The first possibility is that the molecules may begin to rotate about their long molecular axes, giving rise to quasi-smectic phases having long-range positional order within the layers and also long-range out-of-plane order. The long molecular axes can be arranged orthogonal or tilted with respect to the layer planes. The structure of these mesophases are very similar to that found in solid crystals, in that they display periodic ordering of the molecules. In view of this periodic ordering these mesophases are termed *Soft Crystals* and are denoted by the letters E, J, G, H, K and B(cryst),<sup>14</sup> *i.e.* crystal E phase, crystal J phase *etc.*

In the smectic phase (A, B, C, I and F), the periodic ordering of the molecules is absent but the molecules are still arranged in layers but with only short range positional order. There is no out-of-plane ordering of the molecules and once again the molecules may be tilted or orthogonal with respect to the layer plane. Each of these smectic phases is given a different classification letter to denote a particular local arrangement of molecules. A summary of the different classes of crystal and smectic phases is given in Table 1.1.

Isotropic liquid		
Molecules orthogonal within layers	Molecules tilted within layers	
$S_A$	$S_C$	1-D systems
Hexatic $S_B$	$S_I, S_F$	2-D systems
Crystal B, E	Crystal G, H, J, K	3-D systems
Crystalline solid		

**Table 1.1** A summary of the classification of smectic/crystal phases.<sup>15</sup>

The above summary of smectic phases shows that phases which have the molecules arranged orthogonally with respect to the layer plane can be classed as smectic A ( $S_A$ ) (see Figure 1.5), where there is no order of the molecules within the layers, or hexatic smectic B (hexatic  $S_B$ ), where there is local hexagonal packing within the layers, or crystal B and E phases, where there is periodic ordering of the molecules.

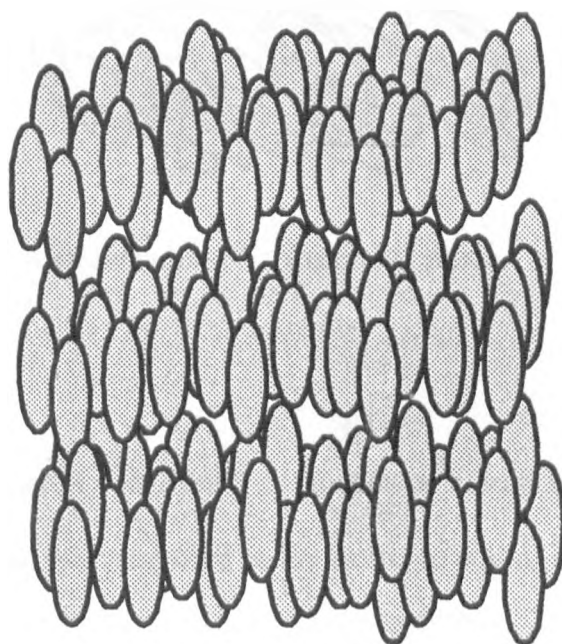


**Figure 1.6** A schematic representation of a smectic A phase.

For smectic phases where the molecules are tilted within the layers there are a number of different types. The structure of the smectic C ( $S_C$ ) phase (see Figure 1.7) is very similar to that of the  $S_A$  phase (see Figure 1.6) except that the molecules are tilted within the layer plane *i.e.* the  $S_C$  phase is a tilted version of the  $S_A$ . Similarly the smectic I ( $S_I$ ) and smectic F ( $S_F$ ) phases are the tilted version of the hexatic  $S_B$  phase. The difference between the  $S_I$  and  $S_F$  phases is that in the  $S_I$  phase, the molecules are tilted towards the corners of the hexagonal net whereas in the  $S_F$  the molecules are tilted towards the faces of the hexagonal net.<sup>16, 17</sup>

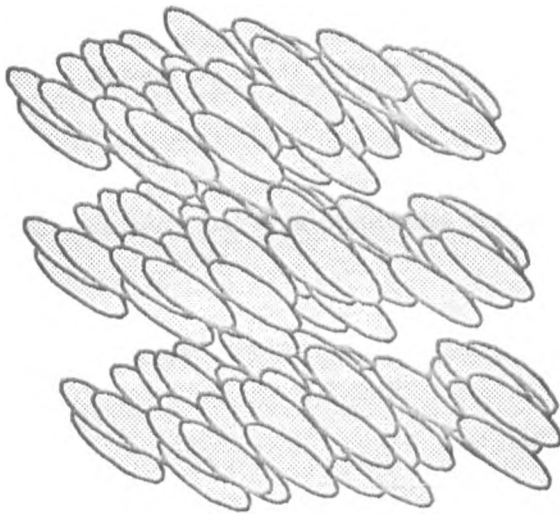
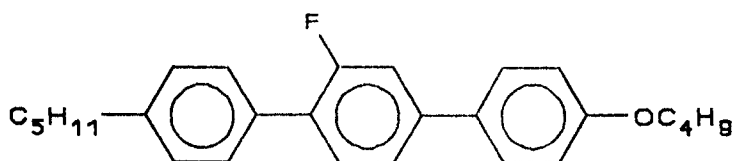
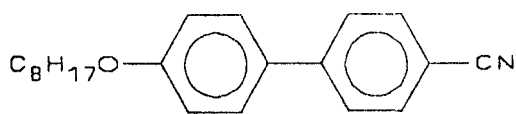


**Figure 1.7** A schematic representation of a smectic C phase.

A liquid crystalline material can exhibit a number of smectic/crystal phases or a nematic phase on heating from the solid to the isotropic liquid.



K 59.5 Cryst.E 85.5  $S_B$  86.5  $S_C$  99.5  $S_A$  144.0 N 176.0 °C I



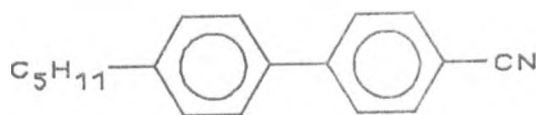
K 54.5  $S_A$  67.0 N 80.0 °C I

**Figure 1.8** Examples of molecules that exhibit smectic and crystal phases.<sup>18, 19</sup>

### 1.4.2 The Nematic Phase.

Another type of mesophase exists in which the long molecular axes of the molecules tend to lie approximately parallel to one another, with no long-range positional or orientational order, this type of mesophase is called the *Nematic Phase*. An example of a molecule that exhibits a nematic phase is shown in Figure 1.9 and a schematic representation of the nematic phase is given in Figure 1.10, the direction of the long molecular axes is given by the *Director* ( $n$ ). Unlike smectic phases there is only one

nematic phase.



K 22.5 N 35.0 °C I

**Figure 1.9** An example of a molecule that exhibits a nematic phase.<sup>8</sup>

Many liquid crystalline materials can exhibit both smectic/crystal and nematic phases see Figure 1.8.

For a more detailed discussion of the different types of liquid crystalline phases, see the review by Leadbetter.<sup>15</sup>

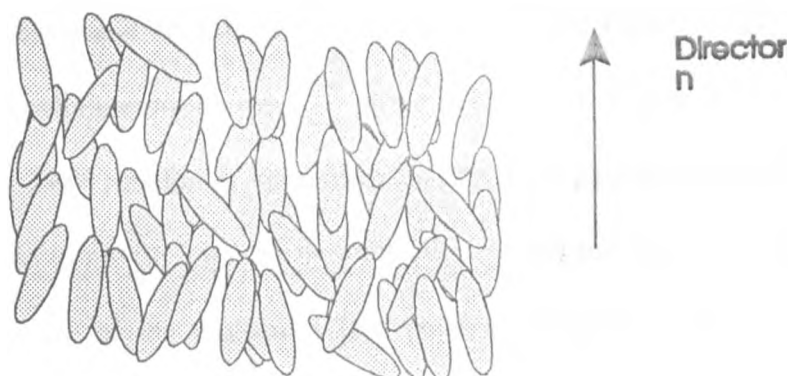


**Figure 1.10** A schematic representation of a nematic phase.

## 1.5 Discussion of Phases Formed by Chiral Liquid Crystalline Materials.

Molecules which possess chirality usually produce liquid crystalline phases which have a helical ordering present throughout the bulk of the material. This is caused by the orientational ordering of the molecules being twisted on passing through the bulk of the material.<sup>20</sup> If the twist of orientational order occurs preferentially in one direction the result is a *Single-Twist* structure. If the helix is formed in more than one direction, a network of helical twists is formed called a *Double-Twist* structure.

### 1.5.1 Chiral Smectic C ( $S_C^*$ ) Phase.

The structure of the  $S_C^*$  phase is very similar to the  $S_C$  phase in that in the  $S_C^*$  phase the molecules (chiral) will still form layers in which the molecules are tilted with respect to the layer plane with no positional order, however a helical twist will now be formed in the  $S_C^*$  phase due to the presence of the chiral centres causing the layers to precess about an axis normal to the layers (see Figure 1.12). An example of a molecule which exhibits the  $S_C^*$  phase is shown in Figure 1.11. The distance required for a  $360^\circ$  rotation of the molecules (the pitch length of the helix) in an  $S_C^*$  phase is related to the tilt angle of the molecules within the layers.<sup>13</sup> Due to the fact that the tilt angle of the molecules is dependent on temperature (the tilt angle  $\theta$  usually increases as the temperature decreases in an  $S_C^*$  phase), the pitch length of the helix is also dependent on temperature. The relationship between tilt angle and temperature is given by

$$\theta(T) = \theta_0(T_C - T)^\alpha$$

where  $T_C$  is the transition temperature;

$T$  is the temperature of the sample;

$\theta_0$  is a constant for the material;

$\alpha$  is an exponent (with a theoretical value of 0.5)

It can be seen that as the temperature is reduced the tilt angle increases, and as a result the helical pitch length is reduced. For  $S_C^*$  phases where the pitch length is in the region of visible light, light will be selectively reflected. As the temperature of the phase is reduced the colour will change from red to blue. This is the inverse of the colours shown on cooling a cholesteric (chiral nematic) phase (see Section 1.5.2). Similar observations can be made for chiral smectic I ( $S_I^*$ ) and smectic F ( $S_F^*$ ) phases.

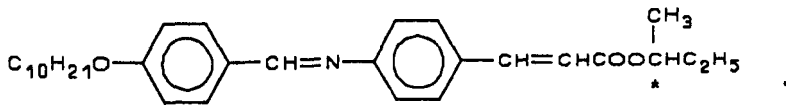


**Figure 1.11** An example of a material that exhibits a chiral smectic C ( $S_C^*$ ) phase.<sup>21</sup>

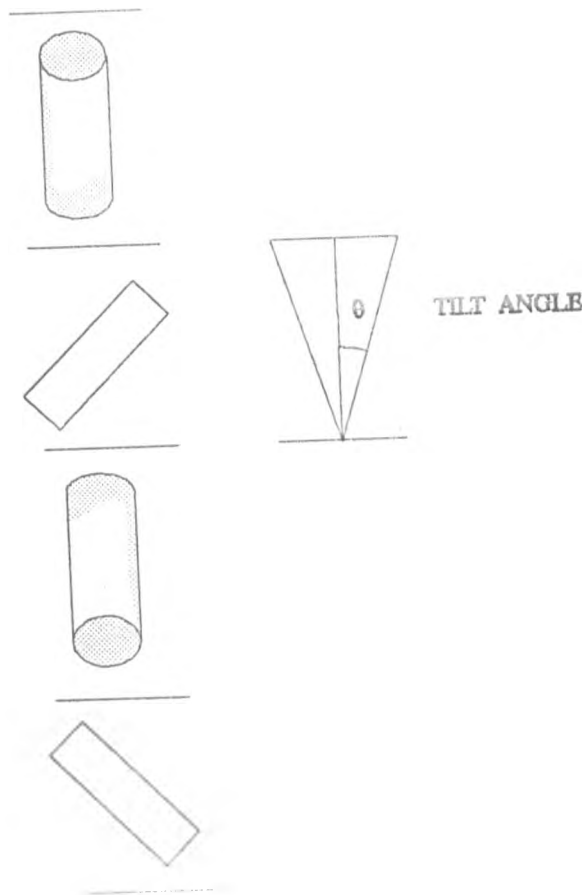
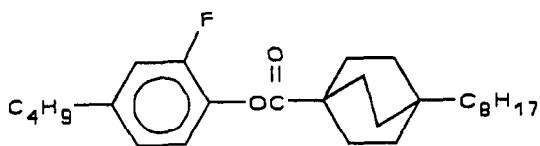


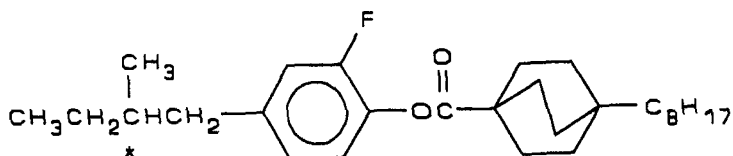
**Figure 1.12** The structure of the chiral smectic C ( $S_C^*$ ) phase.

### 1.5.2 The Cholesteric (Chiral Nematic) Phase.

Molecules that form a cholesteric or chiral nematic ( $N^*$ ) phase are very similar to those which form a nematic phase except that the molecules that form the cholesteric phase possess chirality, see Figure 1.13.



K 10.5 N 44.0 °C I



K 22.0 N\* 29.0 °C I

**Figure 1.13** The relationship between compounds that show nematic and cholesteric phases.<sup>22</sup>

The structure of the cholesteric phase is shown in Figure 1.14. Each cholesteric "slice" in Figure 1.14 is very similar in structure to the nematic phase *i.e.* the molecules are aligned in a preferred direction (the director,  $n$ ). On moving through the cholesteric phase the director rotates giving rise to a macroscopic helix with a single-twist structure. Associated with the helical structure of the cholesteric phase is a parameter called the *Pitch* which governs the light being reflected by the cholesteric phase. If the pitch is in the visible region of the electromagnetic spectrum, then colours can be observed being reflected from this phase. The pitch is sensitive

then colours can be observed being reflected from this phase. The pitch is sensitive to temperature and as the temperature increases, the colour will change from red to blue.<sup>23</sup>

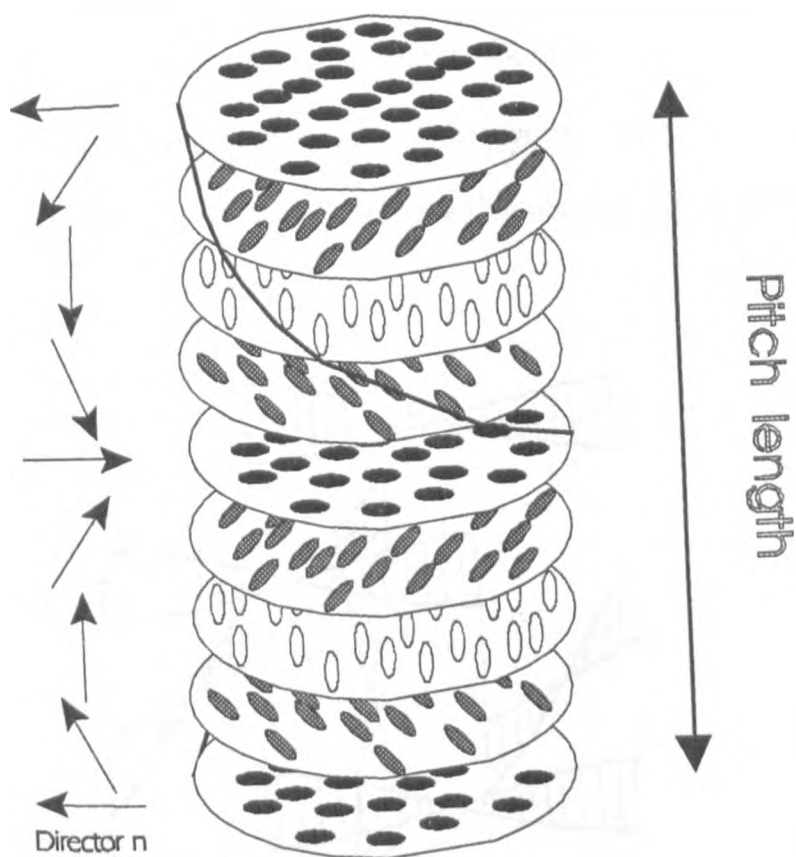


**Figure 1.14** A schematic representation of a cholesteric phase.

### 1.5.3 Blue Phases.

If a helix can be formed from a molecule in two directions *e.g.* perpendicular to the long molecular axis, as in the case of the cholesteric phase, and also parallel to the long molecular axis, then two helices will be formed with their axes perpendicular to

However, the two helices cannot fill space completely and so a two dimensional lattice of defects will be formed (see Figure 1.15). The locations of the defects will be periodic due to the periodicity of the helices. The lattice of defects will extend into three dimensions to give various cubic arrays of defects, which give the necessary structural network required for a range of liquid crystalline phases<sup>20</sup> called *Blue Phases* (BP). Blue phases are very frustrated type of structures which appear after the cholesteric phase but prior to the onset of the isotropic liquid. They have very short temperature ranges and can be best observed by transmission optical microscopy.

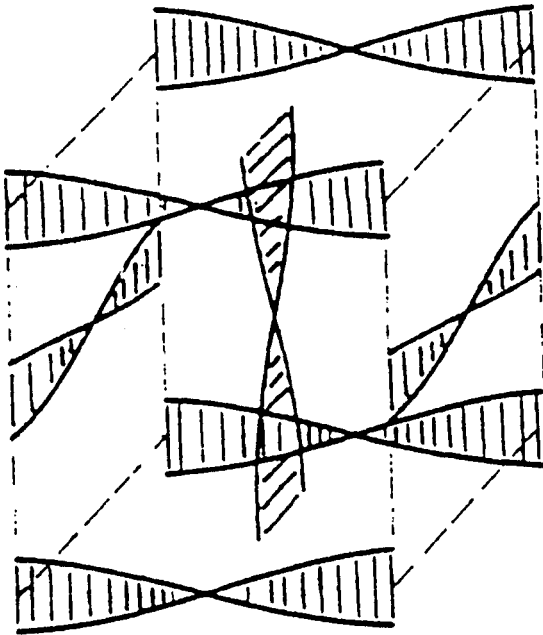


**Figure 1.15** A schematic representation of a cubic blue phase.

### 1.5.4 Smectic A\* Phase.

A new "frustrated smectic phase" has recently been discovered. It was theoretically predicted by Renn and Lubensky<sup>24</sup> to occur in the region of the cholesteric to smectic A phase transition. At this transition the helical ordering of the cholesteric phase gives way to the layered structure of the smectic A phase. Under certain circumstances it is possible that this phase transition can occur *via* an intermediate phase called a *Twist Grain Boundary* phase (TGB). In the TGB phase the molecules try to form a helical structure where the axis of the helix is perpendicular to the long molecular axes of the molecules, but the molecules also try to form a lamellar structure. The two structures are incompatible and cannot coexist without the formation of defects. A lattice of screw dislocations forms which enables a quasi-helical structure to coexist with a layered structure. Small blocks of molecules with S<sub>A</sub>-type structure, separated from each other by screw dislocations, are rotated with respect to each other resulting in a helical structure (see Figure 1.17). The screw dislocations are periodic and form grain boundaries in the phase. The twisted chiral smectic A phase has been found in some esters of "high liquid crystalline chirality", an example is shown in Figure 1.16.

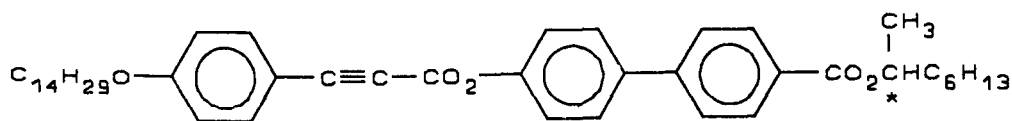
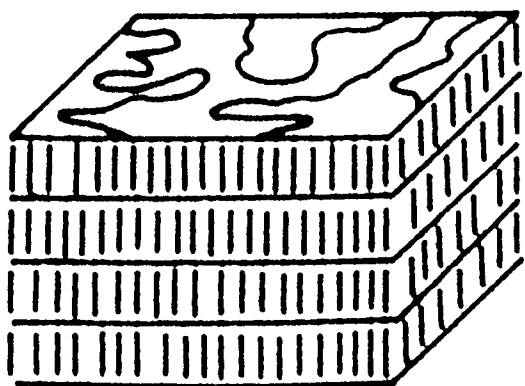
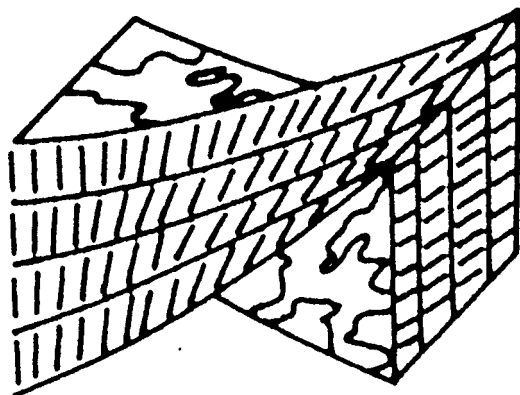


**Figure 1.16** An example of an ester that exhibits a chiral smectic A phase.<sup>25</sup>



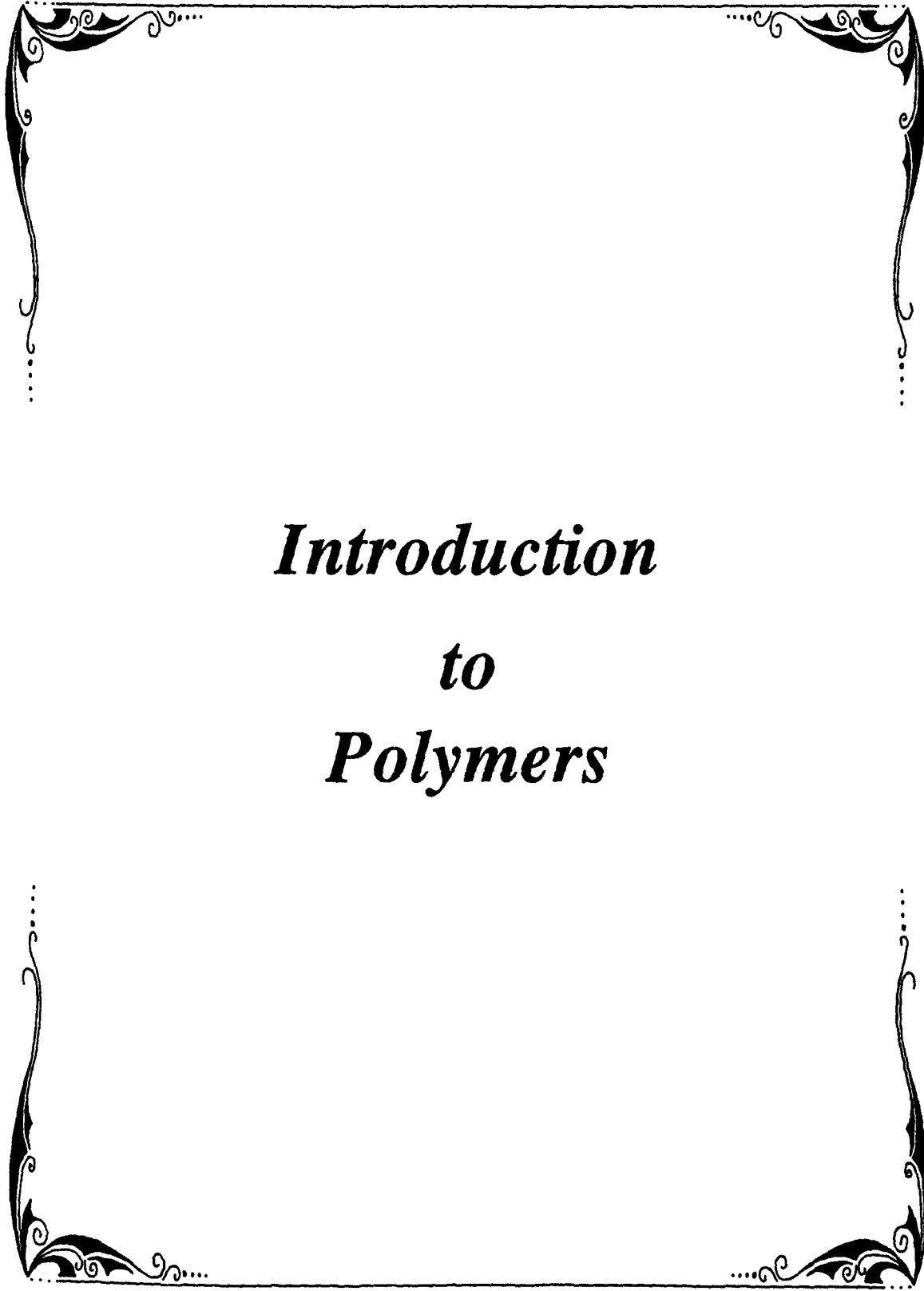


**SMECTIC A  
POLYMER**



**TWISTED A  
POLYMER**

**Figure 1.19** A schematic representation of the structure of a polymeric chiral smectic A phase.



*Introduction*  
*to*  
*Polymers*

## 2. INTRODUCTION TO POLYMERS.

### 2.1 Polymers.

A polymer is defined as a long molecule that contains a chain of repeating monomer units held together by covalent bonds.<sup>28</sup>

In general, polymers are produced by a process known as polymerization in which monomer molecules react together chemically to form either linear chains or a three dimensional network of polymer chains. It is also possible to produce polymers by substituting a preformed polymer backbone with monomer units. Such a process is called a *Polymer-analogous* reaction.

If only one type of monomer unit is employed in the reaction to form a polymer, the resulting species is known as a *Homopolymer*; if two or more different types of monomer are mixed and polymerized, the resulting polymer is called a *Copolymer*. Copolymers are often used to modify the properties of homopolymers because their properties are a combination of the properties of the parent monomers.

### 2.2 Definitions.

The number average molecular mass ( $\bar{M}_n$ ) is defined as the sum of the products of the molar mass of each fraction multiplied by its mole fraction. The number average is

near the peak of the weight - distribution curve (see Figure 2.1) and is the most probable molecular weight<sup>29</sup> of the polymer.

$$\bar{M}_n = \sum X_i M_i$$

where  $X_i$  is the mole fraction of molecules of length  $i$ , and  $M_i$  is the molar mass of molecules which contain  $i$  repeat units.

The weight average molar mass ( $\bar{M}_w$ ) is defined as the sum of the products of the molar mass of each fraction multiplied by its weight fraction.

$$\bar{M}_w = \sum w_i M_i$$

where  $w_i$  is the weight fraction, the mass of molecules of length  $i$  divided by the total mass of all the fractions.

Polydispersity ( $\bar{M}_w/\bar{M}_n = \gamma$ ) gives an indication of the spread of molecular weight distribution of the polymer sample. A monodisperse polymer would have a value  $\gamma = 1.0$ , whereas some types of polymerization lead to a value  $\gamma \approx 2 - 3$ .

One of the most important values associated with polymers is the degree of polymerization ( $\bar{DP}$ ) which gives the number of repeat units of the monomer.

$$\bar{DP} = M/M_0$$

Where  $M$  = the molecular weight of the polymer, *e.g.*  $\bar{M}_n$ , and  $M_0$  is the relative molecular mass of the monomer.

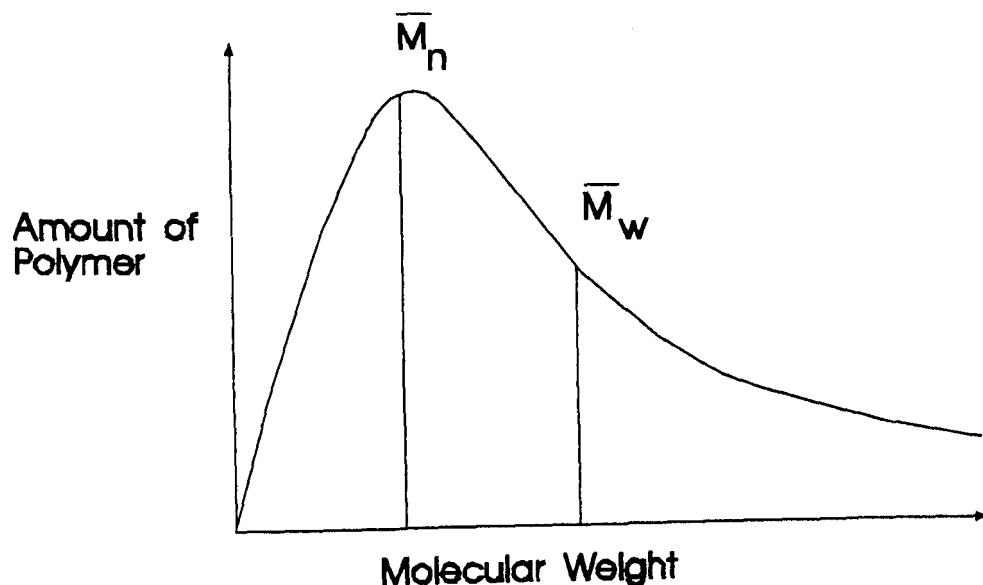


**Figure 2.1** A graph of the distribution of molecular weights of a polymer.

### **2.3 Types of Polymerization.**

There are two major categories of polymerization procedures.

- 1) *Step-Growth Polymerization.*
- 2) *Addition Polymerization.*

#### **2.3.1 Step-Growth Polymerization.**

Step-growth polymerization mainly consists of condensation reactions *i.e.* the reaction between multifunctional organic molecules in which a small molecule, such as water, is eliminated.<sup>30</sup> A good example of a condensation reaction is given in Figure 2.2.



**Figure 2.2** An example of a condensation reaction.

In order for condensation reactions to produce polymers, it is necessary for the monomer species to be able to react at two or more sites *e.g.* a reaction between a dicarboxylic acid and a diol.

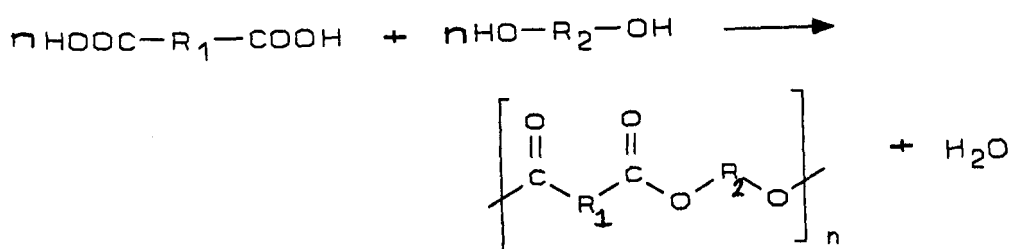


**Figure 2.3** An example of a polycondensation reaction.

The number of sites in a monomer unit which are available to react is the main factor that determines the structure of the final polymer, and is known as the *Functionality* of the monomer. If the monomers have two reactive sites available *i.e.* they are bifunctional, the resulting polymer will be linear. However, if monomers have a functionality greater than two, it is possible that network polymers will be formed.

One disadvantage of condensation reactions is that the polymers which are formed

tend to have low molecular weights due to the reaction being retarded by the presence of the condensate. In cases such as this it is possible to remove the condensate by carrying out the reaction at high temperature and under reduced pressure, in order to improve the degree of polymerization of the final polymer.

Another example of a condensation reaction is the reaction between diamines and dicarboxylic acids to give polyamides (nylons). It is also known for polycondensation reactions not to result in elimination, such as in the production of polyurethanes.<sup>31</sup>

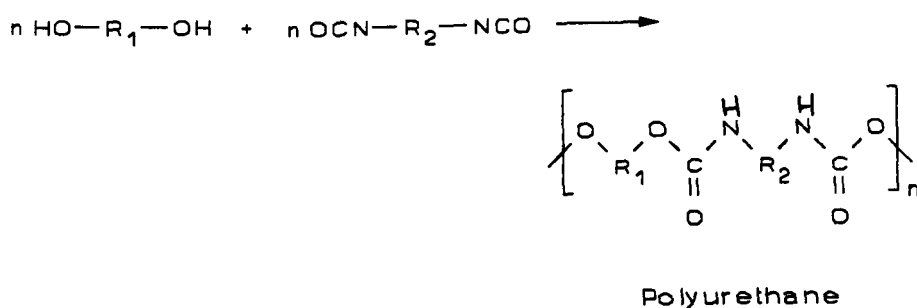


**Figure 2.4** A general example of a reaction that produces polyurethanes.

In some cases an intramolecular condensation may take place, resulting in the formation of a ring structure in preference to a linear polymer, see Figure 2.5. The size of the ring that would be formed is the governing factor of this process; ring sizes of 5, 6 and 7 are particularly stable and in such cases ring structures of this size would be preferred over the formation of a linear polymer chain.

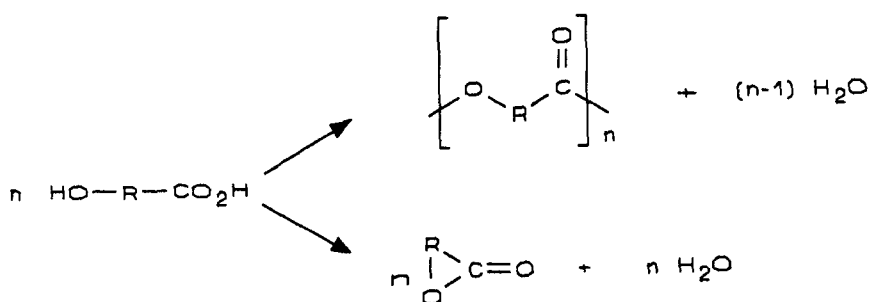


**Figure 2.5** An example of a reaction that can result in a linear polymer or a cyclized monomer.

Condensation reactions rarely give conversions > 98 % and very little high molecular weight polymer is formed. One consequence of this is that the polydispersity of polymers formed by condensation reactions tends to be high, typically in the region of  $\bar{M}_w/\bar{M}_n \approx 2.0$ , thus showing that condensation reactions lead to polymers with a wide distribution of molecular weights. Specialized techniques specific to each monomer system have been developed to try to overcome this problem.<sup>[32 - 35]</sup>

### 2.3.2 Addition Polymerization.

Addition polymerization is the second major type of polymerization.<sup>32</sup> The reaction takes place in three distinct steps; *Initiation*, *Propagation* and *Termination*. The principal mechanism of this type of polymerization is by addition of monomer molecules to a growing chain. Monomers which undergo this type of reaction normally contain a carbon-carbon double bond which is susceptible to attack either by

a free radical or by an anionic initiator to form an active centre. The active centre propagates a growing chain by the addition of monomer molecules, and is eventually neutralized by a termination reaction. The polymerization **only** occurs at the reactive end of a growing chain and this results in long chains being present early on in the reaction, together with unreacted monomer. This is in sharp contrast to step-growth reactions in which *dimers, trimers etc.* are present throughout the course of the reaction.

### **2.3.2.1 Free Radical Initiators.**

Free radicals are species which contain an unpaired electron. These are extremely reactive and will react with monomers containing a carbon-carbon double bond to form an active centre (radical) which is then capable of reacting with further monomer units to give a polymer chain.

### **2.3.2.2 Initiation.**

The radicals formed by the initiator must be stable for a long enough period of time to react with a monomer molecule to form the active centre. The formation of radicals from initiators is normally controlled by the application of an external source such as heat, electromagnetic radiation *etc.* For example, free radicals may be formed by the thermal decomposition of certain peroxides<sup>36</sup> and azo compounds<sup>37</sup>, *e.g.*

benzoyl peroxide (see Figure 2.6).

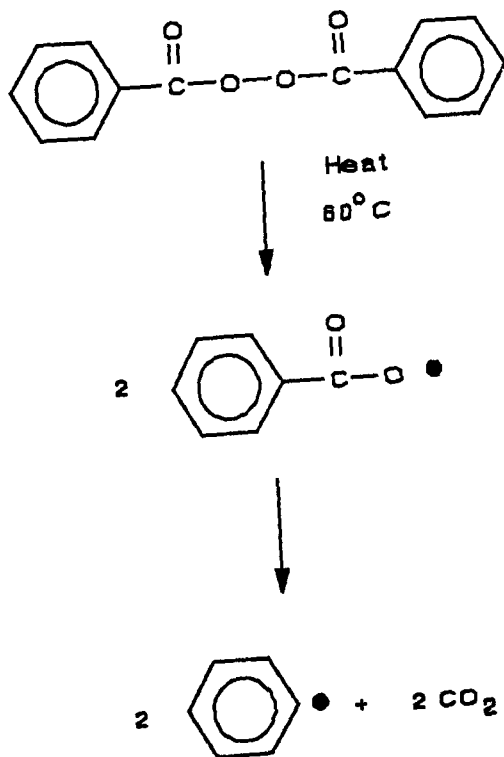


**Figure 2.6** The effect of heat on benzoyl peroxide.

Once formed a radical does not necessarily have to initiate chain growth; if two radicals are unable to diffuse away from each other fast enough, they may recombine. This is due to the confining effect of solvent molecules, the "cage" effect.<sup>38</sup> Other combinations of radical and initiator molecules result in the reduced efficiency of the initiator.

$\alpha,\alpha'$ -Azobisisobutyronitrile (AIBN), a very common source of free radicals, breaks down into cyanopropyl radicals either by the application of heat or ultra-violet radiation (see Figure 2.7).

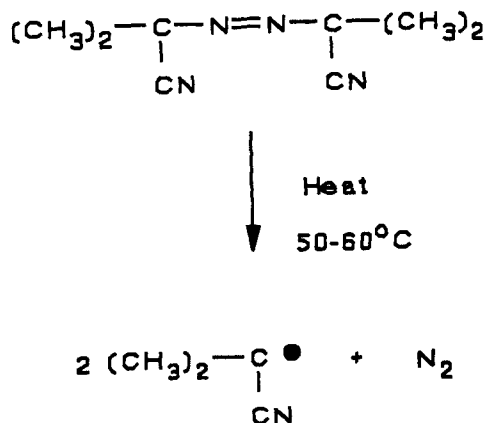


Figure 2.7 The effect of heat on  $\alpha,\alpha'$ -azoisobutyronitrile.

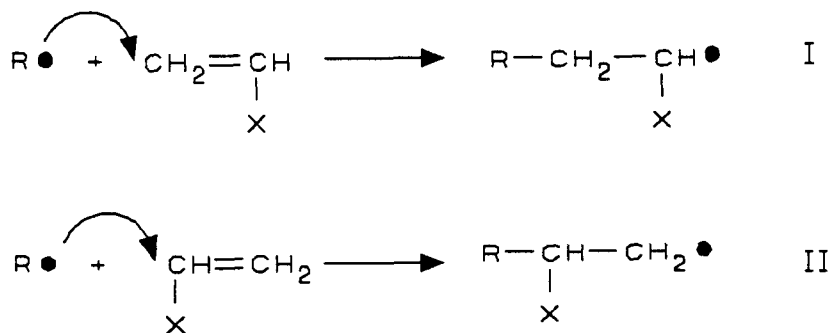
Chemical reactions such as redox reactions may also be used to produce free radicals,<sup>39</sup> and some of these systems are particularly useful when reactions are carried out at low temperatures (see Figure 2.8).



Figure 2.8 A redox reaction that can be used to produce free radicals at low temperatures.

### 2.3.3 Formation of an Active Centre.

The reaction of a monomer molecule with a free radical produces an active centre (see Figure 2.9).



**Figure 2.9** The formation of an active centre.

The amount of the two radicals produced depends on the difference between the activation energies of the two reactions. The activation energy for the formation of the radical with structure II is slightly higher than that for structure I because the X group is usually large and bulky and tends to hinder the approach of the radical  $\dot{\text{R}}$ . Also I is a secondary free radical which is more stable than the primary free radical II. This leads to a greater occurrence of  $\text{R}-\text{CH}_2-\dot{\text{C}}\text{HX}$  radicals.

### 2.3.4 Propagation.

Chain propagation takes place *via* the addition of monomer molecules to the growing

chain. Many monomer additions occur every second and there are two possibilities for the way in which the addition can occur (see Figure 2.10).

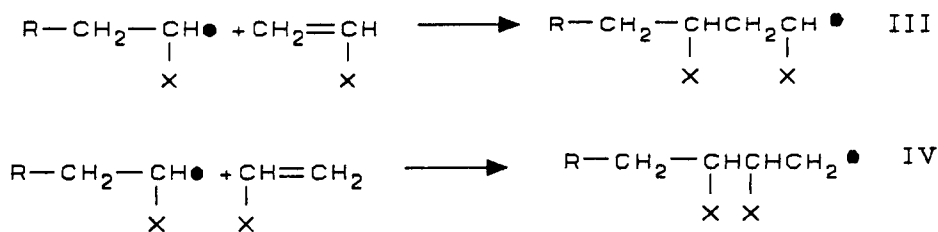


**Figure 2.10** The reaction of a free radical with a monomer unit.

Type III, "head to tail" addition, is favoured mainly due to steric reasons over type IV, "head to head" addition, and results in a polymer chain containing alternating -CH<sub>2</sub>-CHX- groups.<sup>[40 - 42]</sup>

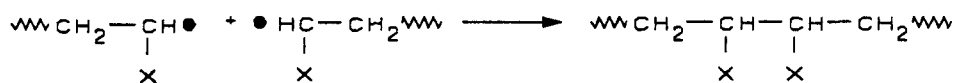
### 2.3.5 Termination.

There are several ways in which the growing chains can be terminated to form covalently bonded molecules (see Figure 2.11).

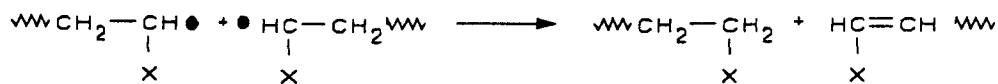
1) *Combination*, in which two growing chains combine in a "head to head" fashion to form a single polymer molecule.

2) *Disproportionation*, in which a hydrogen atom is transferred from one polymer chain to another, to give two polymer chains, one with a saturated end group and the

other with an unsaturated end group.



Combination



Disproportionation

**Figure 2.11** Termination reactions in growing polymer chains.

In most polymer reactions both types of termination processes occur but to different extents, depending upon the system and conditions.<sup>43, 44</sup> Termination can also take place between a growing chain and an unreacted initiator radical (this situation is particularly found when high concentrations of initiator are used). Another process by which chain growth may be halted is chain transfer in which a new active centre is generated and is therefore able to react further (see Figure 2.12).<sup>45</sup>

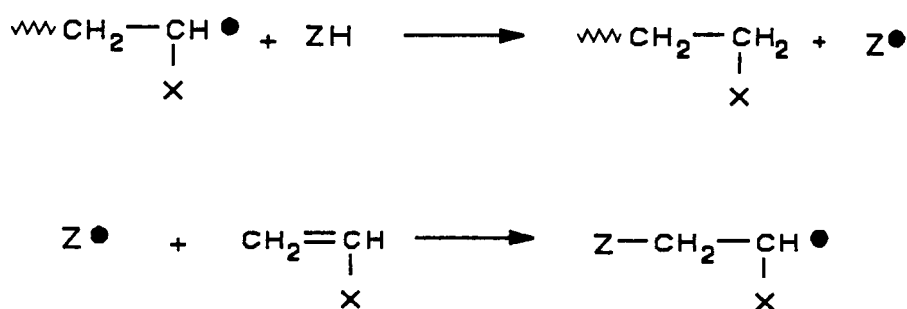


**Figure 2.12** Chain Transfer reaction.

Typical values for the polydispersity of polymers formed by free radical initiated polymerizations are in the region of  $\bar{M}_w/\bar{M}_n \approx 1.5 - 2.0$ . The degree of polymerization in free radical polymerization is proportional to the concentration of the monomer and inversely proportional to the square root of the initiator concentration.

## 2.4 Ionic Polymerization.

This category is divided into two types depending upon whether the polymeric ions are positively or negatively charged. The mechanisms of each reaction are specific to the particular monomer, solvent and initiator system employed. Ionic reactions are often fast and difficult to reproduce. High rates of reaction and degrees of polymerization are possible at low temperatures (typically between  $-20$  and  $-70$  °C). Counter ions are normally involved in the reaction and these can control the

stereochemistry and rate of monomer addition.

Ionic polymerization normally takes place at low temperatures and can offer better control of stereochemistry and polydispersity than free radical polymerization, although reproducibility between batches of polymer is difficult to obtain.

### 2.4.1 Cationic polymerization.

This is the addition of monomer molecules to a positively charged growing chain,<sup>39</sup> [46 - 48] usually initiated by the donation of a proton to a monomer molecule by a strong acid *e.g.* perchloric acid (see Figure 2.13).

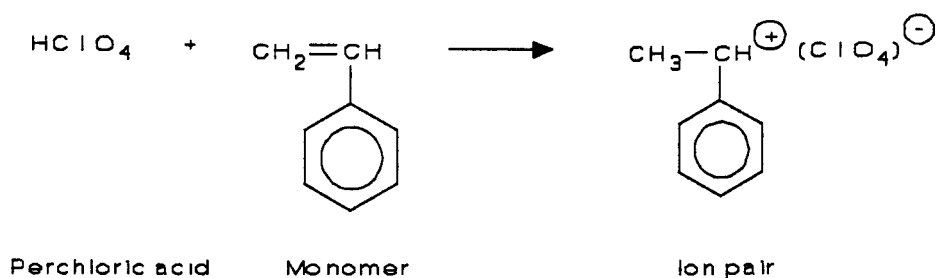


**Figure 2.13** The production of an ion pair by reaction of perchloric acid and a monomer.

The carbonium ion and the perchlorate ion remain closely associated as an ion pair. Other cationic initiators include Lewis acids such as  $\text{BF}_3$  and  $\text{AlCl}_3$ .

Termination occurs by unimolecular rearrangement of the ion pair, or by transfer to

other species in the mixture. The result of this type of polymerization is generally to give short polymer chains. An example of cationic polymerization is shown in Figure 2.14. The results obtained for this type of reaction show that the degree of polymerization and the polydispersity of the resulting polymer are dependent upon the concentrations of reactants that are used.<sup>49</sup> Typical results for such a polymerization are  $\bar{M}_n \approx 6000$ ,  $\bar{M}_w/\bar{M}_n < 1.1$ .

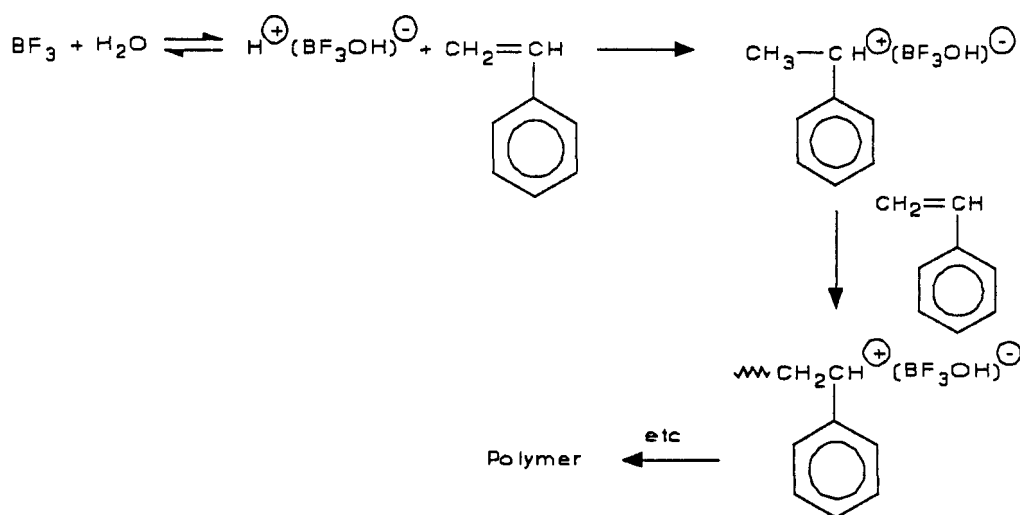


**Figure 2.14** An example of a cationic polymerization.

### 2.4.2 Anionic Polymerization.

Anionic polymerization involves the addition of monomer units to a growing chain containing a negative charge.<sup>50</sup> A monomer containing a strong electronegative charge is essential to stabilise the carbanion (see Figure 2.15).

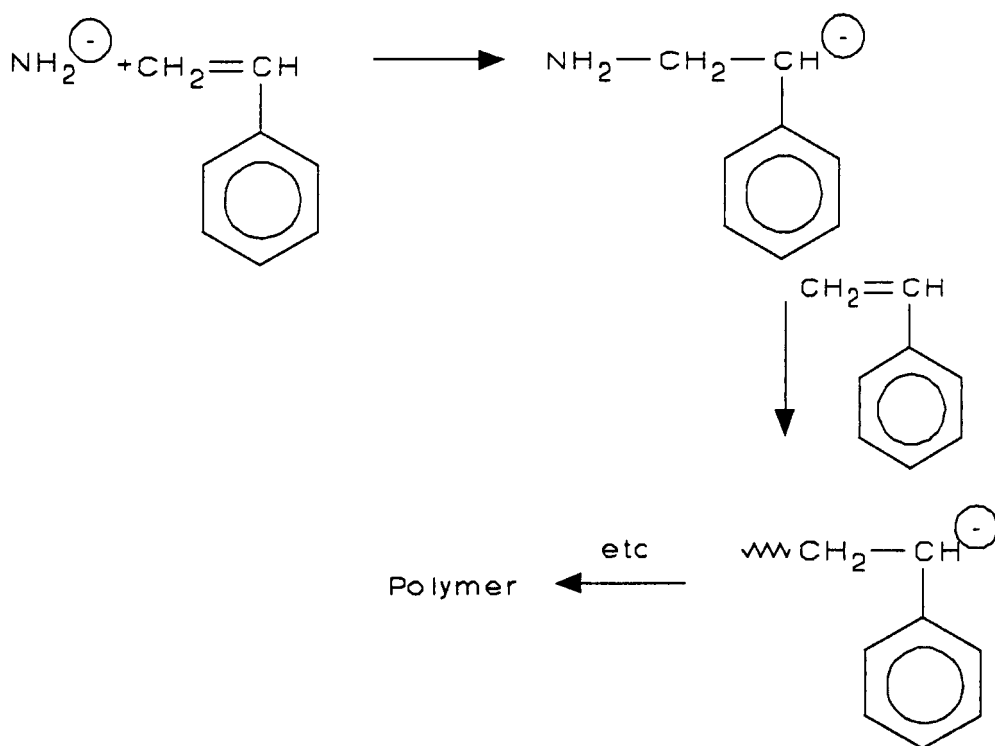


**Figure 2.15** The initiation steps of an anionic polymerization.

Initiation involves the addition of a negatively charged group to the monomer. Propagation takes place *via* the addition of monomer units to active centres, giving rise to "living" polymers,<sup>51, 52</sup> which will only be terminated if impurities are present. In such systems propagation will occur until the supply of the monomer has been exhausted. If a second monomer is now added, propagation will restart until the extra monomer is used. In this way it is possible to produce block copolymers by adding different monomers alternately. The polydispersity of this type of system is typically  $\bar{M}_w/\bar{M}_n \approx 1.3$  (see Figure 2.16).

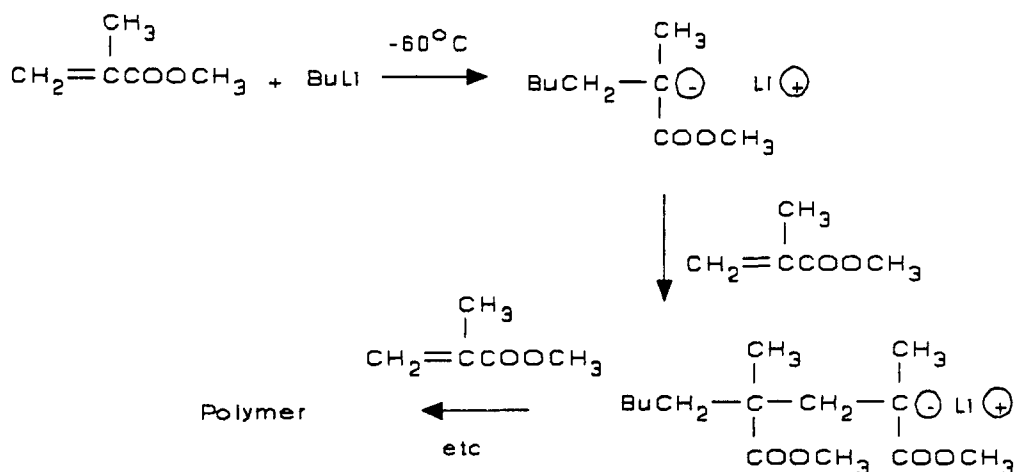


**Figure 2.16** The classical anionic polymerization of methyl methacrylate using butyllithium as initiator.

### 2.4.3 Group Transfer Polymerization.

Group transfer polymerization (GTP) is a modified technique of anionic polymerization, and was developed by Webster and co-workers at DuPont.<sup>51</sup>

The technique involves the polymerization of methacrylic acid esters and other  $\alpha$ -activated olefins using an O-silyl ketene ketal as the initiator in combination with a nucleophilic or electrophilic catalyst (fluorides or Lewis acids respectively).<sup>52</sup> The polymerization is quantitative and gives "living" polymers at room temperature. This is in contrast to classical anionic polymerization which uses hindered alkyl lithium initiators and needs very low temperatures, typically between -20 and -70 °C.

The GTP technique allows control over the degree of polymerization and gives polymers with narrow molecular weight distributions  $\bar{M}_w/\bar{M}_n < 1.3$ .<sup>53</sup>

The proposed mechanism for this reaction is given in Figure 2.17 and involves the activation of the initiator by the fluoride catalyst to form a pentavalent silicon species, which then undergoes a Michael addition to the monomer *via* a hexacoordinated intermediate. The silyl group then migrates to the oxygen of the monomer, forming a new O-silyl ketene ketal which in turn undergoes another Michael addition. It has been shown by labelling experiments that the silyl groups remain attached to the growing chain *i.e.* they do not jump to other chains. The molecular weight of the polymer produced can be controlled by the ratio of monomer to initiator. The "living" polymer produced can either be terminated by the addition of methanol, or polymerized further by the addition of a monomer, which may be the same monomer unit or a different one (block copolymers).

The polymerization of acrylate monomers is more difficult than that of methacrylate monomers because the acrylate monomers contain acidic C-H positions which can undergo deprotonation (metalation).<sup>[54 - 56]</sup>

## 2.4.4 Comparison of Free Radical Polymerization to Group Transfer

### Polymerization.

Free radical polymerization can result in high molecular weight polyacrylates and polymethacrylates with very little control over the molecular weight distribution. In contrast group transfer polymerization produces polymers with molecular weights up to 70,000 with narrow molecular weight distributions  $\bar{M}_w/\bar{M}_n < 1.3$ . The introduction of end groups can be controlled by the termination process of group transfer polymerization, as well as allowing the production of block copolymers by utilising the "living" nature of the polymerization process. Radical polymerization may result in some branching of the polymer backbone, but linear polymer backbones are produced preferentially by group transfer polymerization. It can therefore be seen that group transfer polymerization does offer several advantages over free radical polymerization. However, the GTP technique does have limitations in its application in that, as will be shown later in this thesis, not all monomeric systems can be polymerized by group transfer polymerization.

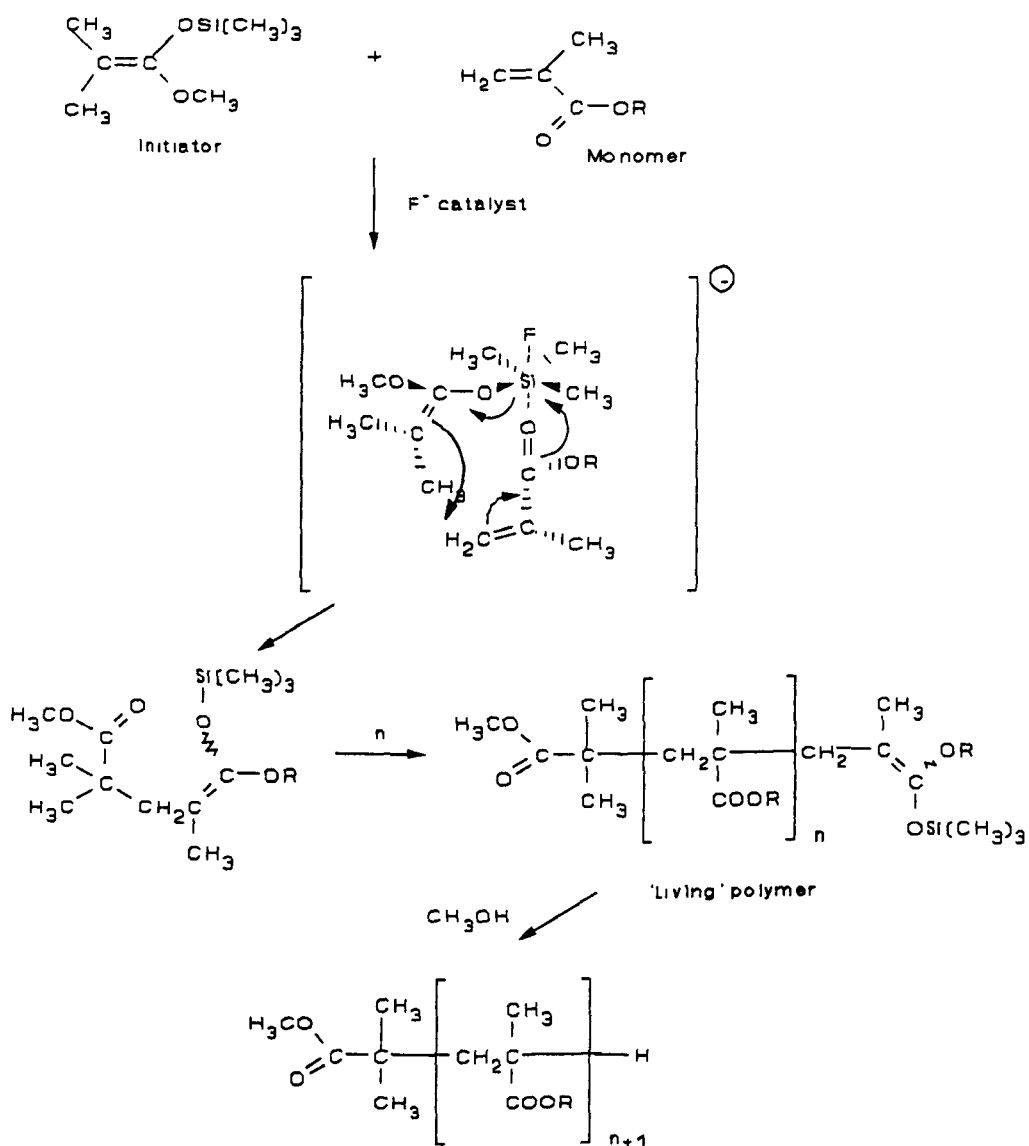
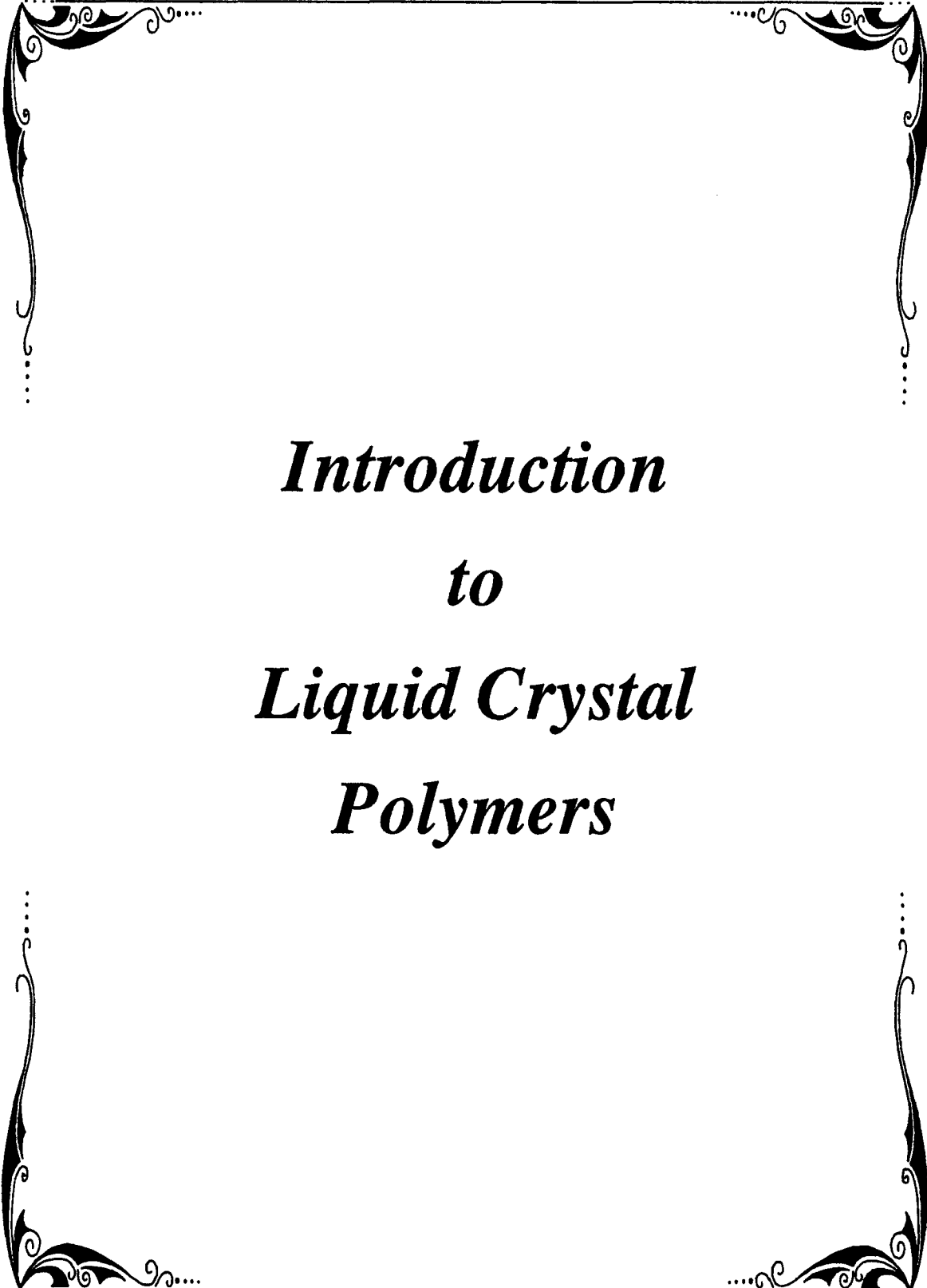


Figure 2.17 The proposed mechanism for group transfer polymerization.<sup>51</sup>



*Introduction*  
*to*  
*Liquid Crystal*  
*Polymers*

### 3. INTRODUCTION TO LIQUID CRYSTAL POLYMERS.

#### 3.1 Introduction.

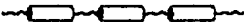
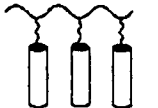
One of the most fascinating features of *Liquid Crystal Polymers* is the possibility of combining liquid crystalline materials, in which the molecules are ordered to give a variety of mesophases, with the random orientation of the polymer backbone. By bringing together liquid crystalline materials and polymers to form liquid crystal polymers, one combines the anisotropic properties of liquid crystalline materials with the rheological and other interesting properties of polymeric materials. These ideas have only been put into practice over the last decade.<sup>57</sup>

There are two obvious ways in which mesogenic moieties can be incorporated into a polymeric system.

- 1) The mesogens are joined in a "head to tail" fashion either directly or by means of a non-mesogenic group, such as a flexible alkyl group, giving rise to *Main Chain Liquid Crystal* (MCLC) polymers.<sup>58</sup>
- 2) The mesogens are joined either directly or by means of a "spacer group" to a polymer backbone giving rise to *Side Chain Liquid Crystal* (SCLC) polymers, in which the mesogenic groups are attached to the polymeric backbone as "pendent groups".<sup>59</sup>

There are two major types of mesogenic groups which can be incorporated into

polymers; amphiphilic and non-amphiphilic. The latter group can be subdivided into calamitic (rod-like mesogens) and discotic (disc-like mesogens). This classification is summarised in Figure 3.1.

	Amphiphilic	Non-amphiphilic	
Monomer		 Calamitic	 Discotic
Main chain polymer			
Side chain polymer		 	

**Figure 3.1** A summary of the different architectures that are possible for liquid crystal polymers.

Examples of all these types of polymer systems have been produced.<sup>60</sup> Since there are such a wide variety of low molar mass mesogens known<sup>61</sup> which can be used as components in conjunction with the wide variety of polymeric backbones, the number of polymeric systems available for study is endless.

The methods of introducing the mesogenic group into the polymer depend upon the type of polymer system required. For polyacrylates and polymethacrylates, the mesogenic unit is synthesized as a monomer unit capable of being polymerized by the methods outlined in Section 5.10. For polysiloxanes, the mesogenic unit is synthesized containing a terminal alkene group which can then be substituted onto a preformed polysiloxane backbone (commercially available from Petrarch) by the use of an appropriate catalyst (see Section 5.10.3). Polyesters can be produced by polycondensation reactions of mesogenic diols and dicarboxylic acids.

### **3.2 Main Chain Liquid Crystal (MCLC) Polymers.**

Main chain liquid crystal polymers were first reported by Robinson<sup>62</sup> in 1958 for a solution of poly- $\gamma$ -benzyl-L-glutamate and other synthetic polypeptides, which gave lyotropic liquid crystalline phases.

#### **3.2.1 Thermotropic MCLC Polymers.**

Thermotropic MCLC polymers were the next class of LC polymers to be examined because of the possibilities that these materials would produce high modulus fibres. Several commercial systems have now been developed by various industrial concerns.<sup>63</sup> Some examples of these systems are given in Figures 3.2 and 3.3.

Eastman Kodak

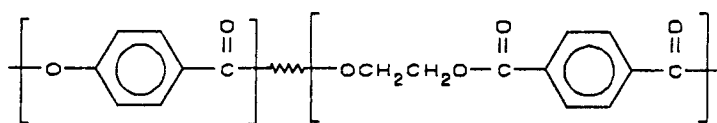
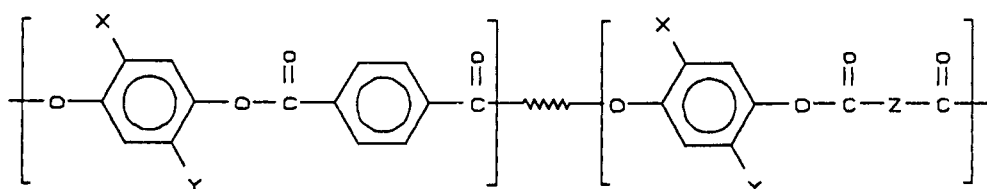


**Figure 3.2** An example of a main chain liquid crystal polymer, produced by Eastman Kodak.<sup>64</sup>

Du Pont



X and Y = -H, -Cl, -Br, -CH<sub>3</sub>

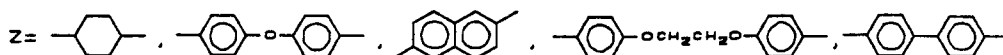


**Figure 3.3** An example of a main chain liquid crystal polymer produced by DuPont.<sup>65</sup>

Main chain liquid crystal polymers are normally produced by stepwise polymerization of bifunctional monomers, to give polyesters or polyamides. One drawback with designing MCLC polymers is that the mesogenic groups must have an elongated, linear structure and this can lead to polymers with extremely high melting temperatures or problems in solubility.<sup>66</sup> In many rigid MCLC polymers, decomposition normally occurs below the melting point of the material, resulting in a non-mesogenic system. For this reason MCLC polymers are synthesized containing

flexible spacer units between the mesogenic groups, to lower the melting point below the decomposition temperature and thus allowing mesophases to be formed. Sometimes it is possible to use solvents, such as concentrated sulphuric acid, to dissolve the MCLC polymer so that the polymer can be easily processed in a lyotropic liquid crystalline phase *e.g.* Kevlar (see Figure 3.4) exhibits a nematic phase when dissolved in concentrated sulphuric acid.

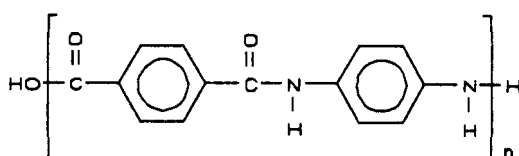
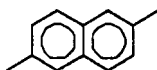


**Figure 3.4** The structure of Kevlar.

There are a number of ways by which the melting point of a MCLC polymer may be lowered.

- 1) Incorporation of lateral chains into the monomer unit, which will act as a lubricant between the rigid polymer chains.<sup>67</sup> Many systems incorporating this type of modification have been prepared using different spacer lengths, different structures for the mesogenic group, and differing amounts of each monomer in a regular or statistically random copolymer system (see Figure 3.5).
- 2) Incorporation of mesogenic groups which will produce kinks in the structure, for example, the structure shown in Figure 3.3 where

Z =



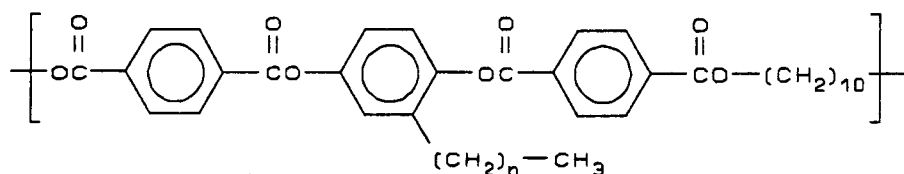


**Figure 3.5** An example of a main chain liquid crystal polymer incorporating different spacer lengths.

### 3.2.2 Phase Behaviour in Main Chain Liquid Crystal (MCLC) Polymers.

The behaviour of liquid crystalline phases found in MCLC polymers is more complicated than that of phases found in low molar mass liquid crystals, due to the fact that all the polymer chains are of different sizes, and hence a polymer has a wide molar mass distribution. Nematic, cholesteric and smectic phases have been found in MCLC polymers.

For rigid-rod polymers, where mesogenic groups are joined directly to form the polymer backbone, the nematic phase exhibited by these polymers may be explained in terms of the statistical arrangement of the centres of gravity of the irregular lengths of the polymer molecules. Following this theory a smectic phase is possible in polymers with regularly repeating monomer units, so that the centres of gravity of the monomer units can become arranged in layers.

For semiflexible polymers incorporating rigid mesogenic units and flexible spacers, the liquid crystalline phase is determined by the distribution of the mesogenic unit within the polymer chain. Short flexible spacers will restrict the movement of the mesogenic moieties and result in the formation of a nematic phase. Longer flexible spacers allow more movement of the mesogenic units and results in the formation of smectic phases. Schematic representations of the nematic and smectic phases formed by polymers with flexible spacer groups are given in Figure 3.6.

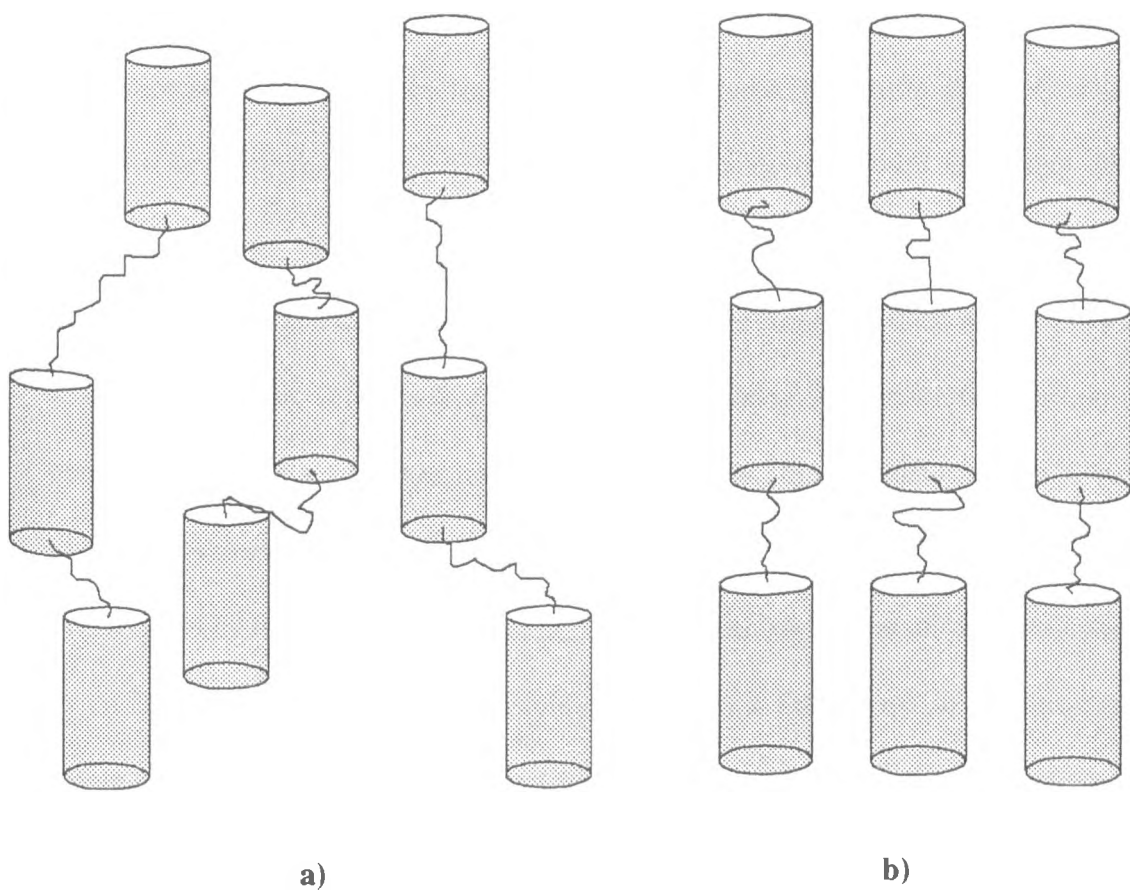


**Figure 3.6** Schematic representations of a) a nematic phase and b) a smectic phase formed by main chain liquid crystal polymers.

The width of the peaks obtained by differential scanning calorimetry (DSC) for phase

transitions exhibited by liquid crystalline polymers are often broader than those obtained for low molar mass materials due to the relatively high polydispersity ( $\bar{M}_w/\bar{M}_n$ ) of the polymeric materials. As a result, biphasic regions are often observed for liquid crystalline polymers in which the mesophase coexists with the isotropic liquid. The transition temperatures that are normally quoted for polymeric liquid crystalline phases are for the temperature of maximum heat flow measured by DSC, ignoring the width of the biphasic region.<sup>68</sup>

The relationship between the width of the biphasic region and the molar mass and polydispersity of the polymer has only been investigated for semiflexible polyesters.<sup>64</sup>

The results show that the biphasic region becomes narrower with increasing degree of polymerization for polydispersities of  $\bar{M}_w/\bar{M}_n = 2.1 - 2.2$ . Semiflexible polymers are easier to characterize than rigid-rod polymers because not only are they soluble in common organic solvents like dichloromethane and tetrahydrofuran (THF), and so can be analyzed by gel permeation chromatography, but their liquid crystal to isotropic phase transitions occur below their decomposition temperatures. The systems investigated by Blumstein<sup>69</sup> show an increase in transition temperatures corresponding to an increase in the degree of polymerization until the degree of polymerization reaches 10, after which point the transition temperatures remain fairly constant.

The length of the flexible spacer group also has an effect on the transition temperature. Increasing the length of the spacer group depresses the transition temperatures and increases the smectic tendencies of the phase.<sup>70, 71</sup>

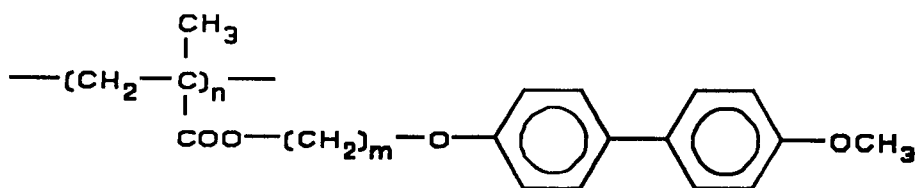
The mechanical properties of main chain polymers are the main reason for the industrial interest shown in these systems. The molecules have macroscopic orientation which improves mechanical properties such as tensile strength, but only along the direction of orientation. The mechanical properties are actually much weaker perpendicular to the orientation direction. It is these properties which facilitates their use as fibres, extrudates and reinforced resins. Liquid crystal main chain polymers can be macroscopically aligned in the nematic phase by flow, or on the application of an electric or magnetic field.

### 3.3 Side Chain Liquid Crystal (SCLC) Polymers.

The synthesis of side chain liquid crystal polymers was first carried out in the 1970's in order to study the kinetics of polymerization of anisotropically ordered molecules, and also the influence of the ordered state on the tacticity of the growing chain. However, many difficulties were encountered due to the inhomogeneity of the reaction mixture.<sup>66</sup>

Direct attachment of mesogenic units to polymer backbones does not generally lead to polymers with liquid crystalline states; instead an amorphous polymer is usually formed. This problem can be overcome by the inclusion of a "flexible spacer" group between the polymer backbone and the mesogenic group.<sup>72, 73</sup> The reason for this is based on a relationship between chemical constitution and liquid crystalline behaviour, similar to that for low molar mass liquid crystals (LMMLC), and can be

explained, in part, by the partial decoupling of the motions between the mesogenic side chain and the chain segments of the polymer backbone. Above the glass transition the polymer backbone adopts a statistically random arrangement but in order for a liquid crystalline state to exist, the flexible spacer must be long enough to allow the mesogenic units to adopt their favoured anisotropic ordering. The fact that no complete decoupling exists has been shown experimentally.<sup>74</sup> Electron spin resonance (ESR) spin probe studies indicate that dynamic coupling of the polymer backbone and mesogenic side chain motions occur *via* the spacer group. <sup>2</sup>H NMR measurements on selectively deuterated polymers have revealed that parts of the spacer group do take part in the anisotropic arrangement of the mesogens.<sup>75</sup> The effect of the flexible spacer group on the liquid crystalline properties of the polymer is shown in Table 3.1. As the length of the flexible spacer group is increased, the clearing point of the polymer decreases and the temperature ranges of the liquid crystalline phases increases.<sup>76</sup>



Spacer length m	Phase transitions / °C	Reference
0	S 255 I	77
2	g 120 N 152 I	78
6	K 119 S 136 I	78
11	g 54 S <sub>C</sub> 87 S <sub>A</sub> 142 I	79

**Table 3.1** A good example of the influence of the length of the flexible spacer group on the phase transitions of polymeric materials demonstrated by poly[ $\omega$ -(4'-methoxybiphenyl-4-oxy)alkyl] methacrylates.<sup>76</sup>

### 3.3.1 Constituents of a Side Chain Liquid Crystal Polymer.

There are many structural features of SCLC polymers which can influence the thermal, physical and rheological properties of these materials. These structural features are as follows:

- 1) the polymer backbone;
- 2) the flexible spacer;
- 3) the mesogenic core;
- 4) the terminal group.

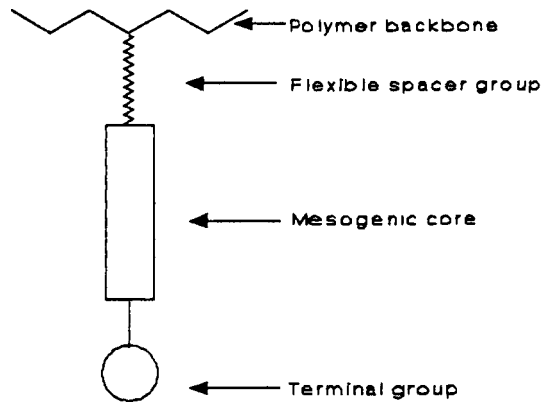


**Figure 3.7** A schematic representation of the main features of a side chain liquid crystal polymer.

### 3.3.2 The Polymer Backbone.

#### 3.3.2.1 Degree of Polymerization.

The polymer backbone has a very large effect on the thermal properties of the SCLC polymers. In particular, the degree of polymerization has a profound effect upon the transition temperatures.<sup>80</sup> The results shown graphically in Figure 3.8, show that there is a very rapid increase in the clearing point as the size of the polymer increases from  $\bar{DP} = 1$  to  $\bar{DP} = 10$ . Beyond this point an increase in  $\bar{DP}$  manifests only a slight

increase in the transition temperatures.

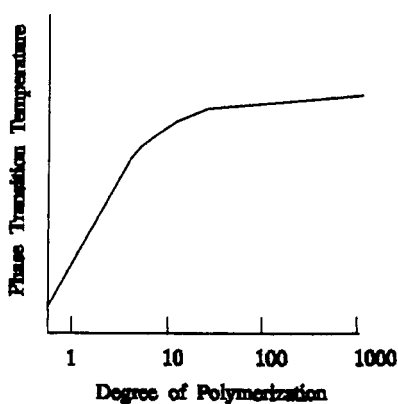


**Figure 3.8** A schematic representation of the variation of phase transition temperatures with degree of polymerization.

One explanation of the above findings is that the increase in degree of polymerization  $\bar{DP}$  creates a denser packing of mesogens which decreases the specific volume at the phase transition. The increase is fastest for low values of  $\bar{DP}$  because the addition of one unit to an existing polymer of say five units has a greater effect than the addition of one unit to a polymer chain containing fifty units. Similar results have been obtained by other groups studying different systems.<sup>81, 82</sup> Another possible explanation of the effect of  $\bar{DP}$  on transition temperatures concerns the terminal end groups of the polymer. A polymer with a low  $\bar{DP}$  has a large number of terminal end groups, which can interact and disrupt the anisotropic nature of the mesogenic groups. A polymer with a larger  $\bar{DP}$  will have less terminal end groups and therefore less disruption of the anisotropy of the system. The conclusion that can be drawn from such results is that the phase transition temperatures of a polymer system will be influenced greatly by its degree of polymerization, meaning that the comparison of the

results found for two polymers will be incomparable unless they have similar or very high values of  $\overline{DP}$ . This is a problem that is encountered widely in the literature, due to the fact that a large amount of data has been published for systems about which no information is given regarding the degree of polymerization or the polydispersity of the polymer backbone. Therefore it can be seen that it is difficult to compare the results found for new polymers with those published by other research groups.

### **3.3.2.2 Polydispersity.**

The polydispersity ( $\overline{M}_w/\overline{M}_n$ ) of a SCLC polymer has a large effect upon the width of phase transition temperatures. In LMM systems the transition temperatures for a particular pure material will be very sharp and reproducible, typically 0.1 °C. However, in polydispersed polymer systems the different lengths of polymer chains, which are characteristic of the polymerization process, give rise to a wide distribution of molecular weights and such systems can be regarded as mixtures of compounds with differing molecular weights. As a result the transition temperatures will not be sharp because short polymer chains will undergo phase transitions at lower temperatures than longer polymer chains. Within the temperature range over which all the chains undergo a transition, two different phases can coexist giving rise to a biphasic region. The phase transition temperature of a polymer is defined as the temperature of maximum heat flow as determined by DSC. The narrower the polydispersity, the smaller the biphasic region will be. Polymerization methods that can produce polymers with narrow polydispersities will therefore be a useful method

of synthesizing SCLC polymers with reproducible and sharp transition temperatures. A major part of the work described in this thesis has been concerned with trying to control the degree of polymerization and polydispersity of SCLC polyacrylates and polymethacrylates.

### 3.3.2.3 Chemical Constitution.

Several different types of polymer backbones have been used for SCLC polymers. The polymer systems which are most common in the field of side chain liquid crystal polymers are polysiloxanes,<sup>83</sup> polyacrylates,<sup>84</sup> polymethacrylates<sup>85</sup> and polyesters.<sup>86</sup> The polymer backbone has a profound effect on the liquid crystalline properties of the polymer due to its stiffness (see Table 3.2). A flexible polymer backbone such as a polysiloxane has a very low glass transition ( $g$  value) ( $\approx -30$  °C), whereas a stiffer backbone, such as a polyacrylate, has a much higher  $g$  value ( $\approx 20$  °C). The polymer backbone also affects the viscosity and rheology of the liquid crystalline phase, and this will be shown later (Section 5.11). The viscosity and rheology of the polymer controls the speed at which liquid crystalline defect textures appear when using polarising light microscopy to characterise the phases exhibited by the polymers. The rotational potential energy of the Si-O bond is low and so conformational changes in the backbone can occur more readily than they can in polymers with hydrocarbon backbones. In general polysiloxanes have lower glass and phase transition temperatures than their corresponding polyacrylates and polymethacrylates, although care must be taken to compare polymers with the same  $\bar{DP}$  and polydispersity.

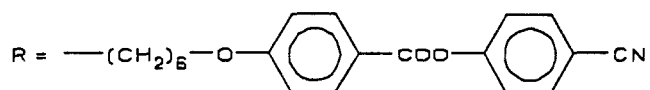
The effects that the polymer backbone can have on the phase transitions of an SCLC polymer are shown in Tables 3.2 and 3.3. Tables 3.2 and 3.3 demonstrate the point that care must be taken when comparing polymers. No data regarding the degree of polymerization or polydispersity is given for any of the polymers. Looking at Table 3.2 there is a decrease in both  $T_g$  transition temperature and phase transition temperature with increasing flexibility of the polymer backbone. Table 3.3 shows the results for a different mesogenic side chain, the results appear to show the reverse of Table 3.2; again no results are given regarding the degree of polymerization or polydispersity of the polymers cited. Another point worth noting is that the trend shown in the isotropization temperature is not shown in the glass transition, this may be an indication that the polymers being compared have greatly differing sizes.

#### **3.3.2.4 Lateral Attachment.**

Another possible variation of the above general structure of a SCLC polymer (Figure 3.7) is that it is not necessary for the mesogenic core to be appended terminally to the polymer backbone *via* the spacer group *i.e.* terminal attachment. As can be seen from Figure 3.9, the attachment of the molecular core may be such that the resulting polymer has mesogenic units appended laterally to the polymer backbone *i.e.* lateral attachment. This means that an extra position is now made available for a further terminal group (groups A and B in Figure 3.9) to be incorporated into the mesogenic core. As a result of lateral attachment, new opportunities are now opened up for altering the thermal and physical properties of the polymer by incorporation of an

$R = \text{---}(\text{CH}_2)_2\text{---O---} \langle \text{benzene ring} \rangle \text{---COO---} \langle \text{benzene ring} \rangle \text{---OCH}_3$	
Polymer backbone	Phase transitions / °C
$\text{---}(\text{CH}_2\text{---}\overset{\text{CH}_3}{\underset{\text{COOR}}{\text{C}}})_n\text{---}$	g 96 N 121 I
$\text{---}(\text{CH}_2\text{---}\overset{\text{H}}{\underset{\text{COOR}}{\text{C}}})_n\text{---}$	g 47 N 77 I
$\text{---}(\text{O---}\overset{\text{CH}_3}{\underset{\text{CH}_2\text{R}}{\text{Si}}})_n\text{---}$	g 15 N 61 I

**Table 3.2** The effect of the polymer backbone on transition temperatures.<sup>87</sup>



Polymer backbone	Phase transitions / °C	Reference
$\text{---}(\text{CH}_2\text{---}\overset{\text{CH}_3}{\underset{\text{COOR}}{\text{C}}})_n\text{---}$	g 55 - 60 N 107 - 110 I	88
$\text{---}(\text{CH}_2\text{---}\overset{\text{H}}{\underset{\text{COOR}}{\text{C}}})_n\text{---}$	g 33 N 133 I	89
$\text{---}(\text{O---}\overset{\text{CH}_3}{\underset{\text{CH}_2\text{R}}{\text{Si}}})_n\text{---}$	g 55 S 185 I	90

**Table 3.3** Influence of the polymer backbone on the phase transitions of polymers.

extra terminal group into the mesogenic core and also by the position of attachment of the mesogenic core with respect to the polymer backbone. Movement of the point of attachment will affect the phase behaviour of the polymers. Lateral attachment decreases the smectic tendency of SCLC polymers to such an extent that SCLC polymers with laterally attached mesogenic cores exhibit either nematic or chiral nematic phases. At present no laterally attached SCLC polymer has exhibited a smectic phase.

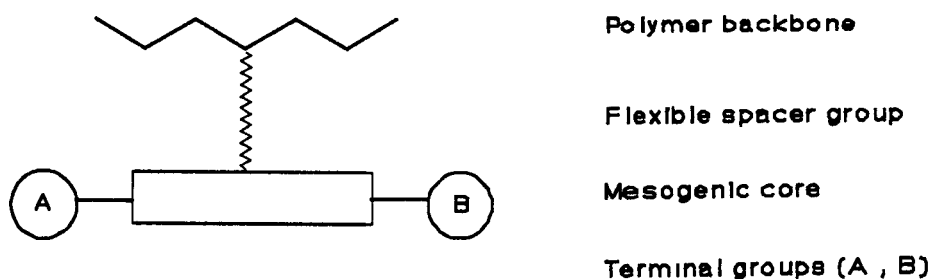


**Figure 3.9** A schematic representation of a laterally attached side chain liquid crystal polymer.

### 3.3.2.5 Linear Polysiloxanes.

Liquid crystalline polysiloxanes can be prepared by a polymer-analogous reaction. The poly(hydrogenmethylsiloxane) (PHMS) backbone can undergo hydrosilylation with a terminal alkenic side chain using an appropriate platinum catalyst. One catalyst for carrying out such a reaction is Speier's catalyst, hexachloroplatinic acid in 2-propanol (see Section 5.10.3.1). The hydrosilylation reaction has been shown to involve Pt-complexes of the alkene and siloxane,<sup>91, 92</sup> as shown in Figure 3.10.

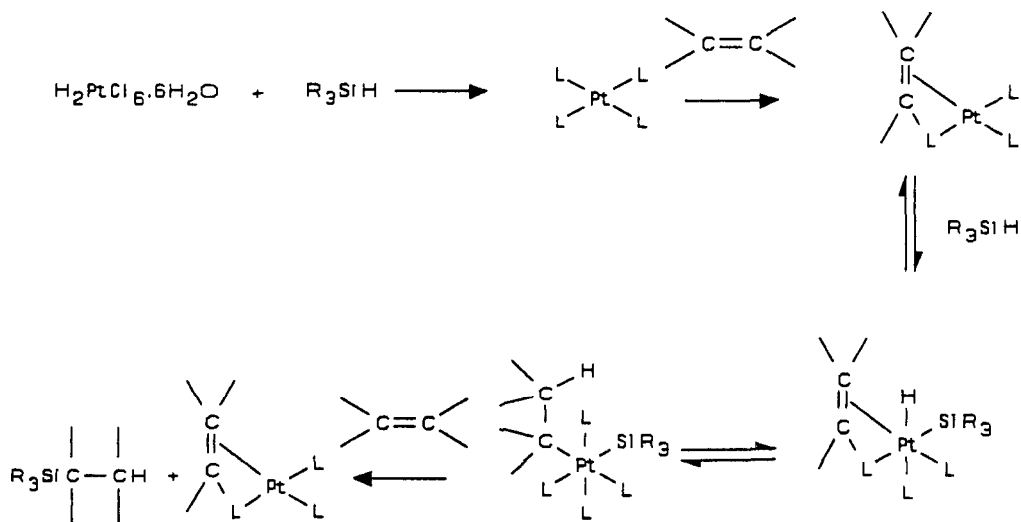


**Figure 3.10** The hydrosilylation reaction.

One restriction of the use of SCLC polysiloxanes is the limited range of PHMS backbones that are commercially available. Since the size of the SCLC polysiloxane can only be altered by using a different size polymer backbone, this type of polymer is entirely dependent upon the commercial availability of a useful size range of PHMS backbones. Even though there are only a few suppliers of PHMS backbones, comparison of SCLC polysiloxanes prepared by different research groups is still very difficult unless comprehensive data is given regarding the degree of polymerization and polydispersity of the polymer backbone.

### 3.3.2.6 Copolymer Linear Polysiloxanes.

The nature of the poly(hydrogenmethylsiloxane) backbone allows for the production of statistically random side chain copolymers to be produced by carrying out the hydrosilylation reaction on a mixture of two or more alkenes, (see Figure 3.11a).

A number of copolymer polysiloxane backbones are commercially available, these copolymer backbones incorporate certain ratios of dimethylsiloxane units into the PHMS backbone, (see Figure 3.11b). Thus the hydrosilylation reaction with a mesogenic alkene results in a polymer containing two differently substituted silicon atoms *i.e.* one silicon atom substituted with two methyl groups, and another silicon atom substituted with one methyl group and one mesogenic group. Once again it should be noted that comparison between different SCLC copolysiloxanes is very difficult due to the different sizes of the homo- and co- polymer backbones. Typical degrees of polymerization for commercially available copolysiloxane backbones are in the range 30 to 100.

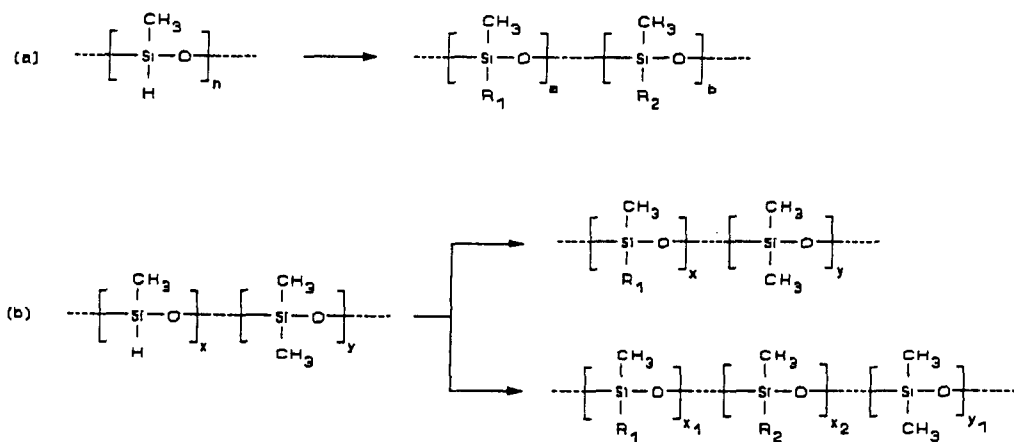
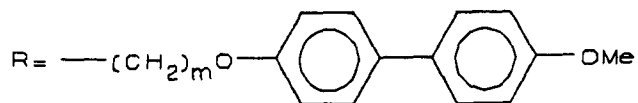
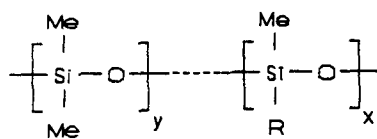


**Figure 3.11** The structures of some commercially available polysiloxane backbones and their analogous SCLC polysiloxanes.

The anisotropic ordering of a liquid crystalline phase can be affected by the flexibility of the polymer backbone.<sup>93, 94</sup> Backbone copolymers have glass and mesophase transition temperatures that are much lower than those for corresponding homopolymers due to the increased flexibility of the backbone.<sup>95, 96, 97</sup> This effect can be clearly seen from the data given in Table 3.4. Also the increase in flexibility of the copolymer backbone produces SCLC copolymers with a consistency of chewing gum, whereas many SCLC homopolymers are hard and brittle, *i.e.* SCLC copolymers have a "softer" rheology. This makes SCLC copolymers easier to handle, and the defect textures exhibited by these polymers are much better defined than those given by homopolymers, and thus means that the identification of the liquid crystalline phases should be much easier for copolymer linear polysiloxanes. The increased flexibility also means that the commercial applications of these copolymers would be much easier than the stiffer homopolymers, *e.g.* it would be much simpler to fill cells and align the samples.



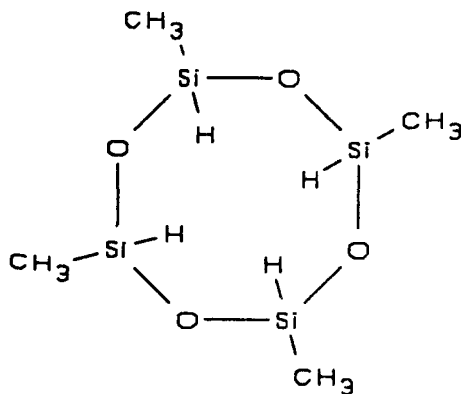
y/x	m	Phase transitions / °C
3/1	3	g -45 I
5/1	3	g -53 I
10/1	3	g -112 I
3/1	5	g -30 S -23 I
5/1	5	g -48 S 6 I
10/1	5	g -114 I
3/1	11	g -31 S 77 I
5/1	11	g -46 S 64 I
10/1	11	g -114 S -16 I

**Table 3.4** The variation of transition temperatures produced by substituting a mesogenic side chain onto different copolymer backbones.<sup>83</sup>

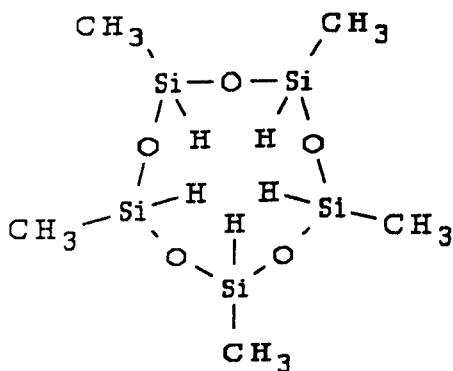
### 3.3.2.7 Cyclic Polysiloxanes.

A novel type of polymer backbone with a known degree of polymerization and narrow polydispersity are cyclic polysiloxanes. The first cyclic liquid crystalline side chain polysiloxanes were synthesized in 1981 by Kreuzer.<sup>98, 99</sup> This type of system consists of a ring structure of Si-O units, each silicon atom has a methyl and a hydrogen substituent, (see Figure 3.12). The hydrogen substituent on the silicon atom can be substituted by an alkene *via* a hydrosilylation reaction (see Section 3.3.2.5).

Due to the nature of these systems each cyclic polysiloxane has a number of isomeric forms. It can be shown that there are 4 isomers for each of the structures shown in Figure 3.12, the isomers are given in Figures 3.13 and 3.14. These isomers have been confirmed by gas chromatographic methods by Semlyen *et al.*<sup>100</sup>



a)



b)

**Figure 3.12** The structures of a) tetramethylcyclotetrasiloxane and b) pentamethylcyclopentasiloxane.

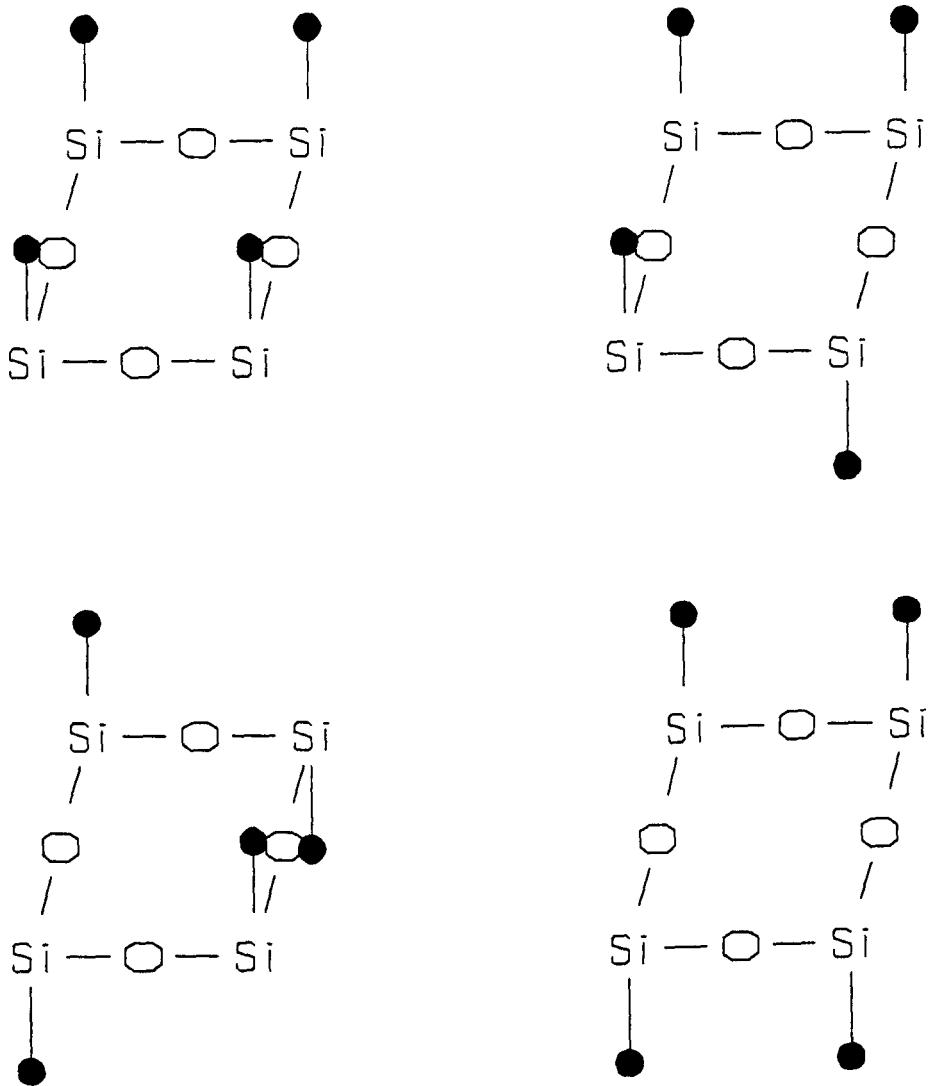


**Figure 3.13** The four isomers of tetramethylcyclotetrasiloxane.

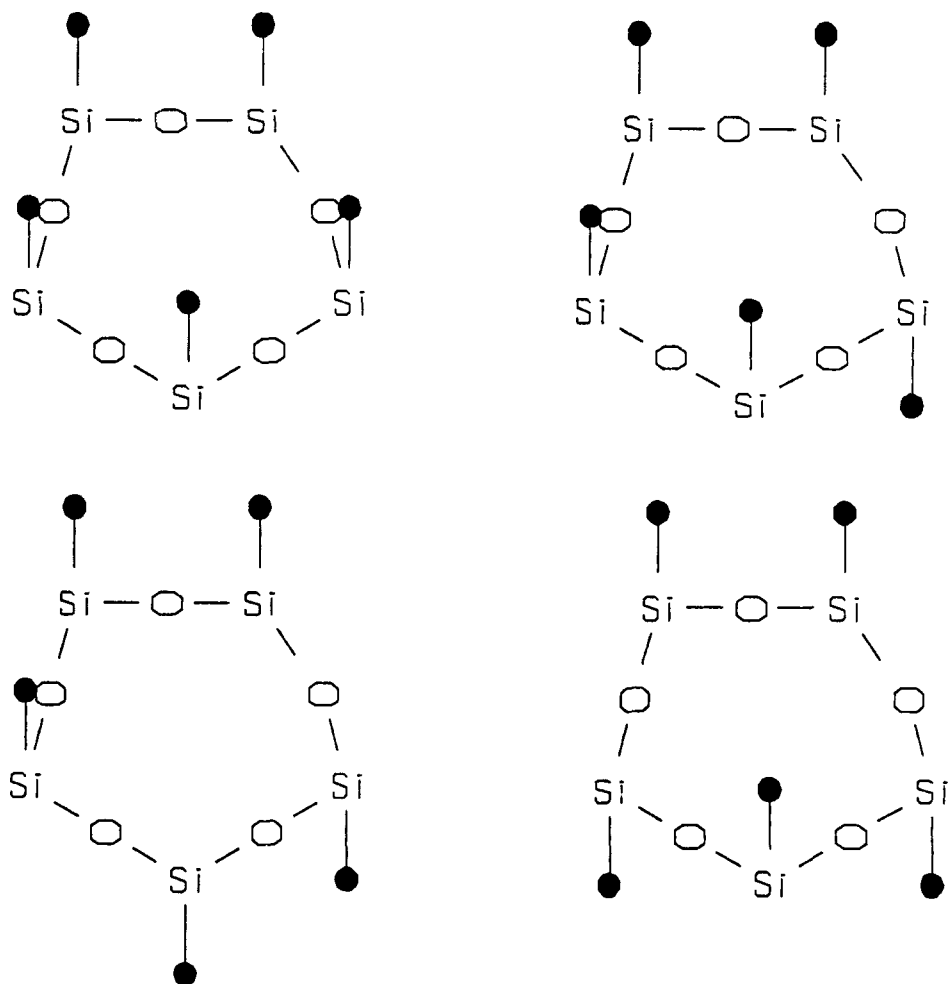


**Figure 3.14** The four isomers of pentamethylcyclopentasiloxane.

Looking at the structures it is possible to think of a SCLC polysiloxane as either a calamitic or a discotic structure. If all the mesogenic substituents were distributed in the equatorial positions the structure would appear discotic (see Figure 3.15a) but if all the mesogenic substituents were distributed in the axial positions a bundle structure would be formed (see Figure 3.15b). The actual arrangement of the mesogenic substituents is probably statistically distributed between axial and equatorial

positions. Most of the liquid crystalline phases exhibited by side chain cyclic polysiloxanes appear to be calamitic liquid crystal phases, however, there do appear to be some specific examples of side chain cyclic polysiloxanes which exhibit phases that seem to be discotic in nature.

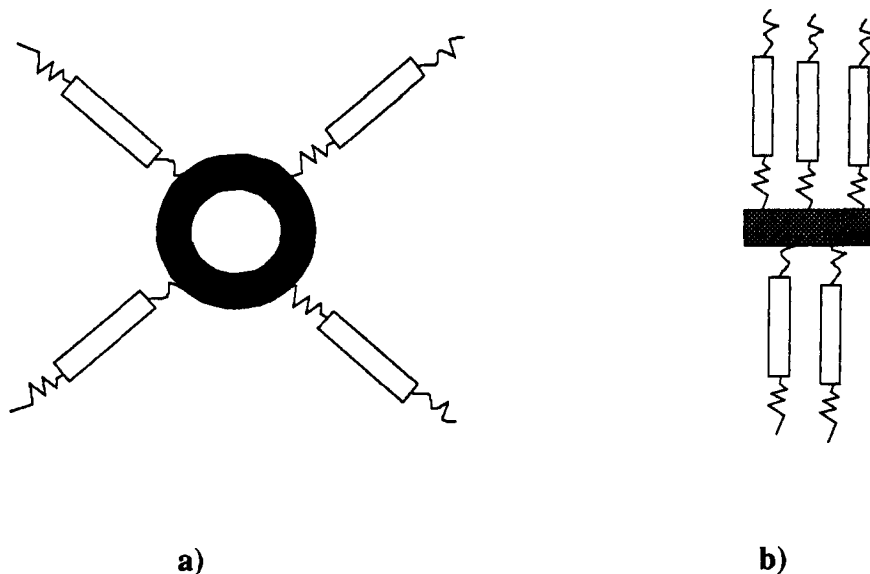


**Figure 3.15** The a) discotic and b) bundle structures for cyclic polysiloxanes.

If a mesogenic side chain is substituted onto a cyclic polysiloxane backbone and onto a linear polysiloxane backbone, the results will show that the liquid crystalline phases produced will probably be the same for each of the different polymer backbones. The temperatures of the phase transitions of cyclic and linear polysiloxanes substituted with the same mesogenic side chain were studied by Richards *et al.*<sup>101</sup> It was found that for polymers with similar numbers of mesogenic substituents on the backbone, the transition temperatures were higher for the cyclic polymers than for the linear polymers (see Figure 3.16). This is due to the absence of terminal end groups in the cyclic polymer, which have the effect of lowering the phase transitions.

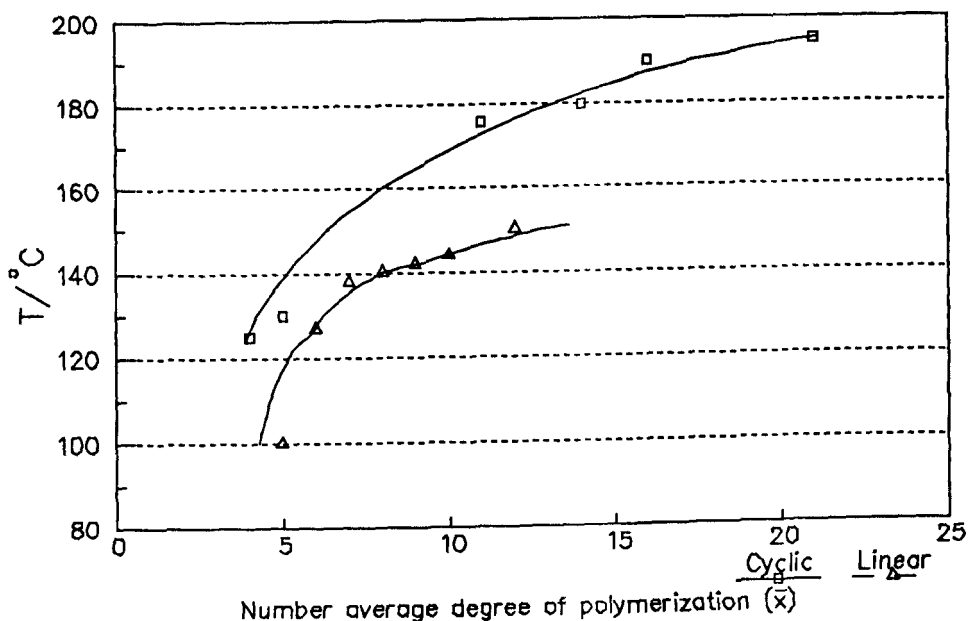
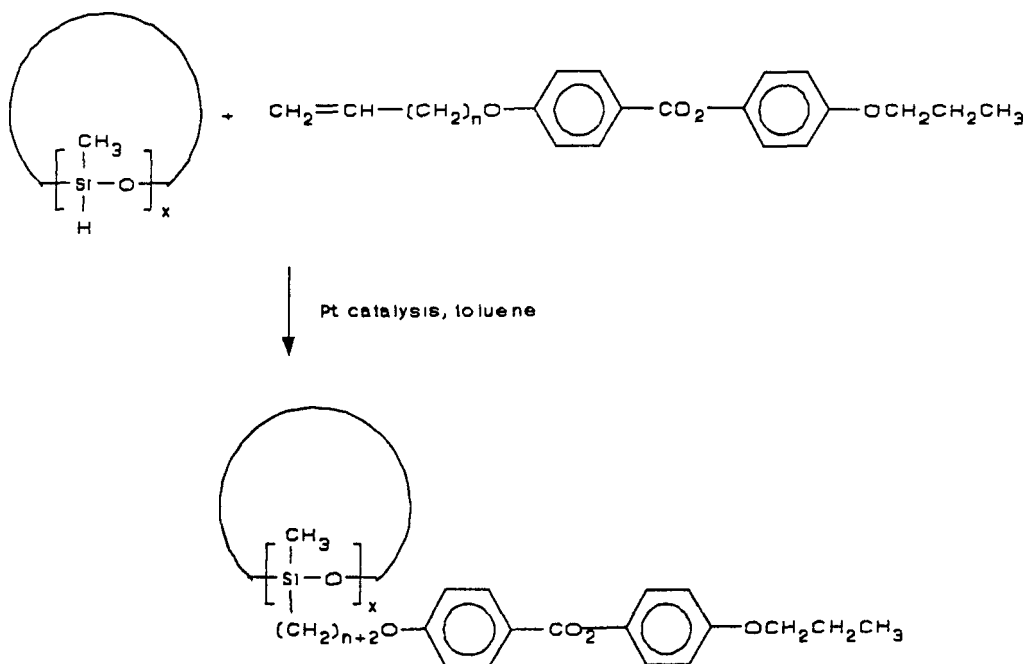


**Figure 3.16** The phase transitions of linear and cyclic polysiloxanes.

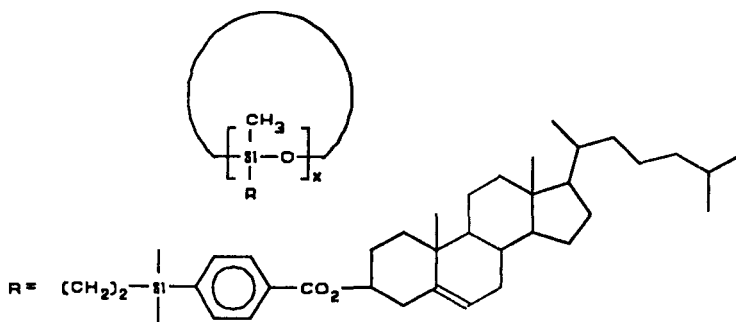
The influence of ring size of the cyclic polysiloxane on phase transition temperatures has also been studied by Kreuzer *et al.*<sup>102</sup> It was found that the transition temperature was not only dependent upon ring size but also on the molecular weight of the attached side chain. For systems with moderate molecular weight side chains (see Figure 3.17), the glass transition temperature  $g$  decreased with increasing size of the siloxane ring, whereas for systems with higher molecular weight side chains (see Figure 3.18), the  $g$  increased with increasing siloxane ring size.



When  $x = 4$  or  $5$ , cyclic polysiloxane backbone is commercially available from Petrarch

n	x	Transition Temperatures / °C
3	4	g 32 N 112 I
3	6	g 30 N 94 I
3	7	g 27 N 89 I

**Figure 3.17** The method of preparing a cyclic polysiloxane with a moderate molecular weight side chain.<sup>102</sup>



x	Transition Temperatures / °C
3	g 63 S <sub>A</sub> 149 I
4	g 67 S <sub>A</sub> 164 I
5	g 80 S <sub>A</sub> 187 I

**Figure 3.18** The structure of a cyclic polysiloxane with a high molecular weight side chain.<sup>102</sup>

The question of whether the liquid crystalline phases produced by cyclic polysiloxanes are calamitic or discotic has been addressed by both Richards and Kreuzer. The results given by Kreuzer<sup>102</sup> show that the phases that are produced are calamitic. Conoscopic observation of the nematic and smectic phases showed that they had positive axiality; discotic phases have negative axiality. The possible arrangement of the structures of cyclic systems in smectic phases is also discussed, and a "bundle" structure in a paired or interdigitated arrangement was proposed (see Figure 3.15b).

### 3.3.2.7 Polymer Architecture.

Synthesising copolymers is a good method for modifying the rheological, thermal and physical properties of SCLC polymers. The incorporation of a variety of components into a liquid crystal system, whether it be low molar mass or polymeric, is often necessary in order to fine-tune the physical properties of the system to meet with the demands of the application. In LMM systems, the "fine-tuning" is achieved by developing mixtures in which the components of the mixture can modify both the thermal and physical properties of the final mixture, *e.g.* to extend the temperature range over which a mixture exhibits liquid crystalline properties. Similar requirements are necessary for SCLC polymers but the situation is more difficult due to the immiscibility of polymers. Copolymers are therefore the only real solution in SCLC polymers in fine-tuning their thermal and physical properties, due to the fact that different homopolymers are not miscible and that many LMM materials are not miscible with polymers. Therefore the obvious solution is to incorporate the different components which control the desired thermal or physical properties of the SCLC polymer onto the same polymer backbone. Control of the amount of each component and its position on the polymer backbone is an important part of SCLC polymer research.

### 3.3.2.8 Mixed Lateral-Terminal Polysiloxanes.

Polysiloxane copolymers containing mesogenic units that are both laterally and terminally attached to the same polymer backbone (see Figure 3.19) have been synthesized by Gray, Hill and Lacey.<sup>96</sup> This was the first time that this type of polymer architecture was used to fine-tune the thermal and physical properties of side chain liquid crystal polysiloxanes. The terminally attached mesogenic side group contained a terminally-positioned cyano-group, which if used as a pendent group in a homopolymer, would certainly produce a SCLC polymer exhibiting a smectic phase. It is therefore extremely difficult to produce a SCLC polymer exhibiting a nematic phase and a positive dielectric anisotropy ( $\Delta E$ ). As mentioned earlier (Section 3.3.2.4) laterally attached mesogenic side groups produce SCLC polymers exhibiting nematic phases, and so what Gray, Hill and Lacey attempted in their study was to modify the properties of the polymer using their lateral-terminal architecture to try to produce SCLC polymers exhibiting a nematic phase and a positive dielectric anisotropy. The structure of the lateral-terminal copolysiloxane used in their study is given in Figure 3.20. From their study they found that the thermal properties of the copolymers depended upon the ratio of the laterally to terminally attached mesogenic side group present in the copolymer. From 0 to 12 % of the lateral substituent present in the copolymer, only a  $S_A$  phase was observed, but when 14 % of the lateral substituent was present a narrow range nematic phase was observed above the  $S_A$  phase. At about 16 - 18 % of the lateral substituent present in the copolymer, the  $S_A$  phase disappeared and the copolymers with a lateral substituent content of greater than 18 % all exhibited a nematic phase only. Thus by modifying the way in which a

mesogenic group is attached to a polymer backbone, SCLC polymers can be made which exhibit a nematic phase and contain a high proportion of a mesogenic side group which incorporates a terminally positioned cyano-group (high  $\Delta E$ ). The transition temperatures of the copolymers remained fairly constant once the lateral component was greater than 30 %.

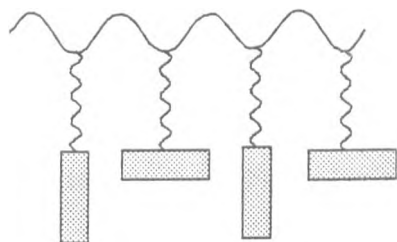


**Figure 3.19** A schematic representation of a polymer with both laterally and terminally appended side chains.

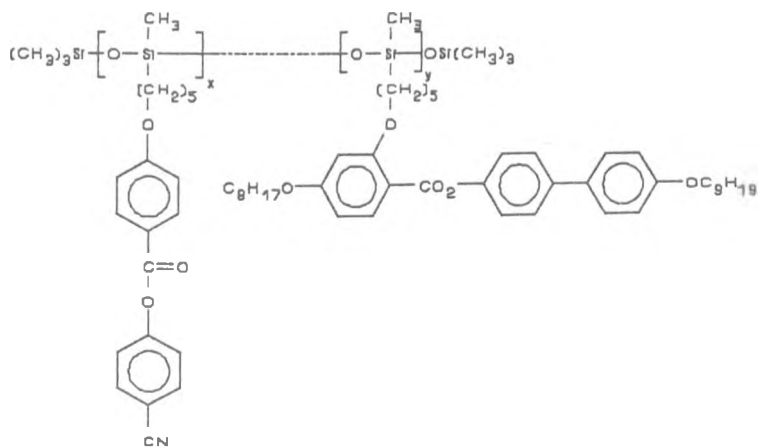


**Figure 3.20** An example of a mixed lateral-terminal copolysiloxane.<sup>103</sup>

In theory it should be possible to achieve similar results for other polymer backbones. However, the question of the amount of each monomer incorporated and the random distribution of the two monomers along the polymer backbone could become important factors in the control of the properties of the SCLC copolymers. Such control could be accessed through the type of method chosen to synthesise the SCLC polymer.

Mesogens can also be incorporated in the polymer backbone itself, as well as in the form of pendent groups (see Figure 3.21).<sup>104</sup> Variations in the polymer backbone can also give rise to systems which are neither linear nor cyclic, for example, star-shaped polymers or cross-shaped polymers (see Tables 3.5 and 3.6).<sup>105</sup>

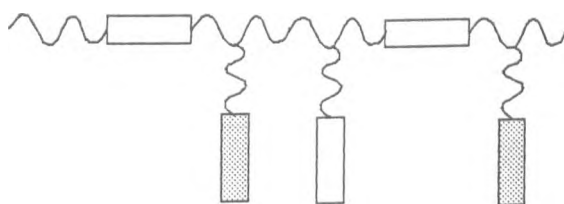
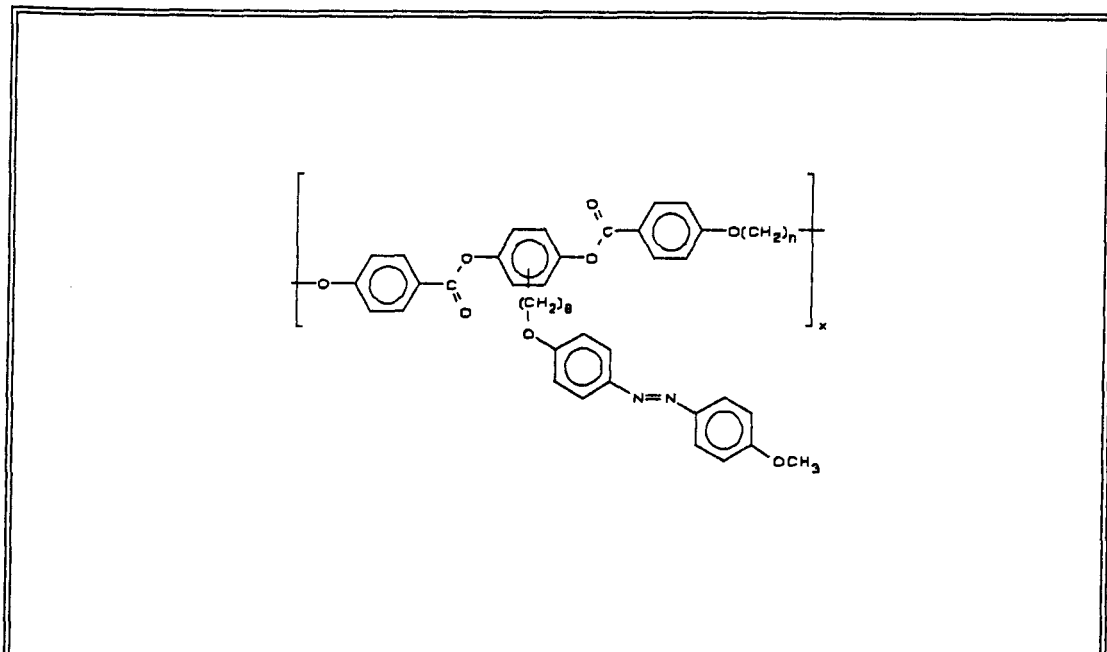
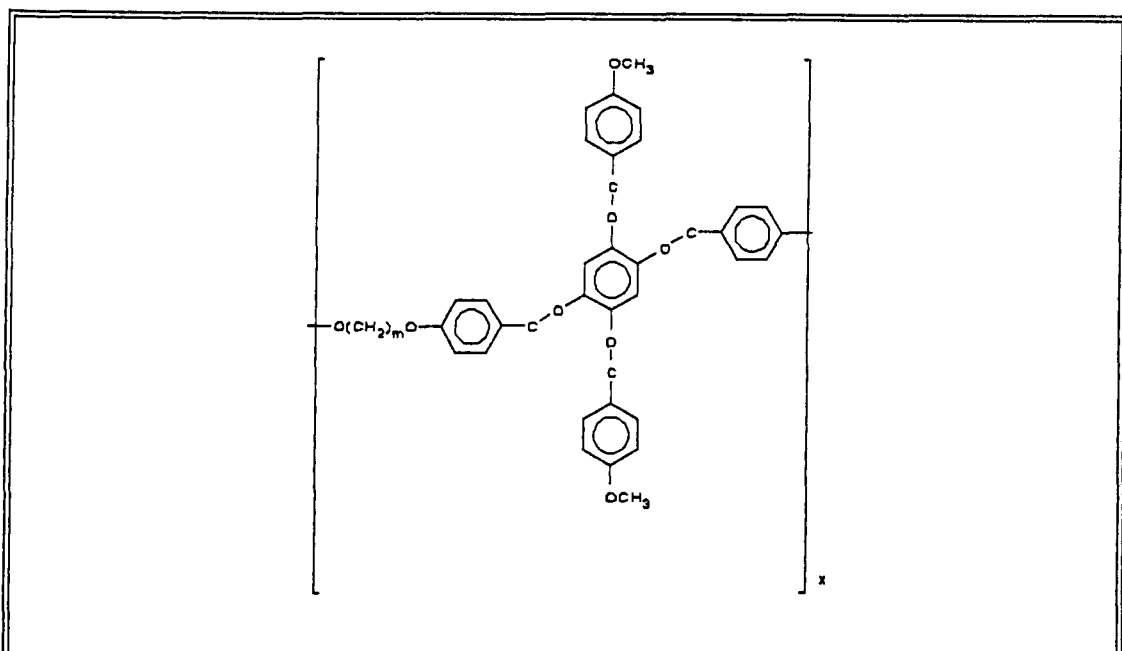


**Figure 3.21** A schematic representation of a polymer containing mesogens in the main and side chains.



n	Phase transitions / °C
9	g 45 N 221 I
6	g 56 N 268 I
2	g 90 N 310 I (dec)

**Table 3.5** Variations in transition temperatures with the length of the spacer group in polymers containing mesogenic units in both the polymer backbone and the side chain.



m	Phase transitions / °C	$\bar{M}_n$
-	g 162 K 186 N 265 I (dec)	-
2	g 203 K 253 N 295 I (dec)	-
6	g 60 N 217 I (dec)	6000
9	g 54 N 214 I (dec)	10000

**Table 3.6** Variations in transition temperature with spacer length for a cross-shaped polymer.

A further method for combining the properties of two mesogens is to attach two mesogenic groups to one polymerizable group *e.g.* an alkene.<sup>106</sup> The forked mesogens produce *en-bloc* polymers (see Table 3.7).

m	x	Phase transitions / °C	Reference
2	2	g 35 K 94 S 98 N 103 I	107
2	6	g 18 S 100 N 113 I	107
6	6	g 4 S 130 I	107

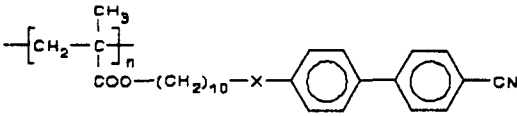
**Table 3.7** The effect of spacer length on the phase transitions of *en-bloc* polymers.

### 3.4 The Flexible Spacer Group.

The flexible spacer group is probably the most important component of a side chain liquid crystal polymer. It allows the statistically random order of the polymer backbone to be partially decoupled from the anisotropically ordered arrangement of the mesogenic units, thus allowing mesophases to be formed.<sup>107</sup> If the flexible spacer group is absent, mesophase formation will be suppressed (see Table 3.9). If the

flexible spacer group is too long crystallisation, an undesirable property of SCLC polymers, will occur.

The chemical constitution of the flexible spacer group is another factor which can influence the properties of the polymer. The flexible spacer group may be alkyl, alkoxy, or even siloxane in nature. It is also possible to change the chemical nature of the anchorage point of the flexible spacer group to the mesogenic core. The effects of changing the nature of the anchorage point on the thermal properties of a SCLC polymer are shown in Table 3.8.<sup>108</sup> Care must be taken when comparing the results given in Table 3.8, since no physical data is given for any of the polymers. The ether linkage and the ester linkage have the same number of atoms in the flexible spacer group and the polymer with the ester linkage has the lower transition temperatures, this is due to the structure being more rigid.

$\left[ \text{CH}_2 - \underset{\text{COO}-(\text{CH}_2)_{10}-\text{X}}{\overset{\text{CH}_3}{\text{C}}} \right]_n$ 	
X	Phase transitions / °C
CH <sub>2</sub> O	g 40 S <sub>A</sub> 121 I
CH <sub>2</sub>	g 30 S <sub>A</sub> 81 I
COO	g 45 S <sub>A</sub> 93 I

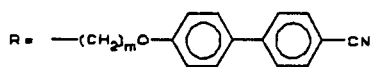
**Table 3.8** The effect of changing the chemical composition of the anchorage point of the flexible spacer group to the mesogenic core.

Table 3.9 gives the phase transitions for a series of SCLC polymers produced using a common 4-cyanobiphenyl based mesogenic side group and a variety of different polymer backbones and flexible spacer group lengths. Once again it must be noted that since no physical data is given for the size of the polymers it is very difficult to compare the results. The polyacrylate and polymethacrylate produced without a flexible spacer group both show extremely high phase transition temperatures, due to the fact that there is no decoupling between the polymer backbone and the mesogenic group. Comparison of polyacrylates and polymethacrylates with the same length flexible spacer groups suggests that the more flexible polyacrylate backbone produces SCLC polymers with higher transition temperatures than the stiffer polymethacrylate

backbone. The much higher phase transition temperatures for the polysiloxanes is probably due to their more flexible backbone. In general there appears to be an increase in phase transition temperature with increasing flexible spacer length, accompanied by a decrease in glass transition temperature and a tendency for the formation of more ordered liquid crystalline phases.

### 3.5 The Mesogenic Core.

The composition of the mesogenic core can be varied as widely in SCLC polymers as it can in LMM liquid crystals. A review of the different types of core structure and their effect on liquid crystalline properties for LMM liquid crystals is given in a review by Toyne.<sup>109</sup> Similar criteria apply to the choice of mesogenic core unit for SCLC polymers. SCLC polymers do not necessarily possess the same phase type as the LMM liquid crystals that they were derived from. For terminally attached SCLC polymers, the stability of the liquid crystalline phase is increased in the polymer with regard to the monomer *i.e.* an increase in transition temperatures is observed, and the monomer may exhibit a nematic phase whereas the corresponding SCLC polymer exhibits a smectic phase. For laterally attached SCLC polymers the reverse is true, *i.e.* monomers exhibiting smectic phases always produce SCLC polymers exhibiting a nematic phase. Most work carried out so far on liquid crystal polymers seems to involve mesogenic core units containing aromatic rings, probably because such SCLC polymers have good phase stabilities and are relatively easy to prepare.



Polymer	m	R'	Phase transitions / °C	Reference
$\text{---}(\text{CH}_2)_m\text{---} \begin{array}{c}   \\ \text{R}' \\   \\ \text{COOR} \end{array}$	0	CH <sub>3</sub>	S 240 I	110
	0	H	S 270 I	110
	2	CH <sub>3</sub>	g 95 I	111, 84
	2	H	g 50 N 112 I	111, 84
	2	H	g 84 K 114 I	113
	3	H	g 54 S <sub>A</sub> 82 I	113
	4	H	g 42 N 229 I	113
	5	CH <sub>3</sub>	g 60 S <sub>A</sub> 120 I	111, 84
	5	H	g 35 S <sub>A</sub> 120 N 124 I	113
	6	CH <sub>3</sub>	g 55 S 100 I	114
	6	H	g 32 N 80 S <sub>A</sub> 124 N 132 I	115
	6	H	g 32 N 80 S <sub>A</sub> 124 N 132 I	113
	11	CH <sub>3</sub>	g 40 S <sub>A</sub> 121 I	111, 84
11	H	g 25 S <sub>C</sub> 30 S <sub>A</sub> 145 I	116	
$\text{---}[\text{O---} \begin{array}{c}   \\ \text{CH}_3 \\   \\ \text{R} \end{array}]_n\text{---}$	3		g 32 S <sub>A</sub> 152 I	89
	3		g 32 S 117 I	117
	4		g 28 S <sub>A</sub> 132 I	89
	5		g 14 S <sub>A</sub> 170 I	89
	5		g 16 S 152 I	117
	6		g 14 S <sub>A</sub> 166 I	89
	11		g -1 S <sub>C</sub> 48 S <sub>A</sub> 157 I	118, 119

**Table 3.9** Influence of the length of the spacer group and the nature of the polymer backbone on the phase transitions of polymers containing 4-cyanobiphenyl based mesogenic groups.

At present structure/property correlations have not extensively been carried out on a large number of SCLC polymers, although work of this type is beginning to be carried out. A study of the effects of varying the core ring system in liquid crystal polysiloxanes was made by Gray, Hill and Lacey.<sup>120</sup> The system that was studied was based on the alkene structure shown in Figure 3.22. The different alkenes were substituted onto a poly(hydrogenmethylsiloxane) backbone (Wacker) which had a  $\bar{DP} = 46 \pm 3$ , and a  $\bar{M}_w/\bar{M}_n = 2.2$ .

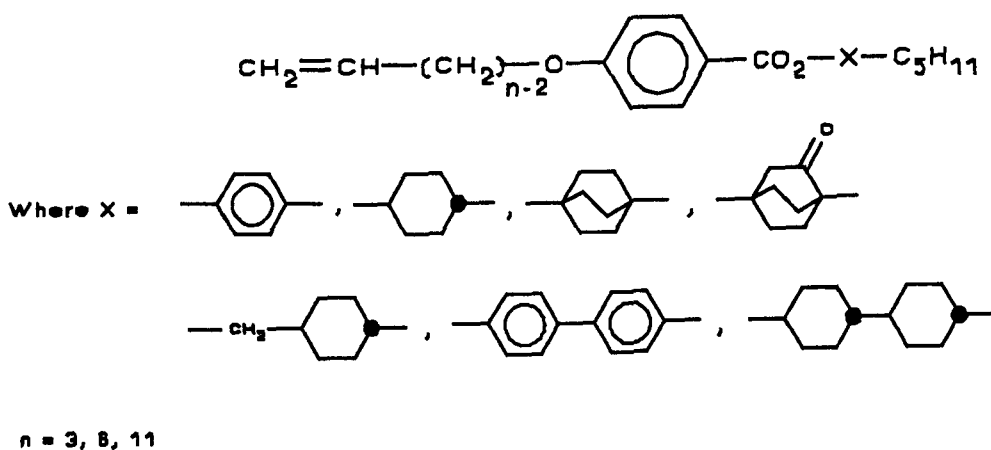


**Figure 3.22** The variety of mesogenic cores that were examined by Gray, Hill and Lacey.<sup>120</sup>

The results from this study are summarised as follows.

- 1) The transition temperatures of the SCLC polymers increase as the length of the spacer group increases.
- 2) The trends of both melting and clearing points show odd-even effects.
- 3) Side chain crystallization occurs in polymers with long spacer lengths.
- 4) The nematic tendency decreases and the smectic tendency increases with increasing length of the spacer group.

5) The efficiency of the ring system X in promoting liquid crystalline properties is shown by the series below.

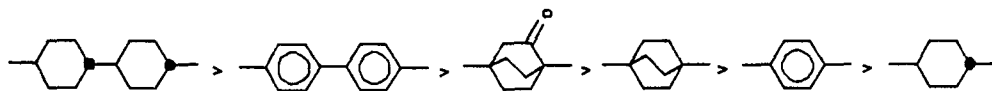


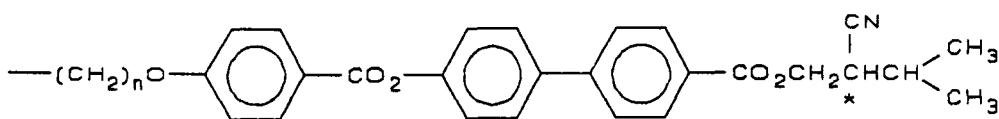
**Figure 3.23** The efficiency of the ring system X in promoting liquid crystal properties.

These results confirm that the trends that were found for SCLC polymers were the same as would be expected by considering the side chains as LMM liquid crystalline materials. This suggests that it may be possible to predict the properties of new SCLC polymers from the mesogenic character of their side chains.

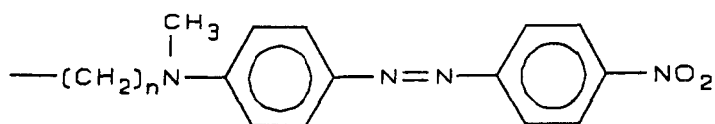
### 3.6 The Terminal Group.

As with the mesogenic core the varieties of terminal groups that can be used in SCLC polymers are almost endless and the choice is usually made from known terminal groups used in LMM liquid crystalline materials according to the effects that they produced in such systems. The effects of incorporating different terminal groups are shown in the review by Toyne<sup>109</sup> and other such reviews of structure/property correlations in LMM liquid crystalline materials. The choice of the terminal group depends on the type of mesophase that is required for a particular application. For example if the SCLC polymer was going to be used in a ferroelectric display device, then the mesogenic side group would have a structure similar to the structure shown

in Figure 3.24a. However if the SCLC polymer was being designed for use in a nonlinear optic device, then the structure shown in Figure 3.24b would be more appropriate. The terminal group is the easiest part of the molecule to change, in order to produce a particular physical/thermal property.



a)

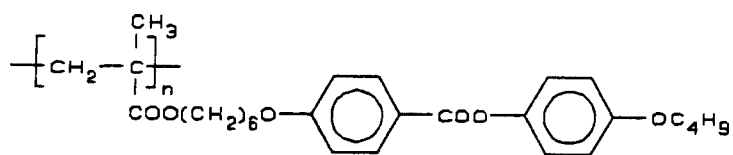


b)

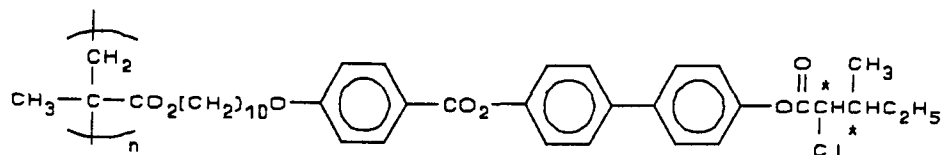
**Figure 3.24** Typical mesogenic side groups for a) ferroelectric, b) nonlinear optic applications.

### 3.7 Summary.

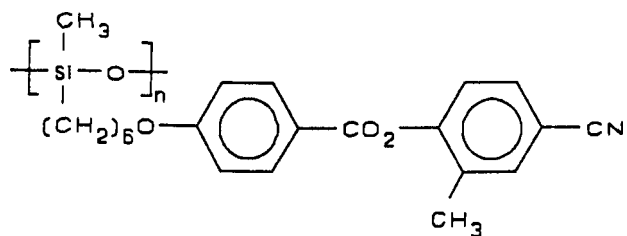
When all the preceding factors are considered the scope for "molecular engineering" in SCLC polymers is vast. The choice of each component will almost certainly be led by the properties required from the material for a particular application. Some typical examples of SCLC polymers and their phase types are given overleaf.



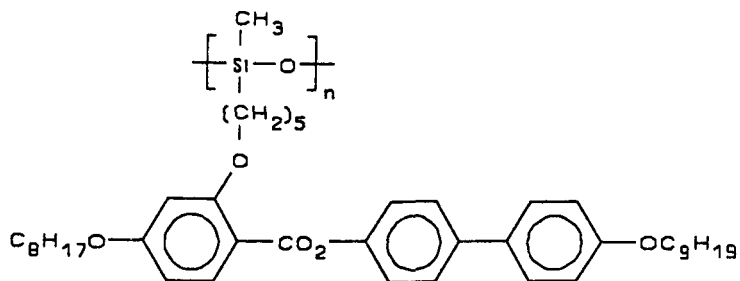
g 39 S<sub>A</sub> 109 N 114 °C I<sup>85</sup>



S<sub>C</sub><sup>\*</sup> 73.0 S<sub>A</sub> 140.0 S<sub>A</sub><sup>\*</sup> 149.0 N<sup>\*</sup> 160.0 °C I<sup>27</sup>

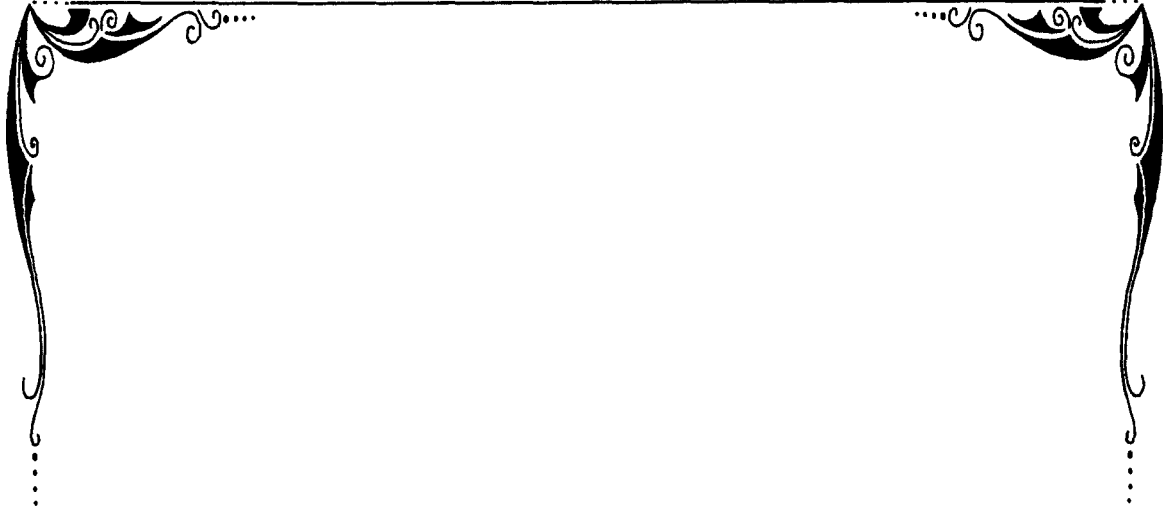


g 7 N 48 °C I<sup>122</sup>

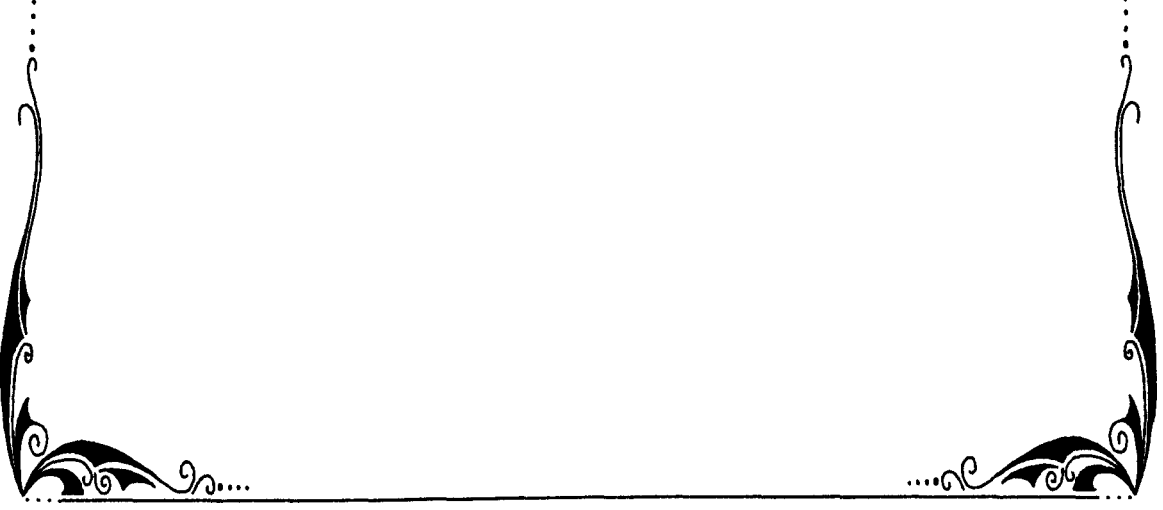


g 48 N 58 °C I<sup>123</sup>

Figure 3.26 Some examples of side chain liquid crystal polymers.



*Aims*



#### 4. AIMS.

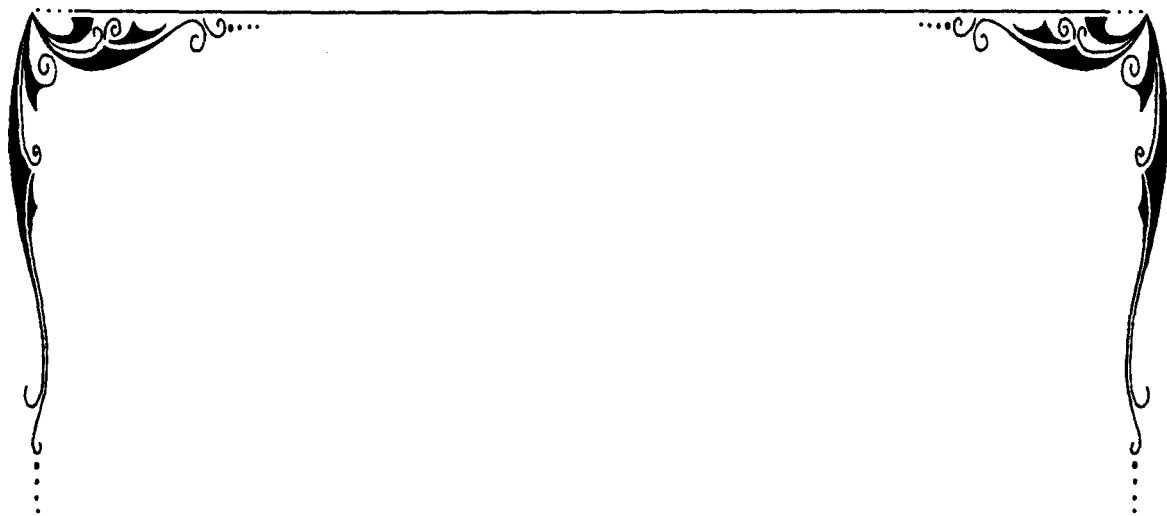
The major aim of the work outlined in this thesis was to investigate procedures by which SCLC polymers could be made with defined and reproducible degrees of polymerization ( $\bar{DP}$ ) and polydispersities ( $\bar{M}_w/\bar{M}_n$ ). Such polymers with well defined  $\bar{DP}$  and  $\bar{M}_w/\bar{M}_n$  values, preferably high  $\bar{DP}$  values and low  $\bar{M}_w/\bar{M}_n$  values, would be very useful polymeric materials in an investigation into the effect of molecular structure of the spacer group, molecular core and terminal group on the thermal, rheological and physical properties of SCLC polymers.

The initial method chosen for carrying out the polymerization of the mesogenic monomers was group transfer polymerization. However, it became clear that the polymerization of mesogenic monomers was not always possible using this type of polymerization, and therefore another method for polymerizing the mesogenic monomers was needed.

An alternative procedure in making SCLC polymers based on acrylate and methacrylate backbones was free radical polymerization, using  $\alpha,\alpha'$ -azoisobutyronitrile (AIBN) as the free radical initiator. By investigating the effects of parameters such as the concentration of the initiator and monomer, the reaction solvent, pressure *etc.*, on the  $\bar{DP}$  and  $\bar{M}_w/\bar{M}_n$  values of the polymer, it was hoped to find a set of optimum conditions for free radical polymerization that would give control over the  $\bar{DP}$  and  $\bar{M}_w/\bar{M}_n$  values of our SCLC polymers.

A new area in liquid crystal research is the use of a cyclic polysiloxane backbones to produce cyclic SCLC polymers. A systematic study was started to study the effect of molecular structure of the pendent group on the thermal, rheological and physical properties of these cyclic SCLC polymers using the hydrosilylation reaction between prepared mesogenic alkenes and commercially available cyclic poly(hydrogenmethylsiloxane) backbones.

The identification of the liquid crystal phases exhibited by the SCLC polymers also became an important part of this work. The identification and alignment of the liquid crystal phases is a very important aspect of liquid crystal research with regard to the commercial and technological applications of SCLC polymers. Work was carried out in this area to align, homeotropically and homogeneously, a number of SCLC polymers using a variety of alignment agents.



# *Experimental*



## 5. EXPERIMENTAL.

### 5.1 Physical Characterization.

Confirmation of the structures of the materials prepared was carried out using a combination of  $^1\text{H}$  nmr spectroscopy (Joel JNM-GX 270 MHz spectrometer), infrared spectroscopy (Perkin-Elmer 783 spectrometer) and mass spectrometry (Finnegan 1020 GC/MS spectrometer). The results obtained were found to be consistent with the predicted structures of the target materials. Chemical purities of the compounds were determined to be single spot by thin layer chromatography (tlc) (silica gel, dichloromethane) unless otherwise stated.

All the final monomers were purified using flash column chromatography (silica gel, dichloromethane) prior to polymerization.

The purity of the monomers and intermediates was checked by reversed phase HPLC (5  $\mu\text{m}$  pore size, 25  $\times$  0.46 cm, ODS Microsorb Dynamax 18 column), using both methanol and a mixture of methanol - water (9:1) as the eluants.

Optical rotations were measured using a ETL-NPL Automatic Polarimeter (143A), using 0.1 g (accurately measured) of the sample in chloroform (10 ml).

The determination of the molecular weights and polydispersities of the polymers ( $\bar{M}_w$ ,  $\bar{M}_n$ ,  $\bar{M}_w/\bar{M}_n$ ) were determined by gel permeation chromatography using a PL-gel

column (5  $\mu\text{m}$ , 30 x 0.75 cm, mixed C column) as the stationary phase and THF as the mobile phase. The column was calibrated using polystyrene standards ( $\bar{M}_p = 1000 - 430500$ ). All values of  $\bar{M}_w$ ,  $\bar{M}_n$ ,  $\bar{M}_w/\bar{M}_n$  given are quoted relative to polystyrene.

Confirmation of the structures of the SCLC polymers was carried out using  $^1\text{H}$  nmr, the peaks produced by polymers tend to occur in the same relative positions but are much broader than the peaks produced by the corresponding monomers. An example of an nmr of a SCLC copolymer is shown in Figure 5.2. The calculation of the relative ratios of each component in the SCLC copolymers produced was based upon the  $^1\text{H}$  nmr. An example of the calculation is given below for the copolymer of XIX + XV (see Figure 5.1).

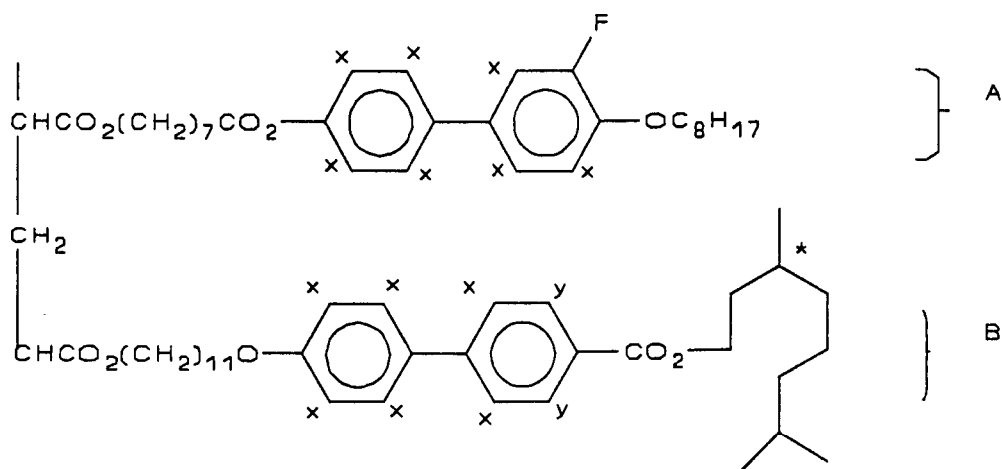


**Figure 5.1** The structure of the copolymer XIX + XV.

The calculation of the relative ratio of each component A and B in the final copolymer is based upon the different  $^1\text{H}$  nmr signal given by the aromatic protons type x and y. The  $^1\text{H}$  nmr for the copolymer of XIX + XV is shown in Figure 5.2, the different signals of type x and y protons can clearly be seen. The calculation of the relative ratios is shown.

Component A contains only 7 x type aromatic protons, component B contains 6 x and 2 y type aromatic protons. From the nmr integration the x type protons have an integration of 7.50, and the y type protons have an integration of 1.00.

$$\text{For y type } 1.00 = 2B$$

$$\text{For x type } 7.50 = 7A + 6B$$

$$\therefore B = 0.500$$

$$\Rightarrow 4.50 = 7A$$

$$\therefore A = 0.640$$

$$\therefore A : B = 0.640 : 0.500$$

$$\Rightarrow 1.28 : 1.00$$

This calculation can be adapted for use with other SCLC copolymers.

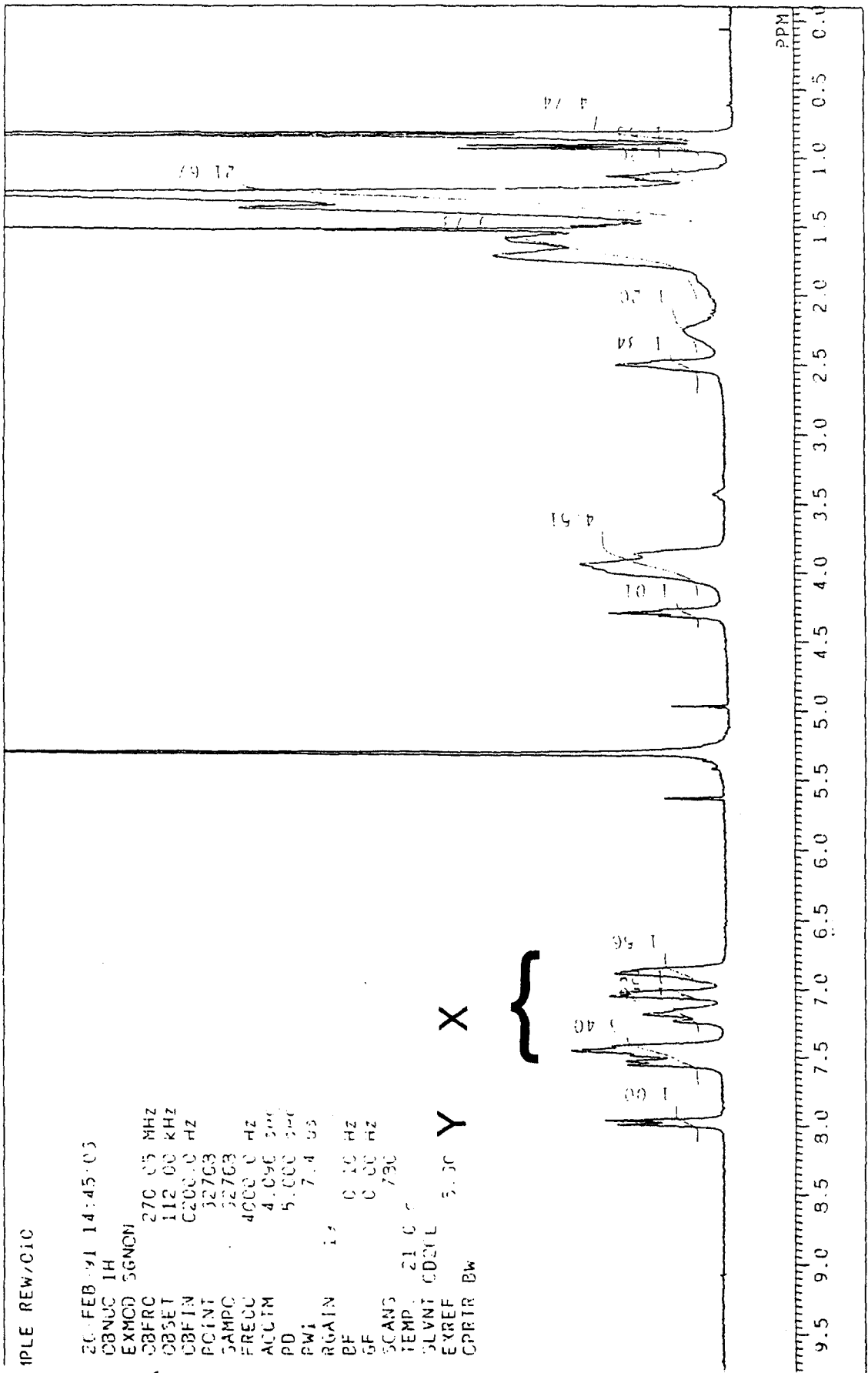


Figure 5.2 The  $^1\text{H}$  nmr of the copolymer XIX + XV.

The phase transitions of the intermediates and final polymers that exhibited liquid crystalline behaviour were investigated by thermal optical microscopy and differential scanning calorimetry. Thermal microscopic studies were made using a Zeiss Universal polarizing light microscope in conjunction with a Mettler FP52 microfurnace and FP5 control unit. Transition temperatures were determined to better than 0.1 °C by this technique. Differential scanning calorimetry was used to determine both the temperatures and heats of transition. These studies were carried out using a Perkin-Elmer DSC 7 calorimeter equipped with a thermal analysis data station. The instrumental accuracy was calibrated against an indium standard (measured  $\Delta H$  28.63  $\text{Jg}^{-1}$ , literature value 28.45  $\text{Jg}^{-1}$ ).

Attempts to obtain the melting points of some of the monomers prepared proved impossible. On heating the samples, decomposition usually occurred below the melting point. The temperature at which decomposition occurred was not reproducible.

## **5.2 Purification of Solvents.**

### **5.2.1 Dry Dichloromethane.**

Dichloromethane was distilled from phosphorus pentoxide immediately prior to use.<sup>124</sup>

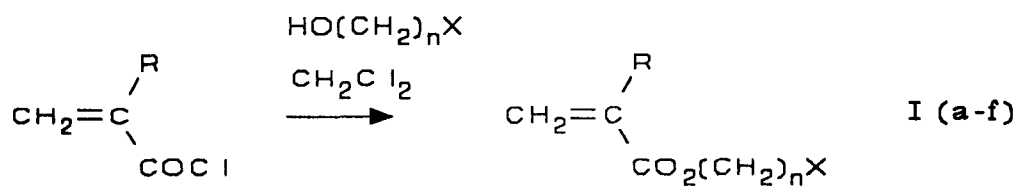
### **5.2.2 Dry Tetrahydrofuran.**

Tetrahydrofuran was distilled from a mixture of sodium wire and benzophenone immediately prior to use.<sup>125</sup>

### **5.2.3 Dry Toluene.**

Dry toluene was stored over dried 4Å molecular sieves and decanted immediately prior to use.

### 5.3 SCHEME 1.



	R	n	X
Ia	H	3	Br
Ib	CH <sub>3</sub>	3	Br
Ic	H	6	Cl
Id	CH <sub>3</sub>	6	Cl
Ie	H	11	Br
If	CH <sub>3</sub>	11	Br

#### 5.3.1 The Preparations of Compounds Ia to If are Exemplified by the Following

##### Preparation of $\omega$ -Bromopropyl acrylate (Ia).

A solution of acryloyl chloride (1.8 g, 0.02 mol) in dry dichloromethane (10 ml) was added dropwise to a stirred solution of 3-bromopropanol (2.8 g, 0.02 mol) and

triethylamine (2.0 g, 0.02 mol) in dry dichloromethane (10 ml). The resulting solution was stirred at room temperature for 4 h, poured into 10 % v/v aqueous hydrochloric acid (50 ml). The organic layer was separated off and the aqueous layer washed with diethyl ether (2 × 25 ml), the combined organic extracts were washed with water and dried (MgSO<sub>4</sub>). The solvent was removed by distillation under reduced pressure at room temperature, to yield an orange oil, 2.3 g (60 %).

$\nu_{\max}$ (capillary film)/cm<sup>-1</sup> 1740 (C=O), 1260 (C-O), 2980 (C-H), 1405 (C-H);  
 $\delta_{\text{H}}$ (CDCl<sub>3</sub>) 2.40 (2H, t, CH<sub>2</sub>CH<sub>2</sub>CH<sub>2</sub>Br), 3.50 (2H, t, CH<sub>2</sub>CH<sub>2</sub>Br), 4.40 (2H, t, COOCH<sub>2</sub>CH<sub>2</sub>), 5.90 (1H, 2xd, OCH=CH<sub>2</sub>), 6.20 (1H, 2xd, OCH=CH<sub>2</sub>), 6.50 (1H, 2xd, OCH=CH<sub>2</sub>);  
m/z 194, 192 (M<sup>+</sup>, 100 %).

The purity of the crude product was checked by thin layer chromatography (tlc) (silica gel, dichloromethane). However no attempt was made to purify compound **Ia** due to the risk of polymerizing the compound by the application of heat.

The following compounds were prepared by using the method outlined for the preparation of compound **Ia**.

### 5.3.2 Preparation of $\omega$ -Bromopropyl methacrylate (Ib).

Methacryloyl chloride	10.4 g, 0.1 mol
Dry dichloromethane	10 ml
3-Bromopropanol	13.96 g, 0.1 mol
Triethylamine	10.0 g, 0.1 mol
Dry dichloromethane	20 ml
Yield	orange oil, 19.0 g (95 %).

$\nu_{\max}$ (capillary film)/ $\text{cm}^{-1}$  1715 (C=O), 1160 (C-O), 2980 (C-H), 1450 (C-H);

$\delta_{\text{H}}$ ( $\text{CDCl}_3$ ) 1.50 (2H, t,  $\text{CH}_2\text{CH}_2\text{CH}_2\text{Br}$ ), 2.50 (2H, t,  $\text{CH}_2\text{CH}_2\text{Br}$ ), 3.40 (2H, t,  $\text{COOCH}_2\text{CH}_2$ ), 4.50 (3H, m,  $\text{OCCH}_3=\text{CH}_2$ ), 5.60 (1H, d,  $\text{OCCH}_3=\text{CH}_2$ ), 6.30 (1H, d,  $\text{OCCH}_3=\text{CH}_2$ );

$m/z$  208, 206 ( $\text{M}^+$ , 100 %).

### 5.3.3 Preparation of $\omega$ -Chlorohexyl acrylate (Ic).

Acryloyl chloride	1.8 g, 0.02 mol
Dry dichloromethane	10 ml
6-Chlorohexanol	2.7 g, 0.02 mol
Triethylamine	2.0 g, 0.02 mol
Dry dichloromethane	10 ml
Yield	yellow oil, 2.7 g (71 %).

$\nu_{\max}$ (capillary film)/ $\text{cm}^{-1}$  1750 (C=O), 1180 (C-O), 2950 (C-H), 1420 (C-H);  
 $\delta_{\text{H}}$ ( $\text{CDCl}_3$ ) 1.75 (8H, m,  $\text{CH}_2(\underline{\text{CH}_2})_4\text{CH}_2\text{Cl}$ ), 3.50 (2H, t,  $\text{CH}_2\underline{\text{CH}_2}\text{Cl}$ ), 4.15 (2H, t,  $\text{COOCH}_2\underline{\text{CH}_2}$ ), 5.85 (1H, 2xd,  $\text{OCH}=\underline{\text{CH}_2}$ ), 6.30 (1H, 2xd,  $\text{OCH}=\underline{\text{CH}_2}$ ), 6.40 (1H, 2xd,  $\text{OCH}=\underline{\text{CH}_2}$ );  
 $m/z$  190 ( $\text{M}^+$ , 100 %).

#### **5.3.4 Preparation of $\omega$ -Chlorohexyl methacrylate (Id).**

Methacryloyl chloride	10.4 g, 0.1 mol
Dry dichloromethane	10 ml
6-Chlorohexanol	13.6 g, 0.1 mol
Triethylamine	10.0 g, 0.1 mol
Dry dichloromethane	20 ml
Yield	yellow oil, 19.4 g (95 %).

$\nu_{\max}$ (capillary film)/ $\text{cm}^{-1}$  1715 (C=O), 1160 (C-O), 2960 (C-H), 1450 (C-H);  
 $\delta_{\text{H}}$ ( $\text{CDCl}_3$ ) 1.50 (8H, m,  $\text{CH}_2(\underline{\text{CH}_2})_4\text{CH}_2\text{Cl}$ ), 2.50 (2H, t,  $\text{CH}_2\underline{\text{CH}_2}\text{Cl}$ ), 3.40 (2H, t,  $\text{COOCH}_2\underline{\text{CH}_2}$ ), 4.50 (3H, m,  $\text{OCCH}_3=\underline{\text{CH}_2}$ ), 5.60 (1H, d,  $\text{OCCH}_3=\underline{\text{CH}_2}$ ), 6.30 (1H, d,  $\text{OCCH}_3=\underline{\text{CH}_2}$ );  
 $m/z$  204 ( $\text{M}^+$ , 100 %).

### 5.3.5 Preparation of $\omega$ -Bromoundecyl acrylate (Ie).

Acryloyl chloride	1.8 g, 0.02 mol
Dry dichloromethane	10 ml
11-Bromoundecanol	5.0 g, 0.02 mol
Triethylamine	2.0 g, 0.02 mol
Dry dichloromethane	10 ml
Yield	orange oil, 18.2 g (60 %).

$\nu_{\max}$  (capillary film)/ $\text{cm}^{-1}$  1750 (C=O), 1180 (C-O), 2950 (C-H), 1420 (C-H);

$\delta_{\text{H}}$ ( $\text{CDCl}_3$ ) 1.40 (18H, m,  $\text{CH}_2(\underline{\text{CH}_2})_9\text{CH}_2\text{Br}$ ), 3.50 (2H, t,  $\text{CH}_2\underline{\text{CH}_2}\text{Br}$ ), 4.25 (2H, t,  $\text{COOCH}_2\underline{\text{CH}_2}$ ), 5.85 (1H, 2xd,  $\text{OCH}=\underline{\text{CH}_2}$ ), 6.10 (1H, 2xd,  $\text{OCH}=\underline{\text{CH}_2}$ ), 6.45 (1H, 2xd,  $\text{OCH}=\underline{\text{CH}_2}$ );

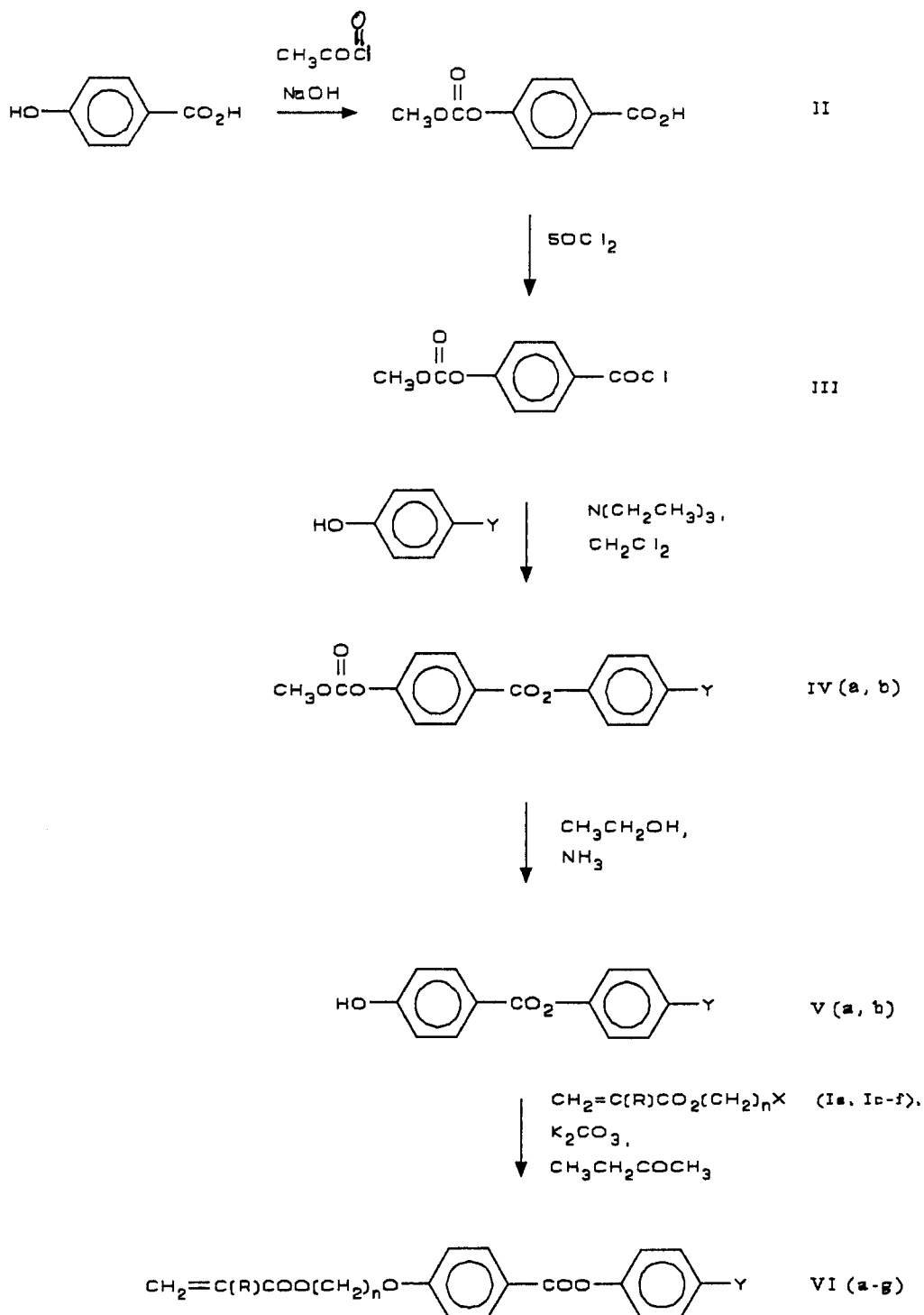
$m/z$  304, 306 ( $\text{M}^+$ , 100 %).

### 5.3.6 Preparation of $\omega$ -Bromoundecyl methacrylate (If).

Methacryloyl chloride	10.4 g, 0.1 mol
Dry dichloromethane	10 ml
11-Bromoundecanol	25.1 g, 0.1 mol
Triethylamine	10.0 g, 0.1 mol
Dry dichloromethane	20 ml
Yield	orange oil, 15.0 g (47 %).

$\nu_{\max}$ (capillary film)/ $\text{cm}^{-1}$  1715 (C=O), 1160 (C-O), 2920 (C-H), 1450 (C-H);  
 $\delta_{\text{H}}$ ( $\text{CDCl}_3$ ) 1.50 (18H, m,  $\text{CH}_2(\underline{\text{CH}_2})_9\text{CH}_2\text{Br}$ ), 2.50 (2H, t,  $\text{CH}_2\underline{\text{CH}_2}\text{Br}$ ), 3.40 (2H, t,  $\text{COOCH}_2\underline{\text{CH}_2}$ ), 4.50 (3H, m,  $\text{OCCH}_3=\underline{\text{CH}_2}$ ), 5.60 (1H, d,  $\text{OCCH}_3=\underline{\text{CH}_2}$ ), 6.30 (1H, d,  $\text{OCCH}_3=\underline{\text{CH}_2}$ );  
 $m/z$  318, 320 ( $\text{M}^+$ , 100 %).

## 5.4 SCHEME 2



IVa, Va, Y = OCH<sub>3</sub>

IVb, Vb, Y = CN

VI (a-g), see Section 5.4.8

#### 5.4.1 Preparation of 4-(Methoxycarbonyloxy)benzoic Acid<sup>126</sup> (II).

4-Hydroxybenzoic acid (10.0 g, 0.073 mol) was added with vigorous stirring to a solution of sodium hydroxide (8.4 g, 0.21 mol) in water (500 ml) maintained at 0 °C. Methyl chloroformate (11.2 g, 0.12 mol) was added slowly to the resulting suspension, and then the reaction mixture was stirred at 0 °C for 4 h. The pH of the reaction mixture was then adjusted to pH 5 by the addition of a mixture of concentrated hydrochloric acid and water (1:1). The voluminous precipitate was filtered off, washed with water and recrystallised (ethanol) to yield

4-(methoxycarbonyloxy)benzoic acid as colourless crystals, 10.7 g (75 %).

m.p. = 83 - 84 °C.

$\nu_{\max}(\text{KBr})/\text{cm}^{-1}$  1740 (C=O), 1670 (C=O), 1400 (C-H);

$\delta_{\text{H}}(\text{CDCl}_3)$  4.0 (3H, s  $\text{CH}_3\text{OCOOAr}$ ), 7.25 (2H, 2xd, ArH), 8.15 (2H, 2xd, ArH);

m/z 196 ( $\text{M}^+$ , 100 %).

#### 5.4.2 Preparation of the Acid Chloride of 4-(Methoxycarbonyloxy)benzoic Acid (III).

4-(Methoxycarbonyloxy)benzoic acid (25.0 g, 0.13 mol) was dissolved in an excess of thionyl chloride (77.0 g, 0.65 mol) and the resulting solution was stirred and heated under reflux for 4 h. The excess thionyl chloride was removed by distillation under reduced pressure and the crude product was used without further purification.

### **5.4.3 Preparation of 4-Methoxyphenyl 4-(methoxycarbonyloxy)benzoate (IVa).**

Triphenylphosphine (7.1 g, 0.027 mol) in dry THF (10 ml) was added dropwise to a stirred solution of 4-(methoxycarbonyloxy)benzoic acid (5.0 g, 0.026 mol), 4-methoxyphenol (3.4 g, 0.027 mol) and diethyl azodicarboxylate (4.7 g, 0.027 mol) in dry THF (20 ml). The resulting solution was stirred at room temperature for 72 h and the solvent removed by distillation under reduced pressure. The crude product was recrystallised (ethanol) to yield compound **IVa** as white crystals, 4.5 g (56 %). The compound exhibited liquid crystal behaviour and had the following transition temperatures.

K (105.9 N) 119.6 °C I.

$\nu_{\max}(\text{KBr}) / \text{cm}^{-1}$  1770 (C=O), 1730 (C=O), 1610 (C-H), 1510 (C-H);

$\delta_{\text{H}}(\text{CDCl}_3)$  3.9 (3H, s,  $\text{CH}_3\text{OCOOAr}$ ), 4.0 (3H, s,  $\text{CH}_3\text{OAr}$ ), 6.95 (2H, m,  $\text{ArH}$ ), 7.15 (2H, m,  $\text{ArH}$ ), 7.35 (2H, m,  $\text{ArH}$ ), 8.25 (2H, m,  $\text{ArH}$ );

$m/z$  302 ( $\text{M}^+$ , 100 %).

### **5.4.4 Preparation of 4-Cyanophenyl 4-(methoxycarbonyloxy)benzoate (IVb).**

The acid chloride (**III**) (5.0 g, 0.023 mol) and 4-cyanophenol (3.2 g, 0.025 mol) were dissolved in dry dichloromethane (20 ml). Triethylamine (2.5 g, 0.025 mol) was added dropwise and the resulting solution stirred at room temperature for 4 h. The solvent was removed by distillation under reduced pressure. The crude product was recrystallised (ethanol) to yield compound **IVb** as a white crystalline solid, 4.0 g (54 %).

m.p. = 117 - 118 °C.

$\nu_{\max}(\text{KBr})/\text{cm}^{-1}$  2220 (C≡N), 1760 (C=O), 1740 (C=O), 1610 (C-H), 1510 (C-H);

$\delta_{\text{H}}(\text{CDCl}_3)$  3.95 (3H, s,  $\text{CH}_3\text{OCOOAr}$ ), 7.40 (4H, m,  $\text{ArH}$ ), 7.75 (2H, m,  $\text{ArH}$ ), 8.30 (2H, m,  $\text{ArH}$ );

m/z 296 ( $\text{M}^+$ , 100 %).

#### **5.4.5 Preparation of 4-Methoxyphenyl 4-hydroxybenzoate (Va).**

4-Methoxyphenyl 4-(methoxycarbonyloxy)benzoate **IVa** (4.5 g, 0.015 mol) was stirred for 2 h in a mixture of ethanol (100 ml) and ammonia (40 ml). The solvent was removed by distillation under reduced pressure and the crude product recrystallised (acetonitrile) to yield compound **Va** as a white solid, 3.3 g (90 %).

m.p. = 90 - 92 °C.

$\nu_{\max}(\text{KBr})/\text{cm}^{-1}$  3380 (C-H), 1710 (C=O), 1600 (C-H), 1340 (C-H);

$\delta_{\text{H}}(\text{CDCl}_3)$  3.85 (3H, s,  $\text{CH}_3\text{OAr}$ ), 6.95 (2H, m,  $\text{ArH}$ ), 7.10 (2H, m,  $\text{ArH}$ ), 7.35 (2H, m,  $\text{ArH}$ ), 8.00 (2H, m,  $\text{ArH}$ );

m/z 244 ( $\text{M}^+$ , 100 %).

#### 5.4.6 Preparation of 4-Cyanophenyl 4-hydroxybenzoate (Vb).

4-Cyanophenyl 4-hydroxybenzoate was prepared using the method outlined for the preparation of 4-methoxyphenyl 4-hydroxybenzoate **Va** (4.5 g, 0.015 mol). The solvent was removed by distillation under reduced pressure and the crude product was recrystallised (acetonitrile) to yield compound **Vb** as a white solid, 2.1 g (72 %).

m.p. = 89 - 92 °C.

$\nu_{\max}(\text{KBr})/\text{cm}^{-1}$  3350 (C-H), 2220 (C≡N), 1760 (C=O), 1600 (C-H);

$\delta_{\text{H}}(\text{CDCl}_3)$  6.95 (2H, m, ArH), 7.40 (2H, m, ArH), 7.75 (2H, m, ArH), 8.10 (2H, m, ArH);

m/z 224 ( $\text{M}^+$ , 100 %).

#### 5.4.7 Preparation of Compounds VIa to VIg.

The preparations of compounds VIa to VIg are exemplified by the following preparation of 4-methoxyphenyl 4-[3-(acryloyloxy)propyloxy]benzoate VIa.

	R	n	Y
VIa	H	3	OCH <sub>3</sub>
VIb	H	6	OCH <sub>3</sub>
VIc	H	11	OCH <sub>3</sub>
VI d	H	6	CN
VIe	CH <sub>3</sub>	6	CN
VI f	H	11	CN
VIg	CH <sub>3</sub>	11	CN

#### 5.4.8 Preparation of 4-Methoxyphenyl

##### 4-[3-(acryloyloxy)propyloxy]benzoate (VIa).

A stirred solution of  $\omega$ -bromopropyl acrylate (0.8 g, 4.1 mmol), 4-methoxyphenyl 4-hydroxybenzoate (1.0 g, 4.1 mmol), potassium carbonate (2.8 g, 20 mmol) and potassium iodide (0.1 g) in dry butanone (100 ml) was heated under reflux for 72 h. The insoluble potassium salts were filtered off and the solvent removed by distillation under reduced pressure, keeping the temperature below 35 °C. The crude product was

purified by flash column chromatography (silica gel, dichloromethane), to yield compound **VIa** as a white solid, 1.0 g (68 %).

m.p. = 45 - 50 °C (dec).

$\nu_{\max}(\text{KBr})/\text{cm}^{-1}$  1740 (C=O), 1710 (C=O), 1260 (C-O), 1405 (C-H), 3380 (C-H), 1600 (C-H), 1340 (C-H);

$\delta_{\text{H}}(\text{CDCl}_3)$  2.40 (2H, t,  $\text{CH}_2\text{CH}_2\text{CH}_2\text{Br}$ ), 3.50 (2H, t,  $\text{CH}_2\text{CH}_2\text{Br}$ ), 3.85 (3H, s,  $\text{CH}_3\text{OAr}$ ), 4.40 (2H, t,  $\text{COOCH}_2\text{CH}_2$ ), 5.90 (1H, 2xd,  $\text{OCH}=\text{CH}_2$ ), 6.20 (1H, 2xd,  $\text{OCH}=\text{CH}_2$ ), 6.50 (1H, 2xd,  $\text{OCH}=\text{CH}_2$ ), 6.95 (2H, m, ArH), 7.10 (2H, m, ArH), 7.35 (2H, m, ArH), 8.00 (2H, m, ArH);

m/z 356 ( $\text{M}^+$ , 100 %).

The following compounds **VIb** - **VIg** were prepared using the method outlined for the preparation of compound **VIa**.

#### **5.4.9 Preparation of 4-Methoxyphenyl 4-[6-(acryloyloxy)hexyloxy]benzoate (VIb).**

$\omega$ -Chlorohexyl acrylate	0.8 g, 4.1 mmol
4-Methoxyphenyl 4-hydroxybenzoate	1.0 g, 4.1 mmol
Potassium carbonate	2.8 g, 20 mmol
Potassium iodide	0.1 g
Dry butanone	100 ml
Yield	white solid, 1.2 g (73 %).
m.p. = 48 - 52 °C (dec).	

$\nu_{\max}(\text{KBr})/\text{cm}^{-1}$  3380 (C-H), 1750 (C=O), 1710 (C=O), 1600 (C-H), 1420 (C-H), 1340 (C-H) 1180 (C-O);

$\delta_{\text{H}}(\text{CDCl}_3)$  1.75 (8H, m,  $\text{CH}_2(\text{CH}_2)_4\text{CH}_2\text{Cl}$ ), 3.50 (2H, t,  $\text{CH}_2\text{CH}_2\text{Cl}$ ), 3.85 (3H, s,  $\text{CH}_3\text{OAr}$ ), 4.15 (2H, t,  $\text{COOCH}_2\text{CH}_2$ ), 5.85 (1H, 2xd,  $\text{OCH}=\text{CH}_2$ ), 6.30 (1H, 2xd,  $\text{OCH}=\text{CH}_2$ ), 6.40 (1H, 2xd,  $\text{OCH}=\text{CH}_2$ ), 6.95 (2H, m, ArH), 7.10 (2H, m, ArH), 7.35 (2H, m, ArH), 8.00 (2H, m, ArH);

$m/z$  398 ( $\text{M}^+$ , 100 %).

#### 5.4.10 Preparation of 4-Methoxyphenyl 4-[11-(acryloyloxy)undecyloxy]benzoate

##### (VIc).

$\omega$ -Bromoundecyl acrylate	1.3 g, 4.1 mmol
4-Methoxyphenyl 4-hydroxybenzoate	1.0 g, 4.2 mmol
Potassium carbonate	2.8 g, 20 mmol
Potassium iodide	0.1 g
Dry butanone	100 ml
Yield	white solid, 1.7 g (88 %).

m.p. = 56 - 60 °C (dec).

$\nu_{\max}(\text{KBr})/\text{cm}^{-1}$  2960 (C-H), 1720 (C=O), 1600 (C-H), 1400 (C-H);

$\delta_{\text{H}}(\text{CDCl}_3)$  1.40 - 1.70 (18H, m,  $(\text{CH}_2)_9$ ), 3.80 (3H, s,  $\text{OCH}_3$ ), 4.10 (4H, m,  $\text{CH}_2\text{O}$ ), 5.80 (1H, 2xd,  $\text{OCH}=\text{CH}_2$ ), 6.1 (1H, 2xd,  $\text{OCH}=\text{CH}_2$ ), 6.4 (1H, 2xd,  $\text{OCH}=\text{CH}_2$ ), 7.00 (6H, m, ArH), 8.10 (2H, m, ArH);

$m/z$  468 ( $\text{M}^+$ , 100 %).

#### **5.4.11 Preparation of 4-Cyanophenyl 4-[6-(acryloyloxy)hexyloxy]benzoate (VIId).**

$\omega$ -Chlorohexyl acrylate	0.8 g, 4.2 mmol
4-Cyanophenyl 4-hydroxybenzoate	1.0 g, 4.2 mmol
Potassium carbonate	2.8 g, 20 mmol
Potassium iodide	0.1 g
Dry butanone	100 ml
Yield	white solid, 1.2 g (71 %).

m.p. = 70 - 72 °C.

$\nu_{\max}(\text{KBr})/\text{cm}^{-1}$  3350 (C-H), 2220 (C $\equiv$ N), 1760 (C=O), 1750 (C=O), 1600 (C-H), 1180 (C-O), 1420 (C-H);

$\delta_{\text{H}}(\text{CDCl}_3)$  1.75 (8H, m, CH<sub>2</sub>(CH<sub>2</sub>)<sub>4</sub>CH<sub>2</sub>Cl), 3.50 (2H, t, CH<sub>2</sub>CH<sub>2</sub>Cl), 4.15 (2H, t, COOCH<sub>2</sub>CH<sub>2</sub>), 5.85 (1H, 2xd, OCH=CH<sub>2</sub>), 6.30 (1H, 2xd, OCH=CH<sub>2</sub>), 6.40 (1H, 2xd, OCH=CH<sub>2</sub>), 6.95 (2H, m, ArH), 7.40 (2H, m, ArH), 7.75 (2H, m, ArH), 8.10 (2H, m, ArH);

m/z 394 (M<sup>+</sup>, 100 %).

#### **5.4.12 Preparation of 4-Cyanophenyl 4-[6-(methacryloyloxy)hexyloxy]benzoate (VIe).**

$\omega$ -Chlorohexyl methacrylate	0.9 g, 4.2 mmol
4-Cyanophenyl 4-hydroxybenzoate	1.0 g, 4.2 mmol
Potassium carbonate	2.8 g, 20 mmol

Potassium iodide	0.1 g
Dry butanone	100 ml
Yield	white solid, 1.1 g (64 %).

m.p. = 65 - 67 °C.

$\nu_{\max}(\text{KBr})/\text{cm}^{-1}$  3350 (C-H), 2220 (C≡N), 1760 (C=O), 1715 (C=O), 1600 (C-H), 1160 (C-O), 1450 (C-H);

$\delta_{\text{H}}(\text{CDCl}_3)$  1.50 (8H, m,  $\text{CH}_2(\text{CH}_2)_4\text{CH}_2\text{Cl}$ ), 2.50 (2H, t,  $\text{CH}_2\text{CH}_2\text{Cl}$ ), 3.40 (2H, t,  $\text{COOCH}_2\text{CH}_2$ ), 4.50 (3H, m,  $\text{OCCH}_3=\text{CH}_2$ ), 5.60 (1H, d,  $\text{OCCH}_3=\text{CH}_2$ ), 6.30 (1H, d,  $\text{OCCH}_3=\text{CH}_2$ ), 6.95 (2H, m, ArH), 7.40 (2H, m, ArH), 7.75 (2H, m, ArH), 8.10 (2H, m, ArH);

m/z 408 ( $\text{M}^+$ , 100 %).

#### **5.4.13 Preparation of 4-Cyanophenyl 4-[11-(acryloyloxy)undecyloxy]benzoate (VI).**

$\omega$ -Bromoundecyl methacrylate	1.3 g, 4.2 mmol
4-Cyanophenyl 4-hydroxybenzoate	1.0 g, 4.2 mmol
Potassium carbonate	2.8 g, 20 mmol
Potassium iodide	0.1 g
Dry butanone	100 ml
Yield	white solid, 1.3 g (74 %).

m.p. = 75 - 79 °C.

$\nu_{\max}(\text{KBr})/\text{cm}^{-1}$  3350 (C-H), 2220 (C≡N), 1750 (C=O), 1715 (C=O), 1600 (C-H), 1180 (C-O), 1420 (C-H);

$\delta_{\text{H}}(\text{CDCl}_3)$  1.40 (18H, m,  $\text{CH}_2(\underline{\text{CH}_2})_9\text{CH}_2\text{Br}$ ), 3.50 (2H, t,  $\text{CH}_2\underline{\text{CH}_2}\text{Br}$ ), 4.25 (2H, t,  $\text{COOCH}_2\underline{\text{CH}_2}$ ), 5.85 (1H, 2xd,  $\text{OCH}=\underline{\text{CH}_2}$ ), 6.10 (1H, 2xd,  $\text{OCH}=\underline{\text{CH}_2}$ ), 6.45 (1H, 2xd,  $\text{OCH}=\underline{\text{CH}_2}$ ), 6.95 (2H, m,  $\text{ArH}$ ), 7.40 (2H, m,  $\text{ArH}$ ), 7.75 (2H, m,  $\text{ArH}$ ), 8.10 (2H, m,  $\text{ArH}$ );

$m/z$  416 ( $\text{M}^+$ , 100 %).

#### 5.4.14 Preparation of 4-Cyanophenyl

##### 4-[11-(methacryloyloxy)undecyloxy]benzoate (VIg).

$\omega$ -Bromoundecyl methacrylate	1.3 g, 4.2 mmol
4-Cyanophenyl 4-hydroxybenzoate	1.0 g, 4.2 mmol
Potassium carbonate	2.8 g, 20 mmol
Potassium iodide	0.1 g
Dry butanone	100 ml
Yield	white solid, 1.7 g (94 %).

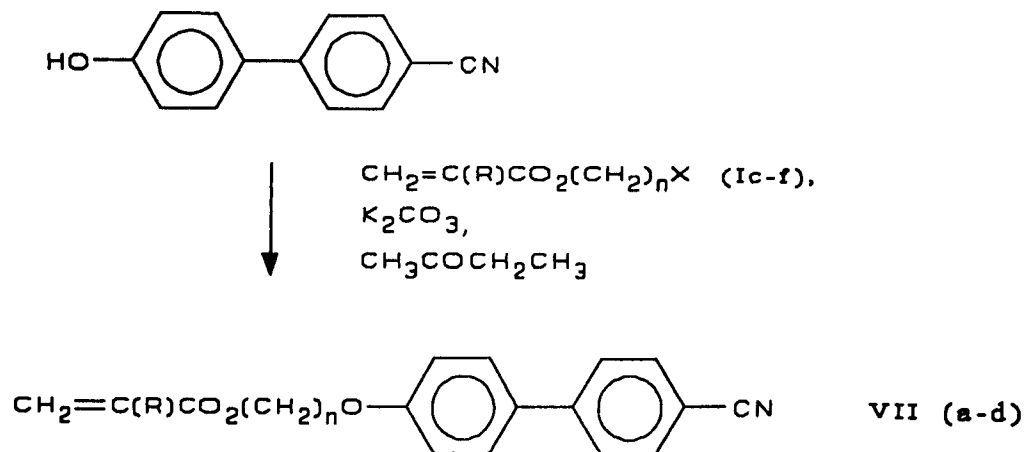
m.p. = 70 - 73 °C.

$\nu_{\text{max}}(\text{KBr})/\text{cm}^{-1}$  3350 (C-H), 2220 ( $\text{C}\equiv\text{N}$ ), 1715 (C=O), 1715 (C=O), 1600 (C-H), 1160 (C-O), 1450 (C-H);

$\delta_{\text{H}}(\text{CDCl}_3)$  1.50 (18H, m,  $\text{CH}_2(\underline{\text{CH}_2})_9\text{CH}_2\text{Br}$ ), 2.50 (2H, t,  $\text{CH}_2\underline{\text{CH}_2}\text{Br}$ ), 3.40 (2H, t,  $\text{COOCH}_2\underline{\text{CH}_2}$ ), 4.50 (3H, m,  $\text{OCCH}_3=\underline{\text{CH}_2}$ ), 5.60 (1H, d,  $\text{OCCH}_3=\underline{\text{CH}_2}$ ), 6.30 (1H, d,  $\text{OCCH}_3=\underline{\text{CH}_2}$ ), 6.95 (2H, m,  $\text{ArH}$ ), 7.40 (2H, m,  $\text{ArH}$ ), 7.75 (2H, m,  $\text{ArH}$ ), 8.10 (2H, m,  $\text{ArH}$ );

$m/z$  430 ( $\text{M}^+$ , 100 %).

### 5.5 SCHEME 3.



X = Cl or Br

	R	n
VIIa	H	6
VIIb	CH <sub>3</sub>	6
VIIc	H	11
VIIId	CH <sub>3</sub>	11

The preparation of compounds VIIa to VIId was carried out using the procedure described for compound VIa (Scheme 2, Section 5.4.8).

### 5.5.1 Preparation of 4'-Cyano-4-[6-(acryloyloxy)hexoxy]biphenyl (VIIa).

$\omega$ -Chlorohexyl acrylate	0.8 g, 4.2 mmol
4'-Cyano-4-hydroxybiphenyl	1.0 g, 4.2 mmol
Potassium carbonate	2.8 g, 20 mmol
Potassium iodide	0.1 g
Dry butanone	100 ml
Yield	white solid, 1.2 g (80 %).

m.p. = 58 - 61 °C.

$\nu_{\max}(\text{KBr})/\text{cm}^{-1}$  3300 (C-H), 2220 (C $\equiv$ N), 1610 (C=O), 1250 (C-O);

$\delta_{\text{H}}(\text{CDCl}_3)$  1.50 (8H, m, CH<sub>2</sub>(CH<sub>2</sub>)<sub>4</sub>CH<sub>2</sub>), 4.00 (2H, t, CO<sub>2</sub>CH<sub>2</sub>OAr), 4.15 (2H, t, COOCH<sub>2</sub>(CH<sub>2</sub>)<sub>4</sub>), 5.75 (1H, d, OCH=CH<sub>2</sub>), 6.10 (1H, d, OCH=CH<sub>2</sub>), 6.45 (1H, d, OCH=CH<sub>2</sub>), 7.00 (2H, m, ArH), 7.55 (2H, m, ArH), 7.65 (4H, m, ArH);

m/z 348 (M<sup>+</sup>, 100 %).

### 5.5.2 Preparation of 4'-Cyano-4-[6-(methacryloyloxy)hexoxy]biphenyl (VIIb).

$\omega$ -Chlorohexyl methacrylate	0.8 g, 4.2 mmol
4'-Cyano-4-hydroxybiphenyl	1.0 g, 4.2 mmol
Potassium carbonate	2.8 g, 20 mmol
Potassium iodide	0.1 g
Dry butanone	100 ml
Yield	white solid, 1.3 g (86 %).

m.p. = 55 - 58 °C.

$\nu_{\max}(\text{KBr})/\text{cm}^{-1}$  3300 (C-H), 2220 (C≡N), 1610 (C=O), 1250 (C-O);

$\delta_{\text{H}}(\text{CDCl}_3)$  1.50 (18H, m,  $\text{CH}_2(\text{CH}_2)_4\text{CH}_2$ ), 4.00 (2H, t,  $\text{CO}_2\text{CH}_2\text{OAr}$ ), 4.20 (2H, t,  $\text{COOCH}_2(\text{CH}_2)_4$ ), 4.55 (3H, d,  $\text{OC}(\text{CH}_3)=\text{CH}_2$ ), 5.55 (1H, d,  $\text{OC}(\text{CH}_3)=\text{CH}_2$ ), 6.10 (1H, d,  $\text{OC}(\text{CH}_3)=\text{CH}_2$ ), 7.00 (2H, m, ArH), 7.55 (2H, m, ArH), 7.65 (4H, m, ArH);  
m/z 362 ( $\text{M}^+$ , 100 %).

### **5.5.3 Preparation of 4'-Cyano-4-[11-(acryloyloxy)undecoxy]biphenyl (VIIc).**

$\omega$ -Bromoundecyl acrylate	1.3 g, 4.2 mmol
4'-Cyano-4-hydroxybiphenyl	1.0 g, 4.2 mmol
Potassium carbonate	2.8 g, 20 mmol
Potassium iodide	0.1 g
Dry butanone	100 ml
Yield	white solid, 1.3 g (72 %).

m.p. = 90 - 91 °C.

The purity of Compound VIIc was checked by HPLC in order to verify the single spot tlc result. The results from the HPLC (methanol and 9:1 mixture of methanol and water were used as eluants) showed that the purity of the compound was 99 %.

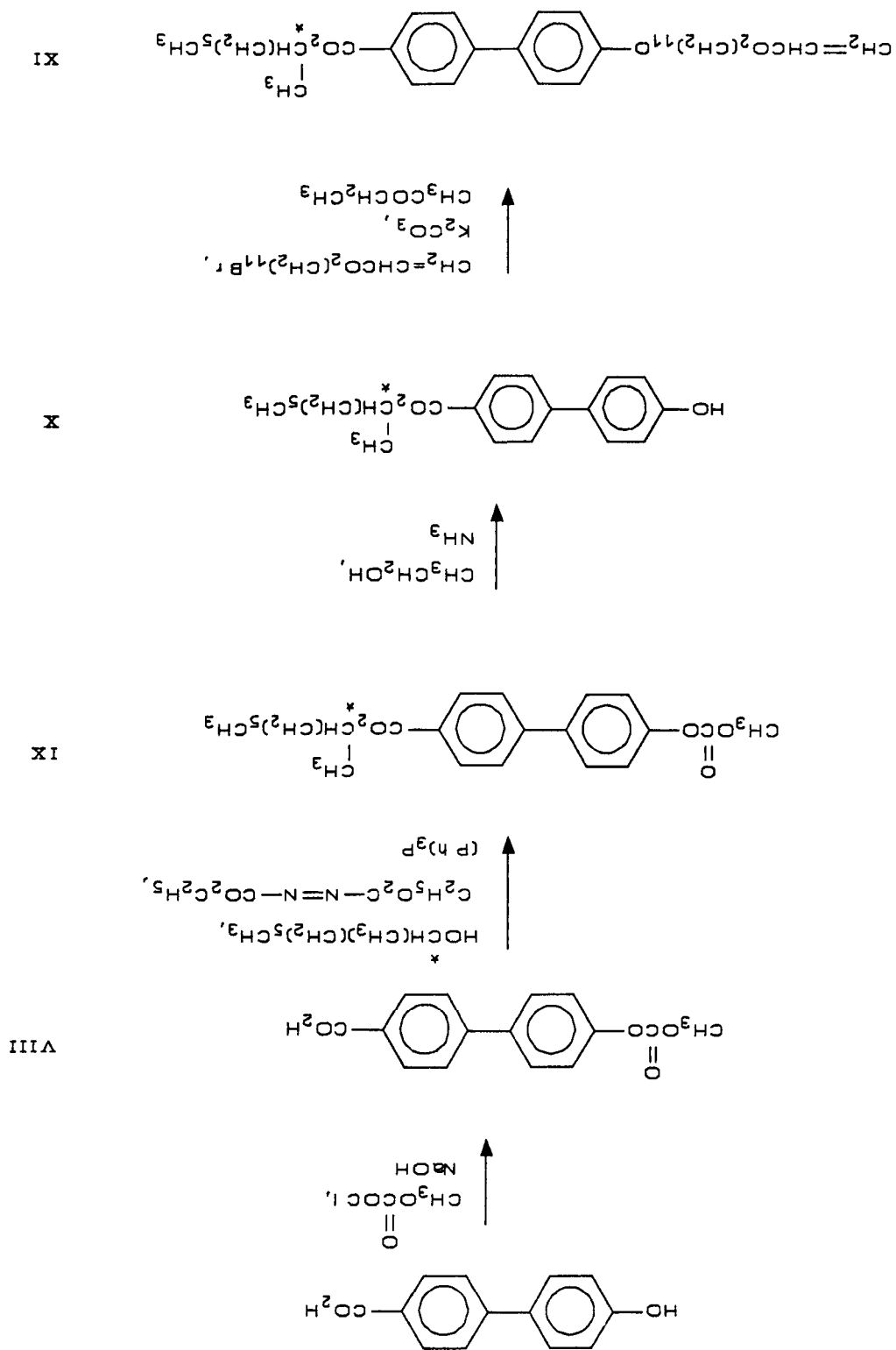
$\nu_{\max}(\text{KBr})/\text{cm}^{-1}$  3300 (C-H), 2220 (C $\equiv$ N), 1610 (C=O), 1250 (C-O);  
 $\delta_{\text{H}}(\text{CDCl}_3)$  1.50 (18H, m, CH<sub>2</sub>(CH<sub>2</sub>)<sub>9</sub>CH<sub>2</sub>), 4.00 (2H, t, CO<sub>2</sub>CH<sub>2</sub>OAr), 4.15 (2H, t, COOCH<sub>2</sub>(CH<sub>2</sub>)<sub>9</sub>), 5.75 (1H, d, OCH=CH<sub>2</sub>), 6.10 (1H, d, OCH=CH<sub>2</sub>), 6.45 (1H, d, OCH=CH<sub>2</sub>), 7.00 (2H, m, ArH), 7.55 (2H, m, ArH), 7.65 (4H, m, ArH);  
 m/z 418 (M<sup>+</sup>, 100 %).

#### **5.5.4 Preparation of 4'-Cyano-4-[11-(methacryloyloxy)undecoxy]biphenyl (VIId).**

$\omega$ -Bromoundecyl methacrylate	1.3 g, 4.2 mmol
4'-Cyano-4-hydroxybiphenyl	1.0 g, 4.2 mmol
Potassium carbonate	2.8 g, 20 mmol
Potassium iodide	0.1 g
Dry butanone	100 ml
Yield	white solid, 1.7 g (89 %).

m.p. = 90 - 92 °C.

$\nu_{\max}(\text{KBr})/\text{cm}^{-1}$  3300 (C-H), 2220 (C $\equiv$ N), 1610 (C=O), 1250 (C-O);  
 $\delta_{\text{H}}(\text{CDCl}_3)$  1.50 (18H, m, CH<sub>2</sub>(CH<sub>2</sub>)<sub>9</sub>CH<sub>2</sub>), 4.00 (2H, t, CO<sub>2</sub>CH<sub>2</sub>OAr), 4.20 (2H, t, COOCH<sub>2</sub>(CH<sub>2</sub>)<sub>9</sub>), 4.55 (3H, d, OC(CH<sub>3</sub>)=CH<sub>2</sub>), 5.55 (1H, d, OC(CH<sub>3</sub>)=CH<sub>2</sub>), 6.10 (1H, d, OC(CH<sub>3</sub>)=CH<sub>2</sub>), 7.00 (2H, m, ArH), 7.55 (2H, m, ArH), 7.65 (4H, m, ArH);  
 m/z 432 (M<sup>+</sup>, 100 %).



### 5.6.1 Preparation of 4'-Methoxycarbonyloxybiphenyl-4-carboxylic acid (VIII).

The preparation of compound VIII was carried out using a similar procedure to that described for the preparation of compound II (Scheme 2, Section 5.4.1).

4'-Hydroxybiphenyl-4-carboxylic acid	5.0 g, 0.023 mol
Sodium hydroxide	2.8 g, 0.07 mol
Water	500 ml
Methyl chloroformate	3.7 g, 0.04 mol

The voluminous white precipitate was filtered off, washed with water and recrystallised (glacial acetic acid) to yield white crystals of compound VIII, 5.1 g (78 %).

K 260 N 290 °C (dec).

$\nu_{\max}(\text{KBr})/\text{cm}^{-1}$  1770 (C=O), 1680 (C=O), 1280 (C-O);

$\delta_{\text{H}}(\text{CDCl}_3)$  3.95 (3H, s,  $\text{CH}_3\text{OCO}$ ), 7.35 (2H, m, ArH), 7.70 (4H, m, ArH), 8.20 (2H, m, ArH);

$m/z$  224 ( $\text{M}^+$ , 100 %).

### 5.6.2 Preparation of (S)-(+)-1-Methylheptyl 4'-methoxycarbonyloxybiphenyl-4-carboxylate (IX).

The preparation of compound IX was carried out using a similar procedure to that described for the preparation of compound IVa (Scheme 2, Section 5.4.3).

Triphenylphosphine	1.9 g, 0.0074 mol
--------------------	-------------------

Dry tetrahydrofuran	10 ml
4'-Methoxycarbonyloxybiphenyl-4-carboxylic acid (VIII)	2.0 g, 0.0074 mol
S-(+)-Octan-2-ol	1.0 g, 0.0074 mol
Diethylazodicarboxylate	1.3 g, 0.0074 mol
Dry tetrahydrofuran	10 ml
Yield	white solid, 1.5 g (54 %).

m.p. 230 - 234 °C.

$[\alpha]_D^{25} = +8.7^\circ$ .

$\nu_{\max}(\text{KBr})/\text{cm}^{-1}$  2970 (C-H), 1750 (C=O), 1650 (C=O), 1440 (C-H), 1250 (C-O);

$\delta_{\text{H}}(\text{CDCl}_3)$  1.50 (15H m  $\text{CH}_2(\text{CH}_2)_6\text{CH}_3$ ), 3.90 (3H, s,  $\text{CH}_3\text{OCO}$ ), 4.00 (2H, t,  $\text{OCH}_2\text{CH}_2$ ), 7.35 (2H, m,  $\text{ArH}$ ), 7.70 (4H, m,  $\text{ArH}$ ), 8.20 (2H, m,  $\text{ArH}$ );

$m/z$  384 ( $\text{M}^+$ , 100 %).

### 5.6.3 Preparation of (S)-(+)-2-Methylheptyl 4'-hydroxybiphenyl-4-carboxylate (X).

The preparation of compound X was carried out using a similar procedure to that described for compound Va (Scheme 2, Section 5.4.6).

(S)-(+)-2-Methylheptyl 4'-methoxycarbonyloxybiphenyl-4-carboxylate (IX)

	1.5 g, 3.9 mmol
Ethanol	50 ml
Ammonia (SG 0.88)	25 ml

Yield white solid, 0.3 g (25 %).

m.p. 79 - 81 °C.

$[\alpha]_{\text{D}}^{25} = +8.6^{\circ}$ .

$\nu_{\text{max}}(\text{KBr})/\text{cm}^{-1}$  2970 (C-H), 1750 (C=O), 1440 (C-H), 1250 (C-O);

$\delta_{\text{H}}(\text{CDCl}_3)$  1.50 (15H m  $\text{CH}_2(\text{CH}_2)_6\text{CH}_3$ ), 4.00 (2H, t,  $\text{OCH}_2\text{CH}_2$ ), 7.35 (2H, m,  $\text{ArH}$ ), 7.70 (4H, m,  $\text{ArH}$ ), 8.20 (2H, m,  $\text{ArH}$ );

m/z 334 ( $\text{M}^+$ , 100 %).

#### 5.6.4 Preparation of (S)-(+)-1-Methylheptyl

##### 4'-[11-(acryloyloxy)undecoxy]biphenyl-4-carboxylate (XI).

The preparation of compound XI was carried out using a similar procedure to that for the preparation of compound VIa (Scheme 2, Section 5.4.8).

$\omega$ -Bromoundecyl acrylate 0.2 g, 0.98 mmol

(S)-(+)-1-Methylheptyl 4'-hydroxybiphenyl-4-carboxylate  
0.3 g, 0.98 mmol

Potassium carbonate 0.9 g, 6.10 mmol

Potassium iodide 0.05 g

Dry butanone 50 ml

Yield white solid, 0.3 g (70 %).

m.p. = 75 °C (dec).

$[\alpha]_{\text{D}}^{25} = +7.6^{\circ}$ .

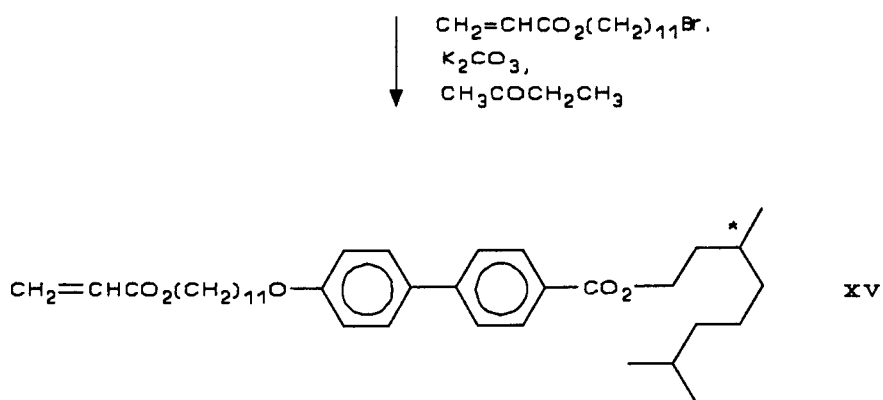
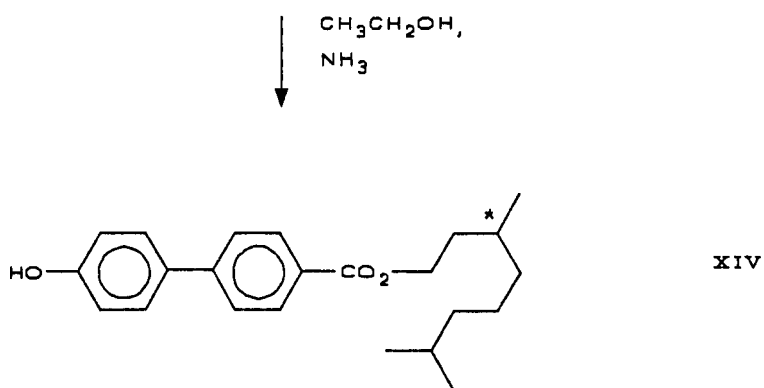
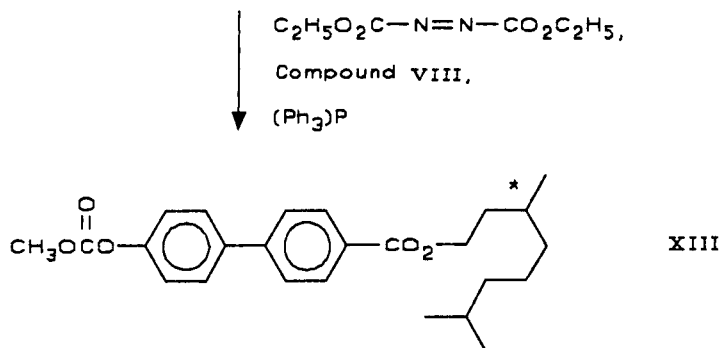
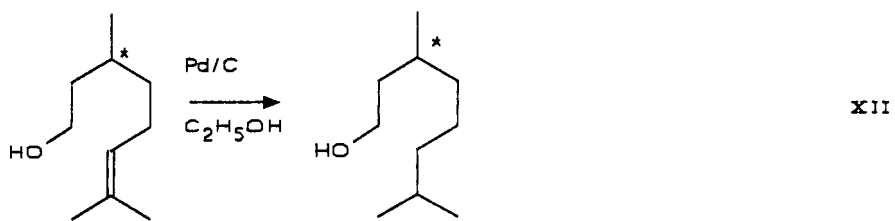
$\nu_{\text{max}}(\text{KBr})/\text{cm}^{-1}$  3300 (C-H), 2970 (C-H), 1610 (C=O), 1750 (C=O), 1440 (C-H),

1250 (C-O);

$\delta_{\text{H}}(\text{CDCl}_3)$  1.50 (33H, m,  $\text{CH}_2(\underline{\text{CH}}_2)_9\text{CH}_2$ ,  $\text{CH}_2(\text{CH}_2)_6\underline{\text{CH}}_3$ ), 4.00 (4H, m,  $\text{OCH}_2\underline{\text{CH}}_2$ ), 4.15 (2H, t,  $\text{COOCH}_2(\underline{\text{CH}}_2)_9$ ), 5.75 (1H, d,  $\text{OCH}=\underline{\text{CH}}_2$ ), 6.10 (1H, d,  $\text{OCH}=\underline{\text{CH}}_2$ ), 6.45 (1H, d,  $\text{OCH}=\underline{\text{CH}}_2$ ), 7.35 (2H, m,  $\text{ArH}$ ), 7.70 (4H, m,  $\text{ArH}$ ), 8.20 (2H, m,  $\text{ArH}$ );

$m/z$  502 ( $\text{M}^+$ , 100 %).

**5.7 SCHEME 5.**



### 5.7.1 Preparation of (S)-(-)-3,7-Dimethyl-1-octanol (XII).

(S)-(-)- $\beta$ -Citronellol (45.0 g, 0.29 mol) and palladium on charcoal (5 %, 4.5 g) in ethanol (500 ml) were stirred under a positive pressure of hydrogen at room temperature until no further hydrogen was taken up (5 h). The palladium on charcoal was filtered off (Hyflo) and the solvent was removed by distillation under reduced pressure. The remaining solution was distilled under reduced pressure, the fraction boiling at 100 - 103 °C, 0.5 mmHg, was collected as a colourless oil, 35.0 g (76 %).

$$[\alpha]_D^{25} = -5.7^\circ.$$

$\nu_{\max}$ (capillary film)/cm<sup>-1</sup> 3350 (O-H), 2980 (C-H), 1100 (C-O);

$\delta_{\text{H}}$ (CDCl<sub>3</sub>) 1.00 (6H, d, CH(CH<sub>3</sub>)<sub>2</sub>), 1.05 (3H, d, CHCH<sub>3</sub>), 1.50 (10H, m, CH<sub>2</sub>(CH<sub>2</sub>)<sub>n</sub>CH<sub>2</sub>), 3.55 (1H, m, HOCH<sub>2</sub>);

m/z 158 (M<sup>+</sup>, 100 %).

### 5.7.2 Preparation of (S)-(-)-3'',7''-Dimethyloctyl 4'-methoxycarbonyloxybiphenyl-4-carboxylate (XIII).

The preparation of compound **XIII** was carried out using a similar procedure to that described for the preparation of compound **IVa** (Scheme 2, Section 5.4.8).

Triphenylphosphine	1.9 g, 0.0074 mol
Dry tetrahydrofuran	10 ml
(S)-(-)-3,7-Dimethyl-1-octanol ( <b>XII</b> )	1.2 g, 0.0074 mol

**4'-Methoxycarbonyloxybiphenyl-4-carboxylic acid (VIII)**

1.7 g, 0.0074 mol

Diethyl azodicarboxylate

1.3 g, 0.0074 mol

Dry tetrahydrofuran

10 ml

Yield

yellow wax, 2.4 g (79 %).

K 234 N 246 °C I.

$[\alpha]_D^{25} = -5.3^\circ$ .

$\nu_{\max}$ (capillary film)/ $\text{cm}^{-1}$  2960 (C-H), 1760 (C=O), 1720 (C=O), 1300 (C-O);

$\delta_{\text{H}}$ ( $\text{CDCl}_3$ ) 1.00 (6H, d,  $\text{CH}(\text{CH}_3)_2$ ), 1.05 (3H, d,  $\text{CHCH}_3$ ), 1.50 (10H, m,

$\text{CH}_2(\text{CH}_2)_n\text{CH}_2$ ), 1.65 (1H, s,  $\text{CH}_3\text{OCO}$ ), 4.40 (2H, m,  $\text{OCH}_2\text{CH}_2$ ), 7.00 (2H, m,

$\text{ArH}$ ), 7.60 (4H, m,  $\text{ArH}$ ), 8.10 (2H, m,  $\text{ArH}$ );

$m/z$  412 ( $\text{M}^+$ , 100 %).

**5.7.3 Preparation of (S)-(-)-3'',7''-Dimethyloctyl 4'-hydroxybiphenyl-4-carboxylate (XIV).**

The preparation of compound XIV was carried out using a similar procedure to that described for the preparation of compound Va (Scheme 2, Section 5.4.5).

**(S)-(-)-3,7-Dimethyloctyl 4'-methoxycarbonyloxybiphenyl-4-carboxylate (XIII)**

1.5 g, mol

Ethanol

50 ml

Ammonia (SG 0.88)

25 ml

Yield

white solid, 1.9 g (90 %).

m.p. 260 °C (dec).

$[\alpha]_D^{25} = -5.9^\circ$ .

$\nu_{\max}(\text{KBr})/\text{cm}^{-1}$  2960 (C-H), 1720 (C=O), 1300 (C-O);

$\delta_{\text{H}}(\text{CDCl}_3)$  1.00 (6H, d,  $\text{CH}(\text{CH}_3)_2$ ), 1.05 (3H, d,  $\text{CHCH}_3$ ), 1.50 (10H, m,  $\text{CH}_2(\text{CH}_2)_n\text{CH}_2$ ), 3.75 (1H, s, ArOH), 4.40 (2H, m,  $\text{OCH}_2\text{CH}_2$ ), 7.00 (2H, m, ArH), 7.60 (4H, m, ArH), 8.10 (2H, m, ArH);

m/z 354 ( $\text{M}^+$ , 100 %).

#### 5.7.4 Preparation of (S)-(-)-3'',7''-Dimethyloctyl

#### 4'-[11-(acryloyloxy)undecyloxy]biphenyl-4-carboxylate (XV).

The preparation of compound XV was carried out using a similar procedure to that described for the preparation of compound VIa (Scheme 2, Section 5.4.8).

$\omega$ -Bromoundecyl acrylate 1.7 g, 5.3 mmol

(S)-(-)-3'',7''-Dimethyloctyl 4'-hydroxybiphenyl-4-carboxylate (XIV)

1.9 g, 5.3 mmol

Potassium carbonate 4.3 g, 33 mmol

Potassium iodide 0.1 g

Dry butanone 100 ml

Yield white solid, 1.5 g (50 %).

$\nu_{\max}(\text{KBr})/\text{cm}^{-1}$  2960 (C-H), 2930 (C-H), 1720 (C=O), 1600 (C=O), 1300 (C-O), 1200 (C-O);

$\delta_{\text{H}}(\text{CDCl}_3)$  1.00 (6H, d,  $\text{CH}(\text{CH}_3)_2$ ), 1.05 (3H, d,  $\text{CHCH}_3$ ), 1.50 (28H, m,

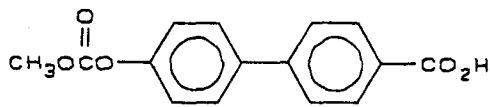
$\text{CH}_2(\underline{\text{CH}_2})_{14}\text{CH}_2$ ), 4.00 (2H, t,  $\text{OCH}_2\underline{\text{CH}_2}$ ), 4.25 (2H, t,  $\text{COOCH}_2(\underline{\text{CH}_2})_9$ ), 4.45 (2H, t,  $\text{COOCH}_2\underline{\text{CH}_2}$ ), 5.90 (1H, 2xd,  $\text{OCH}=\underline{\text{CH}_2}$ ), 6.20 (1H, 2xd,  $\text{OCH}=\underline{\text{CH}_2}$ ), 6.45 (1H, 2xd,  $\text{OCH}=\underline{\text{CH}_2}$ ), 7.00 (2H, m,  $\text{ArH}$ ), 7.60 (4H, m,  $\text{ArH}$ ), 8.10 (2H, m,  $\text{ArH}$ );

$m/z$  578 ( $\text{M}^+$ , 100 %).

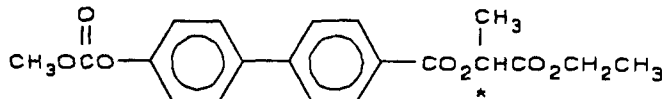
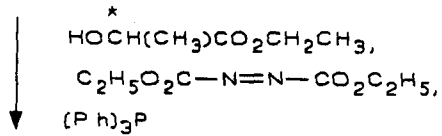
m.p. = 40 - 45 °C (dec).

$[\alpha]_{\text{D}}^{25} = -5.2^\circ$ .

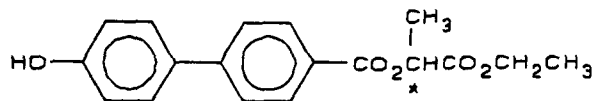
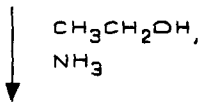
**5.8 SCHEME 6.**



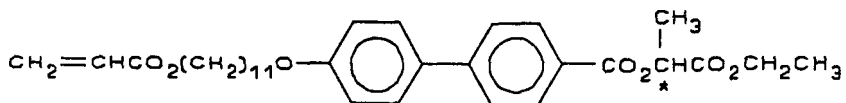
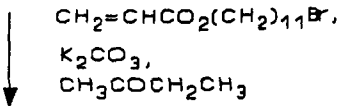
VIII



XVI



XVII



XVIII

**5.8.1 Preparation of (S)-(-)-Ethyl 2-(4'-methoxycarbonyloxybiphenyl-4-carboxyloxy)propanoate (XVI).**

The preparation of compound XVI was carried out using a similar procedure to that described for the preparation of compound IVa (Scheme 2, Section 5.4.3).

Triphenylphosphine	1.9 g, 0.0074 mol
Dry tetrahydrofuran	10 ml
(S)-(-)-Ethyl lactate	0.9 g, 0.0074 mol
4'-Methoxycarbonyloxybiphenyl-4-carboxylic acid (VIII)	2.0 g, 0.0074 mol
Diethyl azodicarboxylate	1.3 g, 0.0074 mol
Dry tetrahydrofuran	10 ml
Yield	white solid, 1.2 g (42 %).

m.p. = 240 °C (dec).

$[\alpha]_{\text{D}}^{25} = -9.5^{\circ}$ .

$\nu_{\text{max}}$ (KBr)/ $\text{cm}^{-1}$  3000 (C-H), 1770 (C=O), 1740 (C=O), 1710 (C=O), 1610 (C-O), 1250 (C-O);

$\delta_{\text{H}}$ ( $\text{CDCl}_3$ ) 1.40 (3H, t,  $\text{CO}_2\text{CH}_2\text{CH}_3$ ), 1.65 (3H, d,  $\text{CO}_2\text{CH}(\text{CH}_3)\text{CO}_2$ ), 3.95 (3H, s,  $\text{CH}_3\text{OCOOAr}$ ), 4.25 (2H, q,  $\text{CO}_2\text{CH}_2\text{CH}_3$ ), 5.35 (1H, q,  $\text{CO}_2\text{CH}(\text{CH}_3)\text{CO}_2$ ), 7.40 (2H, m, ArH), 7.60 (4H, m, ArH), 8.20 (2H, m, ArH);

m/z 372 ( $\text{M}^+$ , 100 %).

## 5.8.2 Preparation of (S)-(-)-Ethyl 2-(4'-hydroxybiphenyl-

### 4-carbonyloxy)propanoate (XVII).

The preparation of compound XVII was carried out using a similar procedure to that for the preparation of compound Va (Scheme 2, Section 5.4.5).

(S)-(-)-Ethyl 2-(4'-methoxycarbonyloxybiphenyl-4-carbonyloxy)propanoate (XVI)

1.2 g, 3.1 mmol

Ethanol 50 ml

Ammonia (SG 0.88) 25 ml

Yield white solid, 0.6 g (58 %).

m.p. = 240 °C.

$[\alpha]_{\text{D}}^{25} = -9.1^{\circ}$ .

$\nu_{\text{max}}(\text{KBr})/\text{cm}^{-1}$  3480 (O-H), 1740 (C=O), 1710 (C=O), 1605 (C-O), 1120 (C-O);

$\delta_{\text{H}}(\text{CDCl}_3)$  1.40 (3H, t,  $\text{CO}_2\text{CH}_2\text{CH}_3$ ), 1.65 (3H, d,  $\text{CO}_2\text{CH}(\text{CH}_3)\text{CO}_2$ ), 4.25 (2H, q,  $\text{CO}_2\text{CH}_2\text{CH}_3$ ), 5.35 (1H, q,  $\text{CO}_2\text{CH}(\text{CH}_3)\text{CO}_2$ ), 7.40 (2H, m, ArH), 7.60 (4H, m, ArH), 8.20 (2H, m, ArH);

m/z 314 ( $\text{M}^+$ , 100 %).

**5.8.3 Preparation of (S)-(-)-Ethyl 2-{4'-[11-(acryloyloxy)undecoxy]biphenyl-4-carboxyloxy}propanoate (XVIII).**

The preparation of compound XVIII was carried out using a similar procedure to that described for the preparation of compound VIa (Scheme 2, Section 5.4.8).

$\omega$ -Bromoundecyl acrylate 0.5 g, 1.8 mmol

(S)-(-)-Ethyl 2-(4'-hydroxybiphenyl-4-carboxyloxy)propanoate (XVII)

0.6 g, 1.8 mmol

Potassium carbonate 1.5 g, 10.9 mmol

Potassium iodide 0.05 g

Dry butanone 50 ml

Yield white solid, 0.5 g (48 %).

$\nu_{\max}(\text{KBr})/\text{cm}^{-1}$  3480 (O-H), 2960 (C-H), 1740 (C=O), 1710 (C=O), 1600 (C=O), 1605 (C-O), 1300 (C-O), 1200 (C-O), 1120 (C-O);

$\delta_{\text{H}}(\text{CDCl}_3)$  1.40 (3H, t,  $\text{CO}_2\text{CH}_2\text{CH}_3$ ), 1.50 (18H, m,  $\text{CH}_2(\text{CH}_2)_9\text{CH}_2$ ), 1.65 (3H, d,  $\text{CO}_2\text{CH}(\text{CH}_3)\text{CO}_2$ ), 4.15 (2H, t,  $\text{COOCH}_2(\text{CH}_2)_9$ ), 4.25 (2H, q,  $\text{CO}_2\text{CH}_2\text{CH}_3$ ), 4.45 (2H, t,  $\text{CH}_2\text{CH}_2\text{OAr}$ ), 5.35 (1H, q,  $\text{CO}_2\text{CH}(\text{CH}_3)\text{CO}_2$ ), 5.90 (1H, 2xd,  $\text{OCH}=\text{CH}_2$ ), 6.20 (1H, 2xd,  $\text{OCH}=\text{CH}_2$ ), 6.45 (1H, 2xd,  $\text{OCH}=\text{CH}_2$ ), 7.40 (2H, m, ArH), 7.60 (4H, m, ArH), 8.20 (2H, m, ArH);

$m/z$  642 ( $\text{M}^+$ , 100 %).

m.p. = 60 °C (dec).

$[\alpha]_{\text{D}}^{25} = -9.3^\circ$ .



The compounds shown in Scheme 7 were prepared by Merck (UK) and compound XIX (40.0 g) was supplied to us for use in our investigations into the optimum conditions necessary for free radical polymerization.

## **5.10 Polymerization Procedures.**

### **5.10.1 Polymerization of Methyl Methacrylate Using Group Transfer**

#### **Polymerization.** <sup>127</sup>

The method we adopted for group transfer polymerization was given to us by Dr J. Nemceck at ICI Chemicals and Polymers. The final procedure that we used for the production of our polymers using group transfer polymerization was a variation on the procedure used by ICI, which produced the most desirable results for our purposes.

#### **5.10.1.1 Purification of Starting Materials.**

Due to the air-sensitive nature of this type of reaction, preparation and handling of the starting materials and apparatus is a very important factor.

#### **5.10.1.1.1 Tetrabutylammonium Fluoride (Catalyst).**

Tetrabutylammonium fluoride was supplied (Aldrich) as a 1.0 M solution in tetrahydrofuran. The solution was diluted to 0.5 M by the addition of dry tetrahydrofuran and then purged to remove oxygen and moisture by slowly bubbling dry nitrogen through the solution for 24 h. Care was taken to ensure that the catalyst remained in solution. The purified solution was stored at 4 °C under an atmosphere of dry nitrogen.

An alternative procedure for the preparation of tetrabutylammonium fluoride was devised in which a 0.5 M solution was made up by dissolving the solid tetrabutylammonium fluoride (Aldrich) into dry tetrahydrofuran (freshly distilled from sodium and benzophenone). The solid was stored *in vacuo* over phosphorus pentoxide when not in use. Once the solution had been made, it was purged with dry nitrogen (to remove oxygen and moisture) and stored at 4 °C under an atmosphere of dry nitrogen.

#### **5.10.1.1.2 Methyl Trimethylsilyl Dimethylketene Acetal (Initiator).**

Methyl trimethylsilyl dimethylketene acetal (Aldrich) was distilled by short-path distillation under vacuum (water pump). The purified compound was stored at 4 °C under an atmosphere of dry nitrogen.

### **5.10.1.1.3 Methyl Methacrylate (Monomer).**

Methyl methacrylate (99 %, Fluka) was passed down a short column (15 cm) of dry neutral alumina, under a positive pressure of dry nitrogen, to remove the inhibitor. The purified monomer was stored at 4 °C under an atmosphere of dry nitrogen.

All the reagents had a useful lifetime of 4 days once they had been purified and stored according to the procedures previously described.

### **5.10.1.2 Group Transfer Polymerization.**

A series of experiments was carried out in order to ascertain the best ratio of monomer:initiator:catalyst. The general procedure for the polymerization of methyl methacrylate is given overleaf. In the course of the experiments the optimum ratio of initiator to catalyst was found, and then this optimum ratio was used with varying amounts of the monomer.

All apparatus used was thoroughly dried (110 °C for 1 h) prior to use, and purged with dry argon throughout the experiment.

The apparatus used for the large scale preparation of poly(methyl methacrylate) using group transfer polymerization had to be built based upon equipment used at ICI Chemicals and Polymers. After a number of modifications the final version of our

group transfer polymerization assembly, seen diagrammatically in Figure 5.3, was made. The apparatus was designed so that the system could be thoroughly purged of all oxygen and moisture prior to use. The subsequent additions of all reagents for the reaction were then carried out *via* syringes, with the appropriate care being taken when handling air-sensitive reagents. The only reagent not added *via* a syringe was the tetrahydrofuran which was distilled from sodium and benzophenone directly into the reaction vessel.

#### **5.10.1.2.1 General Procedure.**

Using the apparatus shown in Figure 5.3, methyl methacrylate (15 g, 0.15 mol) and tetrabutylammonium fluoride (0.5 ml, 0.5 M) were delivered by syringe to the reaction vessel which contained freshly distilled tetrahydrofuran (100 ml), with efficient stirring. Methyl trimethylsilyl dimethylketene acetal (1.0 ml) was added steadily by syringe, the speed of addition was important due to the instantaneous nature of the reaction and the large exotherm that accompanied it. Once the temperature had begun to fall the reaction was complete. Efficient stirring was continued while the reaction mixture was allowed to cool to room temperature (1 h). The reaction mixture was quenched by the addition of methanol (5 ml) *via* a syringe, the reaction mixture was stirred for a further 30 min and then the poly(methyl methacrylate) was precipitated by addition to a large volume of 1:1 methanol:distilled water (1500 ml), with vigorous stirring. The resulting poly(methyl methacrylate) was then filtered off and dried *in vacuo*. Care was taken throughout the described procedure to prevent the introduction

of water or oxygen into the apparatus.

An alternative piece of apparatus was designed which had several advantages over the large apparatus shown in Figure 5.3. A schematic representation of the apparatus, using a Schlenk tube, is shown in Figure 5.4. The advantages of this piece of apparatus were as follows.

- 1) The quantities of reagents could be scaled down ( $\approx 1$  g monomer), which was important when considering the polymerization of mesogenic monomers.
- 2) The whole apparatus could be flame dried prior to use, much faster and more efficiently than the large apparatus.
- 3) Multiple reactions could now be carried out in a day.

Using the Schlenk tube apparatus the reaction procedure was similar to that outlined for the large apparatus except that all the reagents were now scaled down using the quantities necessary to polymerize methyl methacrylate (1.0 g, 0.01 mol).

Results from this investigation into group transfer polymerization are given in the Results and Discussion Section (Section 6.1).

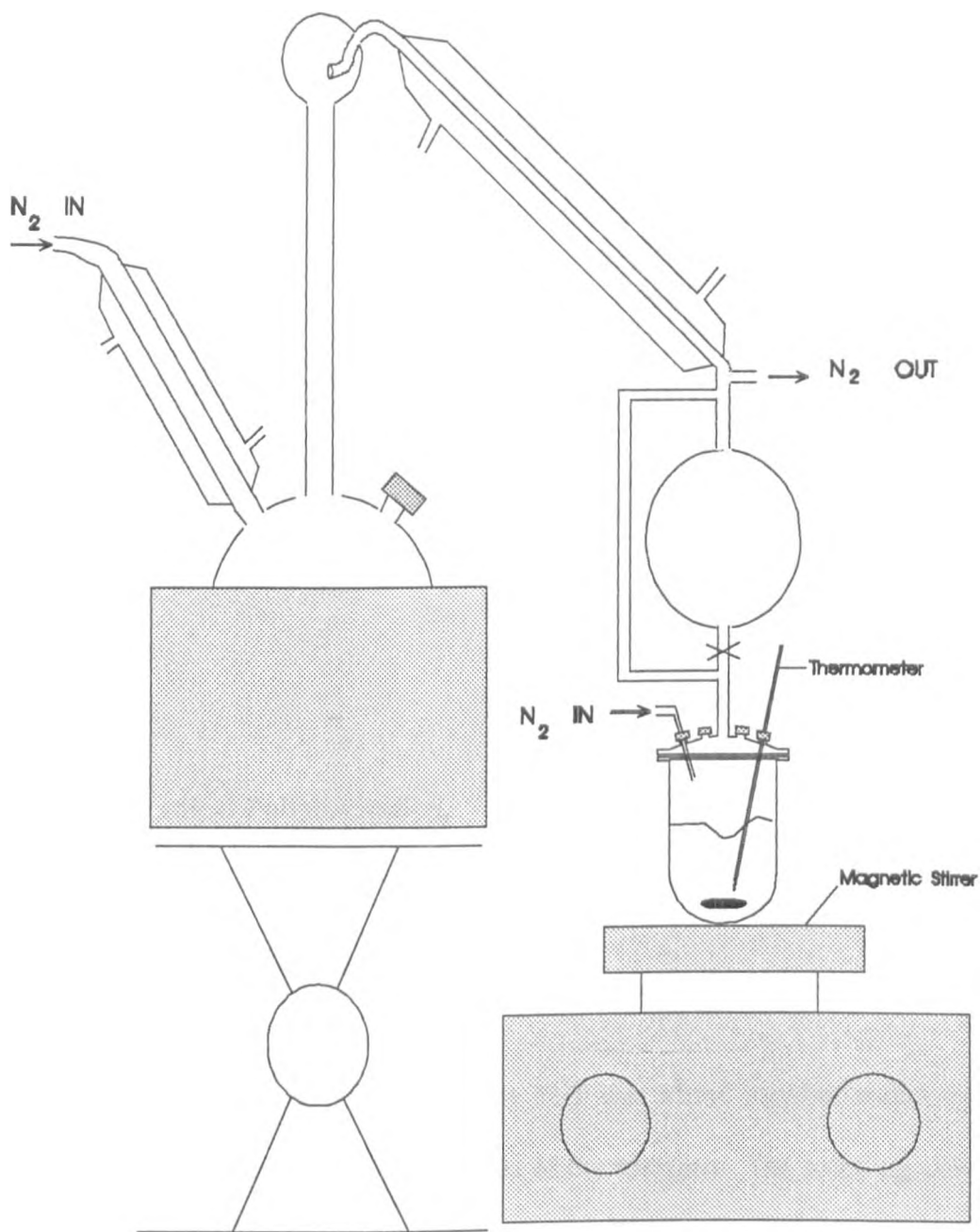


**Figure 5.3** A schematic representation of the large apparatus used to carry out group transfer polymerization.

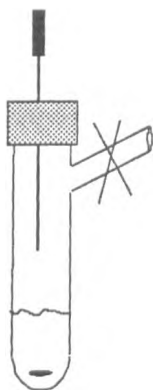


**Figure 5.4** A schematic representation of the modified apparatus for carrying out Group Transfer Polymerization.

## 5.10.2 Free Radical Polymerization.

### 5.10.2.1 Literature Procedure.<sup>128</sup>

A 10 % solution w/w of the monomer in dry THF was stirred together with 1 mol % AIBN for 6 h at 50 °C under an atmosphere of dry nitrogen. The resulting polymer was precipitated by the addition of methanol, filtered off and dried *in vacuo*.

### 5.10.2.2 Modified Procedure.

A solution of the appropriate monomer (1.0 g) and AIBN (1 mol %) in dry dichloromethane (10 ml) was stirred at 50 °C under an atmosphere of dry nitrogen for

24 h. The resulting polymer was precipitated repeatedly from dichloromethane by the addition of methanol until the polymer was free from any residual monomer, monitored by tlc (silica gel, dichloromethane). The polymer was reclaimed from the precipitation by the use of a centrifuge (4500 r.p.m., 30 min). Typically 8 - 10 precipitations were necessary to remove all the residual monomer. Prior to the final precipitation, the solution of polymer in dichloromethane was passed through a micro-pore filter (5  $\mu\text{m}$  pore size) to remove any undissolved solid material.

Results from the investigations into free radical polymerization are given in the Results and Discussion Section (Section 6.2)

### **5.10.3 Preparation of SCLC Cyclic Polysiloxanes.<sup>92</sup>**

The general preparation of the SCLC cyclic polysiloxanes is given below. The transition temperatures and GPC data for these polymers are given in the Results and Discussion Section (Section 6.5). The cyclic polysiloxane backbones used in the work described in this thesis are commercially available from Petrarch.

#### **5.10.3.1 Preparation of Hexachloroplatinic Acid (Speier's catalyst).<sup>130</sup>**

Chloroplatinic acid hexahydrate ( $\text{H}_2\text{PtCl}_6 \cdot 6\text{H}_2\text{O}$ ) (1 g, 2.4 mmol) was dissolved in isopropyl alcohol (20 ml). This stock solution was stored at 4 °C and used within 2

weeks of preparation.

### **5.10.3.2 Hydrosilylation of Cyclic Polysiloxanes.**

To a mixture of the appropriate cyclic polysiloxane (Petrarch)(0.1 g, 1.67 mmol Si-H) and the appropriate side chain alkene (1.83 mmol) in dry toluene (20 ml), the catalyst solution was added to give a Pt/alkene ratio in the range  $1/10^3$  to  $1/10^6$  (the ratio being dependent upon the side chain being used). The mixture was heated under reflux for 5 - 48 h, until no Si-H was detectable by infrared spectroscopy ( $2140\text{ cm}^{-1}$ ). The polymer was isolated by precipitation into methanol. The polymer was purified by precipitation of the polymer in dichloromethane by the addition of methanol. This was repeated until the polymer was free from residual alkene, which was monitored by tlc (silica gel, dichloromethane). The polymer was reclaimed from the precipitation by the use of a centrifuge (4500 r.p.m., 30 min). Typically 8 - 10 precipitations were necessary to remove all the residual alkene. Prior to the final precipitation, the solution of polymer in dichloromethane was passed through a micro-pore filter (5  $\mu\text{m}$  pore size) to remove any undissolved solid material.

### **5.11 Microscopic Identification of Liquid Crystalline Phases.**

The lack of good alignment procedures for SCLC polymers is not just a major obstacle in realising the full potential of these polymers for a number of applications

*e.g.* nonlinear optics, display devices, pyroelectric devices *etc.*, but it is also a major factor as to why phases exhibited by SCLC polymers are difficult to identify. Even in X-ray diffraction studies, which is considered to be one of the most reliable techniques for the identification of phases exhibited by low molar mass (LMM) liquid crystalline materials, difficulties have arisen due to the poor alignment of SCLC polymers using traditional alignment techniques.

The establishment of a good alignment procedure for SCLC polymers is therefore a very important area in liquid crystal polymer research and a substantial part of this thesis is devoted to this theme.

When a sample of a SCLC polymer is heated into its isotropic state on a clean microscope slide under a cover slip, and then allowed to cool to room temperature, the typical "sandy" texture is observed. Unlike LMM liquid crystalline samples which show characteristic defect textures (see Goodby and Gray<sup>131</sup> for a more detailed description of LMM liquid crystal defect textures), SCLC polymer samples often tend only to display the "sandy" texture (see Plate 1). It is not possible to assign the type of liquid crystalline phase from such a texture since it is devoid of textural features. It was found that it was sometimes possible to encourage a defect texture which could be used to identify the phase from a sandy texture by annealing the sample at 5 °C below the phase transition for long periods of time. Annealing times could vary from just a few hours to 2 - 3 days, and in extreme cases up to 2 weeks (see Plate 2). On other occasions, even the annealing process just described failed to produce any change in the sandy texture. Plate 2 shows the focal conic texture of the smectic A

phase formed by annealing the "sandy" texture of Polymer XIX just below its transition temperature. The effect on annealing a SCLC polymer sample to produce an identifiable liquid crystalline defect texture appeared to vary in relation to:

- 1) the type of polymer backbone (polysiloxane, polyacrylate, polymethacrylate, polyester);
- 2) the degree of polymerization ( $\overline{DP}$ );
- 3) the mesogenic side chains.

In order to try to promote the formation of identifiable liquid crystalline defect textures, it was necessary to attempt to physically align the liquid crystalline moieties.

The starting point that was chosen for this investigation were some procedures that had been successfully used for the alignment of LMM liquid crystals.<sup>132</sup> Two particular types of alignment were tried in order to try to enhance the propensity of a SCLC polymer to express both homogeneously and homeotropically aligned defect structures. The homogeneous alignment involved the use of nylon 6,6 and the homeotropic alignment involved the use of trichloro-octadecylsilane. Detailed procedures for carrying out both the alignment techniques are given later.

### **5.11.1 Microscope Slide Preparation.**

Before any aligning agent was applied to the microscope slides, the slides were first cleaned by using the following procedure. The slides were dipped successively in;

- 1) distilled water,
- 2) acetone (AnalaR),
- 3) distilled water,
- 4) 10 % w/w nitric acid solution,
- 5) distilled water,
- 6) acetone (AnalaR),

and then allowed to dry naturally in the air in a dust-free environment. Once dried the aligning agent could then be applied to the microscope slide.

### **5.11.2 Homogeneous Alignment.**

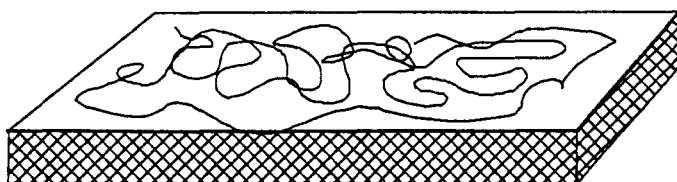
The procedure that was used for this type of alignment was similar to that described by Patel *et al.*<sup>132</sup> A 1 % w/w solution of nylon 6,6 in formic acid was prepared by heating a mixture of the appropriate weights of nylon 6,6 in formic acid, under reflux conditions, until all the nylon had dissolved. Clean dry microscope slides prepared as described in Section 5.11.1, were then dipped into the 1 % nylon solution, removed and allowed to dry vertically at room temperature in a dust-free environment. Once dry the coated slides were rubbed, several times, in one direction on a piece of lint-free cloth using very slight downward pressure. The pressure applied was not sufficient to cause grooves in the nylon surface, but the heat formed by the friction at the nylon surface, means that the temperature was raised above the glass transition temperature for the nylon. The polymer chains in the nylon were then able to move and they became aligned along the direction of rubbing. Once the friction was

removed the temperature cooled rapidly to a temperature below the glass transition temperature of the nylon and the nylon polymer chains were "locked" into their aligned position. The slide was then stored in a dust-free environment until required. The alignment of the SCLC polymer is created by the liquid crystalline moieties aligning along the aligned nylon polymer parallel to the surface of the microscope slide (see Figure 5.5).

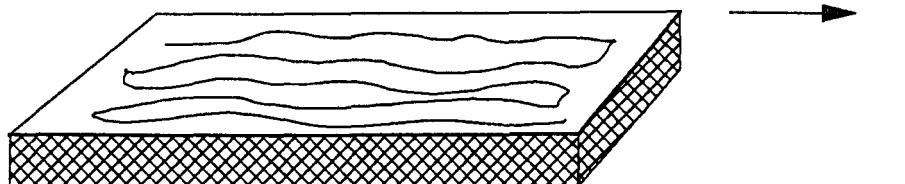
### **5.11.3 Homeotropic Alignment.**

The procedure for the preparation of slides for the production of homeotropic alignment was very similar to that described in Section 5.11.2 for homogeneous alignment, except that the alignment solution that was used was 1 % w/w trichlorooctadecylsilane in dry tetrahydrofuran. Once the slide had been dipped and dried no further treatment of the slide was necessary. Other agents for homogeneous alignment that were tried were trichloro-octylsilane and chlorodimethyloctadecylsilane in dry tetrahydrofuran, however these were less successful than trichlorooctadecylsilane at producing good quality homeotropic alignment. The alignment is caused by the long chains of the silane being held perpendicular at the surface of the microscope slide by the reactive chloro-groups, and the liquid crystalline moieties align themselves with the silane groups using Van der Waals forces (see Figure 5.6).

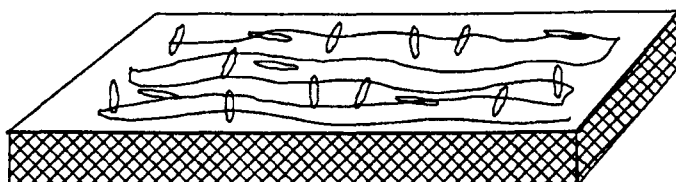
1) Slide dipped in Nylon 6,6



2) Rub in one direction



3) Apply SCLC polymer



4) Anneal just below transition temperature of SCLC polymer

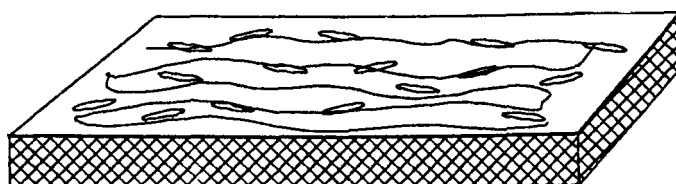


**Figure 5.5** The preparation of homogeneously aligned SCLC polymers.

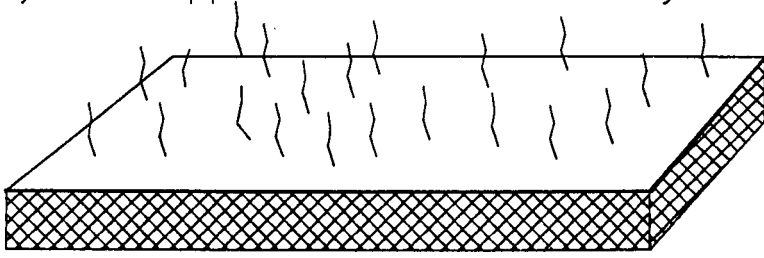
#### **5.11.4 Sample Preparation.**

A small quantity (spatula tip) of the polymer to be examined was placed onto a microscope slide, pretreated with the appropriate aligning agent as outlined in Sections 5.11.2 and 5.11.3, and heated gently into its isotropic state. A microscope cover slip was placed over the isotropic sample, and pressed down firmly so that the polymer melt spread evenly between the microscope slide and the cover slip. The preparation was allowed to cool to room temperature and then examined under the polarising microscope at the appropriate temperatures.

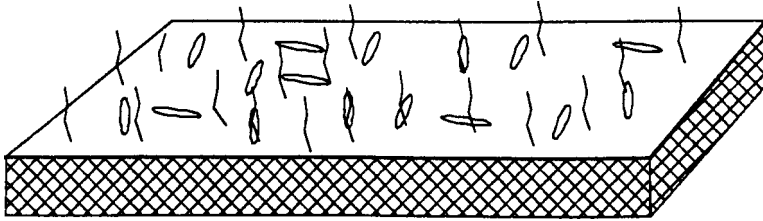
As well as using the techniques described previously to align the polymers described in this thesis, a large number of polymers synthesized by other research groups were also aligned using these techniques and their phase or phases identified by optical microscopy. In particular many samples produced by Merck (UK) were examined this way as part of our collaboration under a MOD contract. Other polymers produced by members of the Liquid Crystal Group at the University of Hull were also examined by these techniques.<sup>27</sup>

The results of work carried out on aligning SCLC polymers are summarised in the Results and Discussion Section (Section 6.1)

1) Slide dipped in trichloro-octadecylsilane



2) Apply SCLC polymer



3) Anneal just below transition temperature of SCLC polymer

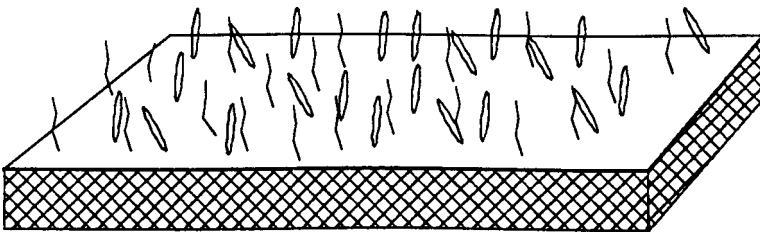


**Figure 5.6** The preparation of homeotropically aligned SCLC polymers.



*Results*  
*and*  
*Discussion*

## **6. RESULTS AND DISCUSSION.**

### **6.1 Group Transfer Polymerization.**

#### **6.1.1 Polymerization of Methyl Methacrylate.**

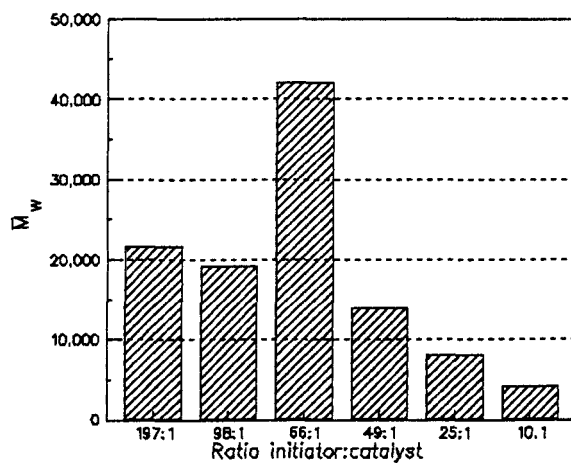
The results obtained for the polymerization of methyl methacrylate by GTP, using the large apparatus in conjunction with the procedure described in Section 5.10.1, are summarised in Table 6.1, and illustrated graphically in Figure 6.1. Methyl methacrylate was chosen as the monomer for this study due to the fact that ICI had demonstrated the technique using this monomer. Therefore it was known that methyl methacrylate could be reproducibly polymerized by the procedures described. The results show that a wide variety of different sized polymers can be produced using a fixed quantity of monomer and varying the ratio of initiator:catalyst. There appears to be an optimum ratio of initiator:catalyst which produces polymers with the highest  $\bar{M}_n$  and  $\bar{M}_w$  values together with the lowest polydispersity ( $\bar{M}_w/\bar{M}_n$ ) values. The optimum conditions found from averaging many replicate reactions suggest that a ratio of initiator:catalyst of around 66:1 consistently produced polymers of maximum size and minimum polydispersity.

A summary of the results found for the polymerization of methyl methacrylate by GTP using the small apparatus in conjunction with the conditions described in Section 5.10.1 is shown in Table 6.2, and illustrated graphically in Figure 6.2. The results indicate the same optimum conditions as those already shown for the large apparatus.

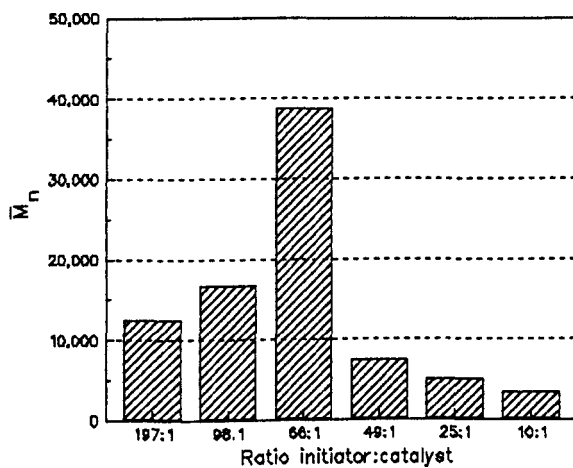
The reaction procedure was identical to that as used on the large apparatus, only the apparatus and the scale of reaction were altered. It was necessary to consider using the small scale apparatus due to the fact that it is not feasible to polymerize at least 10 g of monomer for each polymerization in a research environment. The synthesis of the mesogenic monomers is not practical on such a large scale as would be necessary. The errors due to measuring quantities of reactants are much larger for small quantities. The results shown in Table 6.3, which indicate that although the optimum conditions are 66:1 initiator:catalyst for both large and small scale reactions, the large scale reactions produced much larger polymers. The results of all the GPC work quoted in this thesis are relative to polystyrene standards, therefore the actual figures are not really meaningful but comparisons between polymers with similar structures are valid.

Monomer Volume /ml	Initiator Volume (I) /ml	Catalyst Volume (C) /ml	Ratio Initiator:Catalyst	$\bar{M}_w$	$\bar{M}_n$	$\bar{M}_w/\bar{M}_n$
15.0	1.0	0.05	197:1	21600	12500	1.7
15.0	1.0	0.10	98:1	19200	16700	1.2
15.0	1.0	0.15	66:1	42100	38800	1.1
15.0	1.0	0.20	49:1	14000	7400	1.9
15.0	1.0	0.40	25:1	8140	5050	1.6
15.0	1.0	0.82	10:1	4280	3380	1.3

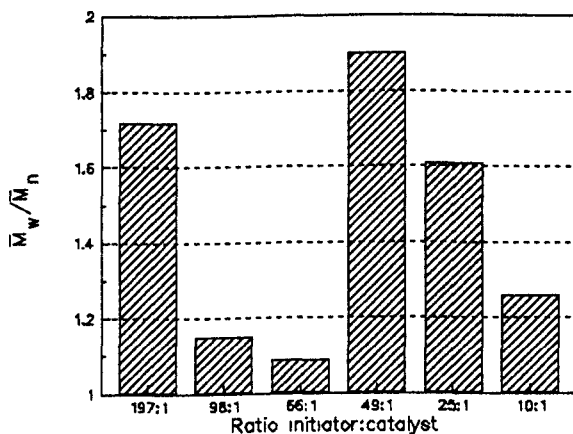
**Table 6.1** GPC data for large scale GTP of methyl methacrylate.



a)



b)

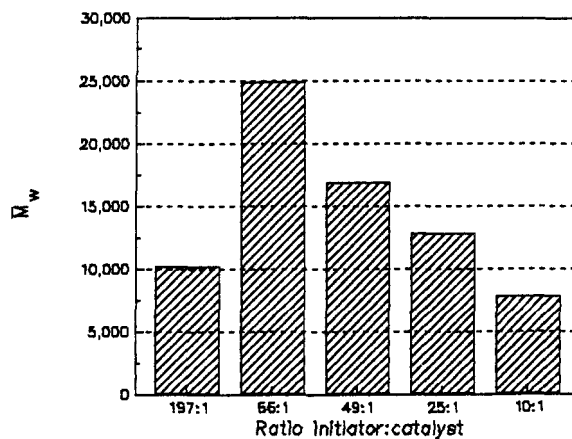


c)

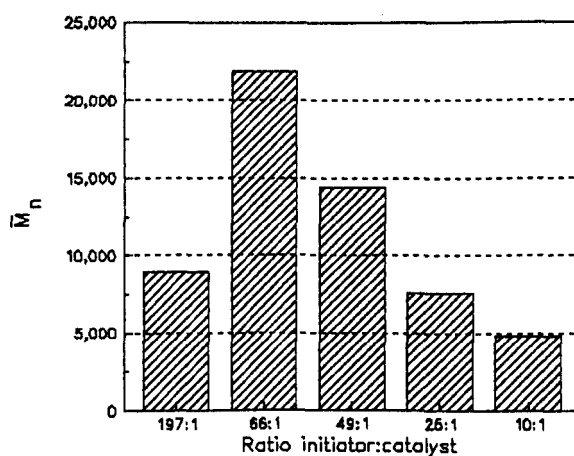
**Figure 6.1** Effect of the ratio of initiator:catalyst (I:C) for the polymerization of methyl methacrylate by GTP (large apparatus).

Monomer Volume /ml	Initiator Volume (I) /ml	Catalyst Volume (C) /ml	Ratio Initiator:Catalyst	$\bar{M}_w$	$\bar{M}_n$	$\bar{M}_w/\bar{M}_n$
1.0	0.003	0.07	197:1	10200	8950	1.1
1.0	0.010	0.07	66:1	24900	21900	1.1
1.0	0.013	0.07	49:1	16900	14400	1.2
1.0	0.027	0.07	25:1	12850	7590	1.7
1.0	0.055	0.07	10:1	7755	4825	1.6

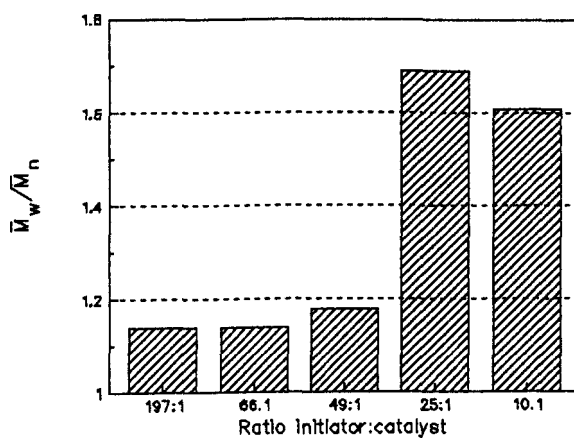
**Table 6.2** GPC data for small scale GTP of methyl methacrylate.



a)



b)



c)

**Figure 6.2** Effect of the ratio of initiator:catalyst (I:C) for the polymerization of methyl methacrylate by GTP (small apparatus).

Initiator:Catalyst	Property	Large Scale	Small Scale	Comments
	$\bar{M}_w$	42100	24900	
66:1	$\bar{M}_n$	38300	21900	Best Results
	$\bar{M}_w/\bar{M}_n$	1.1	1.1	(Highest $\bar{DP}$ )
	$\bar{M}_w$	4280	7755	
10:1	$\bar{M}_n$	3380	4825	Worst Results
	$\bar{M}_w/\bar{M}_n$	1.3	1.6	(lowest $\bar{DP}$ )

**Table 6.3** A comparison of GPC results for large and small scale GTP reactions.

The optimum conditions found from this group of replicate reactions again leads to the conclusion that the ratio of initiator:catalyst should be optimized at 66:1.

The results from both of the above experiments indicate that the ratios of initiator:catalyst which produce the largest  $\bar{M}_n$  and smallest  $\bar{M}_w/\bar{M}_n$  are between 50:1 and 100:1. The larger  $\bar{M}_n$  and  $\bar{M}_w$  values obtained for the polymers produced using the large apparatus were probably due to the difficulty in measuring accurately the quantities of reagents needed for the small apparatus.

In order to investigate whether the polymer system was "living" as is claimed in the literature,<sup>53</sup> a set of experiments was devised in which a further addition of monomer was made after the initial reaction had taken place. Aliquots were taken before and after the addition of a further sample of the monomer, and no significant increase in molecular weight was found after the addition of the extra amount of monomer, leading to the conclusion that under these particular conditions the polymer that was

formed was not "living" once the initial reaction had taken place. This was repeated a number of times and on all occasions the polymer was not "living".

### 6.1.2 Polymerization of Mesogenic Moieties.

The conditions that enabled the production of non-mesogenic polymers with the largest degree of polymerization and smallest polydispersity were used in the attempt to polymerize the mesogenic monomer shown in Figure 6.3. Many attempts were made to polymerize this monomer. A variety of different conditions were used during this part of the study. The starting point was using the large apparatus with 66:1 initiator:catalyst, the conditions that had previously been found to be optimal for the polymerization of methyl methacrylate. After several failures, other ratios of initiator:catalyst (50:1 - 100:1) were tried but with no success. The polymerization of monomer VIIg was also attempted using the small apparatus and various ratios of initiator:catalyst. However these polymerizations did not prove successful, only rarely did any reaction occur at all. It was not possible to correlate the reaction conditions and the  $\bar{M}_w$ ,  $\bar{M}_n$  and  $\bar{M}_w/\bar{M}_n$  values of the polymers. When a reaction did occur, GPC results showed that the product was a small oligomer.

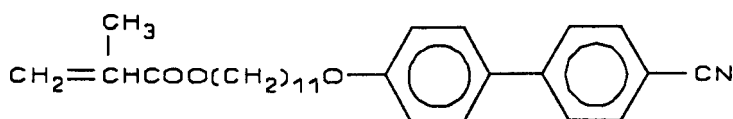


**Figure 6.3** The mesogenic moiety VIIg used for group transfer polymerization.

The monomer shown in Figure 6.3 was polymerized by the above procedure described for GTP on a small scale with the following results;

$$\bar{M}_w = 2220; \bar{M}_n = 2200 (\bar{DP} \approx 5); \bar{M}_w/\bar{M}_n = 1.0.$$

Transition temperatures measured by DSC

$$K 66 S_A 79 \text{ } ^\circ\text{C I}$$

Several attempts were made to polymerize the corresponding acrylate monomer (**VIIIf**), but no polymerization was observed. This observation agrees with literature observations,<sup>53</sup> that it is more difficult to polymerize acrylates than methacrylates.

Even though special attention was paid to exclude all oxygen and moisture from the apparatus and that all reagents used in GTP were very pure, this method of polymerizing mesogenic monomers **VIIIf** and **VIIIfg** failed to produce polymers of high molecular weight.

The major consequence of the failure of the polymerization of mesogenic moieties by group transfer polymerization was that an alternative method for the production of polymers having a high degree of polymerization and a low polydispersity became necessary.

## 6.2 Free Radical Polymerization.

### 6.2.1 Literature Procedure.

Methods for polymerizing mesogenic acrylates and methacrylates using free radical polymerization were available from the literature,<sup>128, 137</sup> and these procedures were chosen as the starting point for the production of side chain liquid crystal polyacrylates and polymethacrylates. In general  $\alpha, \alpha'$ -azoisobutyronitrile (AIBN) was used as the free radical initiator in a dry solvent, such as tetrahydrofuran (THF), under an atmosphere of dry nitrogen. The free radicals were produced from the AIBN by the application of heat to the stirred reaction mixture. The literature procedure given in Section 5.10.2 was used to polymerize the mesogenic monomer **VIII**f several times.

The resulting polymers were analyzed by gel permeation chromatography (GPC) and differential scanning calorimetry (DSC). The results given below show that the polymers that were produced had degrees of polymerization ( $\bar{DP}$ ) between 10 and 15, and polydispersities of 1.2 - 1.5.

$$\bar{M}_w = 5390; \bar{M}_n = 4540 (\bar{DP} \approx 10); \bar{M}_w/\bar{M}_n = 1.2.$$

The transition temperatures measured by DSC

$$g \ 12^\circ S_A \ 129^\circ C \ I$$

In studies involving the investigation of the structure of the polymer on their thermal, rheological and physical properties, polymers with such low  $\bar{DP}$  values are unacceptable due to the variation of transition temperatures with degree of polymerization as

explained in Section 3.3.2.1. It was therefore necessary to refine the polymerization procedure in order to consistently produce polymers with a degree of polymerization around 50. Similar low degrees of polymerization from free radical reactions were also found for other mesogenic systems by a number of research workers including several members of the Liquid Crystal group here at the University of Hull and also by Merck (UK), with whom we were collaborating as part of a MOD contract with the DRA (RSRE, Malvern).

A series of experiments was devised in order to try to increase the  $\bar{DP}$  values of polyacrylates and polymethacrylates produced by using free radical polymerization. The experiments involved changing various parameters of the polymerization process and analysing the effect that the changes had upon the physical properties of the polymers that were produced. Four simple non-mesogenic monomers were chosen for this study *i.e.* methyl methacrylate, methyl acrylate, ethyl methacrylate and ethyl acrylate, and the following parameters of the free radical polymerization procedure were changed consecutively.

- 1) The concentration of initiator.
- 2) The concentration of monomer.
- 3) The reaction solvent.
- 4) The design of the vessel in which the polymerization was carried out.
- 5) The production of free radicals from AIBN by using ultrasound instead of elevated temperatures.

The main aim of this study was to establish the optimum conditions necessary to

produce simple polymers with high molecular weights using free radical polymerization and then to apply these conditions to polymerize mesogenic monomers.

## **6.2.2 Polymerization of Simple Acrylates and Methacrylates.**

### **6.2.2.1 Effect of the Solvent.**

The results of the effect of the solvent on the free radical polymerization of the four non-mesogenic monomers *i.e.* methyl methacrylate, methyl acrylate, ethyl methacrylate and ethyl acrylate, are given in Table 6.4, and summarised graphically in Figures 6.4, 6.5, 6.6 and 6.7. The following amounts of reagents were employed for the free radical polymerization of the monomers using a similar procedure to that outlined in Section 5.10.2.2.

monomer	1.0 g
solvent	10 ml
AIBN	1 mol %

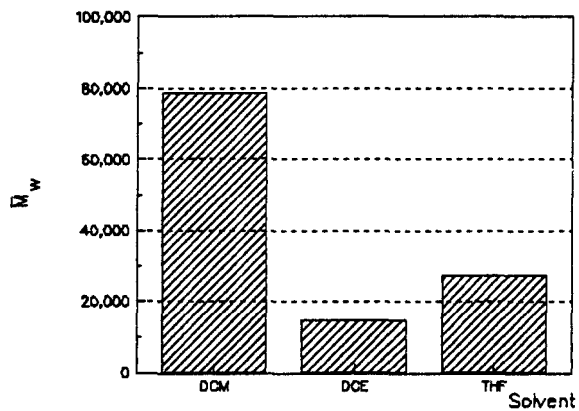
The reaction mixture was heated at 60 °C under an atmosphere of dry nitrogen for 24 h. The choice of solvent for this study from the wide range of commercially available solvents was limited by their ability to dissolve high molecular weight polymers. In order for the polymerization process to produce high molecular weight polymers, the growing free radical polymer chain must remain in solution. Keeping the growing polymer chain in solution means that the chain can react with the

monomer in the solution, thus lengthening the polymer chain. The solvents that were chosen for use throughout this study were, tetrahydrofuran (THF), dichloromethane (a good solvent for polymers that is sometimes used as the mobile phase in GPC) and 1,2-dichloroethane (similar properties to dichloromethane but has a higher boiling point (84 °C)). Benzene and toluene have also been used by other members of the Liquid Crystal group here at the University of Hull, but the use of these solvents in free radical polymerization of acrylates and methacrylates resulted in polymers with a  $\bar{DP}$  of  $\approx 10$ .<sup>134</sup> Toluene was also used as a solvent in a series of experiments carried out to assess the usefulness of ultrasound in the polymerization of mesogenic monomers. The work was carried out at Coventry Polytechnic with the guidance of Dr.P. Lorimer, and involved a variety of different ultrasound generators *e.g.* Kerry ultrasonic bath (35 - 40 kHz), Undatim ultrasonic probe (20, 40, 60 kHz) and the Megason ultrasonic probe (80 kHz).

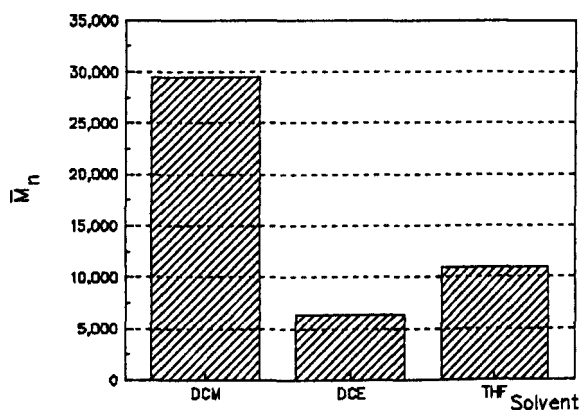
All the reactions carried out at Coventry Polytechnic failed to produce SCLC polymers, even those where heat was used to aid the generation of the radicals. This failure to polymerize the mesogenic monomers was later traced to the use of toluene as the reaction solvent.

Monomer	Solvent	Average of at least three polymerizations		
		$\bar{M}_w$	$\bar{M}_n$	$\bar{M}_w/\bar{M}_n$
Methyl methacrylate	Dichloromethane	78550 ± 15966	29500 ± 13011	3.3 ± 1.2
Methyl methacrylate	1,2-Dichloroethane	14900 ± 4262	6393 ± 2920	2.5 ± 0.4
Methyl methacrylate	Tetrahydrofuran	27400 ± 7321	10900 ± 3327	2.5 ± 0.5
Methyl acrylate	Dichloromethane	375333 ± 46916	167333 ± 24598	2.3 ± 0.6
Methyl acrylate	1,2-Dichloroethane	152000 ± 38053	37200 ± 10325	4.0 ± 2.7
Methyl acrylate	Tetrahydrofuran	15876 ± 4291	6657 ± 2080	2.5 ± 1.3
Ethyl methacrylate	Dichloromethane	222500 ± 36475	131500 ± 15654	1.7 ± 0.4
Ethyl methacrylate	1,2-Dichloroethane	86000 ± 15087	47100 ± 9059	1.8 ± 0.7
Ethyl methacrylate	Tetrahydrofuran	141750 ± 30245	72600 ± 17034	2.0 ± 1.1
Ethyl acrylate	Dichloromethane	198000 ± 7000	27050 ± 850	7.3 ± 0.5
Ethyl acrylate	1,2-Dichloroethane	47150 ± 23050	8615 ± 2485	5.1 ± 1.2
Ethyl acrylate	Tetrahydrofuran	9143 ± 1371	2900 ± 352	3.1 ± 0.5

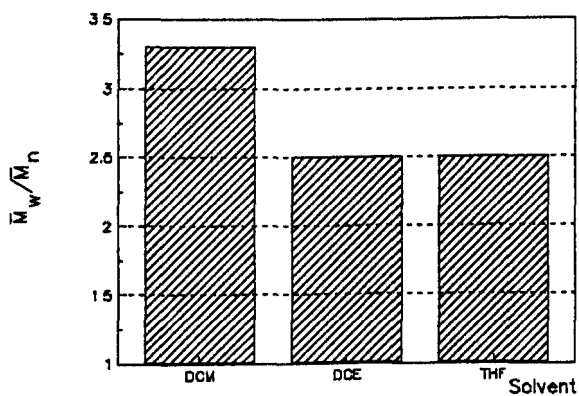
**Table 6.4** The effect of solvent upon the physical properties of free radical polymerization of non-mesogenic monomers.



a)

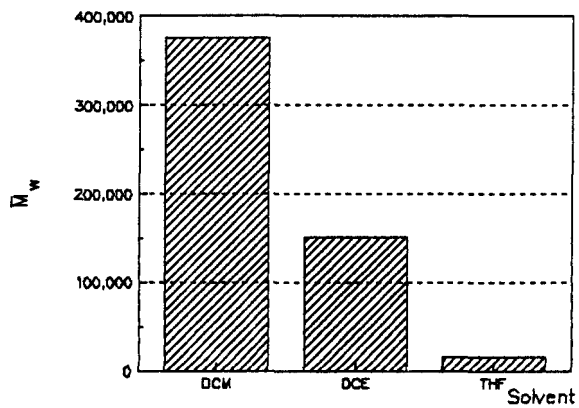


b)

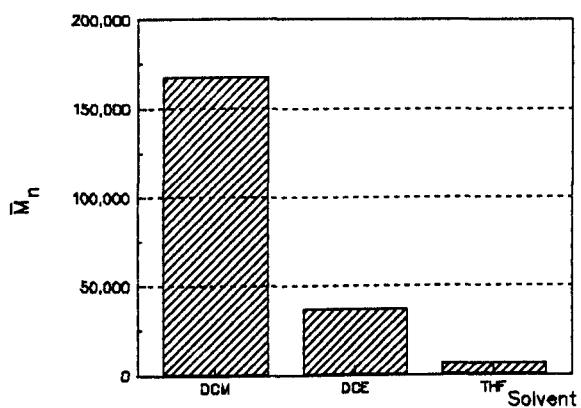


c)

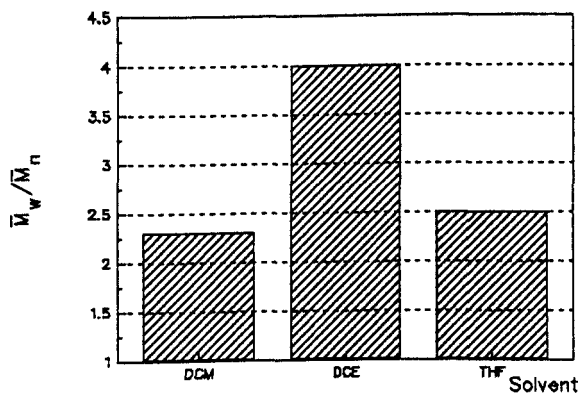
**Figure 6.4** Variation of a)  $\bar{M}_w$ , b)  $\bar{M}_n$  and c)  $\bar{M}_w/\bar{M}_n$  with different solvents for methyl methacrylate.



a)

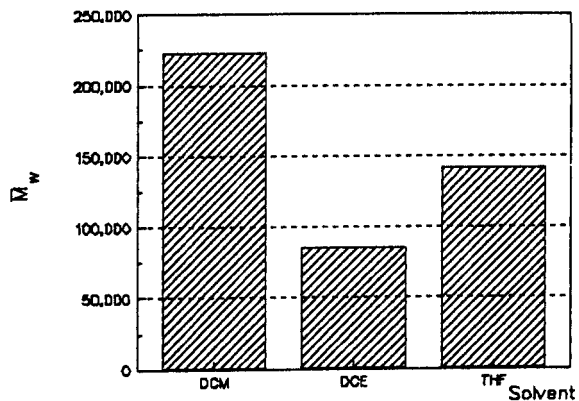


b)

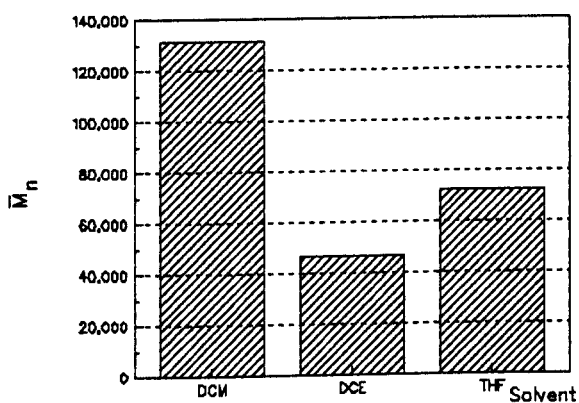


c)

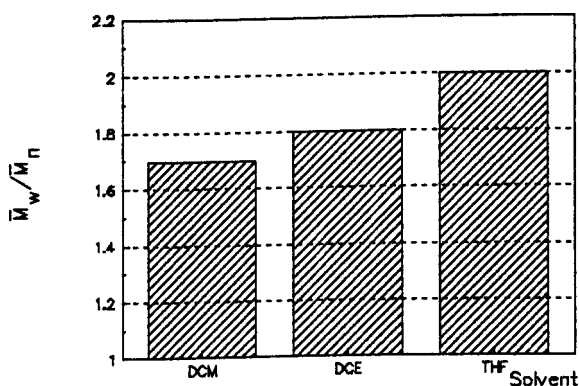
**Figure 6.5** Variation of a)  $\bar{M}_w$ , b)  $\bar{M}_n$  and c)  $\bar{M}_w/\bar{M}_n$  with different solvents for methyl acrylate.



a)

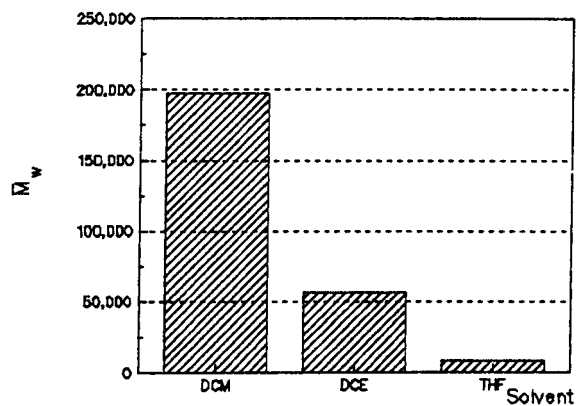


b)

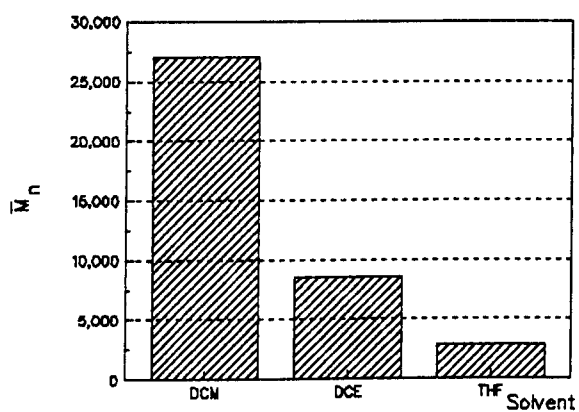


c)

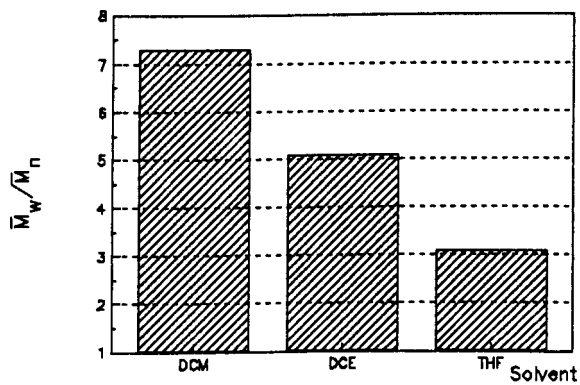
**Figure 6.6** Variation of a)  $\bar{M}_w$ , b)  $\bar{M}_n$  and c)  $\bar{M}_w/\bar{M}_n$  with different solvents for ethyl methacrylate.



a)



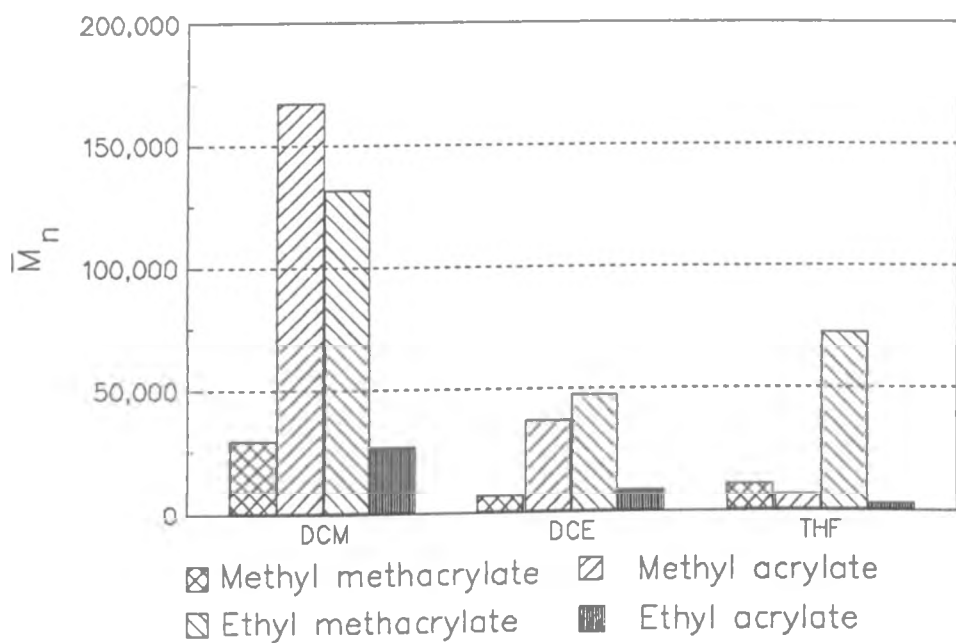
b)



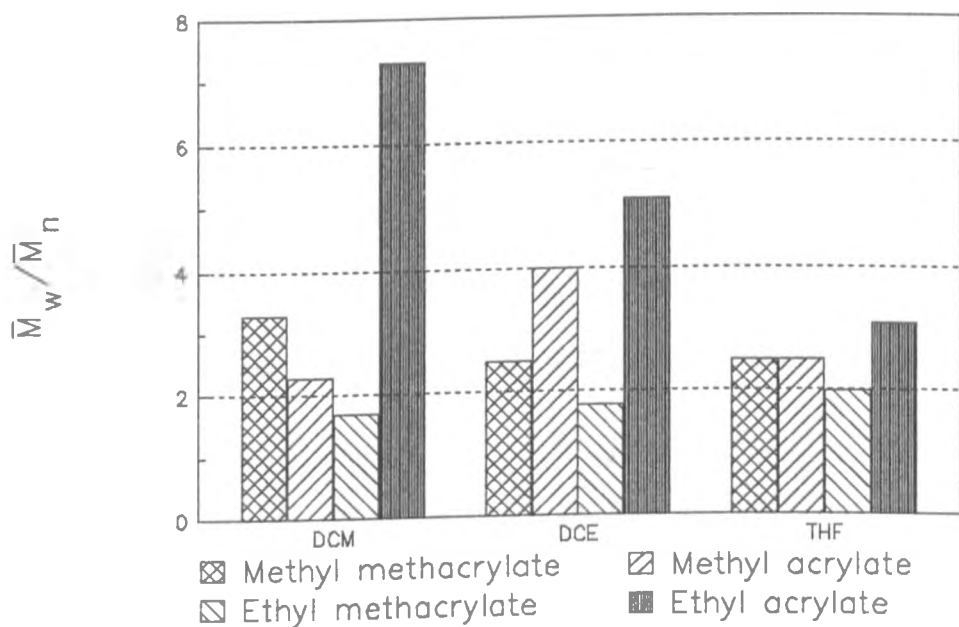
c)

**Figure 6.7** Variation of a)  $\bar{M}_w$ , b)  $\bar{M}_n$  and c)  $\bar{M}_w/\bar{M}_n$  with different solvents for ethyl acrylate.

The results given in Table 6.4, and summarised graphically in Figures 6.4, 6.5, 6.6 and 6.7 show that for all four non-mesogenic systems the polymers having the largest degree of polymerization were produced when dichloromethane was used as the solvent in the polymerization of the monomers. The results that are given in the table correspond to the **average of three sets of results** generated from three separate replicate polymerizations. The resulting polymers were only precipitated once by the addition of methanol. The standard procedure for the purification of mesogenic systems using several precipitations would have reduced the amount of low molecular weight species in the mixture, leading to polymers having reduced polydispersity shifted towards the higher end of the molecular weight range. The polymers were analyzed by GPC which showed that no monomer was present in these non-mesogenic systems even after only one precipitation. This single precipitation procedure was used for all the following results that correspond to non-mesogenic systems. A comparison of the effect of solvent upon the  $\bar{M}_n$  and  $\bar{M}_w/\bar{M}_n$  values of the four non-mesogenic polymers is given in Figure 6.8 a and b. The choice of the parameters  $\bar{M}_n$  and  $\bar{M}_w/\bar{M}_n$  is due to the fact that they are the most important parameters for comparing the polymers. Since the molecular weights of all four of the non-mesogenic systems are very similar, the degree of polymerization ( $\bar{DP} = \bar{M}_n/\bar{M}_0$ ) may be seen as a direct comparison of  $\bar{M}_n$  values. It must be remembered that all the GPC data quoted is relative to polystyrene standards and not an absolute value. Thus the comparison of  $\bar{M}_n$  values is a useful tool to compare the effectiveness of a solvent to promote the propagation stage of the free radical polymerization.



a)



b)

**Figure 6.8** Comparison of the effect of solvent on a)  $\bar{M}_n$  and b)  $\bar{M}_w/\bar{M}_n$  on the four non-mesogenic polymers.

The  $\bar{M}_w/\bar{M}_n$  values are a measure of the efficiency of the solvents in the termination stages of free radical polymerization to produce polymers of equivalent molecular weight.

The aims of this study were to produce polymers with high  $\bar{DP}$  ( $\bar{M}_n$ ) values and low  $\bar{M}_w/\bar{M}_n$  values.

#### Comparing the $\bar{M}_n$ and $\bar{M}_w$ values shown in Figure 6.8a.

- It can be seen from the comparison of  $\bar{M}_n$  values in Figure 6.8a that the order for the effectiveness of the solvents to produce high  $\bar{M}_n$  polymers is dichloromethane » 1,2-dichloroethane » tetrahydrofuran for acrylates and dichloromethane » tetrahydrofuran  $\geq$  1,2-dichloroethane for methacrylates.
- In chlorinated solvents, both methyl acrylate and ethyl methacrylate gave similar results - high  $\bar{M}_w$  and  $\bar{M}_n$ ; whereas methyl methacrylate and ethyl acrylate both gave low  $\bar{M}_w$  and  $\bar{M}_n$  values *e.g.* in dichloromethane methyl acrylate and ethyl methacrylate gave  $\bar{M}_n \approx 150000 - 160000$ ; methyl methacrylate and ethyl acrylate gave  $\bar{M}_n \approx 50000 - 60000$ .
- From this comparison the best choice of solvent is dichloromethane.

#### Comparing the $\bar{M}_w/\bar{M}_n$ values shown in Figure 6.8b.

- For all three solvents the  $\bar{M}_w/\bar{M}_n$  values decrease in the following order  
Ethyl acrylate » methyl methacrylate > methyl acrylate > ethyl methacrylate
- The trends in the values for  $\bar{M}_w/\bar{M}_n$  data are not as clear as the trends in either the  $\bar{M}_w$  or  $\bar{M}_n$  data.

- Apart from the data from poly(ethylacrylate) which is extremely high because of the large variations between  $\bar{M}_w$  and  $\bar{M}_n$ , possibly due to the use of only a single precipitation step.
- In general it can be shown that the values for  $\bar{M}_w/\bar{M}_n$  decrease in the following order  
1,2-dichloroethane (DCE)  $\geq$  dichloromethane (DCM)  $>$  tetrahydrofuran (THF).

The overall conclusions that can be drawn from this study of the effect of solvent upon the polymerization of the four non-mesogenic monomers are as follows.

- Tetrahydrofuran is a good solvent for producing polymers with low  $\bar{DP}$  and  $\bar{M}_w/\bar{M}_n$  values.
- Chlorinated solvents produce polymers with higher  $\bar{DP}$  values and slightly higher  $\bar{M}_w/\bar{M}_n$  values than tetrahydrofuran.
- Dichloromethane produces polymers with the highest  $\bar{DP}$  values.

As this set of results clearly shows the choice of solvent for a free radical polymerization is critical. The properties of the resulting polymer can be changed so drastically simply by changing the solvent, from one extreme of obtaining no polymerized material using toluene to the other in which a polymer so large is produced that it exceeds the calibration range of instruments such as a GPC system, using dichloromethane as a solvent. Other factors also have an effect upon the extent of the polymerization reaction but none seem to be able to "switch the reaction on and off" in the same way that changing the solvent can. Particularly for this type of work, in which the aim is to produce polymers of as large a size as possible, the obvious

choice of solvent is one that will allow the formation of high molecular weight polymers, with the aim of adding more control to the system by altering some of the other parameters.

### 6.2.2.2 Effect of Concentration of AIBN.

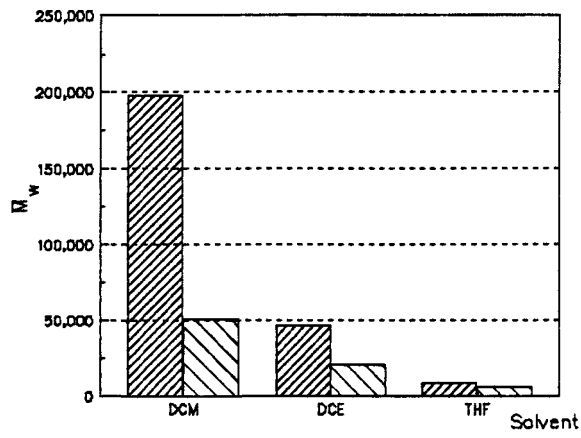
The effect of varying the concentration of AIBN on the  $\bar{M}_w$ ,  $\bar{M}_n$  and  $\bar{M}_w/\bar{M}_n$  values of the polymer was examined by polymerizing ethyl acrylate using different concentrations of AIBN and different solvents. The concentrations of AIBN that were used were the literature amount (1 mol %) and a very large increased amount (40 mol %). The results of the experiment are given in Table 6.5 and shown graphically in Figure 6.9. The results indicate that increasing the concentration of AIBN increases the number of free radical sites which, in turn, results in the formation of a larger number of shorter polymer chains. This is clearly shown in Figure 6.9(c) where the  $\bar{M}_w/\bar{M}_n$  values obtained at 40 mol % AIBN are far lower ( $\approx 2 - 3$ ) than the corresponding values for the 1 mol % AIBN ( $\approx 3 - 7.5$ ). It is interesting to note from Figure 6.9(c) that the  $\bar{M}_w/\bar{M}_n$  values for the 40 mol % AIBN are almost independent of the solvent used, whereas the corresponding values for the 1 mol % AIBN are in the order DCM > DCE > THF, following the trend of highest to lowest  $\bar{M}_w$  and  $\bar{M}_n$  values of the polymer. As expected, the use of dichloromethane in the free radical polymerization of ethyl acrylate gave the highest value of  $\bar{M}_w$  and  $\bar{M}_n$  for both the 1 mol % and 40 mol % concentration level of AIBN. The largest effect of the concentration of AIBN on the free-radical polymerization of ethyl acrylate was on the

$\bar{M}_w$  value for the polymer. When dichloromethane was used as the solvent, the  $\bar{M}_w$  value at 1 mol % AIBN was four times greater than that obtained at 40 mol % AIBN. If the solvent was now changed to 1,2-dichloroethane, the  $\bar{M}_w$  value was doubled by changing the concentration of AIBN from 40 mol % to 1 mol %. There was very little effect of the concentration of AIBN on the  $\bar{M}_w$  values when tetrahydrofuran was used as the solvent.

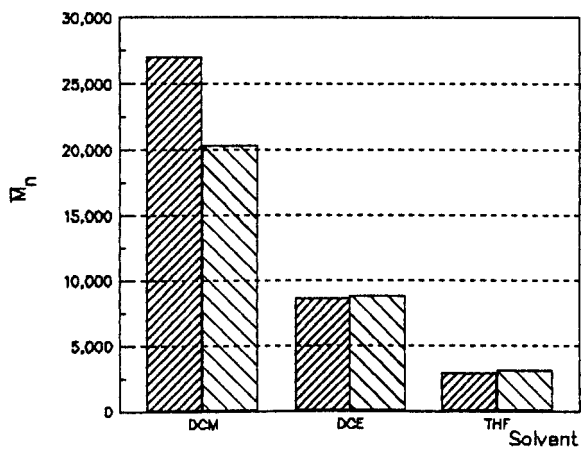
These results clearly show that the use of 1 mol % AIBN in dichloromethane gave the highest degree of polymerization but also the highest polydispersity; the best way of obtaining a low polydispersity was to use a high concentration of AIBN, the disadvantage being the much reduced degree of polymerization.

AIBN Conc	Solvent	$\bar{M}_w$	$\bar{M}_n$	$\bar{M}_w/\bar{M}_n$
1 mol %	Dichloromethane	198000	27050	7.4
1 mol %	1,2-Dichloroethane	47150	8615	5.1
1 mol %	Tetrahydrofuran	9143	2900	3.1
40 mol %	Dichloromethane	51050	20350	2.5
40 mol %	1,2-Dichloroethane	21333	8807	2.5
40 mol %	Tetrahydrofuran	6736	3116	2.1

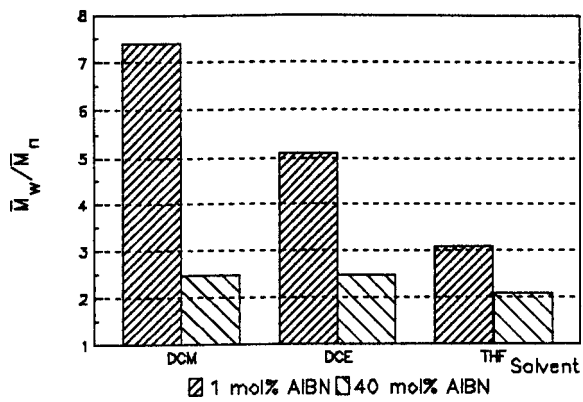
**Table 6.5** The effect of concentration of initiator on the free radical polymerization of ethyl acrylate.



a)



b)



c)

**Figure 6.9** Variation of a)  $\bar{M}_w$ , b)  $\bar{M}_n$  and c)  $\bar{M}_w/\bar{M}_n$  with concentration of AIBN and different solvents, in the free radical polymerization of ethyl acrylate.

### 6.2.2.3 The Effect of Pressure (Sealed Reaction Vessel).

The effect of pressure on the free radical polymerization of monomers was examined by sealing the reactants in a Carius tube. The monomer that was used for this study was methyl methacrylate, the reaction conditions used in the polymerization of methyl methacrylate were as follows.

Methyl methacrylate 5.0 g

AIBN 1 mol %

Solvent 10 ml

The reaction mixture was stirred at 60 °C, under an atmosphere of dry nitrogen in a sealed Carius tube for 24 h.

The results from this study are given in Table 6.6, and shown graphically in Figure 6.10. These results show that by sealing the reactants in a tube under an atmosphere of dry nitrogen, it was possible to negate the effect that solvent alone had on the reaction, in that the  $\bar{DP}$  of the polymer was raised quite considerably by sealing the reactants in a tube. The largest effect was found for THF. In fact the effect of sealing the tube was so dramatic using tetrahydrofuran as the solvent that the 7 fold increase in using a sealed tube produced a polymer with a higher  $\bar{M}_n$  (and  $\bar{DP}$ ) value ( $\bar{M}_n = 73400$ ) than that found for dichloromethane ( $\bar{M}_n = 64800$ ). Possible explanations for this 7 fold increase in  $\bar{M}_n$  value could be as follows.

1) The reagents were sealed in the tube under an atmosphere of dry nitrogen and so as the tube was heated, the solvent would begin to vaporise, which would have resulted in a slight increase in the pressure within the tube. The increased pressure would force the reagents closer together, resulting in a higher probability of a reactive free radical polymer chain colliding with a monomer unit and so extend the growing polymer chain, resulting in polymer chains longer than those formed at atmospheric pressure.

2) The sealed tube prevents the loss of solvent by evaporation. As the expansion of the solvent as it was heated resulted a slight increase in pressure, the solvent that did escape from the liquid surface, condensed on the side of the tube and drained back into the reaction mixture, instead of being lost to the atmosphere, resulting in a more consistent volume of solvent being present in the reaction vessel. The level of solvent may have kept the growing polymer chains in solution during the course of the reaction, and hence allowing the reaction to continue and so produce polymers of higher  $\bar{M}_n$  values.

It is probable that the reason for the improved degree of polymerization may be due to a combination of both these explanations.

Tube type	Solvent	$\bar{M}_w$	$\bar{M}_n$	$\bar{M}_w/\bar{M}_n$
open	Dichloromethane	78550	29500	3.3
open	Tetrahydrofuran	27400	10900	2.5
sealed	Dichloromethane	106000	64800	1.6
sealed	Tetrahydrofuran	141000	73400	1.9

**Table 6.6** The effect of sealed tubes on the free radical polymerization of methyl methacrylate.

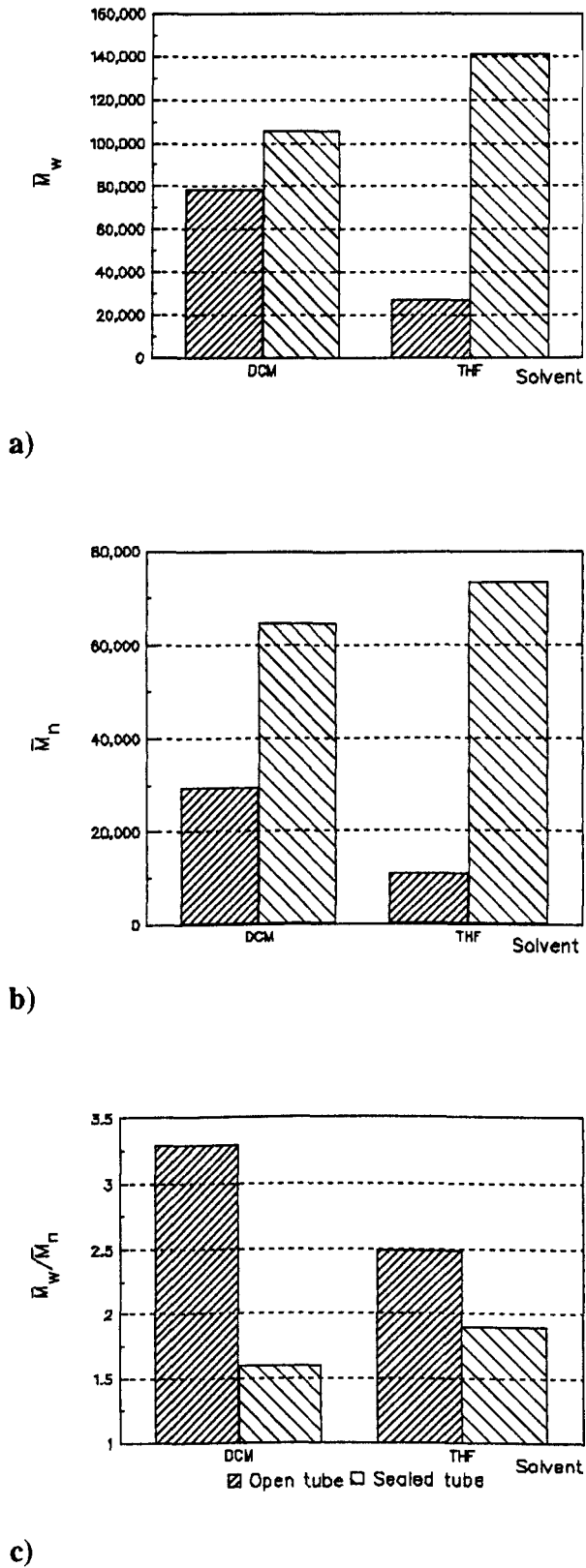


**Figure 6.10** Variation of a)  $\bar{M}_w$ , b)  $\bar{M}_n$  and c)  $\bar{M}_w/\bar{M}_n$  with sealed tubes and different solvents for the free radical polymerization of methyl methacrylate.

#### 6.2.2.4 The Combined Effect of Pressure and Ultrasound.

The effect that both pressure and ultrasound have upon the polymerization process was investigated by the polymerization of methyl methacrylate in two different solvents in sealed tubes. The free radicals were generated from AIBN, either by using the standard procedure of heat (60 °C) or by using an ultrasonic bath (25 - 35 kHz, 40 °C). The reaction conditions were the same as for the previous experiment. The results from this study are given in Table 6.7 and shown graphically in Figure 6.11. The results from this investigation demonstrate that using ultrasound to produce free radicals from AIBN is a good method for polymerizing methyl methacrylate. The temperature that the solution reached in the ultrasonic bath was about 40 °C; this temperature has been shown by Merck (UK)<sup>135</sup> to be insufficient to produce free radicals from AIBN. Therefore the free radicals must have been generated by the action of the ultrasonic radiation upon the AIBN.<sup>136</sup> The application of ultrasound to reactions contained in sealed tubes, enhanced the reaction still further than the sealed tubes alone, increasing both the  $\bar{M}_n$  ( $\bar{DP}$ ) and  $\bar{M}_w$  values of the polymers. The polydispersities ( $\bar{M}_w/\bar{M}_n$ ) of the polymers were also slightly increased on the application of ultrasound where dichloromethane was used as the solvent, but in the case where the solvent was tetrahydrofuran, a decrease in the  $\bar{M}_w/\bar{M}_n$  value was observed. The decrease in the  $\bar{M}_w/\bar{M}_n$  values of polymers on the application of ultrasonic radiation is well known.<sup>137</sup> Ultrasound attacks the polymer chains causing them to break into two roughly equal length radicals, each radical so formed is then capable of recombination with another radical to form a less reactive species. This process has the effect of producing a more uniform degree of polymerization within

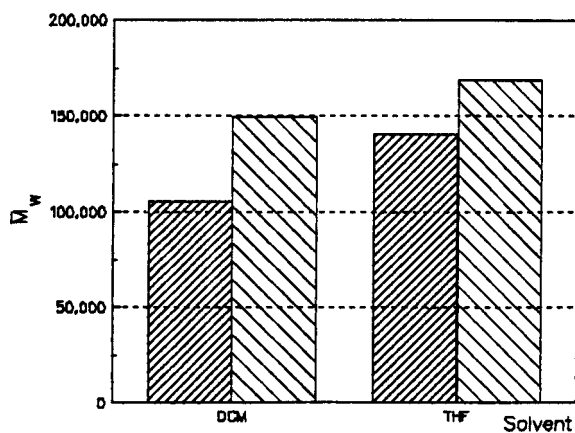
a given polymer system, if the ultrasound is applied for sufficient time.

#### **6.2.2.5 The Effect of Monomer Concentration.**

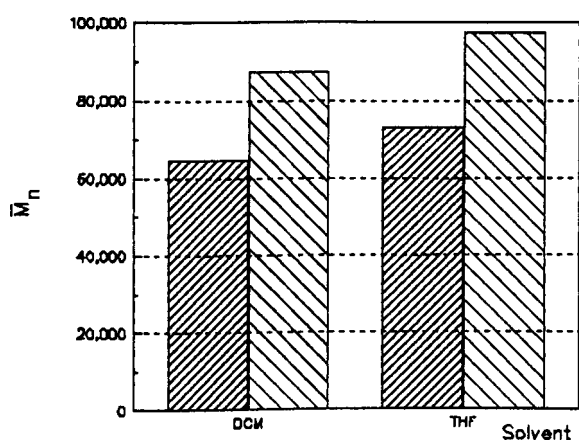
The effect of concentration of the monomer on free radical polymerization was investigated by repeating the previous set of reactions but using a smaller concentration of methyl methacrylate. The concentration of methyl methacrylate used in this series of experiments was chosen to mimic the concentration of the mesogenic monomer that would be present in the reaction. Mesogenic monomers have a much larger molecular weight (typically RMM > 500) than methyl methacrylate (RMM  $\approx$  100). The reaction conditions were the same as for the previous study but using methyl methacrylate (0.2 g) in solvent (10 ml).

Ultrasound	Solvent	$\bar{M}_w$	$\bar{M}_n$	$\bar{M}_w/\bar{M}_n$
No	Dichloromethane	106000	64800	1.6
No	Tetrahydrofuran	141000	73400	1.9
Yes	Dichloromethane	150000	87400	1.7
Yes	Tetrahydrofuran	169000	97500	1.7

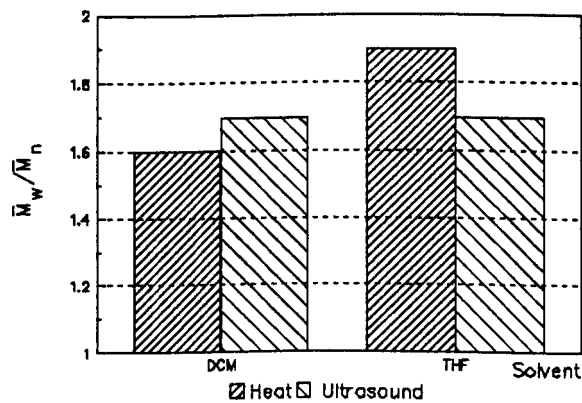
**Table 6.7** The effect of ultrasound on the free radical polymerization of methyl methacrylate.



a)



b)



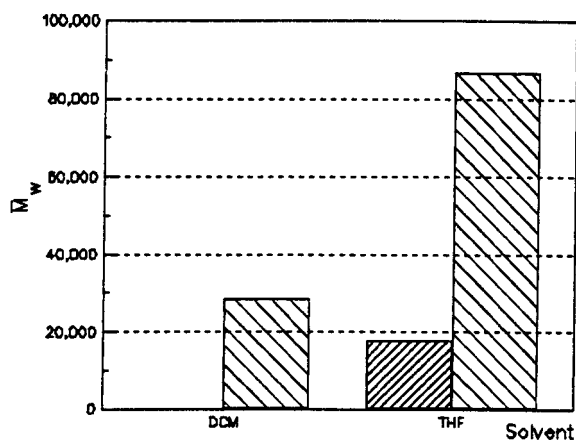
c)

**Figure 6.11** Variation of a)  $\bar{M}_w$ , b)  $\bar{M}_n$  and c)  $\bar{M}_w/\bar{M}_n$  with ultrasound and different solvents in sealed tubes in the polymerization of methyl methacrylate.

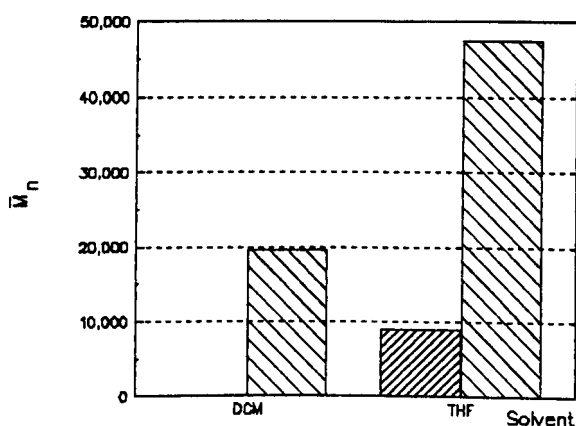
The results shown in Table 6.8 and graphically summarised in Figure 6.12, show the effect that concentration of the monomer has had upon the degree of polymerization of the final polymers. Although the trends in  $\bar{M}_w$ ,  $\bar{M}_n$  and  $\bar{M}_w/\bar{M}_n$  were similar to those found for the free radical polymerization of methyl methacrylate using a higher concentration of the monomer (see Table 6.7 and Figure 6.11), the increase in the  $\bar{M}_w$  and  $\bar{M}_n$  values and the decrease in  $\bar{M}_w/\bar{M}_n$  value on the application of ultrasound were far more dramatic when the monomer was at low concentration (2 mol % instead of the previous 10 mol %). At 10 mol % of monomer and using tetrahydrofuran as the solvent, the increase in  $\bar{M}_w$  and  $\bar{M}_n$  values were 16 and 25 % respectively, but a 5 fold increase was observed when the concentration of monomer was decreased to 2 mol %. The  $\bar{M}_w/\bar{M}_n$  value decreased from 1.9 to 1.7 on the use of ultrasound when 10 mol % of monomer was used, but this decrease was much more severe (2.0 to 1.5) when the monomer concentration was decreased to 2 mol %.

Ultrasound	Solvent	$\bar{M}_w$	$\bar{M}_n$	$\bar{M}_w/\bar{M}_n$
No	Dichloromethane	-	-	-
No	Tetrahydrofuran	17700	8990	2.0
Yes	Dichloromethane	28400	19600	1.8
Yes	Tetrahydrofuran	86500	47600	1.5

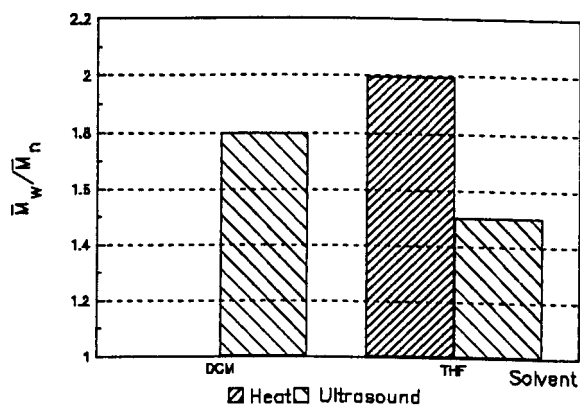
**Table 6.8** The effect of ultrasound on the polymerization of the same concentration of methyl methacrylate as for mesogenic monomers.



a)



b)



c)

**Figure 6.12** Variation of a)  $\bar{M}_w$ , b)  $\bar{M}_n$  and c)  $\bar{M}_w/\bar{M}_n$  with ultrasound and different solvents in sealed tubes in the polymerization of methyl methacrylate (2 mol %).

However, reducing the concentration of monomer also affected the size of the  $\bar{M}_w$ ,  $\bar{M}_n$  and  $\bar{M}_w/\bar{M}_n$  values for the polymer. Taking the results from the free radical polymerization of methyl methacrylate using tetrahydrofuran and ultrasound (polymers with the highest  $\bar{M}_n$  values and lowest  $\bar{M}_w/\bar{M}_n$  values - best combination of polymer properties), at high concentration of the monomer the  $\bar{M}_n$  and  $\bar{M}_w/\bar{M}_n$  values were 97500 and 1.7 respectively. If the concentration of monomer was now decreased to 2 mol %, the  $\bar{M}_n$  and  $\bar{M}_w/\bar{M}_n$  fell to 47600 (half the previous value) and 1.5 respectively.

This effect can be explained by the fact that there was less chance of collision between growing polymer chains and unreacted monomer in the lower concentration situation, resulting in the fact that the polymer chains do not have a chance to grow prior to termination, either by colliding with another free radical or with the walls of the reaction vessel.

#### **6.2.2.6 Summary.**

It has been shown that there are several parameters of the free radical polymerization reaction that can have an effect upon the extent of the reaction, and can therefore be used to control the degree of polymerization and the polydispersity of the polymers produced by such reactions. The parameter which has been shown to have the major effect upon the reaction is the choice of solvent. The wrong choice of solvent could result in no reaction at all taking place.

The choice of conditions for a particular free radical polymerization must be a compromise between the all the possible conditions and the physical properties of the polymer that they will produce. All the subsequent free radical polymerization reactions described in this thesis were carried out using the following standard procedure and conditions, unless otherwise stated.

monomer	1.0 g
dichloromethane	10 ml
AIBN	1 mol %

stirred at 50 °C under an atmosphere of dry nitrogen for 24 h. The resulting polymers were dissolved in dichloromethane and repeatedly precipitated by the addition of methanol until free of unreacted monomer (monitored by tlc; silica gel, dichloromethane) (see Section 5.10.2.2).

### **6.2.3 Free Radical Polymerization of Mesogenic Monomers.**

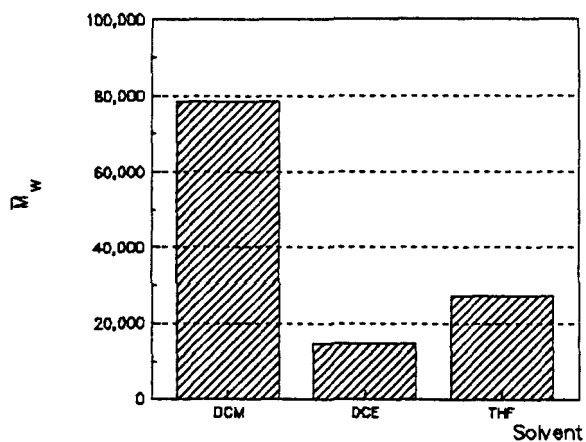
The monomers synthesized by the routes described in Schemes 1 - 7, were polymerized using the conditions described in the previous Section 6.2.2.6. The results are summarised below and the significance of the results is discussed.

The effect of varying the solvent on the polymerization of a mesogenic monomer was examined by polymerizing monomer XIX (1.0 g) in different solvents (10 ml), using AIBN as the initiator. The results given in Table 6.9 and shown graphically in Figure

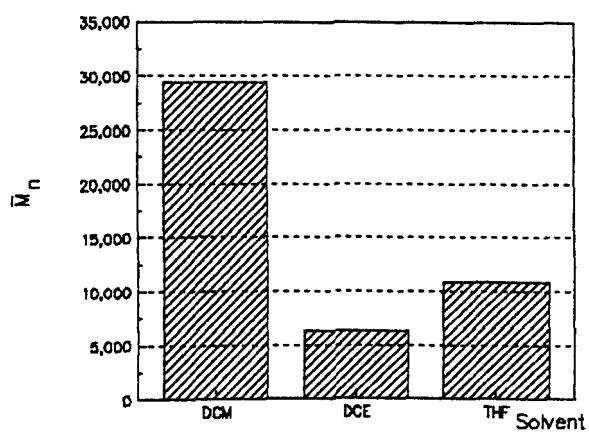
6.13 indicate that changing the reaction solvent from tetrahydrofuran to dichloromethane increases the  $\bar{DP}$  value of the polymer from 8 to 36. This result is similar to the results obtained for the non-mesogenic monomers. Although polymers with a  $\bar{DP}$  value even larger than 36 would be desirable, polymers produced under these conditions have a high enough  $\bar{DP}$  value to be useful. Similar results have been found by Merck (UK).<sup>138</sup> The effect of concentration of the mesogenic monomer was also examined by Merck (UK) and they found that by increasing the concentration of the monomer in the polymerization they also increased the  $\bar{DP}$  value of the polymer. However when the concentration of monomer was increased from 0.1 g/ml to 0.2 g/ml in dichloromethane, the resulting polymer was difficult to dissolve in any of the usual solvents. Subsequent examination of this polymer by GPC showed that it had a molecular weight above the calibration range of the GPC *i.e.* it had a molecular weight > 400,000.

Monomer	Solvent	$\bar{M}_w$	$\bar{M}_n$	$\bar{M}_w/\bar{M}_n$	$\bar{DP}$
<b>XIX</b>	Dichloromethane	78550	29500	3.3	36
<b>XIX</b>	1,2-Dichloroethane	14900	6393	2.5	9
<b>XIX</b>	Tetrahydrofuran	27400	10900	2.5	8

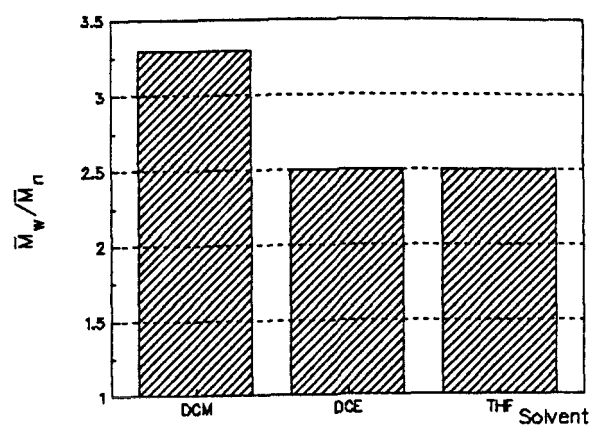
**Table 6.9** The effect of solvents on the physical properties of the free radical polymerization of monomer **XIX**.



a)



b)



c)

**Figure 6.13** Variation of a)  $\bar{M}_w$ , b)  $\bar{M}_n$  and c)  $\bar{M}_w/\bar{M}_n$  with different solvents for Monomer XIX.

One disadvantage of using dichloromethane as the polymerization solvent is that it gave polymers with a slightly higher  $\bar{M}_w/\bar{M}_n$  value. One obvious method of reducing the  $\bar{M}_w/\bar{M}_n$  value of the polymers was to carry out the polymerization using ultrasonic radiation, the reasons for this approach not being taken were.

1) No suitable ultrasonic generator was available for the time scale that was required.

An ultrasound generator was being made by the Department of Physics at the University of Hull, this was not available during the course of this study.

2) There were concerns about the feasibility of using ultrasound in commercial production of these polymers, should they prove commercially useful.

### 6.2.3.1 Polymerization of Monomers VI(a - g).

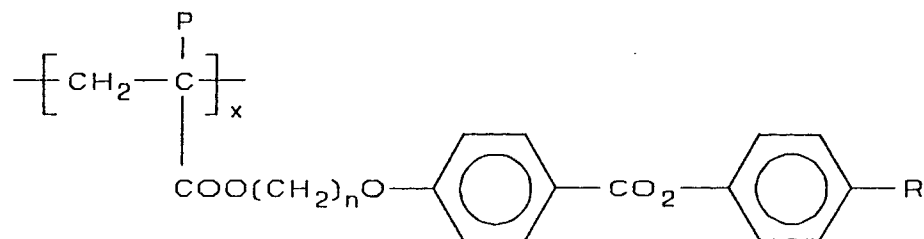
The physical properties of the polymers produced by the free radical polymerization of monomers VI(a - g) are summarised in Table 6.10. This table of results demonstrates the fact that even with all the preceding work regarding polymerization conditions, the reaction was not effectively controlled.

One reaction [the polymerization of monomer VI(b)] resulted in a polymer that had crosslinked to such an extent that it was totally insoluble in solvents such as dichloromethane and tetrahydrofuran, and therefore the molecular weight determination by GPC on this polymer was not possible. Attempts to prepare a microscope slide in

order to examine whether the polymer showed liquid crystal phases failed; the polymer decomposed before melting. The other free radical polymerizations that failed to produce polymer were those involving monomers VI(d, e, g). The reasons why the polymerization process sometimes failed to produce polymers, even though the standard procedure was followed exactly is not fully understood. Some of the possible causes that have been discussed are impurities in the AIBN, moisture or oxygen in the system. Work was planned to repeat the reactions, however lack of time prevented the work being carried out.

The results from the successful polymerizations in the series exhibit some interesting phenomena. The polymer produced from monomer VI(a) which has a spacer length of 3 methylene units between the acrylate backbone and the rigid mesogenic core, has a high  $g$  value  $43.4\text{ }^{\circ}\text{C}$  but exhibits no liquid crystal phases, due to the spacer group being too short to allow the amount of decoupling needed between the polymer backbone and the mesogenic side chains.

The polymer produced from monomer VI(c) has a  $g$  of  $0.7\text{ }^{\circ}\text{C}$ , and exhibits a smectic phase, which is difficult to classify due to the lack of a good defect texture, above the smectic phase there is a nematic phase. The polymer produced from monomer VI(f) is very different with a lower  $g$  value  $-10.4\text{ }^{\circ}\text{C}$  and an unclassified smectic phase which goes isotropic at  $38.4\text{ }^{\circ}\text{C}$ , the only difference in the monomers was the terminal group being methoxy or cyano.



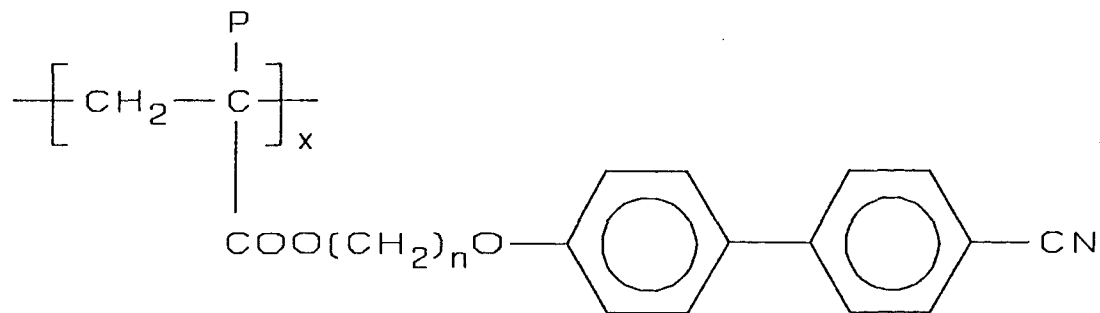
Monomer	P	n	R	$\bar{M}_w$	$\bar{M}_n$	$\bar{M}_w/\bar{M}_n$	g / °C	Transitions / °C by DSC
VIa	H	3	OCH <sub>3</sub>	43000	22900	1.9	43.4	no phases
VIb	H	6	OCH <sub>3</sub>	CROSSLINKED				
VIc	H	11	OCH <sub>3</sub>	25000	15500	1.6	0.7	S <sub>1</sub> 37.2 N 77.6 I
VI d	H	6	CN	FAILED TO POLYMERIZE				
VI e	CH <sub>3</sub>	6	CN	FAILED TO POLYMERIZE				
VI f	H	11	CN	166000	61500	2.7	-10.4	S <sub>1</sub> 38.4 I
VI g	CH <sub>3</sub>	11	CN	FAILED TO POLYMERIZE				

S<sub>1</sub> = unidentified smectic phase.

**Table 6.10** The physical and thermal properties of polymers VI (a - g).

### 6.2.3.2 Polymerization of Monomers VII(a - d).

Table 6.11 shows a summary of the results for the polymerization of monomers VII(a - d). All the monomers were polymerized successfully, the only questionable result is that produced for monomer VII(a) which appears to show no phases above the  $g$  value  $-6.45$  °C. LeBarny<sup>116</sup> suggests a variety of phases for a similar polymer including reentrant nematics and smectics. Attempts were made to repeat the polymerization but a similar result was obtained. The other polymers from the series show high  $g$  values, the  $g$  values for the methacrylates being higher than those for the corresponding acrylates, due to the increased stiffness in the polymer backbone due to the methyl groups. All the polymers exhibit  $S_A$  phases, with only the polymer produced by monomer VII(d) showing another unclassified smectic phase under the  $S_A$  phase.



Monomer	P	n	$\bar{M}_w$	$\bar{M}_n$	$\bar{M}_w/\bar{M}_n$	g / °C	Transitions / °C by DSC
<b>VIIa</b>	H	6	37000	23100	1.6	-6.5	No phases
<b>VIIb</b>	CH <sub>3</sub>	6	36400	22100	1.7	44.3	S <sub>A</sub> 95.4 I
<b>VIIc</b>	H	11	29700	16500	1.8	13.9	S <sub>A</sub> 138.6 I
<b>VIIId</b>	CH <sub>3</sub>	11	101000	59600	1.7	15.3	S <sub>1</sub> 56.8 S <sub>A</sub> 123.5 I

S<sub>1</sub> = unidentified smectic phase.

**Table 6.11** The physical and thermal properties of polymers **VII(a - d)**.

### 6.2.3.3 Polymerization of Monomer XV.

Only the acrylate monomer XV with the long spacer group  $[-(\text{CH}_2)_{11}-]$  was polymerized and the transition temperatures and GPC data for this compound are given in Table 6.12. The polymer exhibits a low  $g$  value ( $-20.9\text{ }^\circ\text{C}$ ) and a cholesteric liquid crystal phase ( $38.4\text{ }^\circ\text{C}$ ). Attempts to produce a series of monomers with this general structure were attempted but the final stage of attaching the acrylate function (compounds I(a - f)) to the mesogenic core (compound XIV) failed and the starting materials broke up into many fragments. Similar reactions were tried using different mesogenic cores which had been used successfully previously but these too failed. It was decided that a new synthetic scheme would have to be devised, to prepare these compounds but unfortunately no time could be spared for this task and no further work was carried out on these polymers.

Monomer	$\bar{M}_w$	$\bar{M}_n$	$\bar{M}_w/\bar{M}_n$	$g / ^\circ\text{C}$	Transitions / $^\circ\text{C}$ by DSC
XV	12600	9740	1.1	-20.9	$\text{N}^* 38.4 \text{ I}$

**Table 6.12** The physical and thermal properties of polymer XV.

### 6.3.1 Free Radical Copolymerization of Mesogenic and Non-Mesogenic Monomers.

A study was carried out which involved the copolymerization of mesogenic acrylates and methacrylates with non-mesogenic acrylates and methacrylates. The aim of this study was to try to increase the degree of polymerization of the liquid crystal polymers without severely disrupting the formation of liquid crystalline phases. It was postulated that one of the reasons why the polymerization of mesogenic systems resulted in polymers with low degrees of polymerization was that the large mesogenic groups cause steric hindrance at the site of polymerization, which thus prevents the acrylate or methacrylate free radicals from interacting to produce the long polymer backbone. It was hoped that by introducing smaller non-mesogenic units, such as methyl methacrylate, it may be possible to reduce the steric hindrance at polymerization sites and allow polymers containing longer chains of mesogenic side-groups to be produced. The incorporation of non-mesogenic groups into SCLC polymers will also affect the physical and thermal properties of these polymers, and this could be of interest in designing SCLC polymers for specific applications. Experiments by Platé, Talroze and Shibaev<sup>139</sup> have shown that the incorporation of increasing amounts of a comonomer (non-mesogenic) into a SCLC polymer had the tendency to reduce both the glass transition temperature and the clearing point, although no details regarding the phase types were given. A summary of their findings is shown in Table 6.13. It can be clearly seen that even with a very large amount of the non-mesogenic monomer of structure (2), the copolymer still exhibited liquid crystalline behaviour. The incorporation of a non-mesogenic acrylate into a

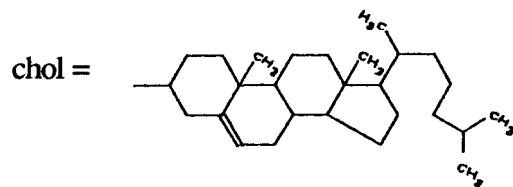
SCLC polymethacrylate had a much more detrimental effect upon both the  $g$  value and the liquid crystalline behaviour of the copolymer than the incorporation of a non-mesogenic methacrylate.

### **6.3.1.1 Methyl Acrylate and Methacrylate as the Non-Mesogenic Monomer.**

In order to investigate the effects of incorporating non-mesogenic monomers, copolymers of a mesogenic acrylate monomer with varying quantities of non-mesogenic monomers were synthesised.

The experiments that were carried out involved mixing different percentages of methyl acrylate or methyl methacrylate to a mesogenic acrylate monomer and then polymerizing the mixture using the standard procedure described in section 6.2.2.6. The results from these experiments and the percentages of mesogenic and non-mesogenic monomers used are given in Table 6.14. The percentage of each component of the copolymer was calculated by the interpretation of the integration of the peaks in the  $^1\text{H}$  nmr (see Section 5.1). The results show that the percentage of each non-mesogenic monomer incorporated into the final polymer was not necessarily the same as the percentage of the monomers that were mixed prior to polymerization. In general the percentage of non-mesogenic component in the final polymer appeared to be higher than in the original mixture of monomers, suggesting that the steric hindrance caused by the large mesogenic side-groups resulted in the monomers with mesogenic side groups being less easily incorporated into the growing free radical

Monomer 1	Monomer 2	% Monomer 2	g / °C	Tcl / °C
$\begin{array}{c} \text{CH}_3 \\   \\ \text{CH}_2=\text{C} \\   \\ \text{CONH}(\text{CH}_2)_{11}\text{COOchol} \end{array}$	$\begin{array}{c} \text{H} \\   \\ \text{CH}_2=\text{C} \\   \\ \text{COOC}_4\text{H}_9 \end{array}$			
		0	120	180
		58	65	160
		63	60	140
$\begin{array}{c} \text{CH}_3 \\   \\ \text{CH}_2=\text{C} \\   \\ \text{CONH}(\text{CH}_2)_{11}\text{COOchol} \end{array}$	$\begin{array}{c} \text{CH}_3 \\   \\ \text{CH}_2=\text{C} \\   \\ \text{COOC}_4\text{H}_9 \end{array}$	83	20	100
		0	120	180
		10	115	180
		33	105	170
		60	85	160

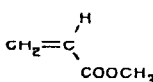
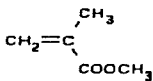


**Table 6.13** The results of the copolymerizations carried out by Platé *et al.*<sup>139</sup>

polymer backbone. Unfortunately there appears to be no general trend in the effect of adding small amounts of the non-mesogenic monomer on the  $\bar{M}_w$  and  $\bar{M}_n$  values of the copolymers except that at high concentrations of the non-mesogenic monomer in the copolymer, high values for  $\bar{M}_w$  and  $\bar{M}_n$  were obtained.

In the case of the copolymers containing methyl acrylate, the  $\bar{M}_w/\bar{M}_n$  values steadily increase as the concentration of non-mesogenic monomer increases, primarily due to the rapid increase in  $\bar{M}_w$  values of the copolymers. This suggests that the methyl acrylate being more reactive than the mesogenic monomer, is being used more rapidly at the outset of the free radical polymerization to form high molecular weight polymers. The rapid rise in the  $\bar{M}_n$  value of the copolymers as the amount of non-mesogenic moiety in the copolymer is increased from 10 to 50 % is indicative of the ease of polymerization due to the presence of the non-mesogenic moiety.

For copolymers containing methyl methacrylate the same trend in the  $\bar{M}_w/\bar{M}_n$  values is observed initially but at high concentrations of the non-mesogenic moiety in the copolymer, the  $\bar{M}_w/\bar{M}_n$  values fall. In this case it could be that the extra methyl group in methyl methacrylate is causing some steric hindrance in the free radical process and therefore is less reactive in a mixed system like this. Only at high concentration of the non-mesogenic moiety in the copolymer do we observe a rapid rise in both  $\bar{M}_w$  and  $\bar{M}_n$  values for the copolymers. This is indicative of the ease of polymerization due to presence of the non-mesogenic moiety.

Mesogenic monomer								
$\text{CH}_2=\text{CHCOO}(\text{CH}_2)_7\text{COO}-\text{C}_6\text{H}_4-\text{C}_6\text{H}_3(\text{F})-\text{OC}_8\text{H}_{17}$								
Comonomer	Polymer	% Comonomer		$\bar{M}_w$	$\bar{M}_n$	$\bar{M}_w/\bar{M}_n$	Tcl / °C Mic	Tcl / °C DSC
		Theoretical	Actual					
	<b>XIX</b>	0	0	36900	26000	1.4	164	164
	<b>XXII</b>	5	11	36200	20900	1.7	157	146
	<b>XXIII</b>	10	12	25600	16100	1.6	155	142
	<b>XXIV</b>	50	52	107000	51000	2.1	102	83
	<b>XXV</b>	80	80	299000	92500	3.2	-	29
	<b>XXVI</b>	5	9	33700	14100	2.4	149	149
	<b>XXVII</b>	10	27	39900	11800	3.4	149	147
	<b>XXVIII</b>	50	72	106000	64100	1.7	-	147
	<b>XXIX</b>	80	90	87400	54500	1.6	-	-

Mic = microscopy, DSC = differential scanning calorimetry

**Table 6.14** The results of the copolymerization of mesogenic and non-mesogenic monomers.

These results confirm the findings by Platé *et al.*,<sup>139</sup> that clearing points of the copolymers fall with increasing amount of non-mesogenic comonomer. The incorporation of a non-mesogenic acrylate into a SCLC polyacrylate had a much more detrimental effect upon the clearing points of the copolymers than the inclusion of the non-mesogenic methacrylate, which had very little effect on the clearing points of the copolymers. The effects that adding different amounts of non-mesogenic comonomer had upon the liquid crystalline phases are shown in the photomicrographs (Plates 2, 8 and 9). The defect texture exhibited by the homopolymer produced from the mesogenic monomer used for these experiments is characteristic of a smectic A ( $S_A$ ) phase (Plate 2). As can be clearly seen from the photomicrographs (Plates 2, 8, 9) the addition of even 5 % of non-mesogenic comonomer (Plate 8) has the effect of disrupting the liquid crystalline order of the phase, making the defect texture indistinguishable. The addition of 27 % of the non-mesogenic component results in a phase which shows no defect texture (Plate 9).

#### **6.3.1.2 Butyl Acrylate and Methacrylate as Non-Mesogenic Monomer.**

Similar results were obtained when the study was repeated using butyl acrylate and butyl methacrylate as the non-mesogenic comonomers. The results are summarised in Table 6.15. It can be clearly seen that there is no general trend suggesting that increasing amounts of non-mesogenic component will produce polymers with increasing  $\bar{M}_w$  and  $\bar{M}_n$  values. Also the trend of decreasing clearing points with increasing amount of non-mesogenic component can be clearly seen, but in this case

the incorporation of the non-mesogenic methacrylate had a much more detrimental effect upon the clearing points of the copolymers than the incorporation of the non-mesogenic acrylate. If we now compare the decrease in the clearing points of the copolymers by the addition of the non-mesogenic moieties to the mesogenic acrylate, then the following efficiency order can be compiled.

Butyl methacrylate » Butyl acrylate > methyl acrylate > methyl methacrylate.

The defect textures are also unidentifiable even for 5 % butyl methacrylate comonomer addition (Plate 10).

This work has been continued at the University of Hull by J. Haley.<sup>140</sup> The experiments were repeated but using the mesogenic methacrylate instead of the mesogenic acrylate. Results from this study along with the corresponding data for the mesogenic acrylates are shown in Table 6.16. The first point to note from the results is the much larger degree of polymerization seen in the methacrylate polymers. Generally polymethacrylates are much easier to polymerize than polyacrylates and hence have larger degrees of polymerization. Another point to note is that the polyacrylate homopolymer produced a  $S_A$  phase, whereas the polymethacrylate homopolymer exhibits a  $S_C$  phase. Due to the variation in  $\bar{M}_w$ ,  $\bar{M}_n$  and  $\bar{M}_w/\bar{M}_n$  values, comparison of the copolymers is difficult. However, it does seem that by adding non-mesogenic methacrylate monomers to a mesogenic monomer, whether it be acrylate or methacrylate, has the effect of reducing the transition temperature by a greater amount than by adding a non-mesogenic acrylate monomer to a similar mesogenic monomer.

Mesogenic monomer								
$\text{CH}_2=\text{CHCOO}(\text{CH}_2)_7\text{COO}-\text{C}_6\text{H}_4-\text{C}_6\text{H}_3(\text{F})-\text{OC}_8\text{H}_{17}$								
Comonomer	Polymer	% Comonomer		$\bar{M}_w$	$\bar{M}_n$	$\bar{M}_w/\bar{M}_n$	Tcl / °C Mic	Tcl / °C DSC
		Theoretical	Actual					
$\text{CH}_2=\underset{\text{COO}(\text{CH}_2)_3\text{CH}_3}{\overset{\text{H}}{\text{C}}}$	<b>XIX</b>	0	0	36900	26000	1.4	164	164
	<b>XXX</b>	5	7	18000	12300	1.5	-	140
	<b>XXXI</b>	10	14	52200	26600	2.0	-	129
	<b>XXXII</b>	20	19	169000	53200	3.2	-	110
	<b>XXXIII</b>	50	46	31800	18200	1.8	-	51
	<b>XXXIV</b>	80	78	23700	11900	2.0	-	-
$\text{CH}_2=\underset{\text{COO}(\text{CH}_2)_3\text{CH}_3}{\overset{\text{CH}_3}{\text{C}}}$	<b>XXXV</b>	5	5	35500	18200	2.0	-	113
	<b>XXXVI</b>	10	11	50000	34000	1.5	-	110
	<b>XXXVII</b>	50	57	76000	43100	1.8	-	11
	<b>XXXVIII</b>	80	80	54200	36000	1.5	-	-

Mic = microscopy, DSC = differential scanning calorimetry

**Table 6.15** The physical and thermal properties of the copolymerization of mesogenic and non-mesogenic monomers.

Polymer	X	Y	% non-mesogenic comonomer		$\bar{M}_w$	$\bar{M}_n$	$\bar{M}_w/\bar{M}_n$	Tcl / °C DSC
			Theoretical	Actual				
<b>XIX</b>	H	-	0	0	36900	26000	1.4	164
<b>XXXIX</b>	CH <sub>3</sub>	-	0	0	268000	107000	2.5	138
<b>XXXI</b>	H	H	10	14	52200	26600	2.0	129
<b>XXXVI</b>	H	CH <sub>3</sub>	10	11	50000	34000	1.5	110
<b>XL</b>	CH <sub>3</sub>	CH <sub>3</sub>	20	10	380000	153000	2.5	111
<b>XLI</b>	CH <sub>3</sub>	H	10	7	287000	174000	1.7	138

**Table 6.16** The physical and thermal properties of copolymerization of mesogenic and non-mesogenic monomers.

The issue is complicated further by work carried out by Merck (UK)<sup>141</sup> as part of our collaboration, suggests improvements in liquid crystal phase identification for similar copolymers with much smaller degrees of polymerization ( $\bar{DP} \approx 11$ ). The copolymers were produced by using 1,2-dichloroethane as the polymerization solvent, the addition of 5 % butyl acrylate, enhanced the formation of an identifiable liquid crystalline defect texture, compared to that of the homopolymer produced from the mesogenic acrylate, without producing a dramatic reduction of the transition temperature of the phase. One possible explanation for this result could be that for a polymer with a  $\bar{DP} \approx 11$ , only a small number (if any) of the non-mesogenic units would be present in each polymer chain, due to the chains themselves being very short. The very low amount of non-mesogenic impurity means that not every polymer chain contains the impurity and the effect it has upon the transition temperature is diluted. The polymer chains which do contain non-mesogenic units may be more flexible and allow the faster formation of liquid crystalline phases.

#### **6.4 Random Mesogenic Copolymers.**

A series of random mesogenic copolymers was synthesized, in which one mesogenic unit was known to form an  $S_C$  phase when polymerized and the other comonomer contained a chiral unit. The purpose of this study was to try and induce chirality into an  $S_C$  phase in order to produce SCLC polymers exhibiting a chiral smectic C ( $S_C^*$ ) phase. The reason for carrying out this study stems from the fact that SCLC polyacrylates and polymethacrylates are not miscible. In LMM liquid crystalline

systems the transition temperatures of the liquid crystal phases can be fine-tuned by mixing the LMM liquid crystal material with different proportions of other mesogenic or non-mesogenic components. In LMM liquid crystals the resulting physical properties of these mixtures are different than those of the components of the mixture (when measured in isolation). Unfortunately it is not possible to fine-tune the physical properties of SCLC polyacrylates or polymethacrylates by the same methods due to the fact that they will not mix with low molar mass materials. Even if the required components are appended to similar polymer backbones it is not possible to mix the different polymers. Any attempt to mix polymers results in phase separation. Therefore the only way to combine different mesogenic and non-mesogenic systems in SCLC polymers is by attaching them to the same polymer backbone. This can be achieved by copolymerizing the components, in an attempt to combine the required constituents of a mixture on the same polymer backbone.

The  $S_C$  forming monomer **XIX** is shown in Figure 6.14, and the chiral monomer was chosen from the other monomers shown in Figure 6.14. Some comonomers which did not possess chirality were also copolymerized to investigate the effect that they had on the system.

A summary of the copolymers that were synthesised and their physical properties is given in Table 6.17. In general the identification of the liquid crystal defect textures was very difficult, even in cases where the copolymer was annealed for 2 weeks, 5 °C below the phase transition, no defect texture was observed. The appearance of the slide was still that of the sandy texture characteristic of a large number of SCLC

polymer phases, irrespective of the liquid crystal phase that they exhibit. In order to identify the liquid crystal phases, some of the samples were sent to the University of Bristol for X-ray diffraction analysis. Some of the preliminary results are described below.

Monomer	Structure
<b>XIX</b>	$\text{CH}_2=\text{CHCO}_2(\text{CH}_2)_7\text{CO}_2\text{-}\langle\text{C}_6\text{H}_4\rangle\text{-}\langle\text{C}_6\text{H}_3(\text{F})\rangle\text{-OC}_8\text{H}_{17}$
<b>XI</b>	$\text{CH}_2=\text{CHCO}_2(\text{CH}_2)_6\text{O-}\langle\text{C}_6\text{H}_4\rangle\text{-}\langle\text{C}_6\text{H}_4\rangle\text{-CO}_2\overset{\text{CH}_3}{\underset{x}{\text{CH}}}(\text{CH}_2)_5\text{CH}_3$
<b>XVIII</b>	$\text{CH}_2=\text{CHCO}_2(\text{CH}_2)_{11}\text{O-}\langle\text{C}_6\text{H}_4\rangle\text{-}\langle\text{C}_6\text{H}_4\rangle\text{-CO}_2\overset{\text{CH}_3}{\underset{x}{\text{CH}}}\text{CO}_2\text{CH}_2\text{CH}_3$
<b>XLII</b>	$\text{CH}_2=\text{CHCO}_2(\text{CH}_2)_{11}\text{O-}\langle\text{C}_6\text{H}_4\rangle\text{-}\langle\text{C}_6\text{H}_4\rangle\text{-CO}_2\text{-}\langle\text{C}_6\text{H}_{10}\text{C}_2\text{CH}_3\rangle \quad (\dagger)$
<b>XV</b>	$\text{CH}_2=\text{CHCO}_2(\text{CH}_2)_{11}\text{O-}\langle\text{C}_6\text{H}_4\rangle\text{-}\langle\text{C}_6\text{H}_4\rangle\text{-CO}_2\text{-}\langle\text{C}_6\text{H}_{10}\text{C}_2\text{CH}_3^*\rangle$

**Figure 6.14** The monomers used for the mesogenic copolymer study.

Monomer 1	Monomer 2	Mass Ratio	$\bar{M}_w$	$\bar{M}_n$	$\bar{M}_w/\bar{M}_n$	Tg / °C	Peak / °C	Peak / °C	Peak / °C	Peak / °C	Tcl / °C
XV	-	-	12600	9740	1.1	-20.9	-	-	-	-	38.4
XIX	-	-	36900	26000	1.4						164.0
XI	XIX	1:1	12800	9470	1.4	-	-	-	-	108.9	143.0
XVIII	XIX	1:1	27900	16400	1.7	-6.2	-	-	-	57.0	96.5
XVIII	XIX	1:5	30300	20900	1.4	-	27.14	71.7	95.0	106.6	127.1
XLII	XIX	1:5	19100	12700	1.5	-0.9	-	-	91.5	116.0	136.3
XV	XIX	1:1	23800	13400	2.1	-	-	-	-	57.7	106.9

**Table 6.17** The physical and thermal properties of the mesogenic copolymers produced by free radical polymerization.

The sample that has been examined so far was the 1:5 copolymer of monomers XVIII + XIX, the DSC and GPC for the copolymer is summarised in Table 6.17, the DSC traces are reproduced in Figures 6.15 and 6.16, and show at least four transitions. A flat plate sample was prepared and orientation of the sample was achieved by cooling the sample from the isotropic state in a magnetic field (9 Tesla).

X-ray diffraction (XRD) patterns were obtained at selected temperatures, at least one in between each transition, on heating and cooling the sample. This was done without taking the sample into the isotropic state. In order to resolve some of the weaker features in the diffraction patterns, exposures of up to six hours were required. X-ray data from this material is still being analyzed. Only the data from the cooling cycle will be discussed. Diffraction patterns were obtained at 110, 95, 76, 46, 20 °C. The diffraction patterns observed at each of the temperatures were almost identical. Along the equatorial plane three strong peaks were observed. The smectic periodicity  $d$ , was about 62 Å, which did not alter with decreasing temperature (see Figure 6.17). Due to the close proximity of the first layer reflection to the beam stop, the smectic periodicity was more accurately estimated from the second and third order reflections. At lower temperatures some weaker peaks were observed (see Figure 6.18). These peaks were indexed as higher order layer reflections as given in Table 6.18 and Table 6.19. At wide angles symmetrical diffuse crescents were observed along the meridian. These wide angle crescents arose from the spatial correlations between the side chain mesogenic units. The fact that the position of the crescents did not move from the meridian plane and that there was no change in the smectic periodicity with decreasing temperatures suggested that the unit cell of all the phases should be orthogonal

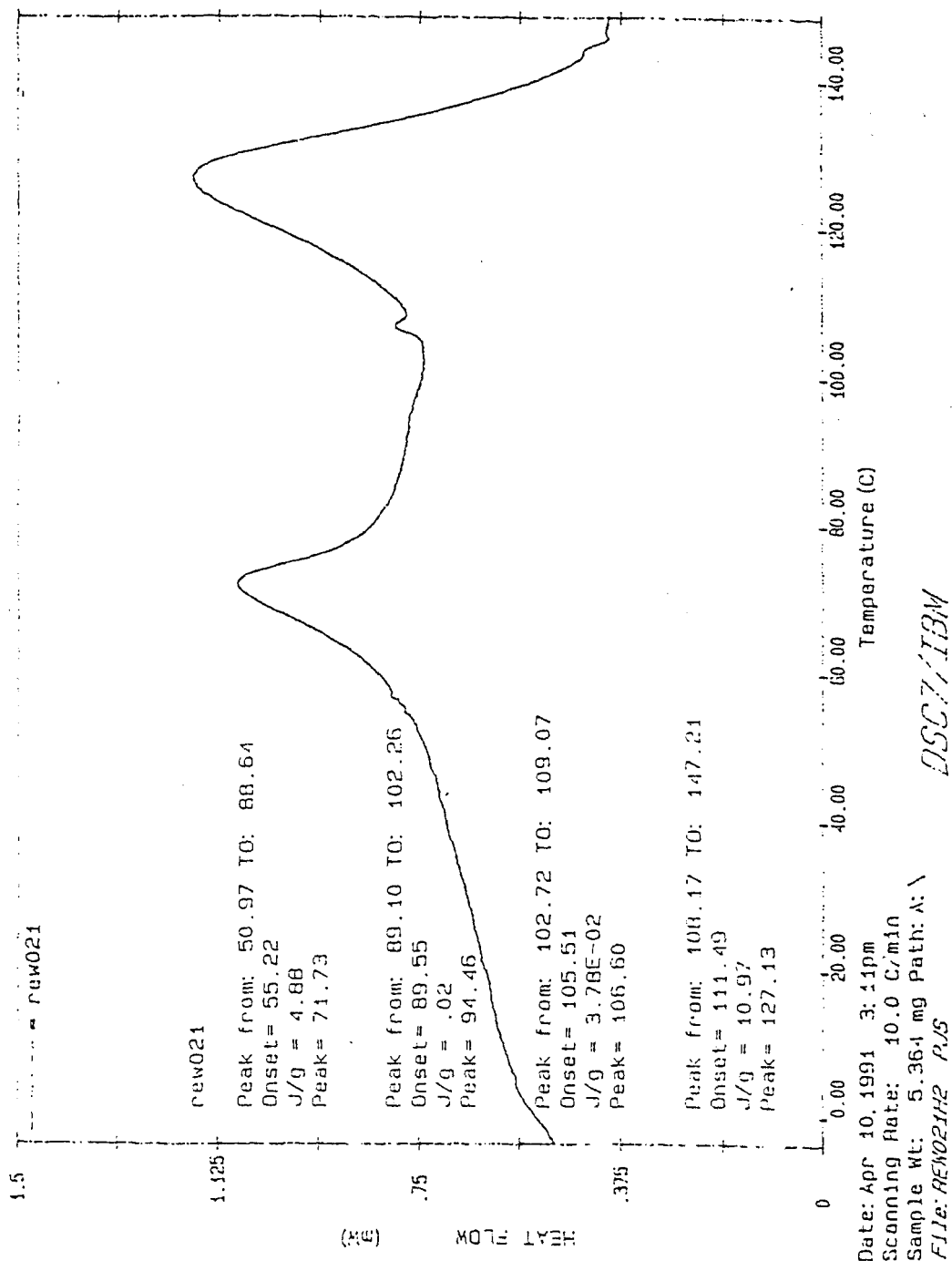
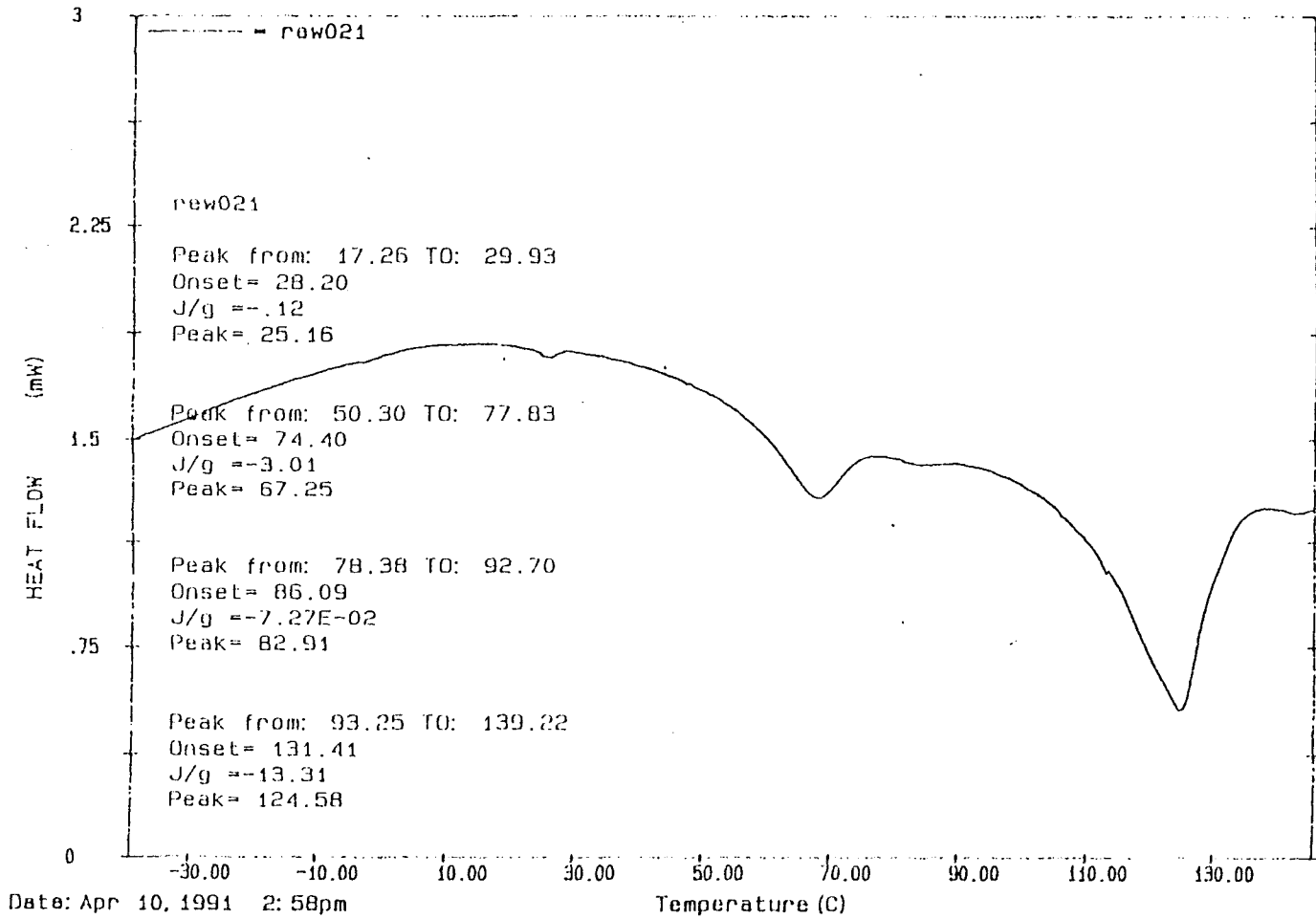


Figure 6.15 The DSC heating curve of the 1:5 copolymer XVIII + XIX.

Figure 6.16 The DSC cooling curve of the 1:5 copolymer XVIII + XIX.

208



Date: Apr 10, 1991 2: 58pm  
Scanning Rate: -10.0 C/min  
Sample Wt: 5.364 mg Path: A:\  
File: REN021C1 PJS

DSC7/IBM

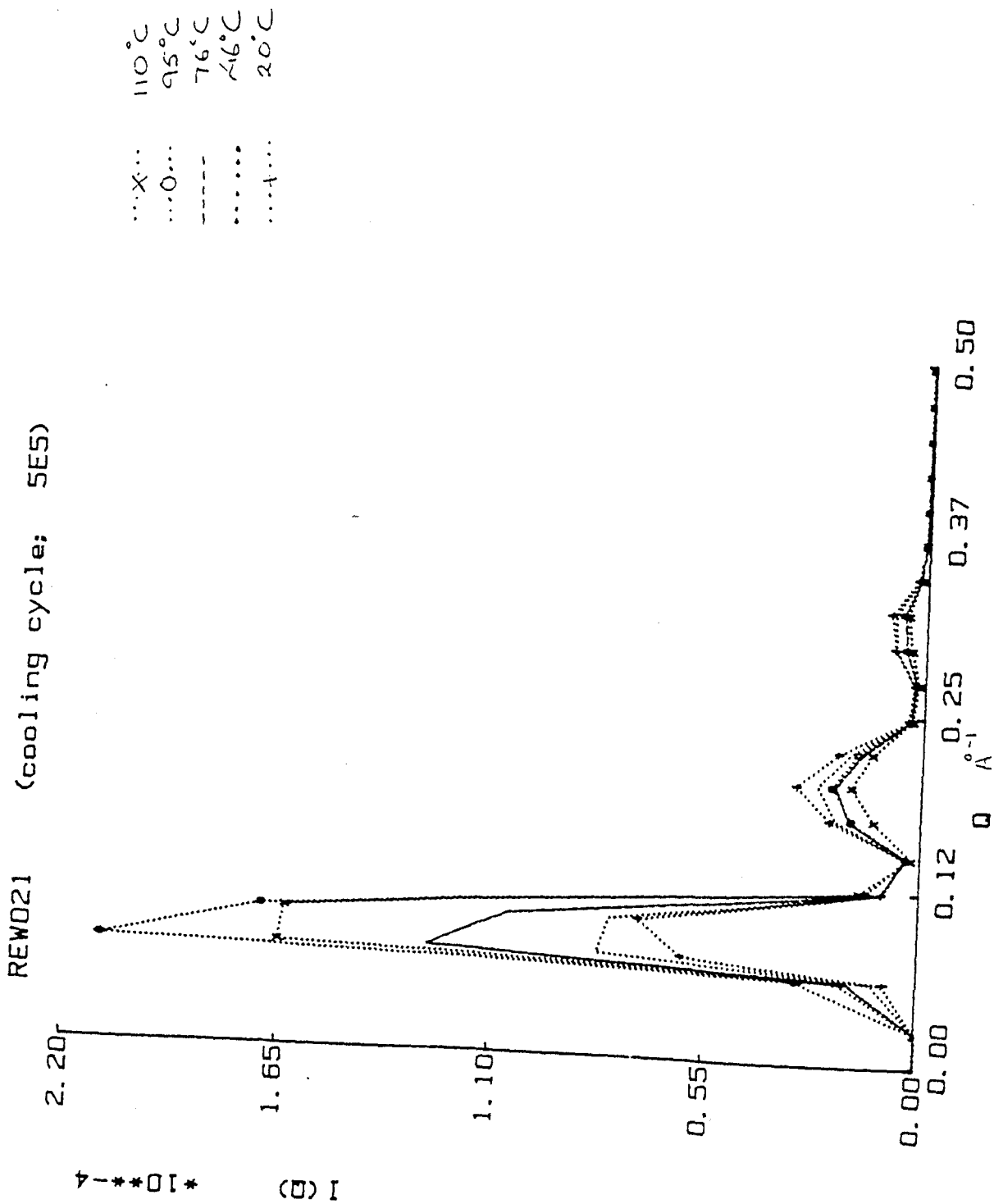
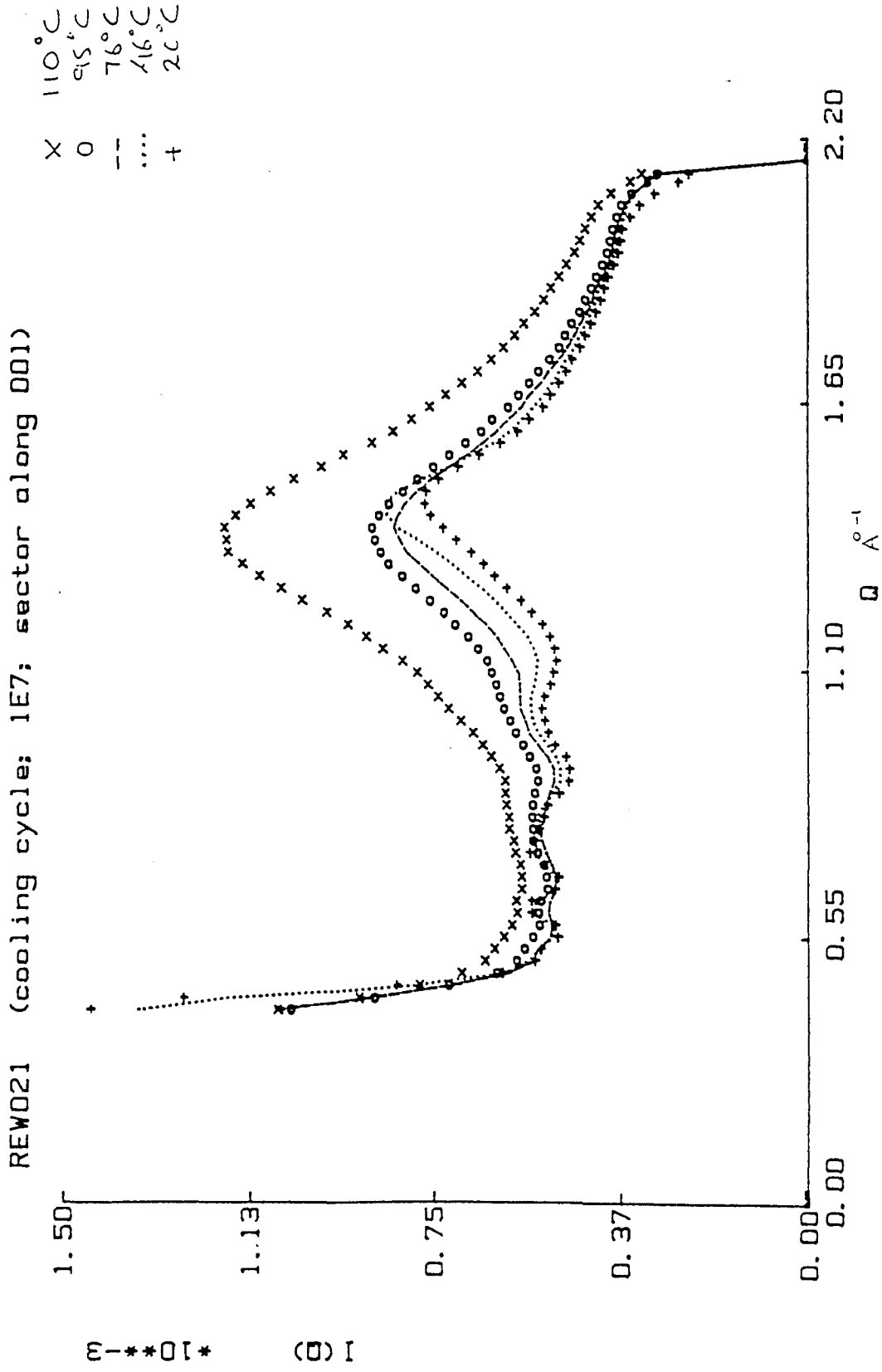


Figure 6.17 The Cooling cycle of the 1:5 copolymer XVIII + XIX.



**Figure 6.18** The cooling cycle 1E7; sector along 001 of the 1:5 copolymer XVIII + XIX.

*i.e.*  $S_A$ ,  $S_B$ , or  $S_E$ . The wide angle peak moved to lower d-spacings (higher  $q$ ) as the temperature decreased (see Figure 6.19). At higher temperatures 110, 95 and 76 °C the peak was diffuse as would be expected from a  $S_A$  phase. At 46 °C the peak was much sharper suggesting a higher ordering within the layers, perhaps a hexatic phase, however the width of the peak suggested that the ordering within the layers was much weaker than that observed in the hexatic phases of low molar mass liquid crystalline materials. At 20 °C the peak moved to a lower d spacing, but there appeared to be a second diffuse peak (in the meridian plane) at  $q > 2.4$ , which was just outside the limits of the detector. This may be a  $S_E$  type phase with weak correlations within the layers.

hkl	$q / \text{\AA}^{-1}$	d-spacing / $\text{\AA}$
001	0.09	72.2
002	0.2	31.4
003	0.31	20.1
004	not observed	
005	0.51	12.3
006	0.61	10.3
007	0.72	8.7
008	0.8	7.9
009	not observed	
0010	1.01	6.3

**Table 6.18** The higher order reflections of the 1:5 copolymer XVIII + XIX.

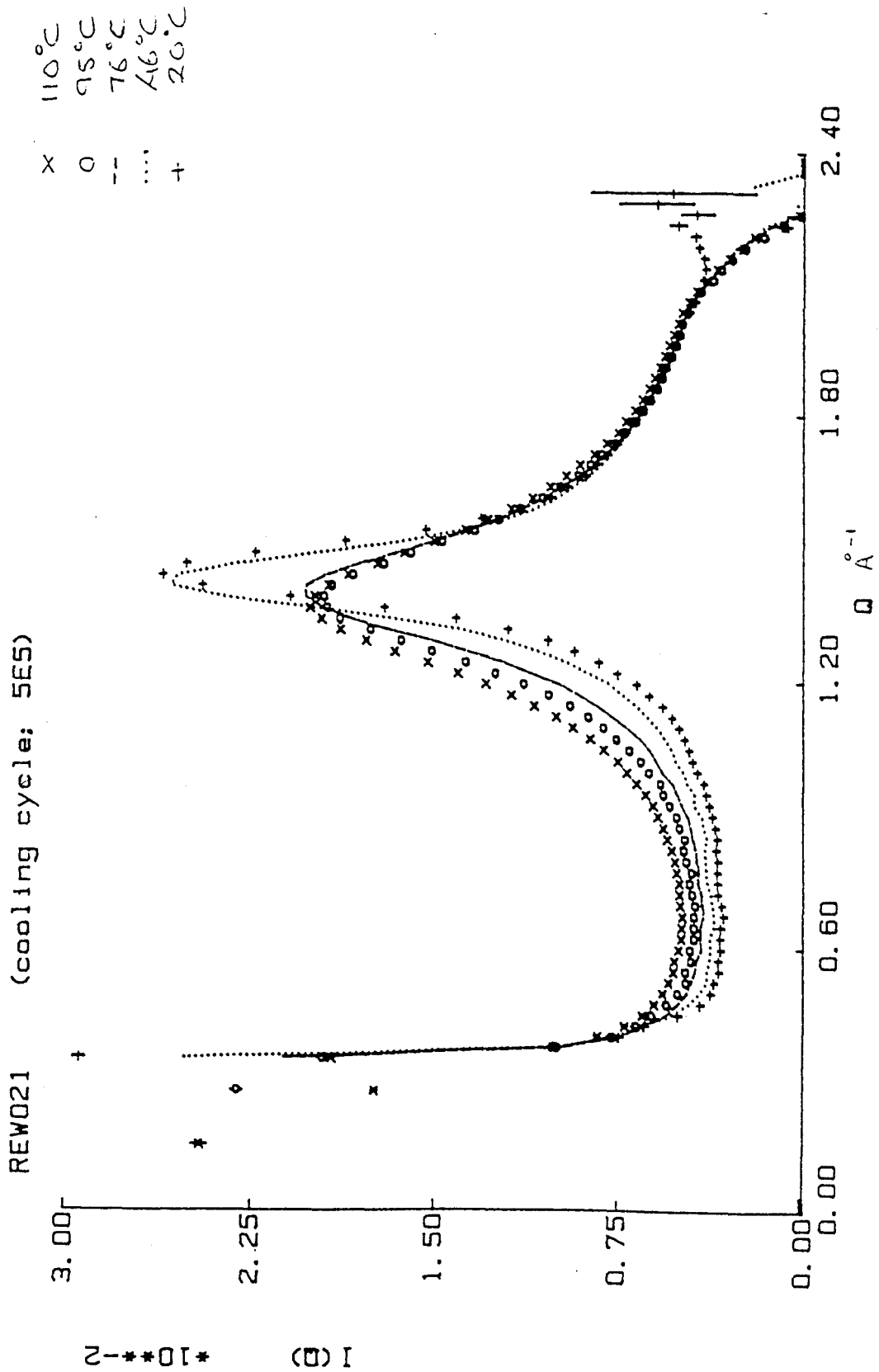


Figure 6.19 The cooling cycle 5E5 of the 1:5 copolymer XVIII + XIX.

Temp / °C	q / Å <sup>-1</sup>	d-spacing / Å
110	1.37	4.57
95	1.39	4.53
76	1.4	4.5
46	1.43	4.4
20	1.45	4.34

**Table 6.19** The variation of layer spacing with temperature for the copolymer.

The phase sequence can be summarised as follows:

110 °C       $S_A$  phase. The smectic periodicity,  $d$  (62 Å) was slightly smaller than twice the molecular lengths of the side chain units, measured from CPK models (see Table 6.20). This indicated that there was some interdigitation of the side chains.  $S_{Ad}$  type structure.

95 °C      Same phase. Layer reflections were stronger suggesting an increase in the ordering with reducing temperature.

76 °C       $S_A$  modification. Intensity of the 001 peak dropped, while the intensity of the 002 and 003 rose. No other changes were observed. This was still the  $S_A$  phase. The changes in the intensity of the 001 peaks suggested some changes in internal structure.

46 °C      Hexatic B phase showed weak inlayer correlations

20 °C      Maybe a  $S_E$  phase showing weak inlayer correlations.

The diagram shows two copolymer units. The top unit has a side chain consisting of a hydrogen atom bonded to a carbon atom, which is also bonded to a CO<sub>2</sub>(CH<sub>2</sub>)<sub>7</sub>CO<sub>2</sub> group, a biphenyl ring system (with a fluorine atom on the second ring), and an OC<sub>8</sub>H<sub>17</sub> group. The bottom unit has a side chain consisting of a hydrogen atom bonded to a carbon atom, which is also bonded to a CO<sub>2</sub>(CH<sub>2</sub>)<sub>11</sub>O group, a biphenyl ring system, and a CO<sub>2</sub>CH(CH<sub>3</sub>)CO<sub>2</sub>C<sub>2</sub>H<sub>5</sub> group. Measurements A, B, C, and D are indicated by horizontal arrows above and below the structures, representing different lengths of the side chain units.

Measurement	Length /Å
A	36.2
B	33.0
C	34.4
D	37.2

**Table 6.20** The length of the side chain units of the copolymer.

## 6.5 Alignment and Phase Identification of SCLC Polymers.

The techniques described in Section 5.11 were used for the alignment and subsequent phase identification of a large number of SCLC polymer samples produced by several research groups. The alignment process, as previously described, is a very time consuming process. It can take up to 2 weeks for an identifiable liquid crystalline defect texture to be formed from a SCLC polymer sample that initially shows the sandy texture. Once a good defect texture has been formed it is then possible to identify the liquid crystalline phase. However, if several phases are present at different temperatures, the annealing process must be carried out each time the temperature is altered. The techniques described in Section 5.11 have been applied to many samples from different research groups, in particular polymers produced by Merck (UK) as part of a collaboration under a MOD contract, and other polymers produced by members of the Liquid Crystal Group at the University of Hull. The technique has been applied to polyacrylates, polymethacrylates, polyesters and linear and cyclic polysiloxanes, with varying amounts of success. Many different phases have been identified after successful alignment including  $S_A$ ,  $S_C$ ,  $S_I$ ,  $S_A^*$ ,<sup>27</sup> and N. This work was reported as a poster at the Macro Group UK meeting at Lancaster (1991).<sup>142</sup>

The typical "sandy" texture of a liquid crystalline phase of a SCLC polymer is shown in Plate 1 for Polymer XIX. Annealing Polymer XIX at 150 °C for 24 h without any aligning agent resulted in the focal conic texture of the  $S_A$  phase (Plate 2).

Two particular examples of polymers supplied by Merck (UK) are shown in Figure 6.20 and 6.21, the results of the alignment are shown in Plates 3, 4, 5, 6 and 7.

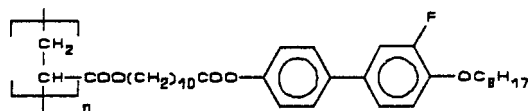


**Figure 6.20** A polyacrylate supplied for phase identification by Merck (UK) (XX).

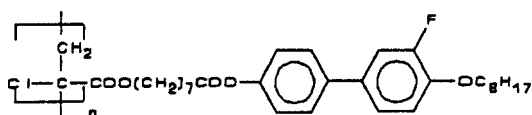


**Figure 6.21** A polychloroacrylate supplied for phase identification by Merck (UK) (XXI).

Examples of the textures formed by both the homogeneous and homeotropic alignment techniques described previously are shown in Plates 3 and 4.

Plate 3 shows a homeotropically aligned smectic C ( $S_C$ ) phase formed by Polymer XXI at 130 °C. The smectic C phase may be identified from the characteristic Schlieren defect texture, similar to the texture exhibited by LMM compounds that exhibit smectic C phases.

Plate 4 shows a homogeneously aligned smectic A ( $S_A$ ) phase formed by Polymer XIX at 150 °C, showing the characteristic focal conic texture.

Plates 5, 6 and 7 are a sequence of plates that show the textures formed by cooling Polymer XX from 105 °C to 30 °C. Plate 5 shows the clean focal conic smectic A phase at 105 °C, which on cooling to 90 °C gives rise to the broken focal conic texture of the smectic C phase (Plate 6). On further cooling this gives rise to an even more patchy defect texture of another smectic phase, possibly a smectic I phase at 30 °C (Plate 7).

It can be seen from the plates, that the defect textures that are formed by SCLC polymers are similar to those shown by LMM liquid crystalline materials showing the same phases, hence if a defect texture can be produced by annealing SCLC polymers, then it should be possible to identify the liquid crystalline phase.

### **6.5.1 Limitations of the Alignment Procedure.**

All the above examples are of SCLC polyacrylates and polymethacrylates. Attempts have been made to use the described alignment procedures for the identification of SCLC polysiloxanes, however it was found that there was much less tendency for a defect texture to form from the sandy texture for polysiloxanes. One possible explanation is that the polysiloxane backbone is much more flexible than either the polyacrylate or polymethacrylate backbone. As a result although the mesogenic side chains will be much more able to move about, once they achieve an position of alignment they are much less likely to be "frozen" into position. Another possible theory is that the extent of alignment is due to the interaction of the polymer backbone

with the nylon aligning agent. If there is less interaction between the polysiloxane backbone and the nylon than occurs between the polyacrylate backbone and the nylon, then it can be seen that there is less likely to be a good alignment in polysiloxanes. If this last statement proves to be true it is possible that other polymer alignment layers may prove more successful at producing "good" defect textures from polysiloxanes and other SCLC polymers with different polymer backbones. The investigation of aligning agents for other types of SCLC polymer backbones was beyond the scope of this investigation.

The success of this technique in producing liquid crystal defect textures that were good enough to identify liquid crystal phases, meant that alignment of many samples was attempted, including samples from Merck (UK) as part of our collaboration and also from within the Liquid Crystal Group at the University of Hull. As a result it was found that the technique worked better for some systems than for others. One major factor that appears to affect the production of identifiable defect textures is the degree of polymerization of the polymer. Polymers with a low degree of polymerization ( $\overline{DP} \approx 10$ ), do not generally produce good defect textures and tend to need long annealing times ( $\approx 7$  days), in cases where the degree of polymerization  $> 30$ , the defect texture appears much faster ( $\approx 4$  h). The mesogenic side chain can also have an effect although no correlation between side chain and the ability to form defect textures has been noted. Mixed mesogenic copolymers in particular proved to very difficult to induce to form good defect textures.

In summary it is often possible to produce identifiable defect textures from SCLC polymers if a wide enough variety of conditions and treatments are employed, and sufficient time is given to the problem. The techniques involved are very intensive on equipment time, due to the need for heating over a period of several days. Attempts were made to use separate ovens for the annealing process, although the transfer process between the oven and the hot stage caused new problems and resulted in the waste of many days of waiting patiently for the textures to form. More work needs to be carried out to improve both the alignment techniques and also to try and free equipment for other purposes.

## 6.6 Cyclic Polymers.

A series of novel cyclic polysiloxanes was produced using a variety of alkenes, some of which were supplied by Merck (UK). The aim of the study of these cyclic systems was to gain some knowledge about the types of phases exhibited by these systems.

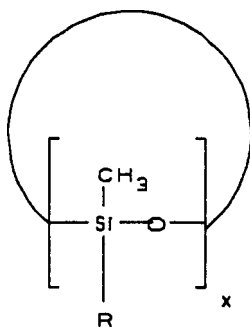


**Figure 6.22** Structure of cyclic polysiloxanes.

The following polymers given in Tables 6.21 to 6.29 were produced by substituting the group R in Figure 6.22 by a mesogenic side chain using the method given in Section 5.10.3.2.

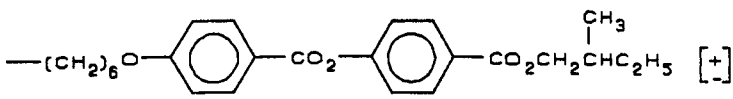
The side chain used in the production of polymer XLIV had been attached to a linear polysiloxane backbone at the University of Hull during previous projects.<sup>143</sup> The linear polysiloxane exhibited a chiral smectic C phase ( $S_C^*$ ). The linear polysiloxane backbone that was used was DOW DC1107 ( $\bar{DP} = 40 \pm 3$ ), the liquid crystalline transition temperatures for this chiral polymer were as follows.

$g -9 T_m 75 S_C^* 75 ^\circ C I$

The results for the cyclic polysiloxanes are given in Tables 6.21 and 6.22. As could be predicted from the work of Richards,<sup>101</sup> the same phase was exhibited by the cyclic polysiloxane as was found for the linear polysiloxane. The phase identification was much easier for the cyclic polysiloxanes, due to the fact that the defect textures that were exhibited by the cyclic polymers formed very quickly and were very similar to those commonly found for LMM materials. The transition temperatures for the cyclic polymers of tetramethyl tetrahydrocyclosiloxane (XLIIIa and XLIVa) seemed to be dependent upon the thermal history of the prepared slides.

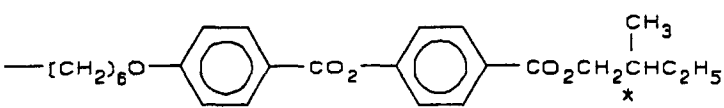
If a freshly prepared slide was annealed at a temperature just below the  $S_C$ -I transition, then the texture exhibited by the sample would be the focal conic  $S_C$  texture with pitch bands (Plate 11). However after 24 h annealing at the same temperature the focal conic fans would have disappeared and given rise to small "butterfly" shaped structures (Plate 12). This defect texture appeared to suggest that

the sample may be exhibiting a discotic phase. Heating and cooling the sample would regenerate the focal conic texture. The sample did not appear to be crystalline at the temperatures at which these effects took place. Another interesting feature was shown by cyclic polymer **XLIIIa**. When heated to about 80 °C the texture appeared to resemble that of the isotropic liquid (*i.e.* uniform dark field of view) but containing small points of light; this texture has been named "the sky at night". It has been postulated that these points of light may correspond to the columns in a discotic liquid crystalline phase. If this sky at night texture was annealed overnight a focal conic smectic C texture appeared. Compounds of this type were sent to Dr R. Richardson for X-ray diffraction studies, some of the preliminary results are given later in Section 6.6. The X-ray analysis has confirmed the presence of the  $S_C$  phase.

						
Polymer	x	$\bar{M}_w$	$\bar{M}_n$	$\bar{M}_w/\bar{M}_n$	Tg / °C	$S_C$ -I / °C
<b>XLIIIa</b>	4	2968	2710	1.1	-30.7	†101.5
<b>XLIIIb</b>	5	3220	2850	1.1	-39.8	33.4

† phase transitions dependant upon thermal history.

**Table 6.21** The physical and thermal properties of Polymers **XLIII(a + b)**.

						
Polymer	x	$\bar{M}_w$	$\bar{M}_n$	$\bar{M}_w/\bar{M}_n$	Tg / °C	S <sub>C-I</sub> / °C
<b>XLIVa</b>	4	2800	2660	1.1	-24.2	†90.0
<b>XLIVb</b>	5	2980	2760	1.1	-22.5	56.1

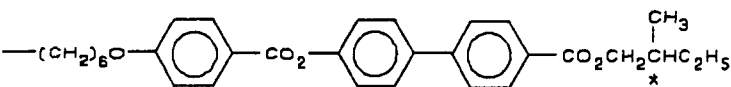
† phase transitions dependant upon thermal history.

**Table 6.22** The physical and thermal properties of Polymers **XLIV(a + b)**.

It can be seen that the S<sub>C-I</sub> transition temperatures for cyclic polymers **XLIII** and **XLIV** are low ≈ 93 °C, which suggests that by careful manipulation of the side chains it may be possible to produce polymers with room temperature S<sub>C</sub> phases. The cyclic polymer **XLIIIa** may be intermediate between a calamitic and a discotic structure, the thermal treatment of the compounds may encourage the preferential formation of one of the forms. One other point to note is that although viscosity measurements were not carried out on these polymers, cyclic polymers seemed to be much less viscous than their linear counterparts and hence were much easier to work with and align.

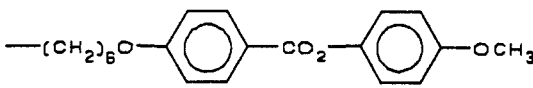
The results shown in Table 6.23 are for the biphenyl analogues of the polymers given in Table 6.22. The effect of adding one benzene ring is very significant; the phase type is unchanged but the transition temperatures for both the biphenyl analogues are very much higher. The g value of both polymers is much higher for the biphenyl

analogues, which means that by cooling these polymers slightly, the  $S_C$  phase could be "frozen" in.

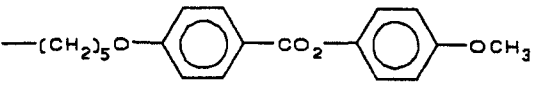
						
Polymer	x	$\bar{M}_w$	$\bar{M}_n$	$\bar{M}_w/\bar{M}_n$	Tg / °C	$S_C^* - I / ^\circ C$
XLVa	4	3580	3310	1.1	8.9	183.5
XLVb	5	4150	3690	1.1	11.5	187.0

**Table 6.23** The physical and thermal properties of Polymers XLV(a + b).

Tables 6.24 and 6.25 show the results of two polymers which have the same mesogenic side chain but different flexible spacer length. The polymers in Table 6.25 had a spacer length shorter by one methylene group. However, the results show that the properties of the polymers are very different. The polymers that have the longer spacer group have much lower glass and nematic to isotropic transition temperatures, and that polymers with the shorter spacer group show an additional phase below the nematic phase, this phase has not yet been identified.

						
Polymer	x	$\bar{M}_w$	$\bar{M}_n$	$\bar{M}_w/\bar{M}_n$	Tg / °C	N-I / °C
<b>XLVIa</b>	4	3340	2370	1.4	-5.0	34.4
<b>XLVIb</b>	5	2710	2290	1.2	-1.7	41.4

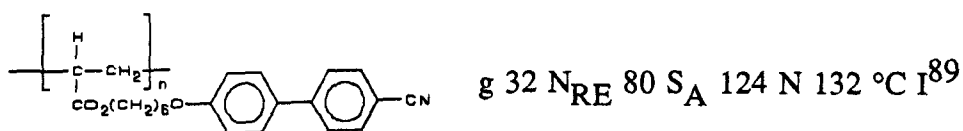
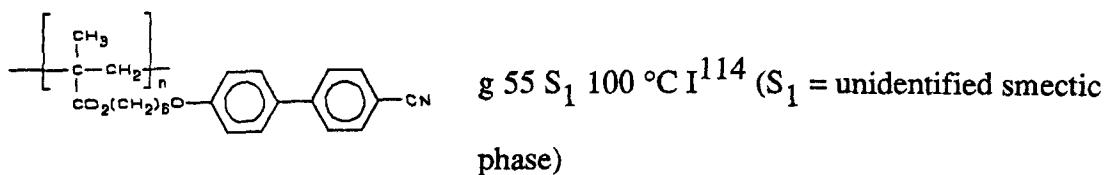
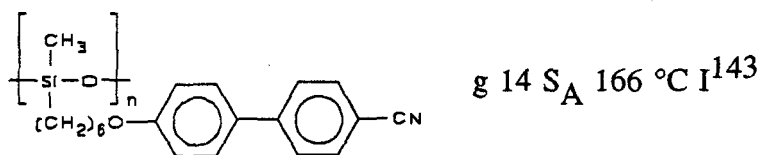
**Table 6.24** The physical and thermal properties of XLVI(a + b).

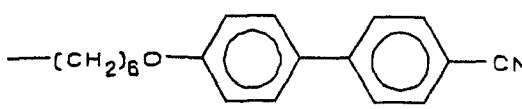
							
Polymer	x	$\bar{M}_w$	$\bar{M}_n$	$\bar{M}_w/\bar{M}_n$	g / °C	Peak / °C	N-I / °C
<b>XLVIIa</b>	4	1840	1758	1.1	9.4	90.7	102.4
<b>XLVIIb</b>	5	2100	1950	1.1	10.7	36.0	95.3

**Table 6.25** The physical and thermal properties of Polymers XLVII(a + b).

The results given in Table 6.26 can be compared to the results given in Table 6.11 for the corresponding polyacrylate and polymethacrylate that had been prepared by free radical polymerization. Both types of polymer exhibit  $S_A$  phases with very similar transition temperatures. The glass transition temperature is very much higher for the polymethacrylate than the cyclic polymers, the g value for the polyacrylate may not be a very representative figure due to the lack of phases in the polymer. Polymers

with this side chain and different polymer backbones are cited in the literature.<sup>143</sup>,  
114, 89



						
Polymer	x	$\bar{M}_w$	$\bar{M}_n$	$\bar{M}_w/\bar{M}_n$	g / °C	$S_A\text{-I} / ^\circ\text{C}$
XLVIIIa	4	1900	1750	1.1	4.9	105.3
XLVIIIb	5	2470	2058	1.2	5.6	86.0

**Table 6.26** The physical and thermal properties of Polymers XLVIII(a + b).

All the side chains used so far in this study have been terminally attached, the results shown in Tables 6.28 and 6.29 are for laterally attached side chains. All of the laterally attached polymers exhibit nematic phases, a feature which is in keeping with the phase types of laterally attached linear polysiloxanes.

Table 6.27 shows a summary of the data given by Gray *et al.*<sup>123</sup> for a series of linear polysiloxanes with laterally attached side chains. Although it is not possible to directly compare the linear polysiloxanes directly with the cyclic polysiloxanes produced in this work. Some relative comparisons may be drawn.

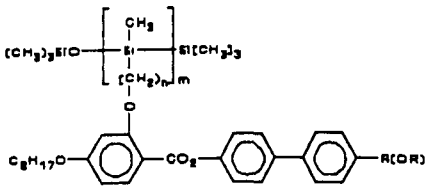
					
Polymer	n	R(OR)	g / °C	K - N / °C	N - I / °C
a	5	C <sub>3</sub> H <sub>7</sub>	8.5		31.7
b	5	C <sub>10</sub> H <sub>21</sub>	1.7		33.9
c	5	OC <sub>5</sub> H <sub>11</sub>	9.3		65.5
d	5	OC <sub>9</sub> H <sub>19</sub>	4.8		58.0
e	5	OC <sub>11</sub> H <sub>23</sub>	9.5		60.5
f	11	OC <sub>9</sub> H <sub>19</sub>		40.4	54.4

Table 6.27 The thermal properties of laterally attached linear polysiloxanes.<sup>123</sup>

1) Comparing **a** and **b**, the length of the alkyl chain makes very little difference to the clearing point of the polymer.

2) Comparing **d** and **f**, the length of the flexible spacer does not have an impact upon the clearing point of the polymer.

Therefore if we compare the linear polysiloxanes with the cyclic polysiloxanes. The cyclic polysiloxanes have lower *g* values than the corresponding linear polysiloxanes, similar to the effect seen for terminally attached side chains. The higher *g* values for the linear polysiloxanes may be due to the higher molecular weight of the polymer.

Polymer	x	$\bar{M}_w$	$\bar{M}_n$	$\bar{M}_w/\bar{M}_n$	Tg / °C	N-I / °C
<b>XLIXa</b>	4	2940	2830	1.0	-11.5	26.8
<b>XLIXb</b>	5	3230	3030	1.1	-11.6	20.9

**Table 6.28** The physical and thermal properties of Polymers **XLIX(a + b)**.

Polymer	x	$\bar{M}_w$	$\bar{M}_n$	$\bar{M}_w/\bar{M}_n$	Tg / °C	N-I / °C
<b>La</b>	4	3190	2920	1.1	-8.4	49.9
<b>Lb</b>	5	3540	3140	1.1	-6.5	47.4

**Table 6.29** The physical and thermal properties of Polymers L(a + b).

The results given in Table 6.30, indicate that not every side chain when attached to a cyclic polysiloxane backbone will form a liquid crystal phase. The polymer shows a low  $g$  value and a melting point at  $-1.8$  °C. Adding another ring to the side chain would probably result in a very interesting polymer.

Polymer	x	$\bar{M}_w$	$\bar{M}_n$	$\bar{M}_w/\bar{M}_n$	Tg / °C	m.p. / °C
<b>LI</b>	5	4000	3510	1.14	-24.6	-1.8

**Table 6.30** The physical and thermal properties of Polymer LI.

### 6.5.1 Mixed Lateral and Terminal Attachment of Side Chains to Cyclic Polysiloxanes.

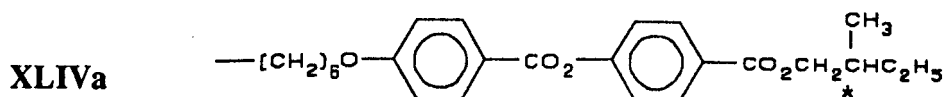
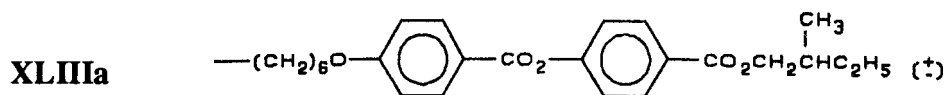
In order to try to modify the properties an attempt was made to substitute equal amounts of a laterally attached side chain **XLIX** and a terminally attached side chain **XLVIII** onto one common cyclic polysiloxane ring, by mixing the side chain alkenes together and then carrying out the hydrosilylation reaction. Only one attempt was made to carry out this kind of reaction due to lack of time before the end of the project. The results summarised in Table 6.31 show that the initial hydrosilylation reaction produced five products when the purity was checked by tlc (silica gel, dichloromethane) after seven precipitations, GPC indicated that there was no monomer present, leading to the conclusion that the product was a mixture of five different polymers. It was found that it was possible to isolate each of the polymers by flash column chromatography (silica gel, dichloromethane). The calculation of the ratio of lateral to terminal component was possible by analysis of the nmr spectrum for each of the fractions, it was found that the fractions varied in composition from 83 % lateral substitution to 77 % terminal substitution. The 77 % terminally substituted fraction showed a smectic A phase with transition temperatures comparable to those given in Table 6.26, and similarly for the 83 % laterally substituted fraction the phase exhibited was nematic with transition temperatures as shown in Table 6.28. Any fraction that contained any percentage of laterally attached side chain greater than 23 % exhibited a nematic phase. Although the purification steps are time consuming this may be a way of modifying the properties of cyclic polysiloxanes.

### 6.5.2 Miscibility of Cyclic Polysiloxanes.

It has been recently found at The University of Hull that cyclic SCLC polymers are miscible. This means that two SCLC cyclic polysiloxanes may be mixed, and the phase transitions exhibited by the mixture will be different than the phase transitions shown by the separate components. This means that the properties of SCLC cyclic polysiloxanes may be fine-tuned in a similar manner to that of LMM liquid crystals. This is a very great advantage compared to linear polymers which cannot be mixed.

### 6.6 X-ray Diffraction Studies on Cyclic Polysiloxanes.

The cyclic structures that were used in these studies were chosen because the phases that the compounds appeared to exhibit were dependent upon the thermal history of the sample. The compounds that were studied contained the side chains shown below substituted into the reactive hydrogen positions of the 4 silicon cyclic polysiloxane.



Polymer	Fraction	% Lateral Component	% Terminal Component	$\bar{M}_w$	$\bar{M}_n$	$\bar{M}_w/\bar{M}_n$	Transition / °C
LII	A	83	17	2750	2400	1.1	N <20 I
LIII	B	64	36	2710	2630	1.0	N 22 I
LIV	C	55	45	2490	2420	1.0	N 40 I
LV	D	-	-	2410	2340	1.0	N 42 I
LVI	E	37	63	2470	2400	1.0	N 65 I
LVII	F	23	77	2760	2460	1.1	S <sub>A</sub> 70 I
	Mixture	43	47	2600	2400	1.1	N 67 I

**Table 6.31** The physical and thermal properties of the fractionated mixed lateral/ terminal cyclic polysiloxane.

X-ray diffraction patterns observed from drawn fibres of both compounds are almost identical (see Figure 6.23). A plot from the regrouped intensity as a function of the scattering vector,  $q$ , shows that even the  $d$ -spacings of the various peaks are the same (see Figure 6.23). This is not surprising since the only difference between the two side chains is that one is a chiral version of the other. The quality of alignment observed was rather poor. A sharp inner ring was observed (at  $q = 0.26$ ) which was stronger along the equatorial plane (perpendicular to the fibre axis) whereas the diffuse outer ring ( $q = 1.35$ ) was stronger along the meridian. This is the kind of pattern that one would expect from a drawn fibre in the  $S_A$  phase. In addition to the above, at least five sets of peaks were also observed ( $q = 0.408, 0.516, 0.580, 0.756$  and  $0.905$ ). These peaks are not usually observed in smectic phases of either low molar mass or from SCLCP materials. Attempts to fit the various peaks to a hexagonal discotic lattice were unsuccessful and there was no splitting of the innermost peak as one would expect from a rectangular discotic phase. However these patterns closely resemble the diffraction patterns observed from ring polymers from the University of York<sup>144</sup> in the crystal phases occurring below the smectic phase. On scanning the regrouped intensities of the outer diffuse peaks radially (in the diffraction patterns from both polymers) there appears to be two pairs of peaks (low tilt  $S_C$  like).

A brief temperature study was carried out on the racemic polymer fibre **XLIIIa** between 27 °C and 53 °C which showed little change in diffraction pattern. It was also possible to draw a fibre at 46 °C where the material was supposed to be isotropic. A further study of these materials is required to determine if there are any mesophases at higher temperatures, which should be done using magnetically oriented samples.

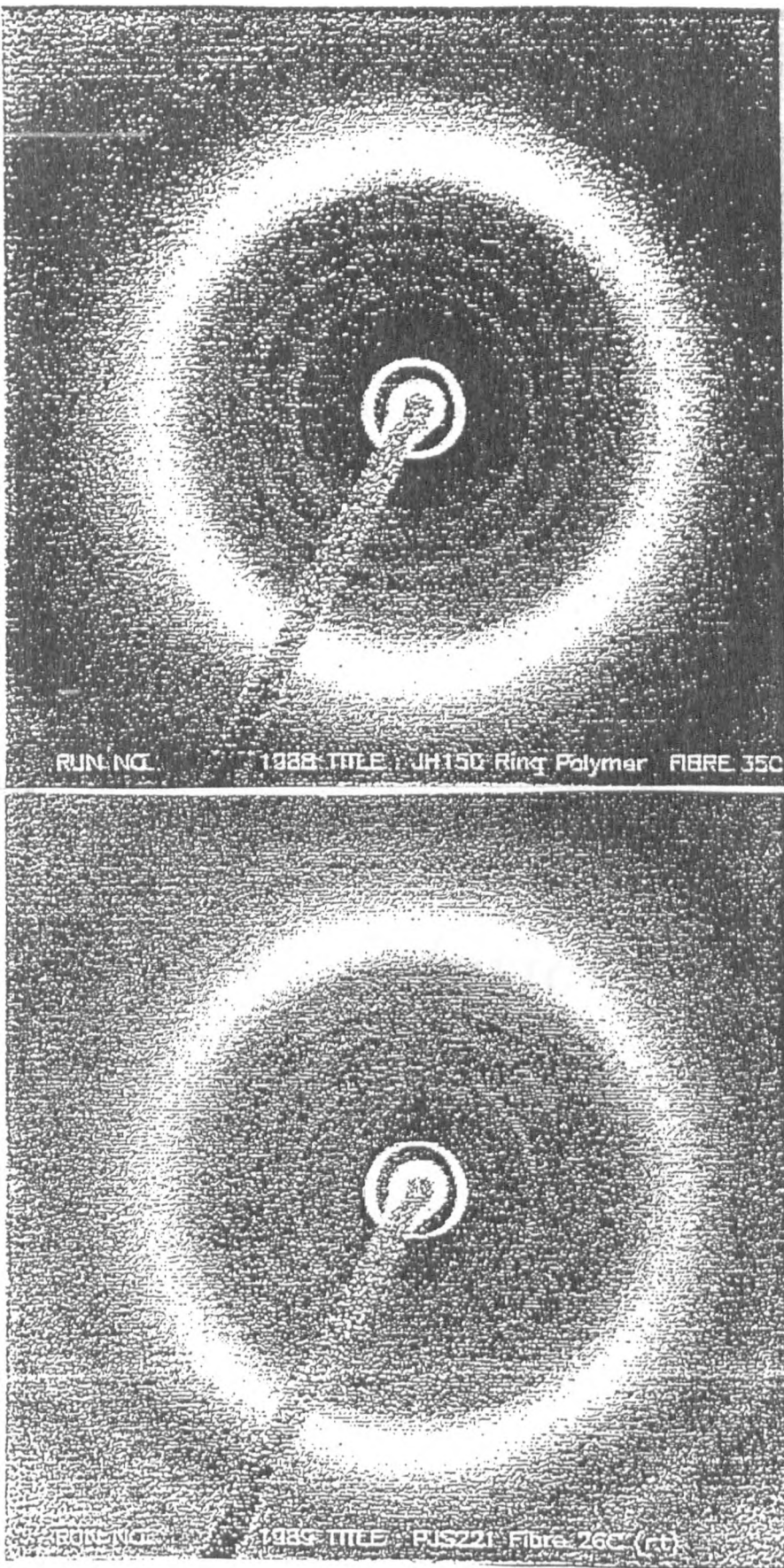
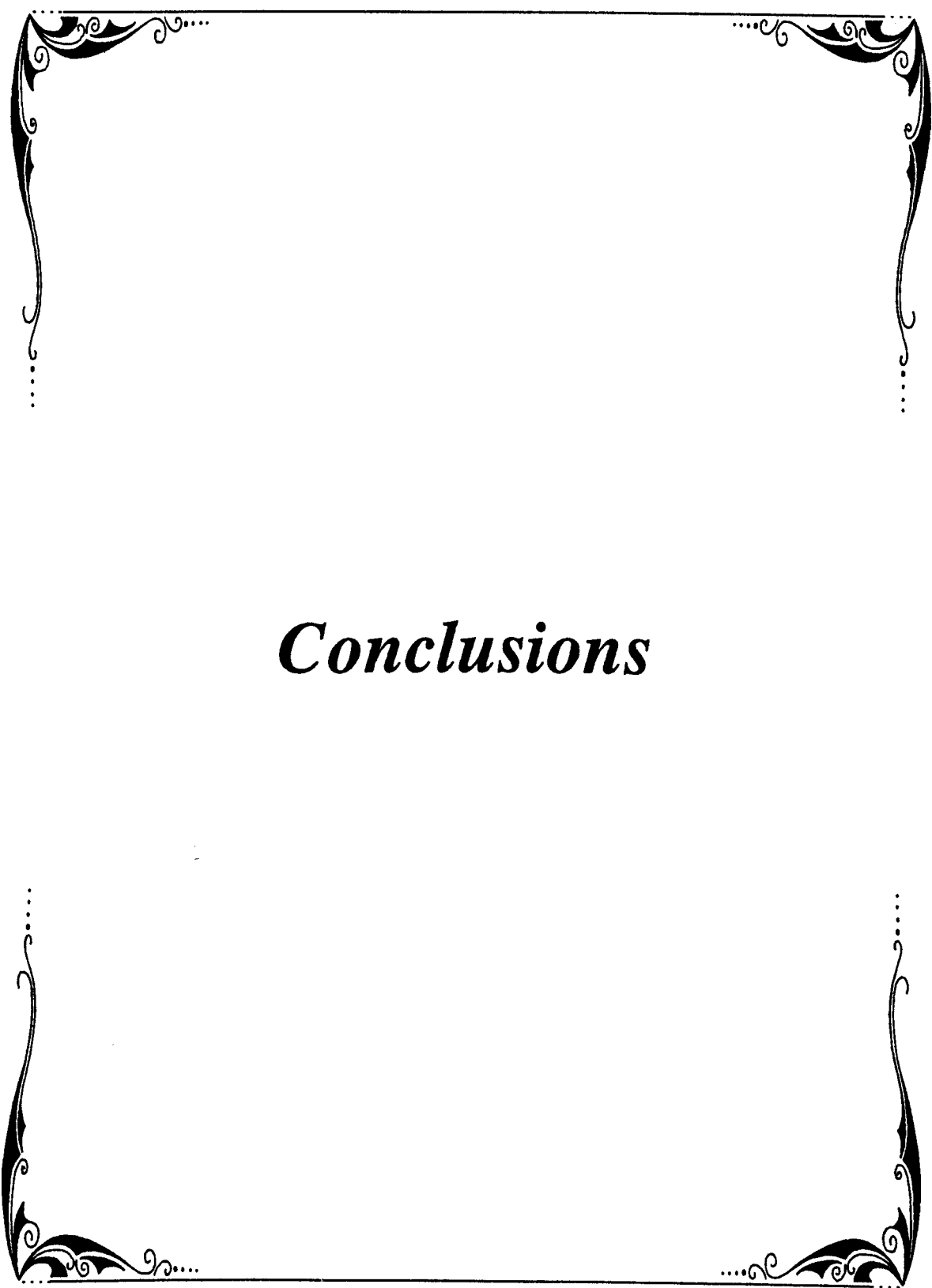


Figure 6.23 The X-ray diffraction patterns of polymers XLIIIa and XLIVa.



# *Conclusions*

## 7. CONCLUSIONS.

Although the initial aims of this work were to produce SCLC polymers with high degrees of polymerization and low polydispersity, it became clear that these criteria could not be met using group transfer polymerization. A large amount of time was spent in designing and building the equipment, and optimizing the reaction conditions for group transfer polymerization using non-mesogenic monomers. Although it was possible to achieve the desired properties when methyl methacrylate was polymerized, whenever mesogenic monomers were introduced into the system, very little polymerization occurred; the best result being oligomers of a mesogenic acrylate. Due to the need for a procedure which would give SCLC polymers with high degrees of polymerization, a different polymerization technique was obviously required.

Free radical polymerization was the alternative method chosen for the polymerization of mesogenic acrylates and methacrylates. The literature procedure for the free radical polymerization of mesogenic acrylates using THF as the solvent, resulted in SCLC polymers with a  $\bar{DP} \approx 10$ , both at The University of Hull and at Merck (UK), with whom we were collaborating, under a MOD contract (DRA, Malvern).

A large amount of work was carried out to try to optimize the conditions necessary in free radical polymerization to produce polymers with high  $\bar{DP}$  and low  $\bar{M}_w/\bar{M}_n$  values. This part of the investigation was carried out using a variety of non-mesogenic monomers. Optimum conditions were found that resulted in polymers with a much higher degrees of polymerization and fairly low polydispersities than those

made by literature procedures. This set of optimum conditions was successfully applied to the polymerization of several mesogenic monomers. Although the degrees of polymerization were lower than would have been preferred ( $> 100$ ), and the polydispersities were higher than would have been preferred  $\bar{M}_w/\bar{M}_n \approx 1.6$ , these SCLC polymers produced stable liquid crystal phase transitions. The homopolymers that were produced exhibited a variety of liquid crystalline phases. Although it could never be said that the polymerization of mesogenic acrylates and methacrylates was easy, using the conditions described in Section 6.2.2.6 of this thesis, it should now be possible to polymerize most mesogenic acrylates and methacrylates successfully to produce SCLC polymers with degrees of polymerization  $> 30$ . Some minor adjustments to the polymerization conditions may be necessary in some cases to maximise the degree of polymerization of the polymers.

One of the techniques that was tried to increase the degree of polymerization of the SCLC polymers was to make random copolymers using mesogenic monomers and incorporating small amounts of non-mesogenic monomers. The reason behind the use of non-mesogenic monomers was to decrease the steric hindrance between the mesogenic groups, allowing a polymer with a larger degree of polymerization to be produced, without detrimentally affecting the liquid crystal phase transitions of the polymer. The results from this work gave no general trends except that the addition of a non-mesogenic monomer gives copolymers with much higher  $\bar{DP}$  values than homopolymers containing the mesogenic side chain only, but with reduced clearing points. The most surprising thing to come out of this study was the fact that copolymers containing up to 80 % non-mesogenic side chain still exhibited liquid

crystalline behaviour.

It was found that the defect textures exhibited by the copolymers became less identifiable on increasing the non-mesogenic content of the copolymers indicating that this technique could not be used to improve the defect textures of SCLC polymers. Such an improvement in the defect textures would have been beneficial in using optical microscopy to identify the phases exhibited by SCLC polymers. However, work carried out by Merck (UK) suggests that if the polymers have a low degree of polymerization ( $\bar{DP} \approx 11$ ), then the formation of an identifiable liquid crystal defect texture is enhanced. This effect could be due to the very small number of non-mesogenic groups that would be incorporated into a polymer chain of only 11 units.

Random copolymers of acrylates and methacrylates were also the focus of another part of this thesis. Mesogenic monomers were mixed prior to free radical polymerization in an attempt to fine-tune the liquid crystalline phases exhibited by the SCLC polymers. The systems that were chosen were designed so that one component of the system would promote the formation of a smectic C phase, while the other component was chosen in order to try to induce chirality into the system. The object of the exercise was to combine the two effects and produce a polymer that exhibited a chiral smectic C phase ( $S_C^*$ ). The results of this work have not yet been fully evaluated due to the difficulty in the identification of the liquid crystalline phases formed by the SCLC copolymers. The only liquid crystal defect structure that is shown by these mixed mesogenic copolymers is the sandy texture common to most SCLC polymers, irrespective of the phase type. A large amount of time was spent trying to promote

the formation of identifiable textures using the alignment techniques described earlier. However, all the techniques that were tried had no real effect on improving the defect textures of the phases. Samples of these materials have been sent to The University of Bristol for X-ray studies. The initial results on one polymer are given in Section 6.4, but further work needs to be carried out in this area. The results from X-ray studies suggest that various liquid crystal phases are present, but unfortunately not an  $S_C$  phase.

The work carried out with respect to the alignment of SCLC polymers has been very successful. It has enabled the identification of many of the polymers produced in connection with this thesis, and also by Merck (UK). The techniques are now used routinely at The University of Hull for the identification of the phases produced by various types of liquid crystalline polymers.

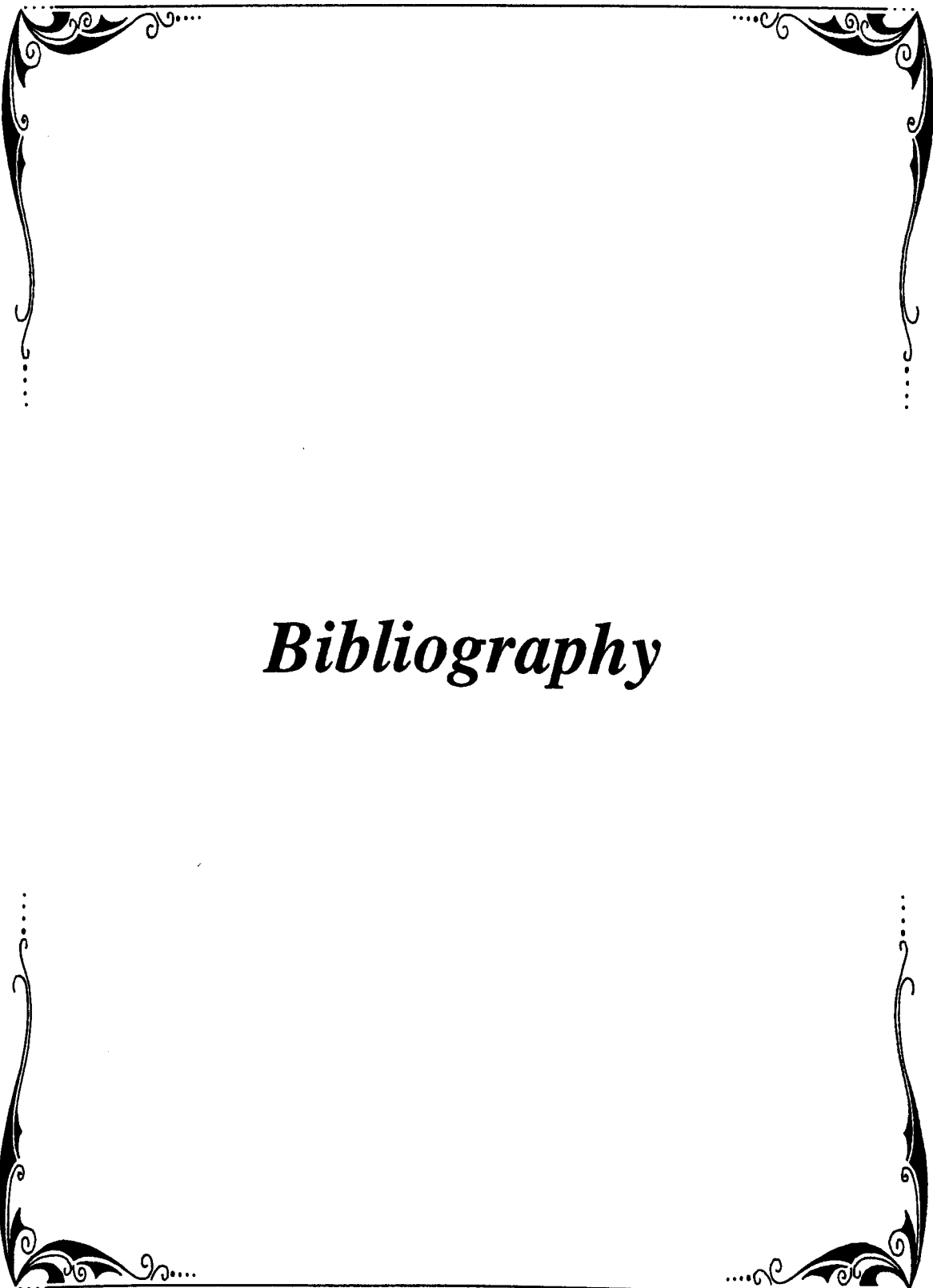
The other major part of this thesis, namely the production of SCLC polymers by the hydrosilylation reaction of mesogenic alkenes to commercially available cyclic polymer backbones containing either 4 or 5 reactive Si-H bonds, resulted in SCLC polymers with a variety of liquid crystalline phase types. One advantage of these cyclic polymers over traditional linear polysiloxanes is that they produce similar liquid crystalline phase transitions to their linear analogues but they possess a much lower viscosity. Hence they are much easier to work with and they also produce identifiable liquid crystal defect textures very quickly. No major difficulties were encountered with the hydrosilylation reaction which means that a variety of mesogenic alkenes can be substituted onto a cyclic polysiloxane. A number of these cyclic polysiloxanes

exhibited  $S_C$  and  $S_C^*$  phases and therefore could be useful as ferro-, pyro- or piezo-electric materials.

Another advantage that cyclic polysiloxanes have over their linear analogues is that they can be used to form mixtures. This means that it is possible to fine-tune the properties of a cyclic polysiloxane by creating mixtures, in the same way as for LMM liquid crystals.

The work reported in this thesis could be described as the first stage in the preparation of a very large number of SCLC polymers prepared for evaluation by the DRA (RSRE, Malvern). The techniques described within this thesis for the production of SCLC polymers using free radical polymerization should be transferable to most monomeric acrylate and methacrylate systems, thus enabling a wide variety of liquid crystalline phases to be produced by polyacrylates and polymethacrylates. The techniques for the enhancement of liquid crystal defect structures should enable the liquid crystalline phases exhibited by the SCLC polymers to be identified by optical microscopy, and hopefully may give some insight into how the phases may be aligned so that they become exploitable for commercial applications.

Much of this work, particularly the studies on the production of novel cyclic polysiloxanes, is being continued in the Liquid Crystal Group at The University of Hull.



# ***Bibliography***

## 8. BIBLIOGRAPHY.

1. F. Reinitzer, *Monatsch. Chem.*, 1888, **9**, 421.
2. O.Z. Lehmann, *Phys. Chem. (Leipzig)*, 1889, **4**, 462.
3. J.W. Goodby, *Chemalog Hi-lites*, 1987, **11**, 3.
4. P.A. Winsor, *Chem. Rev.*, 1968, **68**, 1.
5. P. Ekwall, in "Advances in liquid crystals", ed. G.H. Brown, Academic Press, New York, 1971, vol 1, chap. 1.
6. G.J.T. Tiddy, *Phys. Rep.*, 1980, **57**, 1.
7. E.S. Blackmore and G.J.T. Tiddy, *J. Chem. Soc., Faraday Trans. 2*, 1988, **84(8)**, 1115.
8. G.W. Gray, in "Advances in Liquid Crystal Materials for Applications", BDH Special Publication, BDH Chemicals LTD, Poole, England, 1978.
9. S. Chandrasekhar, B.K. Sadashiva and K.A. Suresh, *Pramana*, 1977, **9**, 471.
10. S. Chandrasekhar, *Phil. Trans. R. Soc. Lond. A*, 1983, **93**, 309.
11. J. Billard, J.C. Dubois, Nguyen Huu Tinh, A. Zann, *Nouv. J. Chim.*, 1978, **2**, 535.
12. D. Coates and G.W. Gray, *Phys. Lett.*, 1973, **45A**, 115.
13. J.W. Goodby, *J. Mater. Chem.*, 1991, **1(3)**, 307.
14. J.W. Goodby, *Mol. Cryst. Liq. Cryst. Lett.*, 1983, **92**, 171.
15. A.J. Leadbetter, in "Thermotropic Liquid Crystals", ed. G.W. Gray, Wiley, Chichester, 1987.
16. P.A.C. Gane, A.J. Leadbetter and P.C. Wrighton, *Mol. Cryst. Liq. Cryst.*, 1981, **66**, 247.

17. J.J. Benetar, J. Doucet and M. Lambert, *Phys. Rev.*, 1979, **A20**, 2505.
18. L.K.M. Chan, G.W. Gray and D. Lacey, *Mol. Cryst. Liq. Cryst.*, 1985, **123**, 185.
19. G.W. Gray, K.J. Harrison and J.A. Nash, *Electron. Lett.*, 1973, **9**, 130.
20. P.P. Crooker, *Liq. Cryst.*, 1989, **5**, 751.
21. R.B. Meyer, L. Liebert, L. Strzelecki and P. Keller, *J. Phys. (Paris) Lett.*, 1975, **69**, 36.
22. D. Lacey, Personal Communication.
23. J.G. Grabmaier, in "Applications of Liquid Crystals", ed. G. Maier, E. Sackmann, J.G. Grabmaier, Springer-Verlag, Berlin-New York, 1975, pp83-160.
24. S.R. Renn and T.C. Lubensky, *Phys. Rev. A*, 1988, **38**, 2132.
25. A.J. Slaney and J.W. Goodby, *J. Mater. Chem.*, 1991, **1(1)**, 5.
26. Y.S. Friedzon, Y.G. Tropsha, V.V. Tsukruk, V.V. Shilov, V.P. Shibaev and Y.S. Lipatov, *J. Polym. Chem. (USSR)*, 1987, **29**, 1371.
27. E.C. Bolton, D. Lacey, P.J. Smith and J.W. Goodby, *Liq. Cryst.*, 1992, **12**, 305.
28. R.J. Young, in "Introduction to Polymers", Chapman and Hall, London, 1981.
29. F.W. Billmeyer, in "Textbook of Polymer Science", Wiley Interscience, New York, 1971.
30. P.J. Flory, in "Principles of Polymer Chemistry", Cornell University Press, Ithaca, New York, 1953.
31. P.W. Morgan and S.L. Kwolek, *J. Chem. Educ.*, 1959, **36**, 182.

32. H. Mark, G. Stafford Whitby eds., in "Collected Papers of Wallace Hume Carothers on High Polymeric Substances", Interscience Publishers, New York, 1940.
33. C.S. Marvel, in "An Introduction to the Organic Chemistry of High Polymers", John Wiley and Sons, New York, 1959.
34. P.W. Morgan, in "Condensation Polymers by Interfacial and Solution Methods", Interscience Div. John Wiley and Sons, New York, 1965.
35. W.R. Sorenson and T.W. Campbell, in "Preparative Methods of Polymer Chemistry", 2nd Ed., Interscience Div., John Wiley and Sons, New York, 1968.
36. O.L. Mageli and J.R. Kolcynski, in "Encyclopedia of Polymer Science and Technology", eds. H.F. Mark, N.G. Gaylord and N.M. Bikales, Interscience Div., John Wiley and Sons, New York, 1967, Vol 9.
37. R. Zand, in "Encyclopedia of Polymer Science and Technology", eds. H.F. Mark, N.G. Gaylord and N.M. Bikales, Interscience Div., John Wiley and Sons, New York, 1967, Vol 2.
38. R.M. Noyes, in "Encyclopedia of Polymer Science and Technology", eds. H.F. Mark, N.G. Gaylord and N.M. Bikales, Interscience Div., John Wiley and Sons, New York, 1967, Vol 2.
39. B. Vollmert, in "Polymer Chemistry", Springer Verlag, New York, 1973.
40. G.C. Eastmond, in "Encyclopedia of Polymer Science and Technology", eds. H.F. Mark, N.G. Gaylord and N.M. Bikales, Interscience Div., John Wiley and Sons, New York, 1967, Vol 7.
41. R.W. Lenz, *Ind. Eng. Chem.*, 1969, **61**(3), 67.

42. R.W. Lenz, *Ind. Eng. Chem.*, 1970, **62**(2), 54.
43. J.C. Bevington, H.W. Melville and R.P. Taylor, *J. Polymer Sci.*, 1954, **12**, 449.
44. J.C. Bevington, H.W. Melville and R.P. Taylor, *J. Polymer Sci.*, 1954, **14**, 463.
45. P.J. Flory, *J. Am. Chem. Soc.*, 1937, **59**, 241.
46. P.H. Plesch, in "Cationic Polymerization and Related Complexes", Academic Press, New York, 1954.
47. A.M. Eastham, in "Encyclopedia of Polymer Science and Technology", eds. H.F. Mark, N.G. Gaylord and N.M. Bikales, Interscience Div., John Wiley and Sons, New York, 1967, Vol 3.
48. R.W. Lenz, in "Organic Chemistry of Synthetic High Polymers", Interscience Div., John Wiley and Sons, New York, 1967.
49. G. Odian, in "Principles of Polymerization", McGraw-Hill Book Co., New York, 1970.
50. M. Swarc, in "Carbanions, Living Polymers and Electron-Transfer Processes", John Wiley and Sons, New York, 1968.
51. W.B. Farnham and D.Y. Sogah, *ACS Polym. Preprints*, 1986, **27**, 167.
52. O.W. Webster, W.R. Hertler, D.Y. Sogah, W.B. Farnham and T.V. Rajanbabu, *J. Am. Chem. Soc.*, 1983, **105**, 5706.
53. M.T. Reetz, *Angew. Chem. Int. Ed. Engl.*, 1988, **27**, 994.
54. M. Morton, in "Anionic Polymerization Principles and Practice", Academic Press, New York, 1983.

55. M. VanBeylen, S. Bywater, G. Smets, M. Swarc and D.J. Worsfold, *Adv. Polym. Sci.*, 1988, **86**, 87.
56. O.W. Webster and D.Y. Sogah, in "Recent Advances in Mechanistic and Synthetic Aspects of Polymerization", eds. M. Fontanille, A. Guyot, Riedel, Dordrecht, 1987.
57. C. Robinson, *Trans. Faraday Soc.*, 1956, **52**, 571.
58. A. Ciferri, in "Polymeric Liquid Crystals", Academic Press, 1982.
59. A. Blumstein and C.S. Hsu, in "Liquid Crystalline Order in Polymers", ed. A. Blumstein, 1978.
60. H. Finkelmann, *Phil. Trans. R. Soc. Lond.*, 1983, A **309**, 105.
61. D. Demus and H. Zschke, in "Flüssige Kristalle in Tabellen", Vol II, VEB Deutscher Verlag für Grundstoffindustrie, Leipzig, German Democratic Republic, 1984.
62. C. Robinson, J.C. Ward and R.B. Beevers, *Faraday Discuss. Chem. Soc.*, 1958, **25**, 29.
63. J.J. Jin, S. Antoun, C. Ober and R.W. Lenz, *Br. Polym. J.*, 1980, **12**, 132.
64. W.J. Jackson and H.F. Kuhfuss, *J. Polym. Sci. Polym. Chem. Ed.*, 1976, **14**, 2043.
65. J.J. Kleinschuster, T.C. Pletcher, J.R. Schaefgen and R.R. Luise, Ger. Offen 2520819 and 2520820 (November 27th) 1975.
66. H. Finkelmann, in "Thermotropic Liquid Crystals", ed. G.W. Gray, John Wiley and Sons, Chichester, 1987.
67. D.G. Gray, in "Polymeric Liquid Crystals", ed. A. Blumstein, Plenum Press, New York, 1985.

68. A. Blumstein, in "Polymeric Liquid Crystals", ed. A. Blumstein, Plenum Press, New York, 1985.
69. A. Blumstein, *Polym. J.*, 1985, **17**, 105.
70. R.W. Lenz, *Faraday Discuss. Chem. Soc.*, 1985, **79**, Paper 2.
71. R.W. Lenz, *Polym. J.*, 1985, **17**, 105.
72. H. Finkelmann and G. Rehage, *Adv. Polym. Sci.*, 1984, **60/61**, 99.
73. V.P. Shibaev and N.A. Platé, *Adv. Polym. Sci.*, 1984, **60/61**, 173.
74. K.H. Wassmer, E. Ohmes, M. Portugall, H. Ringsdorf and G. Kothe, *J. Am. Chem. Soc.*, 1985, **107**, 1511.
75. C. Boeffel, B. Hisgen, V. Pschorn, H. Ringsdorf, H.W. Spiess, *Israel J. Chem.*, 1983, **23**, 388.
76. V. Percec and C. Pugh in "Side Chain Liquid Crystal Polymers", ed. C.B. McArdle, Blackie, Glasgow, 1989.
77. R. Duran, D. Guillon, A. Gramain and A. Skoulios, *Makromol. Chem. Rapid Commun.*, 1987, **8**, 59.
78. H. Finkelmann, M. Happ, M. Portugall and H. Ringsdorf, *Makromol. Chem.*, 1978, **179**, 2541.
79. C.S. Hsu and V. Percec, *Polym. Bull.*, 1987, **17**, 49.
80. H. Stevens, G. Rehage and H. Finkelmann, *Macromolecules*, 1984, **17**, 851.
81. S.G. Kostromin, R.V. Talroze, V.P. Shibaev, N.A. Platé, *Makromol. Chem. Rapid Commun.*, 1982, **3**, 803.
82. M. Portugall, H. Ringsdorf and R. Zentel, *Makromol. Chem.*, 1982, **183**, 2311.

83. G.W. Gray, in "Side Chain Liquid Crystal Polymers", ed. C.B. McArdle, Blackie, Glasgow, 1989.
84. V.P. Shibaev, S.G. Kostromin and N.A. Platé, *Eur. Polym. J.*, 1982, **18**, 651.
85. R. Zentel and H. Ringsdorf, *Makromol. Chem. Rapid Commun.*, 1984, **5**, 393.
86. B. Reck and H. Ringsdorf, *Makromol. Chem., Rapid Commun.*, 1985, **6**, 291.
87. H. Finkelmann, B. Luhmann, G. Rehage and H. Stevens, in "Liquid Crystals and Ordered Fluids", eds. A.C. Griffin, J.F. Johnson, Plenum, New York, 1984, Vol 4.
88. P. Davidson, P. Keller and A.M. Levelut, *J. Phys.*, 1985, **46**, 939.
89. P. LeBarny, G. Ravanx, J.C. Dubois, J.P. Parneix, R. Njenmo, C. Legrand and A.M. Levelut, *S.P.I.E.*, 1986, **56**, 682.
90. P.A. Gemmell, G.W. Gray and D. Lacey, *Mol. Cryst. Liq. Cryst.*, 1985, **122**, 205.
91. C.S. Cundy, B.M. Kingston and M.F. Lappert, *Adv. Organomet. Chem.*, 1973, **11**, 253.
92. G.W. Gray, D. Lacey, G. Nestor and M.S. White, *Makromol. Chem., Rapid Commun.*, 1986, **7**, 71.
93. C. Casagrande, P. Farbre, M. Veyssie, C. Weill, H. Finkelmann, *Mol. Cryst. Liq. Cryst.*, 1984, **113**, 193.
94. L. Strzelecki and L. Liebert, *Bull. Soc. Chim. Fr.*, 1973, 597.

95. H. Ringsdorf and A. Schneller, *Makromol. Chem. Rapid Commun.*, 1982, **3**, 557.
96. H. Ringsdorf, H.W. Schmidt, H. Eilingsfeld and K.H. Etzbach, *Makromol. Chem.*, 1987, **188**, 1355.
97. H. Ringsdorf and R. Wustefeld, Int. Conf. on Liquid Crystalline Polymers, Bordeaux, Abstract 10P1.
98. F.H. Kreuzer, *Proceedings II Freiburger, Arbeitstagung Flüssigkristalle*, 1981, P5.
99. F.H. Kreuzer, M. Gawhary, R. Winkler, H. Finkelmann, E.P. 0060335, 1981.
100. M.S. Beevers and J.A. Semlyen, *Polymer*, 1971, **12**(6), 378.
101. R.D.C. Richards, W.D. Hawthorne, J.S. Hill, M.S. White, D. Lacey, J.A. Semlyen, G.W. Gray and T.C. Kendrick, *J. Chem. Soc. Chem. Commun.*, 1990, 95.
102. F.H. Kreuzer, D. Andrejewski, W. Haas, N. Haberle, G. Riedl, P. Spes, *Mol. Cryst. Liq. Cryst.*, 1991, **199**, 345.
103. G.W. Gray, J.S. Hill and D. Lacey, *Angew. Chem. Int. Ed. Engl. Adv. Mater.*, 1989, **28**, 1120.
104. B. Reck and H. Ringsdorf, *Makromol. Chem. Rapid Commun.*, 1986, **7**, 389.
105. S. Berg, V. Krone and H. Ringsdorf, *Makromol. Chem. Rapid Commun.*, 1986, **7**, 381.
106. S. Diele, B. Hisgen, B. Reck and H. Ringsdorf, *Makromol. Chem. Rapid Commun.*, 1986, **7**, 267.

107. M. Engel, B. Hisgen, R. Keller, W. Kreuder, B. Reck, H. Ringsdorf, H.W. Schmidt and P. Tschirner, *Pure Appl. Chem.*, 1985, **57**, 1009.
108. R.V. Talroze, S.G. Kostromin, V.P. Shibaev, N.A. Platé, H. Kresse, K. Zauer and D. Demus, *Makromol. Chem. Rapid Commun.*, 1981, **2**, 305.
109. K.J. Toyne, in "Thermotropic Liquid Crystals", ed. G.W. Gray, John Wiley and Sons, Chichester, 1987.
110. A.K. Amiloglu, A. Ledwith, P.A. Gemmell, G.W. Gray and D. Lacey, *Polymer*, 1984, **25**, 1342.
111. S.G. Kostromin, V.V. Simitsyn, R.V. Talroze and V.P. Shibaev, *Polym. Sci. USSR*, 1984, **26**, 370.
113. J.C. Dubois, G. Decobert, P. LeBarny, S. Esselin, C. Friedrich, C. Noël, *Mol. Cryst. Liq. Cryst.*, 1986, **139**, 349.
114. V.P. Shibaev and N.A. Platé, *Pure Appl. Chem.*, 1985, **57**, 1589.
115. P. LeBarny, J.C. Dubois, C. Friedrich, C. Noël, *Polym. Bull.*, 1986, **15**, 341.
116. S.G. Kostromin, V.V. Simitsyn, R.V. Talroze, V.P. Shibaev and N.A. Platé, *Makromol. Chem. Rapid Commun.*, 1982, **3**, 809.
117. H. Ringsdorf, J. Schneider and A. Schuster, 3rd Int. Conf. on Langmuir-Blodgett Films, Göttingen, FRG, 1987.
118. C.S. Hsu, J.M. Rodriguez-Parada and V. Percec, *J. Polym. Sci. Polym. Chem. Ed.*, 1987, **25**, 2425.
119. C.S. Hsu and V. Percec, *Polym. Bull.*, 1987, **18**, 91.
120. G.W. Gray, J.S. Hill and D. Lacey, *Makromol. Chem.*, 1990, **191**, 2227.

122. G. Nestor, M.S. White, G.W. Gray, D. Lacey and K.J. Toyne, *Makromol. Chem.*, 1987, **188**, 2759.
123. G.W. Gray, J.S. Hill and D. Lacey, *Mol. Cryst. Liq. Cryst. Letts.*, 1990, **7(2)**, 47.
124. D.D. Perrin, W.L.F. Armarego and D.R. Perrin, in "Purification of Laboratory Chemicals", Pergamon Press, Oxford, 1980, pp205.
125. D.D. Perrin, W.L.F. Armarego and D.R. Perrin, in "Purification of Laboratory Chemicals", Pergamon Press, Oxford, 1980, pp427.
126. E. Chin and J.W. Goodby, *Mol. Cryst. Liq. Cryst.*, 1986, **141**, 311.
127. J. Nemceck, personal communication.
128. H. Finkelmann, H. Ringsdorf, W. Siol, J.H. Wendorff, *ACS Symp. Series*, 1978, **74**, 22.
130. R. Benkeser and J. Kang, *J. Organomet. Chem.*, 1980, **185**, C9.
131. J.W. Goodby and G.W. Gray, in "Smectic Liquid Crystals: Textures and Structures", Blackie Press, Glasgow-London, 1984.
132. J.S. Patel, T.M. Leslie and J.W. Goodby, *Ferroelectrics*, 1984, **59**, 137.
133. H. Finkelmann, J. Koldehoff and H. Ringsdorf, *Angew. Chem.*, 1978, **90**, 922.
134. E.C. Bolton, personal communication.
135. M. Verral, personal communication.

136. P.J. Lorimer in "Sonochemistry, Theory, Applications and Uses of Ultrasound in Chemistry", John Wiley and Sons, Chichester, 1988.
137. P.J. Lorimer in "Critical Reports on Applied Chemistry. Vol 28 Chemistry with Ultrasound". Ed. T.J. Mason, Elsevier, Barking, 1990.
138. M. Verral, personal communication.
139. N.A. Platé, R.V. Talroze and V.P. Shibaev, *Makromol. Chem. Suppl.*, 1984, 8, 47.
140. J. Haley and D. Lacey, personal communication.
141. M. Verral personal communication.
142. P.J. Smith, J.W. Goodby and D. Lacey, Poster at Macro Group UK Meeting, University of Lancaster, March 1991.
143. G. Nestor, PhD Thesis, University of Hull, 1988.
144. A. Cherodian, R. Richardson, personal communication.



**Plate 1** The characteristic "sandy" texture of a side chain liquid crystal polymer. Polymer **XIX**, 150 °C (x100).

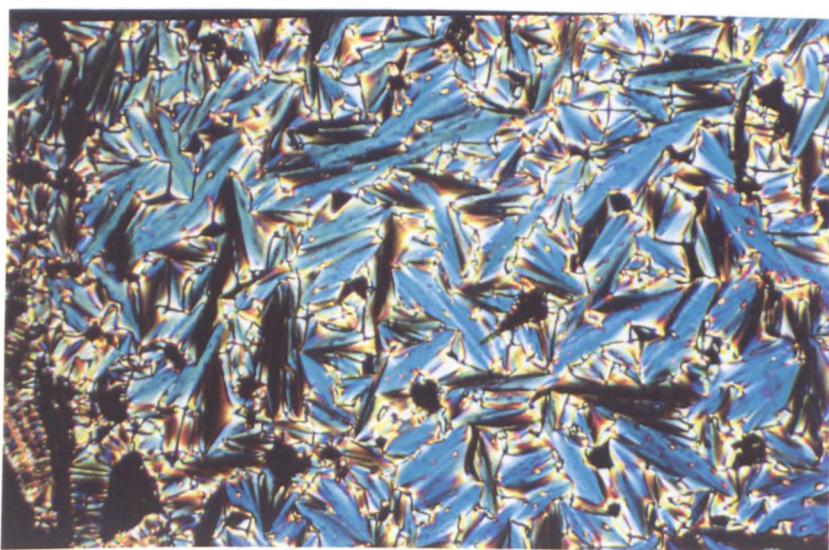


**Plate 2** The Focal conic texture of the smectic A phase of Polymer **XIX**, no alignment, 150 °C (x100).

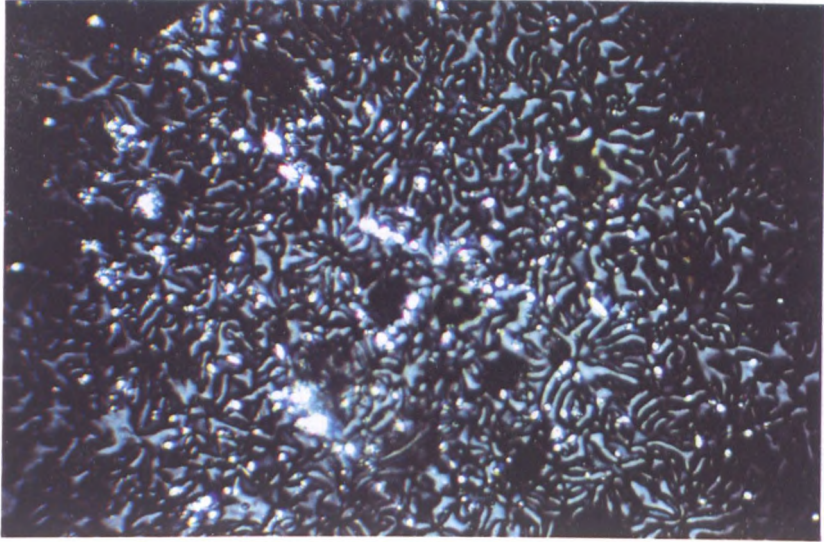


**Plate 3** The schlieren texture of the smectic C phase of Polymer XXI, aligned homeotropically, 130 °C (x100).

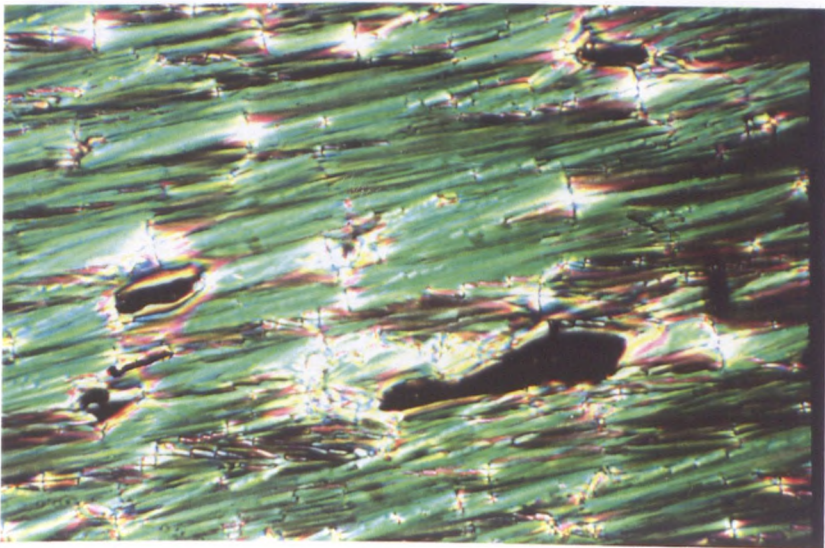


**Plate 4** The focal conic texture of the smectic A phase of Polymer XX, homogeneously aligned, 150 °C (x100).

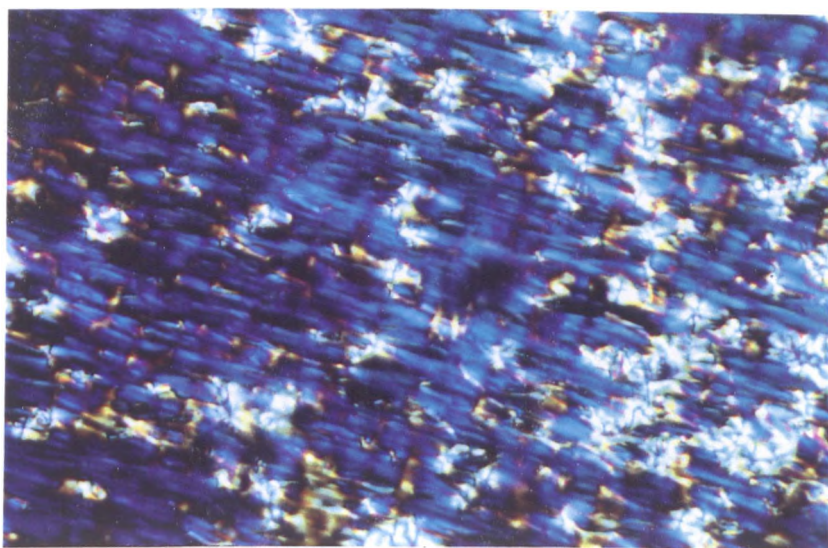


**Plate 5** The focal conic smectic A texture of Polymer XX, homogeneously aligned, 105 °C (x100).

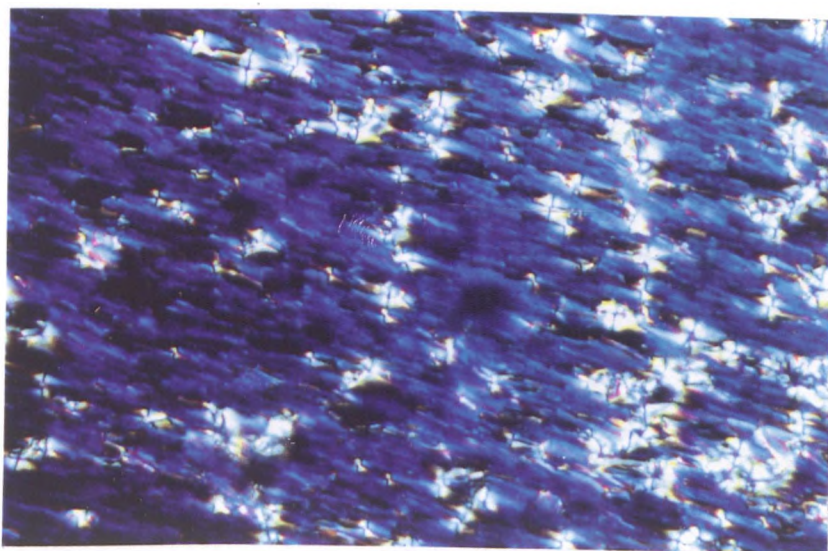


**Plate 6** The broken focal conic smectic C texture of Polymer XX, homogeneously aligned, cooled from the smectic A phase, 90 °C (x100).

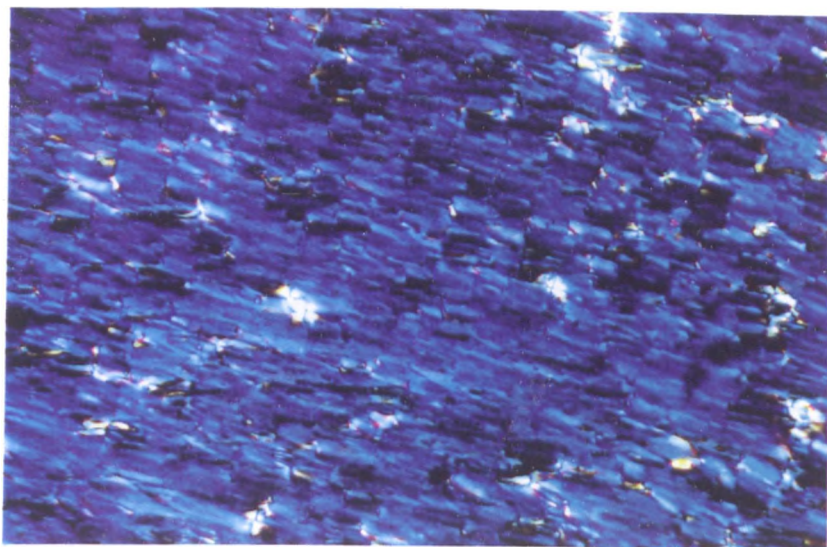


**Plate 7** The broken focal conic texture of the smectic I phase of Polymer XX, homogeneously aligned, cooled from the smectic C phase, 30 °C (x100).



**Plate 8** The texture of Polymer XXVI, 145 °C (x100).

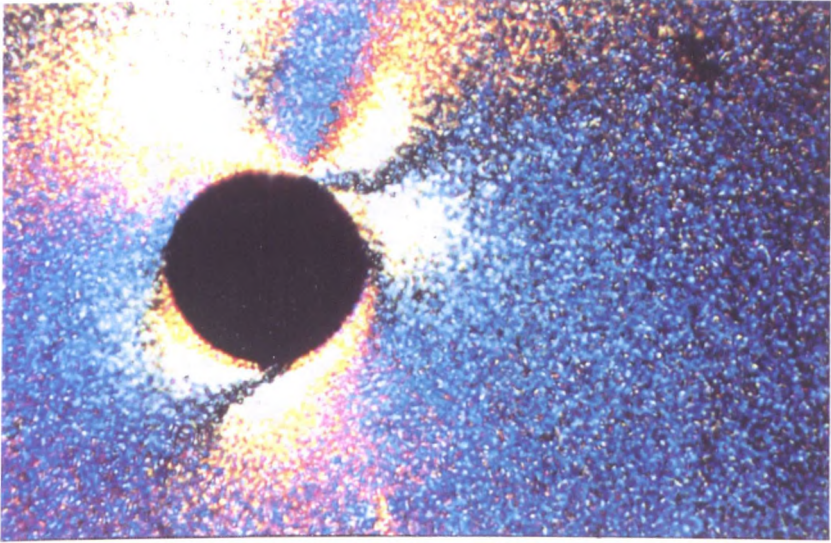


Plate 9 The texture of Polymer XXVII, 130 °C (x100).

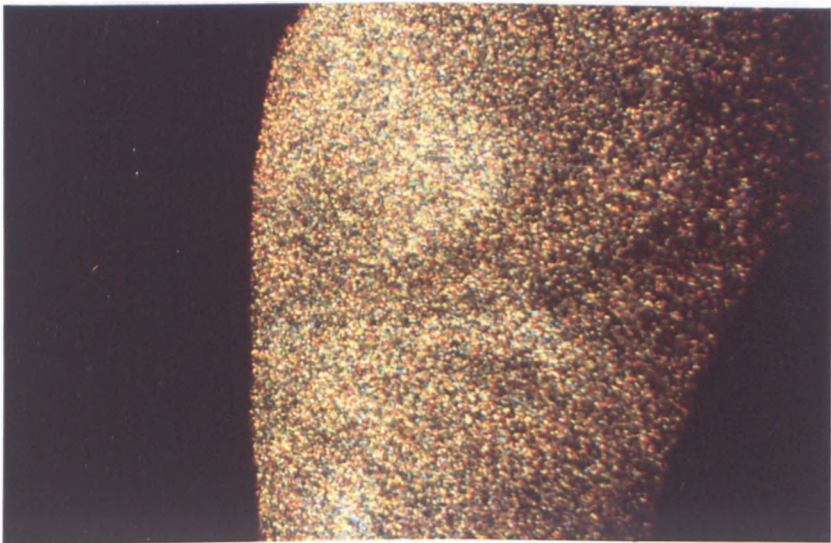
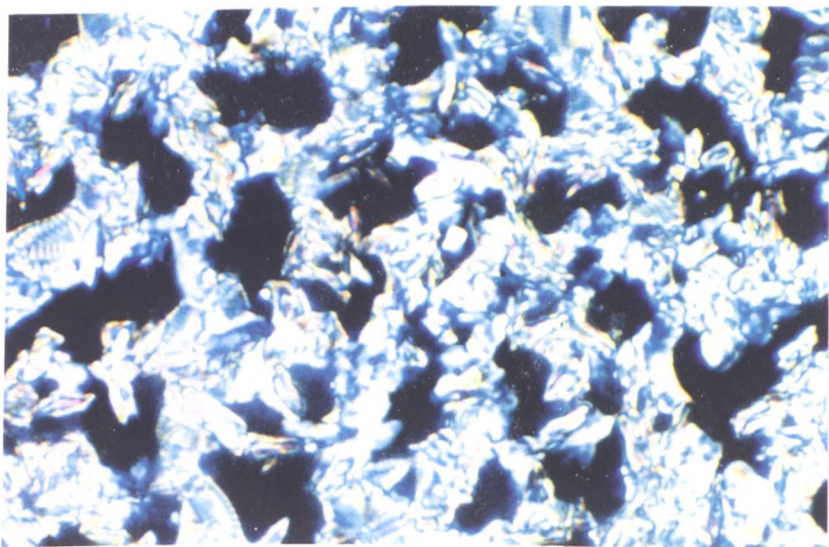
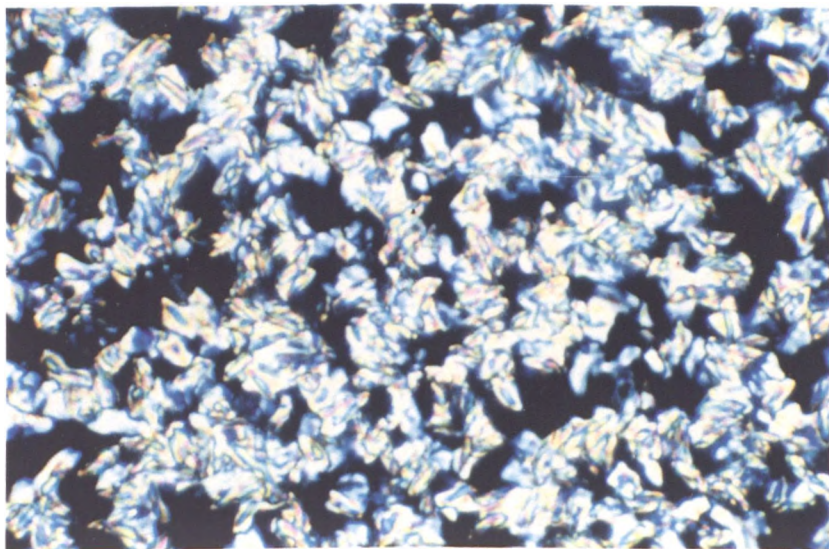


Plate 10 The texture of Polymer XXXV, 100 °C (x100).



**Plate 11** The focal conic texture of the chiral smectic C phase of Polymer XLIVa, 25 °C (x100).



**Plate 12** The "discotic" texture of Polymer XLIVa, 25 °C after 24 h. (x100).